

© 2011 by Onur Pekcan. All rights reserved.

SOFT COMPUTING BASED PARAMETER IDENTIFICATION IN PAVEMENTS  
AND GEOMECHANICAL SYSTEMS

BY

ONUR PEKCAN

DISSERTATION

Submitted in partial fulfillment of the requirements  
for the degree of Doctor of Philosophy in Civil Engineering  
in the Graduate College of the  
University of Illinois at Urbana-Champaign, 2011

Urbana, Illinois

Doctoral Committee:

Professor Erol Tutumluer, Director of Research  
Professor Jamshid Ghaboussi, Co-Director of Research  
Professor Marshall Thompson  
Professor Imad Al-Qadi



# Abstract

Accurate estimation of road pavement geometry and layer material properties through the use of proper nondestructive testing and sensor technologies is essential for evaluating pavement's structural condition and determining options for maintenance and rehabilitation. For these purposes, pavement deflection basins produced by the nondestructive Falling Weight Deflectometer (FWD) test data are commonly used. The nondestructive FWD test drops weights on the pavement to simulate traffic loads and measures the created pavement deflection basins. Backcalculation of pavement geometry and layer properties using FWD deflections is a difficult inverse problem, and the solution with conventional mathematical methods is often challenging due to the ill-posed nature of the problem.

In this dissertation, a hybrid algorithm was developed to seek robust and fast solutions to this inverse problem. The algorithm is based on soft computing techniques, mainly Artificial Neural Networks (ANNs) and Genetic Algorithms (GAs) as well as the use of numerical analysis techniques to properly simulate the geomechanical system. A widely used pavement layered analysis program ILLI-PAVE was employed in the analyses of flexible pavements of various pavement types; including full-depth asphalt and conventional flexible pavements, were built on either lime stabilized soils or untreated subgrade. Nonlinear properties of the subgrade soil and the base course aggregate as transportation geomaterials were also considered. A computer program, Soft Computing Based System Identifier or SOFTSYS, was developed. In SOFTSYS, ANNs were used as surrogate models to provide faster solutions of the nonlinear finite element program

ILLI-PAVE. The deflections obtained from FWD tests in the field were matched with the predictions obtained from the numerical simulations to develop SOFTSYS models.

The solution to the inverse problem for multi-layered pavements is computationally hard to achieve and is often not feasible due to field variability and quality of the collected data. The primary difficulty in the analysis arises from the substantial increase in the degree of non-uniqueness of the mapping from the pavement layer parameters to the FWD deflections. The insensitivity of some layer properties lowered SOFTSYS model performances. Still, SOFTSYS models were shown to work effectively with the synthetic data obtained from ILLI-PAVE finite element solutions.

In general, SOFTSYS solutions very closely matched the ILLI-PAVE mechanistic pavement analysis results. For SOFTSYS validation, field collected FWD data were successfully used to predict pavement layer thicknesses and layer moduli of in-service flexible pavements. Some of the very promising SOFTSYS results indicated average absolute errors on the order of 2%, 7%, and 4% for the Hot Mix Asphalt (HMA) thickness estimation of full-depth asphalt pavements, full-depth pavements on lime stabilized soils and conventional flexible pavements, respectively.

The field validations of SOFTSYS data also produced meaningful results. The thickness data obtained from Ground Penetrating Radar testing matched reasonably well with predictions from SOFTSYS models. The differences observed in the HMA and lime stabilized soil layer thicknesses observed were attributed to deflection data variability from FWD tests. The backcalculated asphalt concrete layer thickness results matched better in the case of full-depth asphalt flexible pavements built on lime stabilized soils compared to conventional flexible pavements. Overall, SOFTSYS was capable of producing reliable thickness estimates despite the variability of field constructed asphalt layer thicknesses.

*To my mother, for the benefit of mankind.*

# Acknowledgments

My Ph.D. was a long journey, during which I received help from many people. First, I would like to thank to my advisors Professor Erol Tutumluer and Professor Jamshid Ghaboussi for their contributions in this dissertation. Dr. Tutumluer's positive attitude and kindness always made me comfortable when I had to handle many things at the same time. He was also supportive in my decisions, the most extreme of which was to undertake the responsibility of studying for an M.S. degree in Computer Science.

Secondly, I wish to express my sincere gratitude to my co-supervisor, Dr. Ghaboussi. I was extremely happy to join his research group at the beginning of my Ph.D. studies. Dr. Ghaboussi's innovative solutions made the problems easier for me to solve; the main idea of this thesis actually belongs to him. I am thankful to him for sharing these ideas generously. In addition, I would like to thank him for his endless support during hard times. Knocking his door was always fruitful and made me think about how I could come up with different solutions to my research problems. I also learned many things from him about the academic world, the facts of which I was not really aware of before. In all, I have learned a great deal from him.

I would like to thank my committee members Dr. Marshall Thompson and Dr. Imad Al-Qadi. I always admired Dr. Thompson's deep love for his subjects, both pavement and geotechnical engineering problems. I will always remember his contributions, especially his practical approaches to challenging engineering problems. The field work in this thesis would not have been possible without him. Similarly, Dr. Al-Qadi's positive attitude towards me always made me comfortable, and his enthusiasm motivated me to learn

more about my subject matter. He always brought challenging questions to the table. Thinking about the solutions to these problems actually made my life easier at the later stages of my thesis. Throughout, I learned a lot from his intellectual and leadership characteristics. Therefore, I need to thank him for being an exemplary person for young engineering students. I also thank Dr. Al-Qadi's students, Jongeun Baek and Wei Xie, and my office-mate Abdullah Akçe for their help during the Ground Penetrating Radar testing of Staley Road. Finally, I am also grateful to Mr. Douglas Steele from Applied Research Associates, Inc. for his help in providing the data and performing field tests for this research.

This project would not have been possible without the support of Dr. David Goldberg. His great enthusiasm for always exploring further in science always motivated me during this thesis project. I know that I will continue to learn from him in the future as I do regular thinking about the world and humanity.

There were many friends whom I would like to thank. First, I am grateful to Nejan Huvaj Sarihan, for her help during my graduate study at UIUC. I always felt better when Nejan and her husband Süleyman were around us. I also would like to thank Barış Aktemur, Nur Pehlivanoğlu, İsmail Çağrı Özcan, Nihan Doğramacı Aksoylar and Cenk Aksoylar for being very good friends and Emre Akbaş for always answering with great patience my boring questions about basic computer concepts and Latex. There have been many friends with whom I shared the Chambana experience. I do not even attempt to name them individually since I am sure I will fail to mention them all.

This experience was an important one in which I have learned the “to-do’s” and “not-to-do’s” of my life. This would not have been possible without my wife’s continuous support. She was always with me in hard times. I hope my next stop will be my dream adventure. Last, but not the least, I owe my deepest gratitude to my mother.

# Table of Contents

<b>List of Tables</b> . . . . .	<b>x</b>
<b>List of Figures</b> . . . . .	<b>xii</b>
<b>List of Abbreviations</b> . . . . .	<b>xvii</b>
<b>List of Symbols</b> . . . . .	<b>xix</b>
<b>Chapter 1 Introduction</b> . . . . .	<b>1</b>
1.1 Problem Statement and Overview . . . . .	1
1.2 Research Objectives . . . . .	4
1.3 Research Methodology . . . . .	5
1.4 Thesis Organization . . . . .	7
<b>Chapter 2 Literature Review</b> . . . . .	<b>8</b>
2.1 Backcalculation Problem . . . . .	8
2.2 Falling Weight Deflectometer . . . . .	9
2.3 Backcalculation Methods . . . . .	11
2.4 Soft Computing Methods . . . . .	13
2.4.1 Artificial Neural Networks . . . . .	14
2.4.1.1 Backpropagation Learning Algorithm . . . . .	15
2.4.1.2 Pavement Layer Backcalculation Using ANNs . . . . .	20
2.4.2 Genetic Algorithms . . . . .	22
2.4.2.1 Genetic Algorithm Operators . . . . .	25
2.4.2.2 Genetic Algorithms in Backcalculation Analysis . . . . .	29
<b>Chapter 3 Development of Artificial Neural Network Based Structural Models</b>	<b>31</b>
3.1 ILLI-PAVE Finite Element Modeling . . . . .	31
3.1.1 Falling Weight Deflectometer Simulation . . . . .	33
3.1.1.1 Pavement Layer Characterization . . . . .	37
3.2 Lime Stabilization . . . . .	39
3.2.1 Preliminary Analyses of Lime Stabilized Sections . . . . .	41
3.2.1.1 Full-depth Asphalt Pavements on Lime Stabilized Soils . . . . .	44
3.2.1.2 Conventional Flexible Pavements on Lime Stabilized Soils . . . . .	45
3.3 ILLI-PAVE Database For Flexible Pavements . . . . .	49

3.4	ANN Structural Models . . . . .	53
3.4.1	Forward Analysis Models . . . . .	55
3.4.1.1	Performances of the Developed ANN Models . . . . .	57
3.4.2	Backcalculation Models . . . . .	62
3.4.2.1	Performances of the Developed ANN Models . . . . .	69
3.5	Field Validation . . . . .	74
3.5.1	US 50 (FAP 327, old FA 409) . . . . .	80
3.5.2	US 20 (FAP 301, old FA 401) . . . . .	81
3.5.3	Roseville Bypass . . . . .	81
3.5.4	Staley Road . . . . .	81
3.5.5	High Cross Road (FA 808) . . . . .	82
3.5.6	Sand Pit Road (Henry County) . . . . .	88
3.6	Summary . . . . .	90
<b>Chapter 4</b>	<b>Soft Computing Based System Analyzer: SOFTSYS . . . . .</b>	<b>91</b>
4.1	Introduction . . . . .	91
4.2	Basics of SOFTSYS . . . . .	91
4.2.1	SOFTSYS Algorithm and Implementation . . . . .	93
4.2.1.1	Defining Pavement Type and Backcalculation Model . . . . .	94
4.2.1.2	Entering FWD Data . . . . .	94
4.2.1.3	Population Initialization . . . . .	95
4.2.1.4	Running ANN Forward Analysis . . . . .	95
4.2.1.5	Fitness Evaluation of Population . . . . .	96
4.2.1.6	Checking Termination Criterion . . . . .	96
4.2.1.7	Encoding Variables . . . . .	97
4.2.1.8	Selection of Child Genotypes . . . . .	97
4.2.1.9	Crossover and Mutation of Variables . . . . .	97
4.2.1.10	Decoding of Genotypes . . . . .	97
4.2.2	Development of SOFTSYS Models . . . . .	98
4.3	SOFTSYS Validation with Synthetic Data Sets . . . . .	101
4.3.1	Full-depth Asphalt Pavements . . . . .	104
4.3.2	Full-depth Asphalt Pavements on Lime Stabilized Soils . . . . .	105
4.3.3	Conventional Flexible Pavements . . . . .	107
4.4	Field Validations . . . . .	110
4.4.1	US 50 (FAP 327, old FA 409) . . . . .	110
4.4.2	US 20 (FAP 301, old FA 401) . . . . .	113
4.4.3	Roseville Bypass . . . . .	115
4.4.4	Staley Road . . . . .	119
4.4.5	High Cross Road (FA 808) . . . . .	120
4.4.6	Sand Pit Road (Henry County) . . . . .	121
4.5	Comparison of SOFTSYS with ANN-PRO . . . . .	124
4.6	Summary . . . . .	125

<b>Chapter 5 Backcalculation of Layer Thickness and Moduli for Flexible Pavements</b>	<b>127</b>
5.1 Introduction	127
5.1.1 Significance	128
5.1.2 Objective	129
5.2 SOFTSYS Models for Thickness Determination	130
5.2.1 Full-depth Asphalt Pavements	133
5.2.2 Full-depth Asphalt Pavements on Lime Stabilized Soils	135
5.2.3 Conventional Flexible Pavements	138
5.2.4 Sensitivity and Uniqueness Issues for Three-Layered Systems	147
5.3 Field Validations	148
5.3.1 US 50 (FAP 327, old FA 409)	148
5.3.2 US 20 (FAP 301, old FA 401)	149
5.3.3 Roseville Bypass	152
5.3.4 Staley Road	154
5.3.5 High Cross Road (FA 808)	162
5.3.6 Sand Pit Road (Henry County)	165
5.4 Summary	167
<b>Chapter 6 Summary, Conclusions, and Future Work</b>	<b>170</b>
6.1 Summary	170
6.2 Conclusions	173
6.3 Future Work	178
<b>References</b>	<b>181</b>
<b>Vita</b>	<b>190</b>



# List of Tables

3.1	Falling Weight Deflectometer Sensor Spacing . . . . .	33
3.2	Typical Resilient Property Data for Granular Materials (after Rada and Witczak [1981]) . . . . .	39
3.3	Ranges of FDP-LSSs Studied in the ILLI-PAVE Preliminary Analyses . . .	44
3.4	Ranges of CFP-LSSs Studied in the ILLI-PAVE Preliminary Analyses . . .	47
3.5	Geometries and Material Properties of Full-Depth Flexible Pavements Analyzed . . . . .	52
3.6	Geometries and Material Properties of Conventional Flexible Pavements Analyzed . . . . .	52
3.7	Geometries and Material Properties of Full-Depth Flexible Pavements on Lime Stabilized Soils Analyzed . . . . .	54
3.8	Geometries and Material Properties of Conventional Flexible Pavements on Lime Stabilized Soils Analyzed . . . . .	54
3.9	Forward Artificial Neural Network Models for Flexible Pavements . . . . .	56
3.10	Backcalculation ANN Models for Full-Depth Asphalt Pavements . . . . .	68
3.11	Backcalculation ANN Models for Conventional Flexible Pavements . . . . .	68
3.12	Backcalculation ANN Models for Full-Depth Asphalt Pavements on Lime Stabilized Soils . . . . .	68
3.13	Backcalculation ANN Models for Conventional Flexible Pavements on Lime Stabilized Soils . . . . .	68
4.1	Descriptions of SOFTSYS Models Developed to Estimate Layer Moduli of Different Types of Pavements . . . . .	103
5.1	Asphalt Thickness Variability for Various Flexible Pavements Constructed in the State of Illinois . . . . .	132
5.2	SOFTSYS Models Developed to Estimate Thicknesses and Moduli of Different Pavement Types . . . . .	134
5.3	Backcalculation Results of SOFTSYS for a Given FWD Data Chosen from ILLI-PAVE Database Developed for FDP-LSS . . . . .	148
5.4	Effect of Lime Stabilized Soil Layer's Thickness on Pavement Responses ( $t_{AC} = 8$ in., $E_{AC} = 900$ ksi, $E_{LSS} = 100$ ksi, $E_{Ri} = 9$ ksi) . . . . .	149
5.5	Effect of Lime Stabilized Soil Layer's Thickness on Pavement Responses ( $t_{AC} = 8$ in., $E_{AC} = 500$ ksi, $E_{LSS} = 100$ ksi, $E_{Ri} = 9$ ksi) . . . . .	151

5.6	Effect of Lime Stabilized Soil Layer's Modulus on Pavement Responses ( $t_{AC} = 8$ in., $t_{LSS} = 12$ in., $E_{AC} = 900$ ksi, $E_{Ri} = 9$ ksi) . . . . .	151
5.7	Backcalculation Results of SOFTSYS for a Given FWD Data Chosen from ILLI-PAVE Database Developed for CFP . . . . .	152
5.8	Effect of Granular Base Layer's Thickness on Pavement Responses ( $t_{AC} =$ 9 in., $E_{AC} = 1300$ ksi, $K_{GB} = 5$ ksi, $E_{Ri} = 9$ ksi) . . . . .	154
5.9	Effect of Granular Base Layer's Thickness on Pavement Responses ( $t_{AC} =$ 9 in., $E_{AC} = 100$ ksi, $K_{GB} = 5$ ksi, $E_{Ri} = 9$ ksi) . . . . .	156
5.10	Effect of Granular Base Layer's Stiffness on Pavement Responses ( $t_{AC} = 9$ in., $t_{GB} = 12$ in., $E_{AC} = 1300$ ksi, $E_{Ri} = 9$ ksi) . . . . .	157
5.11	GPR Test Conditions Along Staley Road Pavement Sections . . . . .	159

# List of Figures

2.1	Dynatest Falling Weight Deflectometer Device. . . . .	9
2.2	Haversine Loading Applied by FWD. . . . .	10
2.3	Locations of FWD Sensors and Schematic Drawing. . . . .	11
2.4	Traditional Iterative Backcalculation Procedure [Meier, 1995]. . . . .	12
2.5	A Typical Backpropagation Neural Network. . . . .	16
2.6	Schematic Representation of an Information Processing Element in Backpropagation Neural Networks (adopted from [Tutumluer, 1995]). . . .	17
2.7	Direct Pavement Backcalculation Procedure Using a Neural Network. . . .	21
2.8	ANN Training Curves. . . . .	22
2.9	Crossover Methods (adopted from [Burke & Kendall, 2005]). . . . .	28
3.1	ILLI-PAVE 2005 Finite Element Software for Pavement Analysis. . . . .	32
3.2	Locations of Critical Pavement Responses and Deflections for Pavements Built on Unmodified Subgrade. . . . .	34
3.3	Locations of Critical Pavement Responses and Deflections for Pavements Built on Lime Stabilized Soils. . . . .	35
3.4	Finite Element Mesh for Full-Depth Pavements on Lime Stabilized Subgrade.	36
3.5	Bilinear Model to Characterize Stress Dependency of Fine-Grained Soils. .	38
3.6	Relationship Between $K$ (Shown as $K_1$ ) and $n$ (Shown as $K_2$ ) Values for Granular Materials Identified by Rada and Witczak [1981] (Reproduced from the Original Figure). . . . .	40
3.7	Typical Stress-Strain Curves for Natural and Lime Treated Soils [Transportation Research Board, 1987] (Reproduced from the Original Figure). . . . .	42
3.8	Immediate Effects of Lime Treatment without Curing on Modulus Deformation [Neubauer & Thompson, 1972] (Reproduced from the Original Figure). . . . .	42
3.9	Typical Stress-Strain Curves for Immediate Effects of Lime Treatment (a) Vicksburg Buckshot Clay (b) Ava B. [McDonald, 1969] (Reproduced from the Original Figure). . . . .	43
3.10	Generalized Stress-Strain Relationship for Cured Soil-Lime Mixtures [Thompson, 1966] (Reproduced from the Original Figure). . . . .	43
3.11	ILLI-PAVE Comparisons between FDP-LSS and FDP with No Lime. . . .	46
3.12	ILLI-PAVE Comparisons between CFP-LSS and CFP with No Lime. . . .	48

3.13	Randomly Selected Inputs Shown in an MS Excel File for ILLI-PAVE Analyses. . . . .	50
3.14	ILLI-PAVE Input Data Generator. . . . .	50
3.15	ILLI-PAVE Auto Analysis Engine. . . . .	51
3.16	Sample MS Excel Database Used to Train ANN Models. . . . .	51
3.17	Comparisons of ANN Structural Model Predictions with ILLI-PAVE Results for Full-depth Asphalt Pavement Surface Deflections (in mils). . . .	58
3.18	Comparisons of ANN Structural Model Predictions with ILLI-PAVE Results for Full-depth Asphalt Pavement Critical Pavement Responses (Strains in micro-strain and Stress in psi). . . . .	59
3.19	Comparisons of ANN Structural Model Predictions with ILLI-PAVE Results for Conventional Flexible Pavement Surface Deflections (in mils). .	60
3.20	Comparisons of ANN Structural Model Predictions with ILLI-PAVE Results for Conventional Flexible Pavement Critical Pavement Responses (Strains in micro-strain and Stress in psi). . . . .	61
3.21	Comparisons of ANN Structural Model Predictions with ILLI-PAVE Results for Surface Deflections (in mils) of Full-depth Asphalt Pavements Built on Lime Stabilized Soils. . . . .	63
3.22	Comparisons of ANN Structural Model Predictions with ILLI-PAVE Critical Pavement Responses of Full-depth Asphalt Pavements Built on Lime Stabilized Soils (Strains in micro-strain and Stress in psi). . . . .	64
3.23	Comparisons of ANN Structural Model Predictions with ILLI-PAVE Results for Surface Deflections (in mils) of Conventional Flexible Pavements Built on Lime Stabilized Soils. . . . .	65
3.24	Comparisons of ANN Structural Model Predictions with ILLI-PAVE Critical Pavement Responses of Conventional Flexible Pavements Built on Lime Stabilized Soils (Strains in micro-strain and Stress in psi). . . . .	66
3.25	Performances of ANN Backcalculation Models for Predicting Layer Moduli (in psi) of Full-depth Asphalt Pavements. . . . .	70
3.26	Performances of ANN Backcalculation Models for Predicting Critical Pavement Responses of Full-depth Asphalt Pavements (Strains in micro-strain and Stress in psi). . . . .	71
3.27	Performances of ANN Backcalculation Models for Predicting Layer Moduli (in psi) of Conventional Flexible Pavements. . . . .	72
3.28	Performances of ANN Backcalculation Models for Predicting Critical Pavement Responses of Conventional Flexible Pavements (Strains in micro-strain and Stress in psi). . . . .	73
3.29	Performances of ANN Backcalculation Models for Predicting Layer Moduli (in psi) of Full-depth Asphalt Pavements Built on Lime Stabilized Soils. . . . .	75
3.30	Performances of ANN Backcalculation Models for Predicting Critical Pavement Responses of Full-depth Asphalt Pavements Built on Lime Stabilized Soils (Strains in micro-strain and Stress in psi). . . . .	76

3.31	Performances of ANN Backcalculation Models For Predicting Layer Moduli (in psi) of Conventional Flexible Pavements Built on Lime Stabilized Soils. . . . .	77
3.32	Performances of ANN Backcalculation Models for Predicting Critical Pavement Responses of Conventional Flexible Pavements Built on Lime Stabilized Soils (Strains in micro-strain and Stress in psi). . . . .	78
3.33	Performances of FDP ANN Models for US 50. . . . .	83
3.34	Performances of FDP ANN Models for US 20. . . . .	84
3.35	Performances of FDP-LSS ANN Models for Roseville Bypass. . . . .	85
3.36	Performances of FDP-LSS ANN Models for Staley Road. . . . .	86
3.37	Performances of FDP-LSS ANN Models for High Cross Road. . . . .	87
3.38	Performances of CFP ANN Models for Sand Pit Road. . . . .	89
4.1	Effect of Population Size on the Performance of SOFTSYS for a Random IP-SYNTH Station. . . . .	100
4.2	Effect of Number of Generations on the Performance of SOFTSYS for a Random IP-SYNTH Station. . . . .	101
4.3	Effect of Crossover Rate, $p_c$ , on the Performance of SOFTSYS for a Random IP-SYNTH Station. . . . .	102
4.4	Effect of Mutation Rate, $p_m$ , on the Performance of SOFTSYS for a Random IP-SYNTH Station. . . . .	102
4.5	Performances of SOFTSYS Backcalculation Models for Predicting Layer Moduli (in psi) of Full-depth Asphalt Pavements Using $D_0, D_{12}, D_{24}$ and $D_{36}$ as Inputs. . . . .	105
4.6	Progress Curves of SOFTSYS Model FDP-PM1-FWD4 for Random IP-SYNTH Stations. . . . .	106
4.7	Performances of SOFTSYS Backcalculation Models for Predicting Layer Moduli (in psi) of Full-depth Asphalt Pavements Using Seven Deflections. . . . .	106
4.8	Performances of SOFTSYS Backcalculation Models for Predicting Layer Moduli (in psi) of Full-depth Asphalt Pavements Built on Lime Stabilized Soils Using Four Deflections. . . . .	108
4.9	Performances of SOFTSYS Backcalculation Models for Predicting Layer Moduli (in psi) of Full-depth Asphalt Pavements Built on Lime Stabilized Soils Using Seven Deflections. . . . .	109
4.10	Performances of SOFTSYS Backcalculation Models for Predicting Layer Moduli (in psi) of Conventional Flexible Pavements Using Four Deflections. . . . .	111
4.11	Performances of SOFTSYS Backcalculation Models for Predicting Layer Moduli (in psi) of Conventional Flexible Pavements Using Seven Deflections. . . . .	112
4.12	Performances of FDP-PM1-FWD4 SOFTSYS Model for US 50. . . . .	114
4.13	Performances of FDP-PM1-FWD4 SOFTSYS Model for US 20. . . . .	116
4.14	Performances of FDP-LSS-PM1-FWD4 SOFTSYS Model for Roseville Bypass. . . . .	118
4.15	Performances of FDP-LSS-PM1-FWD4 SOFTSYS Model for Staley Road. . . . .	120

4.16	Performances of FDP-LSS-PM1-FWD4 SOFTSYS Model for High Cross Road. . . . .	122
4.17	Performances of CFP-PM1-FWD4 SOFTSYS Model for Sand Pit Road. . .	123
5.1	Typical Pavement System Geometry and Properties to be Determined. . .	127
5.2	Performance Results of SOFTSYS Backcalculation Model FDP-PM2-FWD4 for Predicting AC Layer Thickness (in inches) and Layer Moduli (in psi) of Full-depth Asphalt Pavements Using Four Deflections. . . . .	136
5.3	Performance Results of SOFTSYS Backcalculation Model FDP-PM2-FWD7 for Predicting AC Layer Thickness (in inches) and Layer Moduli (in psi) of Full-depth Asphalt Pavements Using Seven Deflections. . . . .	137
5.4	Performance Results of SOFTSYS Backcalculation Model FDP-LSS-PM2-FWD4 for Predicting Layer Thicknesses (in inches) and Layer Moduli (in psi) of Full-depth Asphalt Pavements Built on Lime Stabilized Soils Using Four Deflections. . . . .	139
5.5	Performance Results of SOFTSYS Backcalculation Model FDP-LSS-PM2-FWD7 for Predicting Layer Thicknesses (in inches) and Layer Moduli (in psi) of Full-depth Asphalt Pavements Built on Lime Stabilized Soils Using Seven Deflections. . . . .	140
5.6	Performance Results of SOFTSYS Backcalculation Model FDP-LSS-PM3-FWD4 for Predicting AC Layer Thickness (in inches) and Layer Moduli (in psi) of Full-depth Asphalt Pavements Built on Lime Stabilized Soils Using Four Deflections. . . . .	141
5.7	Performance Results of SOFTSYS Backcalculation Model FDP-LSS-PM3-FWD7 for Predicting AC Layer Thickness (in inches) and Layer Moduli (in psi) of Full-depth Asphalt Pavements Built on Lime Stabilized Soils Using Seven Deflections. . . . .	142
5.8	Performance Results of SOFTSYS Backcalculation Model CFP-PM2-FWD4 for Predicting Layer Thicknesses (in inches) and Layer Moduli (in psi) of Conventional Flexible Pavements Using Four Deflections. . . . .	143
5.9	Performance Results of SOFTSYS Backcalculation Model CFP-PM2-FWD7 for Predicting Layer Thicknesses (in inches) and Layer Moduli (in psi) of Conventional Flexible Pavements Using Seven Deflections. . . . .	144
5.10	Performance Results of SOFTSYS Backcalculation Model CFP-PM3-FWD4 for Predicting AC Layer Thickness (in inches) and Layer Moduli (in psi) of Conventional Flexible Pavements Using Four Deflections. . . . .	145

5.11	Performance Results of SOFTSYS Backcalculation Model CFP-PM3-FWD7 for Predicting AC Layer Thickness (in inches) and Layer Moduli (in psi) of Conventional Flexible Pavements Using Seven Deflections. . . . .	146
5.12	Performance Results of SOFTSYS Model FDP-PM2-FWD4 for US 50. . .	150
5.13	Performance Results of SOFTSYS Model FDP-PM2-FWD4 for US 20. . .	153
5.14	Performance Results of SOFTSYS FDP-LSS-PM3-FWD4 Models for Roseville Bypass. . . . .	155
5.15	Location of Staley Road and Test Sections. . . . .	158
5.16	Locations of FWD Tests Along the Staley Road Sections. . . . .	159
5.17	GPR Test Results: North Bound - Right Wheel Path. . . . .	160
5.18	GPR Test Results: South Bound - Right Wheel Path. . . . .	161
5.19	Estimation of AC layer thicknesses using SOFTSYS FDP-LSS-PM3-FWD4 model on Staley Road in Illinois. . . . .	163
5.20	Estimation of Pavement Layer Properties Using SOFTSYS FDP-LSS-PM3-FWD4 Model on Staley Road in Illinois (cont.). . . . .	164
5.21	Estimation of Pavement Layer Properties Using SOFTSYS FDP-LSS-PM3-FWD4 Model on Staley Road in Illinois (cont.). . . . .	165
5.22	Performance Results of SOFTSYS FDP-LSS-PM3-FWD4 Models for High Cross Road. . . . .	166
5.23	Performance Results of SOFTSYS CFP-PM2-FWD4 Model for Sand Pit Road. . . . .	168

# List of Abbreviations

AAE	Average Absolute Error
AASHTO	American Association of State Highway and Transportation Officials
AC	Asphalt Concrete
ANN	Artificial Neural Network
ANN-Pro	Artificial Neural Network for Professionals Software
CFP	Conventional Flexible Pavement
CFP-LSS	Conventional Flexible Pavement on Lime Stabilized Soils
DOT	Department of Transportation
EC	Evolutionary Computation
FDP	Full-depth Asphalt Flexible Pavement
FDP-LSS	Full-depth Asphalt Flexible Pavement on Lime Stabilized Soils
FE	Finite Element
FS	Fuzzy System
FEM	Finite Element Method
FWD	Falling Weight Deflectometer
GA	Genetic Algorithm
GB	Granular Base
GPR	Ground Penetrating Radar
HMA	Hot-mix Asphalt
IDOT	Illinois Department of Transportation



IHR	Illinois Highway Research
ILLI-PAVE	Two Dimensional Finite Element Software Developed for Pavement Analysis and Design
LSS	Lime Stabilized (or Modified) Subgrade
MEPDG	Mechanistic-Empirical Pavement Design Guide
MS	Microsoft Corporation
MSE	Mean Squared Error
NCHRP	National Cooperative Highway Research Program
NDT	Nondestructive Testing
SG	Fine-grained Subgrade
SGA	Simple Genetic Algorithm
SHA	State Highway Agency
SHRP	Strategic Highway Research Program
SOFTSYS	Soft Computing Based Pavement and Geomaterial System Analyzer
TRB	Transportation Research Board

# List of Symbols

$\alpha$	Momentum term used in backpropagation neural network
$Bias_i$	Bias term of node $i$
$d$	Number of falling weight deflectometer sensors
$\delta$	Delta term of the generalized delta rule
$D_i$	Surface deflection value obtained at a distance $i$ from the center of FWD loading
$\varepsilon_{SG}$	Vertical strain at the top of subgrade layer
$\varepsilon_{AC}$	Horizontal strain at the top of asphalt layer
$\eta$	Learning rate used in backpropagation neural network
$E$	Squared error term in backpropagation neural network
$E_{AC}$	Elastic modulus of asphalt layer
$E_{LSS}$	Elastic modulus of lime stabilized soil layer
$E_{Ri}$	Breakpoint resilient modulus of subgrade layer
$K$	$K - \theta$ model parameter obtained from multiple regression analyses of repeated load triaxial test data
$K_i$	$i^{th}$ slope in the bilinear model
$M_R$	Resilient modulus
$n$	$K - \theta$ model parameter obtained from multiple regression analyses of repeated load triaxial test data
$N$	Number of input signals from previous nodes in a neural network
$\nu_{AC}$	Poisson's ratio of asphalt layer
$\nu_{LSS}$	Poisson's ratio of lime stabilized soil layer

$O_i$	Outputs of backpropagation neural network
$p_c$	Crossover probability
$p_m$	Mutation probability
$p_s$	Swapping probability
$Q_u$	The unconfined compressive strength
$\sigma_{DEV}$	Deviator stress at the top of subgrade layer
$\sigma_{di}$	Breakpoint deviator stress
$\sigma_{dll}$	The lower limit deviator stress in the bilinear model
$\sigma_{dul}$	The upper limit deviator stress in the bilinear model
$\sigma_v$	Vertical stress at the top of subgrade layer
$t$	Each iteration of backpropagation neural network
$t_{AC}$	Thickness of asphalt concrete layer
$t_{LSS}$	Thickness of lime stabilized subgrade layer
$\varpi$	Constant to emphasize the difference between the calculated and measured deflections
$W_{ij}$	Connection weight between neurons $i$ and $j$
$X_j$	Value of signal coming from previous node $j$
$y_i$	Activation threshold
$Z_i$	Net input signal

# Chapter 1

## Introduction

### 1.1 Problem Statement and Overview

State Highway Agencies (SHAs) determine the strategies for annual pavement maintenance and rehabilitation activities mostly based on the pavements' structural conditions. Accurately determining the remaining life of in-service pavements require precise information about pavement geometry and layer material properties. Generally nondestructive testing (NDT) technologies can provide such information. Falling Weight Deflectometer (FWD) test is one of the most common NDT methods, which produces deflections on the surface of a pavement as a result of load application. Pavement deflection basins obtained from FWD test are used to backcalculate the layer properties. Due to the recent American Association of State Highway and Transportation Officials (AASHTO) move towards adopting mechanistic-based pavement analysis, backcalculation using FWD data demands the use of advanced multi-layered finite element (FE) solutions for accurate analyses of pavement structural conditions. For example, Illinois Department of Transportation (IDOT) uses backcalculation algorithms developed based on statistical interpretations of the ILLI-PAVE, two dimensional finite element software developed for pavement analysis and design, solutions for evaluating the pavements' structural conditions [Thompson, 1989]. Recently, use of Artificial Neural Network (ANN) models trained with ILLI-PAVE FE solutions made considerable improvements over the these algorithms currently used by IDOT [Ceylan *et al.*, 2004, 2005; Pekcan *et al.*, 2006].

ANNs, as a sub-class of soft computing techniques, have been widely used in the last two decades. They have been successfully applied for tasks requiring intelligence such as deduction, reasoning, planning and learning. ANNs can solve broad range of problems involving but not limited to classification, regression and optimization. Their capabilities in exploring huge data sets and for organizing complex information make ANNs viable alternatives compared to more-traditional methods that use numerical and statistical approaches. Because of their performance, ANNs' use is found in all areas of pavement engineering: materials characterization/modeling, pavement distress classification, pavement structural modeling, pavement performance prediction, and, finally, pavement rehabilitation in the forms of nondestructive evaluation and remaining life estimation [Transportation Research Board, 1999]. Several successful studies using ANNs to predict the pavement layer moduli used FWD deflection data [Goktepe *et al.*, 2006; Gucunski & Krstic, 1996; Gucunski *et al.*, 1998; Ioannides *et al.*, 1996; Khazanovich & Roesler, 1997; Kim & Kim, 1998; Lacroix, 2008; Lee *et al.*, 1998; Meier *et al.*, 1997; Meier & Rix, 1993, 1994, 1995; Saltan & Terzi, 2004, 2008; Sharma & Das, 2008; Williams & Gucunski, 1995].

Numerous transportation organizations have also acknowledged the importance of ANNs; the Federal Highway Administration, National Cooperative Highway Research Program (NCHRP) 1-37A, Mechanistic-Empirical Pavement Design Guide (MEPDG) research team have recognized ANNs as progressive and very powerful computing techniques and took advantage of ANN models in preparing the MEPDG concrete pavement analysis package [ARA Incorporated & Program, 2004]. In addition, a recent Transportation Research Board (TRB) subcommittee was focused on "Applications of Nontraditional Computing Tools Including Neural Networks" for providing guidance to practitioners to have a better understanding about ANNs and to further clarify the so-called black box concept and at the same time encourage the use of ANNs and other computational intelligence techniques in pavement engineering applications related to

transportation facilities. The power of ANNs in pattern recognition and their superiority for correlating nonlinear relationships between the inputs and outputs of a problem make them an excellent tool for the structural evaluation of pavements using both static and dynamic deflection basins. Among the various State DOTs and government agencies that have already used ANNs in nondestructive evaluation of pavements are:

1. The Kansas DOT used ANN-based distress models to predict longitudinal joint spalling for concrete pavements [Basheer & Najjar, 1996].
2. The Waterways Experiment Station employed ANNs as surrogates for WESLEA in a computer program for backcalculating pavement layer moduli and drastically cutting the processing time [Meier *et al.*, 1997].
3. The Texas DOT developed a methodology based on ANNs to compute the remaining life of flexible pavements and compare results with field data from the Texas Mobile Load Simulator [Abdallah *et al.*, 2000].
4. The Iowa DOT used ANN-based backcalculation models for flexible, rigid, and composite pavements and developed a computer program for the use of Iowa DOT [Ceylan *et al.*, 2007].
5. The Texas DOT also conducted a research study to evaluate the structural integrity of pavements and to predict their performances through ANN models developed using FWD data [Abdallah & Nazarian, 2009].

In recent successful applications at the University of Illinois, the use of ANNs was introduced for backcalculating the pavement layer moduli and predicting the critical pavement responses directly from the FWD deflection basins [Ceylan *et al.*, 2004]. The ILLI-PAVE 2005 FE program [Elliott & Thompson, 1985; Gomez-Ramirez & Thompson, 2001; Thompson, 1987, 1992, 1994], extensively tested and validated for over three decades, has been used as the primary analysis tool for the solution of full-depth and conventional flexible pavement responses under the standard 9,000 lb. FWD loading. ANN

models trained with the results of the ILLI-PAVE FE solutions have been found to be viable alternatives to backcalculate the pavement layer moduli and predict the critical pavement responses based on the FWD deflection data. The trained ANN models are capable of backcalculating the pavement layer moduli and predicting the critical pavement responses successfully. These predictions are generally much better than those of traditionally used ILLI-PAVE algorithms. These predictions also provide an advantage when used in mechanistic-based pavement design procedures.

When properly trained ANN models are used as surrogate advanced ILLI-PAVE structural models to backcalculate pavement layer properties; the speed of these ANN models provides an advantage over traditional backcalculation schemes. With the addition of powerful and robust searching algorithms, such as Genetic Algorithms (GAs), pavement layer thicknesses can also be estimated from just the FWD deflection basins. Thickness variability is a real issue in the field, and coring is not always an option to determine layer thickness. It is also one of the key inputs to pavement management systems. With these ideas in mind, the SOFTSYS approach has been developed in this thesis to the extent that its full potential is demonstrated on the basis of its promise for nondestructive pavement analysis.

## **1.2 Research Objectives**

The first objective in this thesis is to develop ANN models based on the ILLI-PAVE FE solutions as a pavement evaluation toolbox for

1. rapidly and more accurately backcalculating in-service pavement layer properties;
2. predicting critical stress and strain responses of in-service pavements in real time from the measured FWD deflection data; and
3. incorporating these predicted critical pavement responses, such as tensile strain for asphalt fatigue, directly into mechanistic pavement analysis and design procedures.

The second objective is to develop the framework SOFTSYS, Soft Computing Based Pavement and Geomaterial System Analyzer, with the purpose of

1. reliably determining pavement thickness for Full-depth Asphalt Pavements (FDPs) as well as the pavement layer properties using FWD deflection basin data without any coring requirements in the field;
2. extending the possibility of using SOFTSYS for multi-layered systems such as Full-depth Asphalt Pavements on Lime Stabilized Soils (FDP-LSSs) and Conventional Flexible Pavements (CFPs) having unbound aggregate base courses in order to cover wider ranges of pavements; and
3. validating the results of SOFTSYS with the field data obtained using Ground Penetrating Radar (GPR) as well as the core thickness data obtained from the road sections.

The overall intent of this thesis is to solve pavement layer backcalculation problems fast and accurately. Since the solution is computationally hard because of ill-posedness, several strategies are developed to relax the mathematical difficulties. Using these, both inverse and forward computational approaches are investigated to obtain layer properties of various types of flexible pavements including layer thicknesses. The outcome of this work is expected to facilitate proper pavement condition assessments and rehabilitation strategies.

## **1.3 Research Methodology**

The research has accomplished the following tasks as a means to achieving the study goals:

1. Identify the types and properties of different flexible pavement layers existing in Illinois.
2. Conduct ILLI-PAVE FE runs on the commonly found constructed flexible pavement sections considering stress-dependent pavement layer behavior. A database of FE



runs has been developed covering the different pavement layer thicknesses, layer moduli, and deformation characteristics of the pavement layers.

3. Develop forward and backcalculation type ANN models based on the ILLI-PAVE FE solutions for the evaluation of flexible pavement systems. Different ANN architectures have been searched and trained to determine the optimum network architecture (or model) that best captures the behavior of various pavement sections in Illinois. Some of the network architectures are designed for directly predicting the critical pavement responses (maximum stresses and strains) from the FWD deflection basins. These networks can directly be used to implement the mechanistic-based pavement design concepts.
4. Use both existing FWD data, available and gathered from previous studies, and new field FWD data, collected in recent years by engineers running FWD tests, to validate the ANN models.
5. Prepare an ANN based forward and backcalculation structural analysis toolbox as user-friendly software, and demonstrate the use of this toolbox with real world examples and applications.
6. Develop the framework SOFTSYS for evaluating in-service flexible pavements with the purpose of determining pavement layer thicknesses as well as the layer properties from FWD data without the need for pavement coring.
7. Compare and verify SOFTSYS results with those of the nonlinear ILLI-PAVE based FE solutions.
8. Develop models for SOFTSYS full-depth and conventional asphalt pavement layer properties and thicknesses and calibrate these models linking to the actual field FWD data available. The results are verified with the actual field data. The variability in the thickness as well as other pavement properties is a critical issue. GPR is selected as a reliable alternative of determining thicknesses of pavement sections. As-constructed thickness information is also required to determine the HMA thickness of the

pavements. Therefore, along with the FWD testing, GPR testing was also performed on selected Full-depth Asphalt Pavement sections.

## **1.4 Thesis Organization**

Chapter 2 of this thesis introduces FWD testing as the most popular NDT and evaluation approach for pavement and gives a complete literature review of backcalculation methods, including the background information on the advanced methods used in this study, i.e., ANNs and GAs. The development of ANN based structural models is described in Chapter 3 for full-depth asphalt and conventional type pavements found/constructed in Illinois on both natural and lime stabilized subgrade soils. The developed ANN models are also validated with field FWD data in Chapter 3. Chapter 4 introduces a new SOFTSYS approach based on the combined use of ANNs and GAs for pavement layer modulus determinations applied mainly to full-depth asphalt pavements and conventional flexible pavements. Chapter 5 focuses on the determination of both modulus and thickness properties of full-depth asphalt and multi-layered pavements using the SOFTSYS approach. Field validations are also provided in this chapter. Finally, a summary, major findings, conclusions and recommended future research are given in Chapter 6.

# **Chapter 2**

## **Literature Review**

### **2.1 Backcalculation Problem**

In transportation geotechnics, determining pavement layer properties using surface deflections is commonly referred to as backcalculation. The backcalculation of layer properties including pavement layer moduli and even layer thicknesses from surface deflection measurements plays a major role in the structural evaluation of pavements, design of overlays and management of in-service pavements. Two approaches are mainly used to determine the existing condition of a pavement: destructive or nondestructive. In the last three decades, improvements in technology have caused NDT methods to be used more widely since there is neither disturbance to the integrity of the material nor the necessity of sampling it. Moreover, NDTs are quite easy to use: they are repeatable, and can be performed much faster than destructive tests. These advantages result in a reduced overall cost in the long run when compared to destructive testing methods. Against all the advantages, however, the reliability of NDT methods certainly depends on accurate interpretations of test results and the precise determination of the pavement layer material properties, such as pavement layer modulus and layer thickness. FWD testing is the most popular NDT method for evaluating pavements. It provides pavement surface deflections, as recorded by several offset sensors, in response to a constant load dropped from a specific distance at a certain frequency. These deflections are used for the structural evaluation of pavements.

## 2.2 Falling Weight Deflectometer

FWDs are NDT devices which exert an impulsive load on the pavement and record the resulting deflections on the pavement surfaces at several distances from the load. As the name implies, an FWD imparts its test load by means of a specified weight (usually between 110 and 660 lb.) falling a given distance (up to 16 in.) and striking a buffered plate resting on the pavement surface (see Figure 2.1). It can produce a peak dynamic force typically between 1,500 and 24,000 lb. in 25 – 30 milliseconds (see Figure 2.2). The load is transmitted from the rubber buffers to the pavement through a 5.91 in. radius steel plate underlain by a rubber pad, which helps applying the load uniformly on the pavement surface. The FWD impulse load duration of 25 to 30 milliseconds approximates the same load duration of a vehicle traveling at 40 to 50 mph [Ullidtz & Stubstad, 1985].



**Figure 2.1:** Dynatest Falling Weight Deflectometer Device.

Deflections with FWD equipment are typically measured at the center of the load and up to six other locations. A typical test configuration is shown in Figure 2.3. One advantage

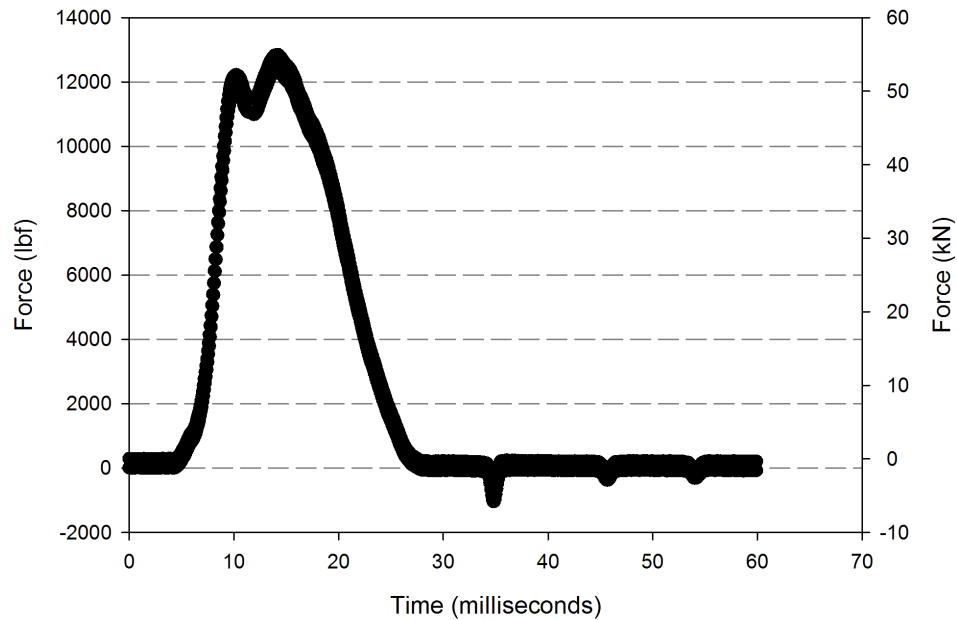


**Figure 2.2:** Haversine Loading Applied by FWD.

of FWD is that it replicates the load histories and deflections produced by moving vehicles better than any other testing equipment. This deflection profile or basin is primarily affected by the properties of individual pavement layers as well as the magnitude and frequency of the loading [Shahin, 2005]. In comparing elastic properties calculated from an earlier Dynaflect test with results from the FWD, it was found that dynamic effects were less important in the FWD results due to the higher frequencies of loading [Roesset & Shao, 1985]. Hoffman and Thompson [1981] compared the FWD with the Road Rater Model 400B and the Benkelman Beam NDT equipment. They concluded that the FWD produced a deflection which best represented conditions under a moving wheel load. Since FWD is the device that best duplicate the deflections of a moving truck [Ullidtz & Stubstad, 1985], it has been widely accepted throughout the world. Among the many FWDs described in the literature, the following are the three most commonly used and commercially available:

1. Dynatest Model 8000 (Dynatest Consulting, Inc.);
2. KUAB FWD Models 50 and 150 (KUAB America); and

### 3. JILS FWD (Foundation Mechanics, Inc.).

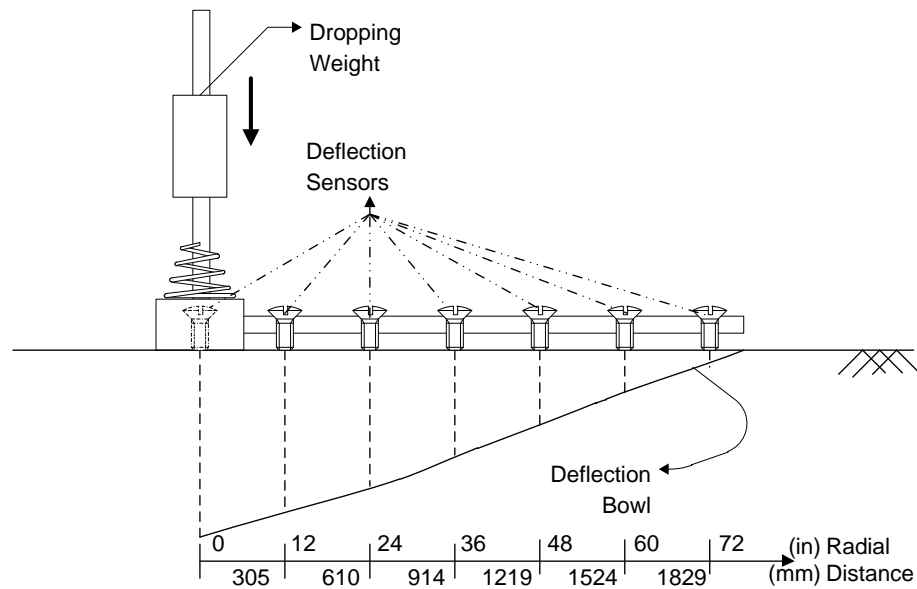


**Figure 2.3:** Locations of FWD Sensors and Schematic Drawing.

FWD test deflection basins can be successfully interpreted to identify the existing condition of a pavement under traffic loading. For example, at a specified temperature, small deflections may indicate a strong pavement structure, while larger ones might indicate a weaker section. Diagnosing the current conditions of pavements, however, requires accurate determination of mechanical properties through evaluation of FWD data.

## 2.3 Backcalculation Methods

The concept of backcalculation for pavements became popular in the last three decades along with the wide use of mechanistic-empirical methods in the design of pavements and developments in pavement management systems. Backcalculation approaches for obtaining pavement moduli using NDT data can be grouped into three methods [Anderson, 1988]:

- Simplified methods
- Gradient relaxation methods
- Direct interpolation methods

Many of the above methods were proposed using several simplifications, such as assuming a constant thickness of pavement layers throughout the testing or uniform pavement layer properties along the depth. Neither simplified methods [Ullidtz, 1973; Van der Loo, 1982] nor direct interpolation methods [Uzan *et al.*, 1988] received a lot of attention by the research community for several reasons. Still, there are other studies using backcalculation by various researchers to solve the pavement layer backcalculation problem [Anderson, 1989; Uzan *et al.*, 1989; Vakili, 2008]. The most common of these are gradient relaxation methods. In this type, a mathematical model of the pavement is usually constructed and subjected to the appropriate NDT load to obtain surface deflections as a function of pavement layer properties. These models can then be run with various layer properties until a satisfactory solution set is found for which the measured deflection basin is produced (see Figure 2.4).

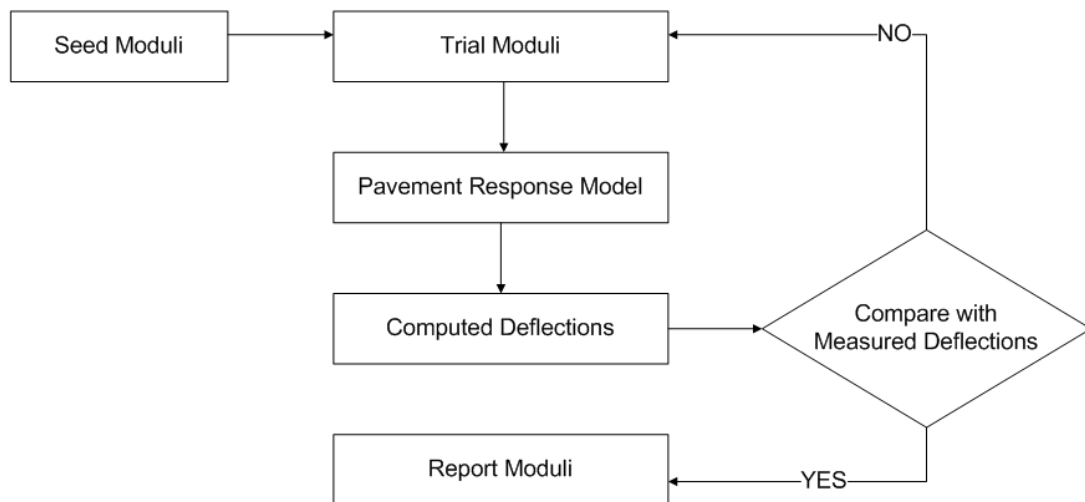


**Figure 2.4:** Traditional Iterative Backcalculation Procedure [Meier, 1995].

Alkasawneh [2007] summarized the main steps of the backcalculation as follows:

- Define the input parameters of the pavement system, including thickness of each layer, Poisson's ratio, etc.
- Assume moduli seed values for the pavement system. Seed moduli values can be assumed based on experience or typical moduli values. Moduli values can differ based on the forward method implemented in the backcalculation program.
- Calculate the pavement deflections, using the forward program, at the FWD geophone locations (along the surface).
- Compare the calculated deflections with the measured deflections. If the difference between the calculated and measured deflections is acceptable, then the assumed layer moduli are the actual moduli. Otherwise, the assumed layer moduli are not the actual moduli and the assumed moduli should be refined.
- Repeat steps if necessary.

In addition, many computational methods were proposed. Linear regression methods, ANNs, GAs, and Fuzzy Systems (FSs) were mainly utilized as backcalculation techniques. A recent study by Goktepe *et al.* [2006] provides an extensive summary of these methods. Particularly, many researchers found soft computing methods to be useful due to their advantages such as non-universality and noise tolerance [Ghaboussi, 2001; Ghaboussi & Wu, 1998]. These methods can properly deal with the difficulties existing in the backcalculation problem. As a sub-class of soft computing methods, the development of ANNs and GAs for pavement backcalculation studies will be reviewed.

## 2.4 Soft Computing Methods

There are generally two categories of inverse problems in engineering. In the first one, the characteristics of an engineering system are known and the inputs (or excitations) to the



system are found by looking at the known outputs. In the second, the characteristics of the engineering system are determined using the known inputs and outputs [Ghaboussi, 2010]. (The most detailed classification of inverse problems is provided in Liu and Han [2003]). The FWD backcalculation problem, which falls into the second category, can be solved efficiently by a collection of techniques called soft computing.

Soft computing methods can analyze engineering problems by mimicking nature's problem solving strategies such as reduction in disorder and learning [Ghaboussi, 2010]. These tools are fundamentally different than classical mathematical methods in the sense that they can solve problems approximately with a tolerable precision and uncertainty [Ghaboussi, 2001, 2010]. The major soft computing tools are ANNs, FSs and Evolutionary Computation (EC) [Zadeh, 1994]. Each sub-branch has many variations that can be adopted to solve specific problems. In this chapter, ANNs and GAs are introduced and their theories are briefly presented.

### **2.4.1 Artificial Neural Networks**

ANNs are computational models for information processing, which can be trained to perform certain tasks. Usually classified as a sub-class of soft computing tools, ANNs' fundamental properties are derived from biological systems [Haykin, 1999; Hertz *et al.*, 1991; Reed & Marks, 1999]. ANNs are attractive because of the following features [Ghaboussi, 2001]:

- They are, to some extent, tolerant of errors in a data set (imprecision tolerance).
- They are valid primarily within the ranges of the training data (non-universality).
- Unlike mathematical functions, various ANNs can represent the same computational model (functional uniqueness) within a given level of error.

For computationally complex problems, ANNs are quite robust and practical. In many civil engineering applications, they serve as innovative tools that can capture nonlinear

relationships between inputs and outputs of natural phenomena in situations where numerical methods such as non-linear regression tools do not succeed because of the complex nature of the problem [Ghaboussi & Wu, 1998]. The most widely used ANN is a multilayered, feed-forward neural network, which is composed of perceptrons. A perceptron is an information processing element which behaves according to characteristics of the input and a predefined set of rules [Rosenblatt, 1958]. Essential to feed-forward neural networks are a feed-forward propagation rule, a network architecture (i.e., the number of hidden layers, artificial neurons, and the structure defining their connectivity), and a learning rule.

The most commonly used learning rule is the error backpropagation algorithm (i.e., the generalized delta rule). Backpropagation neural networks are feed-forward neural networks that utilize the error backpropagation learning rule. Shown in Figure 2.5 is a common backpropagation neural network similar to that used in this dissertation. The multilayered back-propagation ANN has one input layer, one output layer, and a set of constructed processing elements (artificial neurons) called hidden layers. Inserted between the input and output layers are the hidden layers. The network operation is composed of a highly nonlinear functional mapping of the neurons in hidden layers between the input and output variables.

#### **2.4.1.1 Backpropagation Learning Algorithm**

Backpropagation algorithm was proposed by Rumelhart [1986]. It is a generalization of the least mean squared algorithm that minimizes the mean squared error (MSE) between the actual and desired outputs of the network. The network connections are defined using weights, which simply represent the effect of one neuron on another. The minimization of error is achieved through changing these network weights. In a backpropagation neural network, each neuron,  $i$ , receives several input signals  $X_j$  coming from previous nodes or neurons,  $j$ . The signals carry valuable information, and they are processed by taking

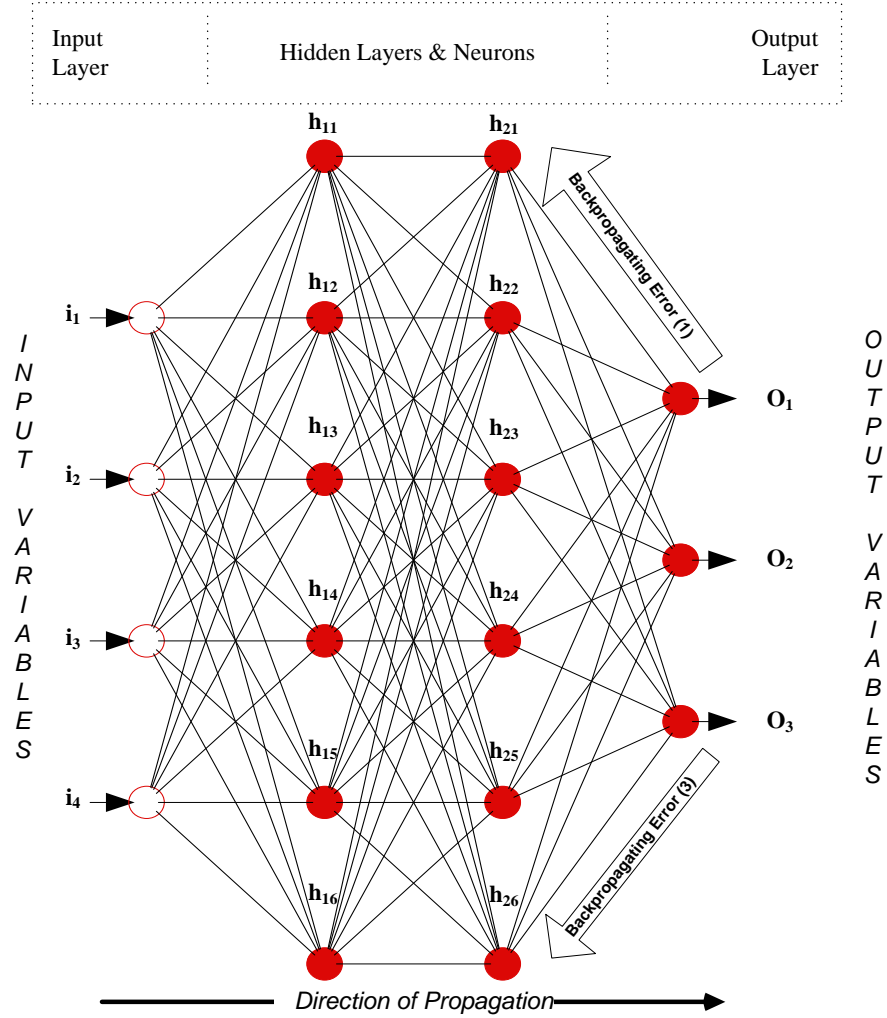


**Figure 2.5:** A Typical Backpropagation Neural Network.

into account their connection weights  $W_{ij}$  (see Figure 2.6). Each neuron has an internal threshold level above which it is activated. The activation is based on the input coming from the other neurons of different layers and a bias term that represents an outer source to the processing element. The input signals are linked to the internal activation level using Equation 2.1:

$$Z_i = \sum_{j=1}^N (W_{ij}X_j) - Bias_i \quad (2.1)$$

where

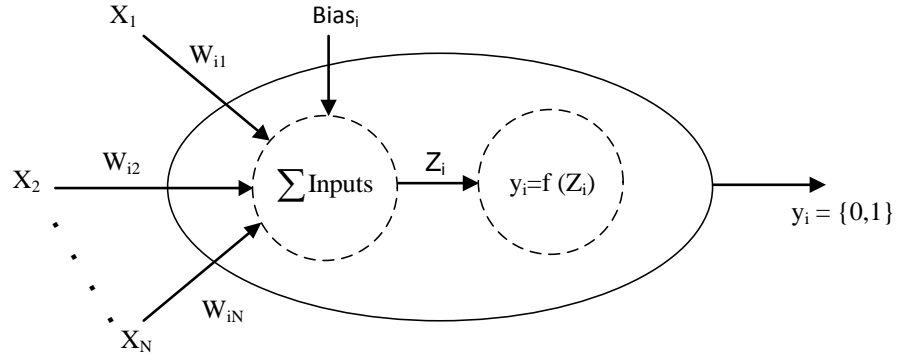


**Figure 2.6:** Schematic Representation of an Information Processing Element in Backpropagation Neural Networks (adopted from [Tutumluer, 1995]).

$Z_i$  = Net input signal;

$W_{ij}$  = Connection weight between neurons  $i$  and  $j$ ;

$X_j$  = Value of signal coming from previous node  $j$ ;

$Bias_i$  = Bias term of node  $i$  (contributes to the activation threshold value);

$N$  = Number of input signals from previous nodes.

The output of the neuron is dependent on the activation threshold,  $y_i$  (Equation 2.2). If the neuron is activated (or fired), then the output signal is dictated by a transfer function  $f(x)$ . The function  $f$  is bounded, monotonically increasing, invertible and everywhere differentiable, such as a tanh or sigmoid function [Mehrotra *et al.*, 1997]. Equations 2.3 and 2.4 are commonly used sigmoid and hyperbolic tangent sigmoid functions, respectively [Harrington, 1993].

$$y_i = f(Z_i) \quad (2.2)$$

$$f(x) = \frac{1}{(1 + e^{-x})} \quad (2.3)$$

$$f(x) = \frac{2}{(1 + e^{-2x})} - 1 \quad (2.4)$$

The activation of a single neuron is calculated for all nodes in the network. The squared error terms  $E^k$  between the outputs  $y_i$  and the desired values  $d_i$  (actual values in the output layer) are calculated using Equation 2.5. The term  $\frac{1}{2}$  is added in order to calculate the derivative more easily at the next stage.

$$E^k = \frac{1}{2} \sum_i [d_i^k - y_i^k]^2 \quad (2.5)$$

where  $i$  shows the individual neurons, and  $k$  represents the individual samples from the training data set. The derivative of the error term,  $E$ , with respect to the connection weight  $W_{ij}$  is minimized using Equation 2.6. It is expected that ANN will produce results that are close to the desired outputs within a given level of tolerance:

$$\Delta W_{ij} = -\eta \frac{\partial E}{\partial W_{ij}} = -\eta \sum_k \left( \frac{\partial E^k}{\partial W_{ij}} \right) \quad (2.6)$$

where  $\eta$  is a learning rate, which is a measure of the step length of each iteration in the negative gradient direction. In general, very small values of  $\eta$  result in slow convergence, which is not desired. On the contrary, choosing large values may cause oscillations around the global minimum and convergence problems. Reaching a local minimum can also be prevented by using an appropriate  $\eta$  in the search. At this stage, the learning problem is narrowed down to calculating the gradient of the error function with respect to its connection weights. The derivative term  $(\frac{\partial E^k}{\partial W_{ij}})$  can be simplified through the chain rule as:

$$-\frac{\partial E^k}{\partial W_{ij}} = -\frac{\partial E^k}{\partial y_i} \frac{\partial y_i}{\partial Z_i} \frac{\partial Z_i}{\partial W_{ij}} = -\delta_i^k \frac{\partial Z_i}{\partial W_{ij}} = -\delta_i^k X_j \quad (2.7)$$

in which the multiplication of the first two terms is defined as the delta term,  $\delta_i^k$ . For hidden layers, this term is expressed by Equation 2.8.

$$\delta_i^k = f'(Z_i^k) \sum_r \delta_r^k W_{ir} \quad (2.8)$$

where  $r$  represents the network nodes in the upstream of the network. This stage can be viewed as the backward propagation of the activations coming from the output layer.

The weight update for each iteration  $t$  is then performed using Equation 2.9:

$$\Delta W_{ij}(t+1) = \eta \sum_k \delta_i^k X_j^k + \alpha \Delta W_{ij}(t) \quad (2.9)$$

where  $\alpha$  is the momentum (or acceleration) term added to eliminate the convergence problems. When  $\alpha$  is introduced, usually  $\eta$  is kept small. The summation is done over all individual data in the training set. Similarly, the bias term  $Bias_i$  is also updated through iterations by Equation 2.10:

$$\Delta Bias_i(t+1) = \eta \sum_k \delta_i^k + \alpha \Delta Bias_i(t) \quad (2.10)$$

The network processes each cycle iteratively for every sample in the training data set. While doing that, the choice of the parameters  $\alpha$  and  $\eta$  is very crucial to achieving a stable solution. Finally, when a sufficiently small MSE is calculated, the iterations are stopped and network weights are finalized.

Currently, there are no precise methods for determining the ideal number of layers and nodes in these layers for a specific problem. However, as the complexity of the learning problem increases an increase in both parameters can customarily be expected. Moreover, a function approximation theorem proposed by Kolmogorov [1957] can be re-interpreted as the use of a 3-layer neural network with appropriate activation functions to approximate

any arbitrary function, although there are several critiques of this work [Giroso & Poggio, 1989; Kúrková, 1991] in the literature.

#### **2.4.1.2 Pavement Layer Backcalculation Using ANNs**

When FWD backcalculation is considered, an ANN model can be trained to map deflection basins back onto their corresponding pavement layer moduli. One way to train such a network would be to use experimentally determined deflection basins along with independently measured pavement layer thicknesses and moduli. However, it is often difficult to obtain representative, undisturbed samples with which to make a laboratory determination of the pavement moduli. Furthermore, because laboratory testing is expensive, there is an insufficient quantity of experimental data covering a broad-enough range of pavement layer moduli and pavement layer thicknesses to successfully train a neural network [Meier, 1995]. Instead, synthetic deflection basins calculated using pavement analysis programs such as ILLI-PAVE can be used to create synthetic deflection basins. Using FEM as the analysis tool allows precise control of the pavement layer properties used to train the network. The basic neural network training procedure developed for this study can be considered as a closed loop (see Figure 2.7). A mathematical model is used to calculate a synthetic deflection basin for a presumed set of pavement layer properties. The ANN is then taught to perform the inverse operation of mapping the synthetic deflection basin back onto the presumed set of properties. At first, the neural network produces a random mapping; however, by repeating the training process many times for many different pavement profiles, the neural network will eventually learn the appropriate inversion function [Meier, 1995].

Trained ANN models need to be tested based on an independent data set within their training ranges. A sufficiently wide data set obtained from the pavement analysis can be chosen independently considering the given ranges of material and geometry properties and used as the testing data set for the verification of proper ANN learning. The remaining data

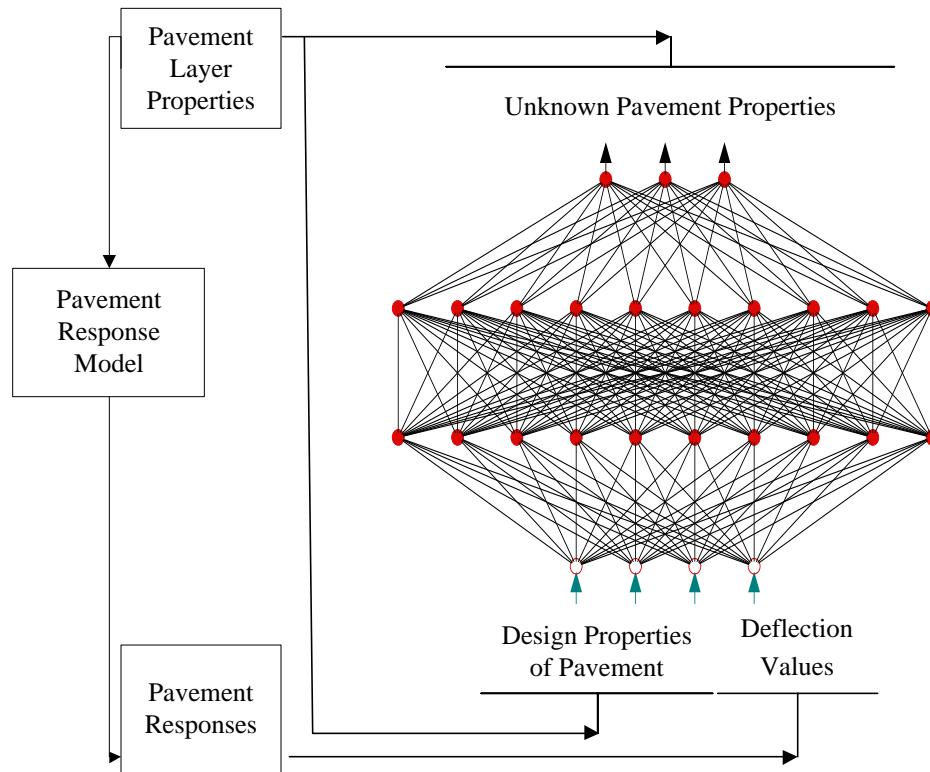


**Figure 2.7:** Direct Pavement Backcalculation Procedure Using a Neural Network.

are then used for the training and learning procedure. Whether the trained ANN models are capable of producing the same database (with the given inputs to obtain outputs or vice versa) can be checked quickly in this manner. Figures 2.8(a) and 2.8(b) show proper and improper learning curves for training and testing data sets. Although ANNs are very powerful tools, sometimes they may not work due to improper learning because of the quality and/or quantity of the data [Tutumluer & Meijer, 1996]. Improper learning causes ANNs to memorize the given training data set and to lose the capability of generalization [Reed & Marks, 1999]. This concept is known as “overfitting”. Although training takes a long computation time, testing is often much faster (on the order of microseconds) with the already set-weighted connections. This feature also facilitates the use of trained ANNs as quick pavement analysis tools by a field engineer without the need for any complex inputs.



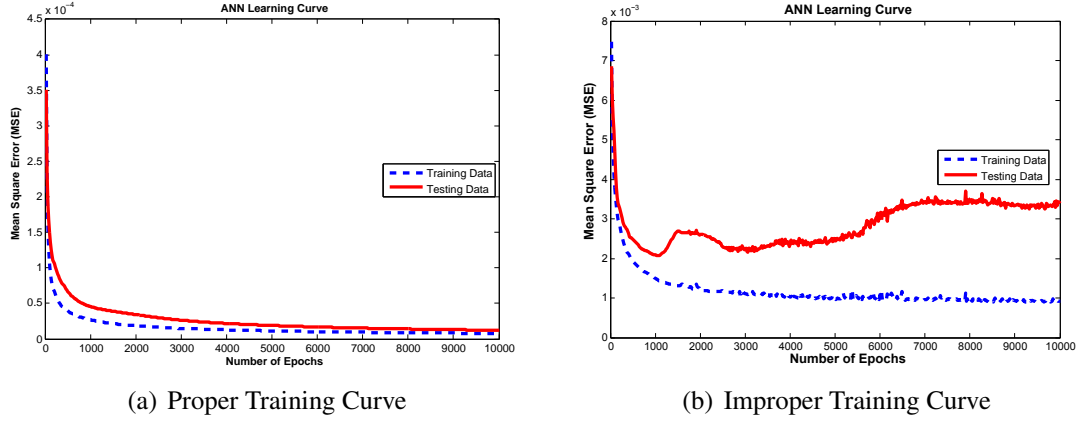


**Figure 2.8:** ANN Training Curves.

## 2.4.2 Genetic Algorithms

Computational information models that operate on the basis of the natural evolutionary process and genetics are known as GAs [Bäck, 1996; Bäck *et al.*, 2000; De Jong, 2006]. Using evolution-based search techniques suggested by the process of natural selection [Darwin, 1859; Mayr, 1987] and with the power of randomness, these algorithms obtain robust solutions for engineering problems. Because they do not require previous knowledge of the problem domain. For the past 30 years they have been very widely used alternatives to classical solution approaches. Numerous successful solutions with GAs have been found for search and optimization problems [Beasley, 2000; Freitas, 2002; Goldberg, 1989].

The application of GAs for problems that require solutions using optimization or engineering design strategies has been well researched [Michalewicz, 1996]. GA based solutions have many advantages compared to those developed based on mathematics and heuristic search [Rasheed & Hirsh, 1997]. Some advantages include:

- GAs are global search methods and are very effective for searching multi-modal and deceptive problem domains where finding reliable solutions is generally harder than conventional techniques.

- They can accomplish fitness (or objective) evaluations and apply genetic operators separately for each candidate making GAs suitable for parallel computation which is an increasingly researched subject in computer science.
- They can handle ill-posed and deceptive objective functions without requiring gradient information which is an essential component of mathematical formulations.
- GAs easily facilitate the incorporation of discrete, continuous, and mixed variables into the problem formulation and the encoding of constraints.

These advantages make GAs suitable tools for solving highly nonlinear, noisy and discontinuous problems [Cox, 2005]. On the contrary, (1) a complete dependence on the fitness function, (2) the sensitivity of solutions to GA parameters and (3) the type of encoding need to be treated carefully when developing GA based solution strategies are the disadvantages.

GAs operate in four conceptually different ways than other methodologies [Goldberg, 1989]: (1) the parameters of GAs are only representations (or encodings), not the parameters themselves; (2) many candidate solutions are created simultaneously as opposed to working on a single one; (3) GAs do not need any additional information such as derivatives and only utilize the objective information; and (4) GAs use probabilistic random rules, not deterministic ones, for appropriately performing random directed search.

GAs derive some of their fundamental properties from biological systems. The terminology used in GAs is therefore similar to that used in biology and genetics. For example, GAs use strings that represent problem variables using a predefined encoding strategy. Each option for encoding characterizes potential solutions to the problem. These strings are referred to as *chromosomes*. These options are taken from a finite set or representation for properly encoding variables and are referred to as *genes*; and the values of the genes are called *alleles*. The encoded parameter in the GA string is called the

*genotype* and the decoded form of genotype is called the *phenotype* [Burke & Kendall, 2005].

In order to apply genetic pressure effectively and to produce better solutions, GAs also use a *fitness function* as a measure of the quality of the obtained solutions. Definition of the objective function is problem dependent. For scientific problems, it is generally based on a computational model. For problems such as those in social sciences, it is a function in which a comparison can be made and better solutions are chosen by humans.

As an evolutionary strategy, GAs use a population of solutions. A *population* is a compilation of candidates, i.e., possible solutions, in one generation. Usually the user specifies the population size, which is an important factor affecting the GAs' performance and scalability. If population sizes are not chosen carefully, premature solutions may be obtained or the GA operation time may be extensive [Burke & Kendall, 2005].

The GA operation follows these steps:

1. *Initialization*: The possible solutions are usually created randomly. Domain knowledge or other information such as constraints are included when generating the candidates.
2. *Evaluation*: The fitness function and the termination criteria both indicate maturity of the solutions. Using the fitness function, the initial candidate solutions are evaluated. Then these solutions are tested against termination criteria. If the criteria for termination are satisfied, then the solution with the highest fitness among the population members is chosen as the solution to the problem. Otherwise, evolution is continued through the first generation, with the chromosomes in the initial candidates being the parental ones of the next generation.
3. *Selection*: Selection is a mechanism that provides more chance to survive for solution candidates with higher fitness values. It is the driving force of the survival-of-the-fittest mechanism on the candidate solutions. Better members are chosen and their genomic structure is preserved through generations.

4. *Recombination*: This step involves the generation of new candidate solutions (i.e., offspring) in the next generation from the two or more parental solutions. The expectation from this combination is to obtain better candidates such that the parental traits will be inherited.
5. *Mutation*: Mutation is the operator through which a single candidate solution is modified randomly to create population diversity. Mutation can be applied to each gene with a relatively small probability. As in recombination or selection operators, there are also many mutation techniques.
6. *Replacement*: The offspring of the parental population are inserted into the new generation using replacement. Many options are available for applying replacement such as steady state replacement, and elitist replacement, etc.
7. Steps 2 to 6 are repeated until sufficiently good quality solutions are obtained, i.e., the termination criteria are satisfied.

Each of the above operators has been studied in the literature. As a result, the individual techniques have been improved for specific types of problems. However, the progress in the development of GA theory was very slow compared to that of its operators. The schema theorem and the principle of minimal building blocks as defined by Holland [1975] and Goldberg [1989] are still actively used; they almost became the standards in explaining the behavior of GAs. Both theories mention the selection of a representation of fixed length that encodes the parameters of the problem in binary form. This representation is widely used in many applications [Bäck *et al.*, 1997; Ghaboussi, 2001].

#### **2.4.2.1 Genetic Algorithm Operators**

Genetic Algorithm operations are carried out through many operators each of which has a special task in mimicking the evolutionary process. The details of these tasks are explained below.

**Selection:** There are two main selection mechanisms defined for GAs [Baker, 1985; Burke & Kendall, 2005; Goldberg & Kalyanmoy, 1991]:

- *Fitness Proportional Selection Methods:* In this category are roulette-wheel selection [Goldberg, 1989; Holland, 1975] and stochastic universal selection [Baker, 1985]. Roulette-wheel selection is a widely used mechanism utilized in GAs. A fitness value is assigned to each individual given the fitness function, and the solution candidates of the population are selected according to these values. Each individual in the population will have a probability of selection  $p(x)$  based on its fitness value  $f(x)$  divided by the sum of the fitness values of the population. This simply suggests that an individual with higher fitness will have an increased chance of being selected for recombination; those individuals with low fitness may be eliminated completely when creating the next generation.
- *Ordinal Selection Methods:* Ordinal methods operate differently than those based on fitness proportions. They are more effective as there is no need to work with fitness. These methods mainly include tournament selection [Goldberg, 1989] and truncation selection [Muhlenbein & Schlierkamp-Voosen, 1993]. In tournament selection, certain numbers of individuals compete against each other. Then the parents are either eliminated from the original pool (called tournament selection without replacement), or not (called tournament selection without selection). The best individual in the selected group of chromosomes wins the tournament and is selected as the parent. This scheme is repeated as often as individuals must be selected. The general principle is that if the tournament size is larger, weak individuals have a smaller chance to be selected. In truncation selection the candidate solutions are ranked by their fitness, and the top  $(1/k)^{th}$  of the individuals get  $k$  copies each in the reproduction pool. After the chromosome is selected for reproduction, it enters into the parental pool for creating next generations.

**Recombination - Crossover:** The selected individuals are inserted into the mating pool to continue applying the genetic operators of evolution. The crossover operation is the first operator after the selection. It is performed on selected individuals to create the new members of the next generation. As for selection methods, many crossover operators are available in the literature [Beasley *et al.*, 1993; Booker *et al.*, 1997; Goldberg, 1989; Lima *et al.*, 2005; Sastry & Goldberg, 2004]. Although properly designing a crossover operator may require problem-specific knowledge, in this section problem independent crossover operators are described. The rule of thumb is that these operators may not be the best option; they are the first alternative to try. The traditional crossover operators perform random selection of two individuals and combine them with a probability  $p_c$ , called the crossover probability. For this purpose, first a uniform random number is created and it is then compared to  $p_c$ . If the random number is less than  $p_c$ , then selected individuals are recombined. Otherwise, the traits of these individuals are transferred to the offspring without any change. Usually sensitivity analyses are needed to determine a good value for  $p_c$  or the value is determined based on the theoretical explanations of GA. Two most frequently used crossover operators are described below.

- *One- and Two-Point Crossover:* In this category, there are two types of crossover operators: one-point (Figure 2.9(a)) and two-point crossover (Figure 2.9(b)). The principle is that the chromosomes are exchanged based on a predefined location called *locus*, which is determined according to the  $p_c$  values. Finally, this can be extended for any number of loci, which is generally called the k-point crossover.
- *Uniform Crossover:* This method is based on the exchange of uniform crossover between the pair of randomly selected chromosomes with a certain probability,  $p_s$ , known as the swapping probability [Spears & De Jong, 1991; Syswerda, 1989], which is generally taken to be 0.5. Figure 2.9(c) shows the alleles that are exchanged when a uniform operator is applied.

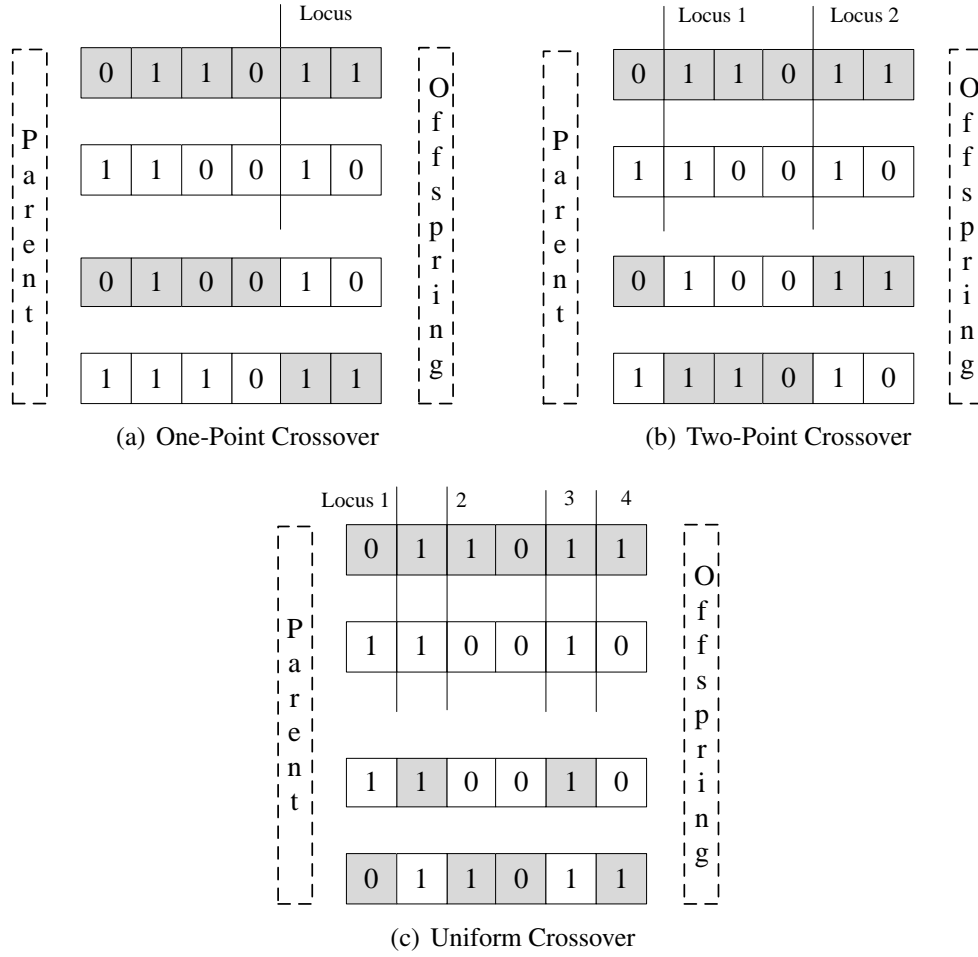


**Figure 2.9:** Crossover Methods (adopted from [Burke & Kendall, 2005]).

In addition to the above crossover techniques, other GAs are described in the literature such as Uniform Order-Based Crossover, Order-Based Crossover, Cycle Crossover and Partially Matched Crossover.

**Mutation:** In GAs, better candidates are generally expected through the generations. Although the crossover operator provides diversity to the population if the two parents have the same genetic structure, then the crossover operator will not function at all. If the same genetic structure is observed in both members, the same parental characteristics are transferred to next generations forever. In order to prevent this action, mutation operation is applied to the parental chromosomes. Mutation generally is a small change to the

characteristics of the population to provide diversity to prevent the similarity of parental strings. The most important effect of mutation is that it helps in searching the entire solution space effectively. The building blocks are generally not destroyed; on the contrary, mutation may help introduce new building blocks to the solution space [Sastry *et al.*, 2005].

Mutation is applied with a certain probability  $p_m$ . In general, the probability value is chosen to be very low in order not to affect the parental traits. The random search in the neighborhood of individuals is performed through mutation. Depending on the number of candidates in the population, increasing  $p_m$  results in more alterations, which may greatly change the diversity of population. The most widespread mutation operator is the bitwise mutation, where each bit in the binary string is replaced with its opposite binary pair; that is, if the bit is 0, then it is changed to 1, or vice versa. Other mutation operators are described in the literature such as mutation clock, directed mutation operator, adaptive mutation, etc., and choosing or designing the appropriate one for a specific problem generally requires knowledge of the domain.

**Replacement:** Replacement is a strategy to introduce the newly created members into a better parental population. Similarly to crossover, replacement is also performed to preserve diversity in the population. The decision to keep the parental members in the population is made based on the candidates' fitness. Those with better fitness are kept and the others are replaced with the offspring. Many replacement strategies are also available to perform replacement; among those, delete-all, steady-state, and steady-state-no-duplicates are frequently used.

#### **2.4.2.2 Genetic Algorithms in Backcalculation Analysis**

GAs were successfully implemented for the solution of pavement layer backcalculation problem. A binary coded simple GA with single-point crossover, mutation and ranking selection mechanism was first successfully introduced as a novel method for



backcalculation of pavement layer moduli [Fwa *et al.*, 1997]. In that study, a deflection based objective function was utilized, which seeks to match deflections calculated from one of the two different deflection computation approaches (BISAR or Odemark equivalent layer method), with that from FWD testing. It was also proved that the simple GA approach performed better when compared to the backcalculation programs that are used in practice such as MICHBACK, MODULUS, EVERCALC and EVERCALC-Alt. A similar approach was later developed for backcalculation of pavement layers, with the deflection values obtained from elastic layer system analyses [Kameyama *et al.*, 1997]. The method of heuristic crossover for floating point implementation was used along with a dynamic mutation operator. Moreover, the implemented ranking selection was modified through eliminating the similar chromosomes to prevent premature convergence. Reddy *et al.* [2002] developed a GA based backcalculation program that implements the same philosophy using the ELAYER program to compute surface deflections. Reddy *et al.* [2004] also determined a set of optimum parameters for backcalculating pavement layer properties using elastic programs. The optimal set of GA parameters (population size, crossover and mutation probabilities, etc.) was determined using a heuristic approach implemented through running the GA based backcalculation program called BACKGA. Recently, Park *et al.* [2010] also implemented GAs to solve backcalculation problems using a software program called GAPAVE.

The previous studies proved that GAs were effective in searching the solution space of the backcalculation problem. However, all those methodologies use the solutions of elastic layered programs or the programs usually employed at the design stage of pavement construction to match the deflections obtained from FWD testing. On the other hand, natural conditions for pavements induce high nonlinearity in material behavior. Therefore, the modeling of pavement requires consideration of nonlinear pavement layer properties, which makes the solution of the backcalculation problem difficult.

# **Chapter 3**

## **Development of Artificial Neural Network Based Structural Models**

In this chapter, the development of ANN structural models for both forward and backcalculation pavement structural analyses is introduced. Forward analysis models are used to analyze pavement sections without the need for using a pavement analysis program, whereas the backcalculation models are used to backcalculate pavement layer properties directly from FWD test results. Considering the ANN model development stages, nonlinear FE modeling of flexible pavements is discussed first along with its relevant aspects regarding pavement layer characterization. Lime stabilization of pavement weak subgrades is also described to address the need for performing separate analyses for pavements built on lime stabilized sections. The process of ANN model training is explained next by giving details of the additional computer programs also developed for collecting and processing the synthetically generated data from thousands of FE analyses. Finally, the details of the developed forward and backcalculation analysis ANN structural models are given with their performance validations accomplished through the use of field FWD data.

### **3.1 ILLI-PAVE Finite Element Modeling**

The ILLI-PAVE 2005 FE program, the most recent version of this extensively tested and validated ILLI-PAVE pavement analysis program used for over three decades, was used as an advanced structural model for solving deflection profiles and responses of the typical Illinois FDPs and CFPs, FDP-LSSs and CFP-LSSs. ILLI-PAVE uses an axisymmetric

revolution of the cross-section to model the layered flexible pavement structure. Unlike the linear elastic theory commonly used in pavement analysis, nonlinear unbound aggregate base and subgrade soil characterization models are used in the ILLI-PAVE program to account for the typical hardening behavior of base course granular materials and the softening nature of fine-grained subgrade soils under increasing stress states. Among the several modifications implemented in the new ILLI-PAVE 2005 FE code are

1. increased number of elements (degrees of freedom);
2. new/updated material models for the granular materials and subgrade soils;
3. enhanced iterative solution methods;
4. Fortran 90 coding and compilation; and
5. a new user-friendly Borland Delphi pre-/post-processing interface to assist in the analysis [Gomez-Ramirez *et al.*, 2002](see Figure 3.1).

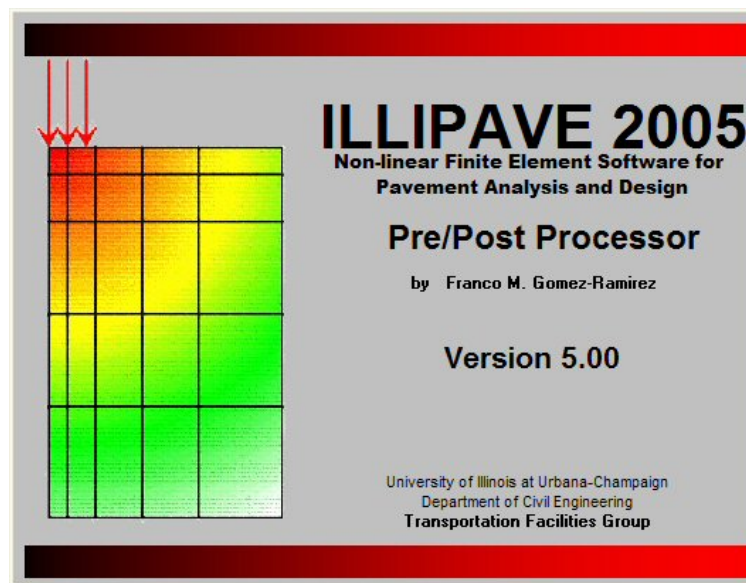


**Figure 3.1:** ILLI-PAVE 2005 Finite Element Software for Pavement Analysis.

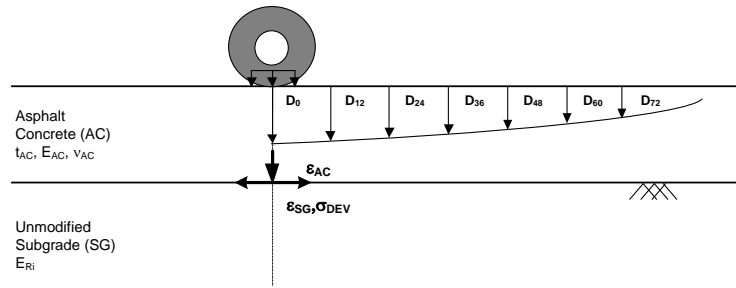
### 3.1.1 Falling Weight Deflectometer Simulation

Pavement FE modeling was performed in this study using an axisymmetric FE mesh for all pavement sections considered. Using the ILLI-PAVE FE program, FWD tests on flexible pavements were modeled with the standard 9-kip equivalent single axle loading applied as uniform pressure of 80 psi over a circular area of 5.91 in. radius. The FE mesh was selected according to the uniform spacing option of the FWD sensors as follows: 0 in., 8 in., 12 in., 18 in., 24 in., 36 in., 48 in., 60 in. and 72 in. away from the center of the FWD plate. The surface deflections corresponding to the locations of these FWD sensors were abbreviated as  $D_0$ ,  $D_8$ ,  $D_{12}$ ,  $D_{18}$ ,  $D_{24}$ ,  $D_{36}$ ,  $D_{48}$ ,  $D_{60}$ , and  $D_{72}$ , respectively.

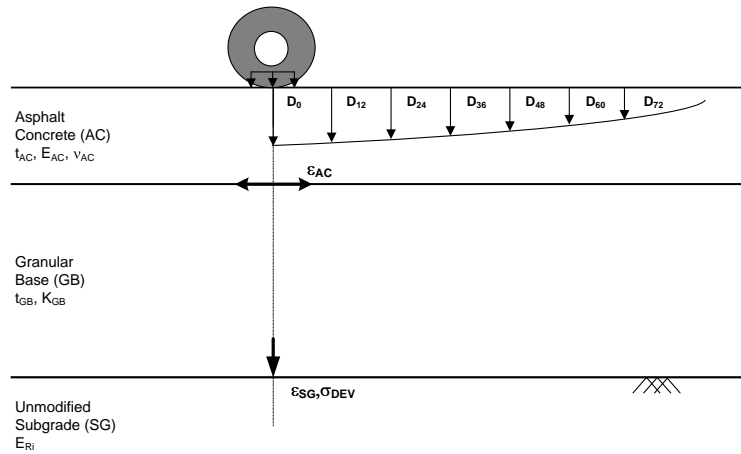
These deflections are in conformity with the uniform spacing commonly used in FWD testing by many state highway agencies (Table 3.1). Typically, finer mesh spacing was used in the loaded area with the horizontal spacing adjusted according to the locations of the geophones used in FWD tests. In addition to the deflections, the critical pavement responses, i.e., horizontal strain at the bottom of AC layer ( $\epsilon_{AC}$ ), vertical strain at the top of the subgrade ( $\epsilon_{AC}$ ), and the vertical deviator stress on top of the subgrade ( $\sigma_{DEV}$ ) directly at the centerline of the FWD loading, were also extracted from ILLI-PAVE results. Figures 3.2 and 3.3 show the locations of these responses obtained from different types of flexible pavements. These critical pavement responses play a crucial role in the context of mechanistic-empirical asphalt pavement design procedures as they directly relate to major failure mechanisms due to excessive fatigue cracking and rutting in the wheel paths.

**Table 3.1:** Falling Weight Deflectometer Sensor Spacing

Sensor Spacing (in.)	0	8	12	18	24	36	48	60	72
Uniform (used in this study)	+		+		+	+	+	+	+
State Highway Research Program (SHRP)	+	+	+	+	+	+		+	

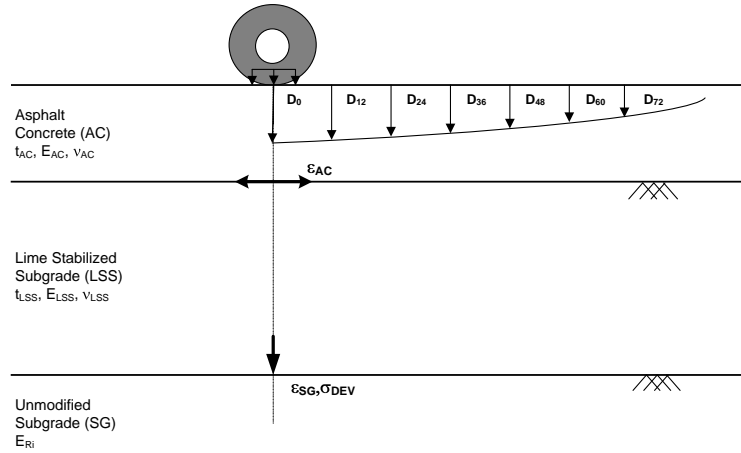


(a) Full-depth Asphalt Pavements

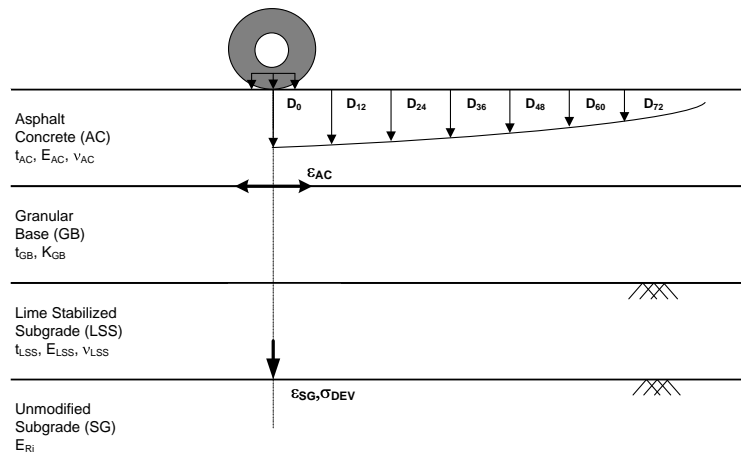


(b) Conventional Flexible Pavements

**Figure 3.2:** Locations of Critical Pavement Responses and Deflections for Pavements Built on Unmodified Subgrade.



(a) Full-depth Asphalt Pavements Built on Lime Stabilized Soils



(b) Conventional Flexible Pavements Built on Lime Stabilized Soils

**Figure 3.3:** Locations of Critical Pavement Responses and Deflections for Pavements Built on Lime Stabilized Soils.

A total analysis depth of 300 in. was selected for all pavements analyzed. Depending on the thicknesses of the layers, an aspect ratio of 1 was mainly used in the finite elements with a limiting value of 4 to get consistent pavement response predictions from ILLI-PAVE FE analyses [Pekcan *et al.*, 2006]. The vertical and horizontal spacings in the FE mesh were chosen appropriately so that there was neither numerical instability nor inconsistency in the results due to meshing. Figure 3.4 shows a sample ILLI-PAVE FE mesh that was used in the analyses of FDP-LSS. The thicknesses of all layers were selected to have appropriate ranges encountered for most flexible pavements in Illinois.

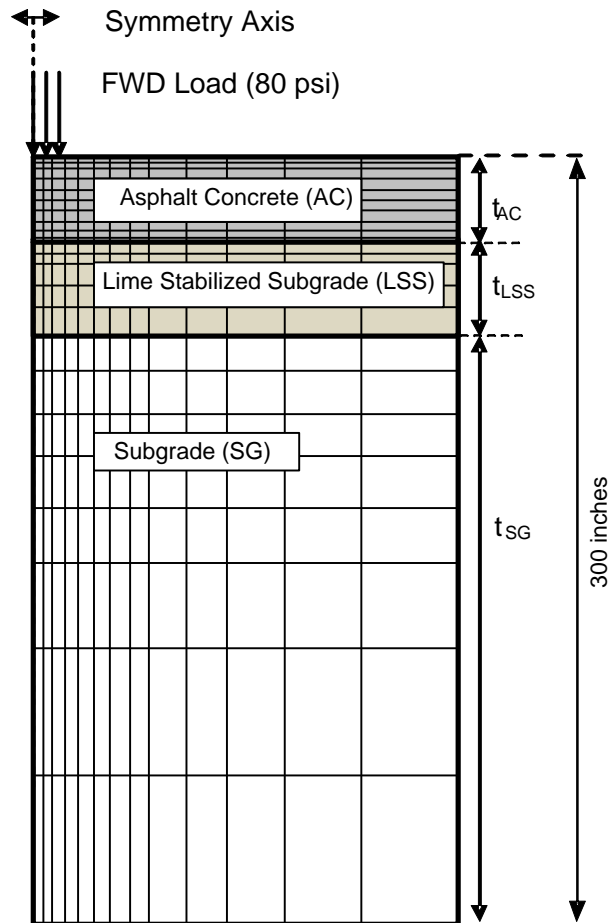


**Figure 3.4:** Finite Element Mesh for Full-Depth Pavements on Lime Stabilized Subgrade.

### 3.1.1.1 Pavement Layer Characterization

Adequately characterizing pavement layer behavior plays a crucial role for an accurate backcalculation of the layer moduli. Accordingly, modeling of FDP and CFP requires accurate material characterizations for the AC, GB and fine-grained subgrade soil layers. After material shakedown has taken place due to construction loading and early trafficking of the pavements, most of the deformations under a passing truck wheel are recoverable and hence considered resilient or elastic. The resilient modulus ( $M_R$ ), defined by repeated wheel load stress divided by recoverable strain, is therefore the elastic modulus often used to describe flexible pavement layer behavior under traffic loading. In ILLI-PAVE FE models of the different flexible pavements analyzed, the AC surface course was always represented with elastic properties, layer modulus  $E_{AC}$  and Poisson's ratio  $\nu_{AC}$ , for the instant loading during FWD testing. The value of  $\nu_{AC}$  was taken constant as 0.35.

The modeling of fine-grained subgrade soils, mainly encountered in Illinois, has received more attention in the last three decades since it has a major impact on all the responses predicted under traffic loading within the context of Mechanistical-Empirical design. Fine-grained subgrade soils exhibit nonlinear behavior when subjected to traffic loading [Ceylan *et al.*, 2005; Thompson & Robnett, 1979]. The subgrade stiffness characterized by  $M_R$  is usually expressed as a function of the applied deviator stress through nonlinear modulus response models. These models were developed based on the results of repeated load triaxial tests, which form the basis of evaluating resilient properties of fine-grained soils [AASHTO, 1999].

Illinois subgrade soils are mostly fine-grained, exhibit stress softening behavior, and can be characterized using the bilinear arithmetic model [Thompson & Elliott, 1985; Thompson & Robnett, 1979] with the modulus-deviator stress relationship shown in Figure 3.5. The upper limit deviator stress in the bilinear model,  $\sigma_{dul}$ , is dependent on the breakpoint modulus,  $E_{Ri}$ , which is also a function of the unconfined compressive strength,  $Q_u$ ,



expressed by Equation 3.1 [Thompson & Robnett, 1979].  $E_{Ri}$  is a characteristic property of the fine-grained soil often computed for Illinois soils at a breakpoint deviator stress  $\sigma_{di}$  of 6 psi. The corresponding values and parameters of the bilinear model used in the analyses are also given in Figure 3.5.

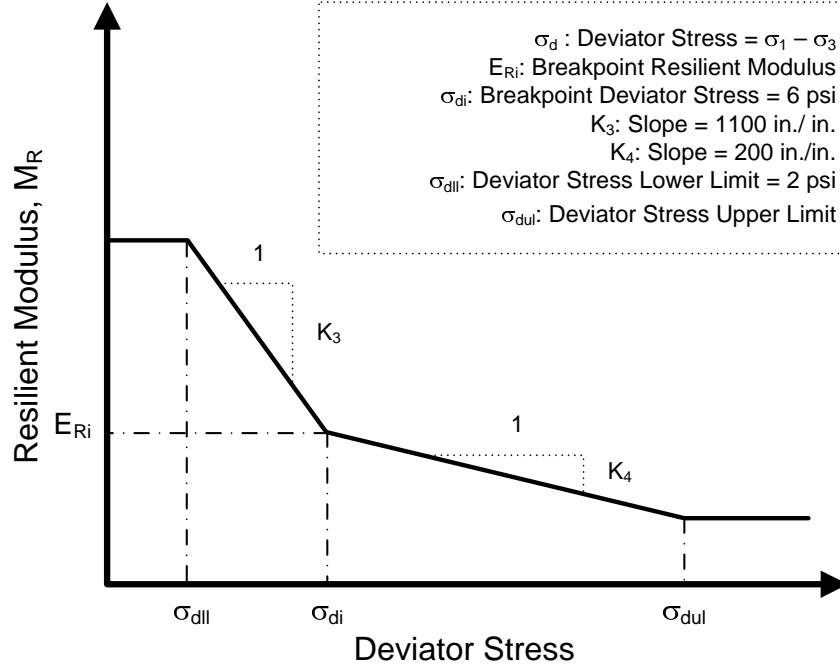


**Figure 3.5:** Bilinear Model to Characterize Stress Dependency of Fine-Grained Soils.

$$\sigma_{dul}(psi) = Q_u(psi) = \frac{E_{Ri} \cdot (ksi) - 0.86}{0.307} \quad (3.1)$$

The GB layer provides the essential load transfer in a conventional flexible pavement. The effect of this layer is predominant in determining the fatigue behavior of the AC layer. The well-known  $K - \theta$  model [Hicks & Monismith, 1971] was used in our modeling study to characterize the stress dependency of elastic, i.e., resilient modulus in ILLI-PAVE analyses. In this model, the modulus stress dependency is considered by the use of two model parameters, “K” and “n”. The model parameter “n” is correlated to K-parameter

according to Equation 3.2, where  $K$  is in psi. A major advantage of the given equation is that the unbound aggregate modulus characterization model then only requires one model parameter.  $K - \theta$  model parameters of different granular materials ( $K$  and  $n$  values) are also given in Table 3.2. Typical “ $K$ ” values range from 3 ksi to 12 ksi based on the comprehensive granular material database compiled by Rada and Witczak [1981] (Figure 3.6). Poisson’s ratio was taken as 0.35 when  $K \geq 5$  ksi, otherwise it was assumed 0.40.

$$\log_{10}(K) = 4.657 - 1.807 * n \quad (3.2)$$

**Table 3.2:** Typical Resilient Property Data for Granular Materials (after Rada and Witczak [1981])

Granular Material  Type	Number of  Data Points	K (psi) <sup>1</sup>		n <sup>1</sup>	
		Mean	Standard Deviation	Mean	Standard Deviation
Silty Sands	8	1620	780	0.62	0.13
Sand-Gravel	37	4480	4300	0.53	0.17
Sand-Aggregate Blends	78	4350	2630	0.59	0.13
Crushed Stone	115	7210	7490	0.45	0.23

<sup>1</sup>  $E_R = K\theta_n$  where  $E_R$  is Resilient modulus and  $K$ ,  $n$  are model parameters obtained from multiple regression analyses of repeated load triaxial test data.

## 3.2 Lime Stabilization

Pavement design and performance requirements often necessitate the use of a treated subgrade when pavements are to be constructed on soft and weak subgrade soils. Lime stabilization is commonly utilized for this purpose as an effective and inexpensive ground improvement technique in the area of transportation geotechnics. Application of lime,

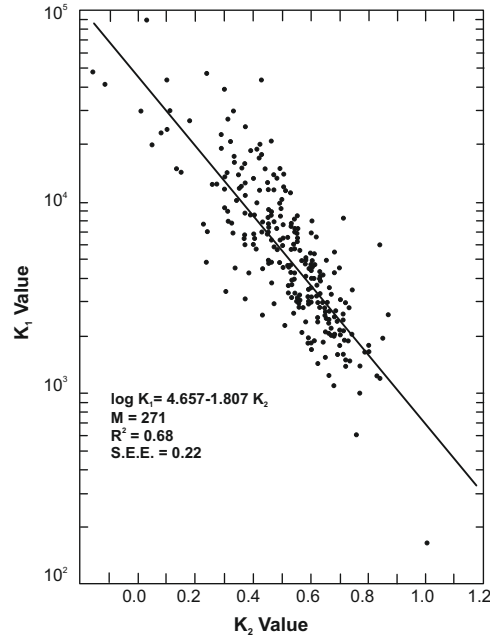


**Figure 3.6:** Relationship Between K (Shown as  $K_1$ ) and  $n$  (Shown as  $K_2$ ) Values for Granular Materials Identified by Rada and Witczak [1981] (Reproduced from the Original Figure).

especially in clayey soils, results in a major improvement in the strength and deformation characteristics. Moreover, it significantly improves the long term moisture and rutting susceptibilities of fine-grained soils while also providing a working platform and the needed expediency in the construction of transportation facilities [Transportation Research Board, 1987]. Lime stabilization helps control the stiffness variability in soil layers, which is one of the most challenging problems in numerical modeling of geomaterials [Hausmann, 1990]. Various geotechnical applications can be found in the literature [Moseley & Kirsch, 2004]. Its improvement effects on the engineering properties of fine-grained soils or the fine portion of granular soils facilitate the use of the lime stabilized subgrade (LSS) as modified pavement layers. The lime stabilization of clayey subgrade soils has been a popular stabilization technique in the State of Illinois.

In Illinois, the existence and added performance of a LSS is usually ignored in pavement design and field evaluation. This is because the LSS layer is often constructed to establish a stable working platform for the construction equipment and not directly considered

as an improved structural layer coefficient in the design of pavements [Little, 1999]. Even though it is not taken into account in pavement design, the long term effect of LSS in the pavement structure is certainly reflected in the FWD deflection basins to affect the backcalculated layer properties. A proper ANN backcalculation model should therefore consider the contribution of the LSS layer to measured FWD deflection basins and pavement performance.

Although soil-lime reactions are complex considering the generalized compressive stress-strain relations for cured and uncured soil-lime mixtures [Little, 1999; Transportation Research Board, 1987], in ILLI-PAVE FE analyses, it was assumed that the LSS layer exhibited linear elastic behavior. Figure 3.7 shows the effect of lime on vertical compressive stress-strain responses of fine grained subgrade soils [Thompson, 1966]. Figure 3.8 shows the effect of lime stabilization on stress-strain characteristics that occur without curing [Neubauer & Thompson, 1972]. Figure 3.9(a) and (b) show the immediate effects of lime treatment on soils compacted at the wet side of optimum moisture contents [McDonald, 1969]. Figure 3.10 shows a generalized stress-strain curve developed as a result of an extensive study of Illinois soils stabilized with lime [Thompson, 1966]. In summary, the reviewed studies provided adequate support for modeling the LSS layer using elastic layer properties  $E_{LSS}$  and  $\nu_{LSS}$ . The value of  $\nu_{LSS}$  was selected to be 0.31 and remained constant with stress levels [Transportation Research Board, 1987].

### **3.2.1 Preliminary Analyses of Lime Stabilized Sections**

The contributions of an existing LSS layer and the nonlinear behavior of underlying subgrade on FWD deflection profiles and pavement response predictions might inherently be modeled using ANNs. The main objective of this section is therefore to prove that lime stabilization has a definite impact on pavement performance for flexible pavements including FDPs and CFPs. Then, ANN based models can be developed for backcalculation and forward analyses of flexible pavements including FDP-LSSs and CFP-LSSs. Proper

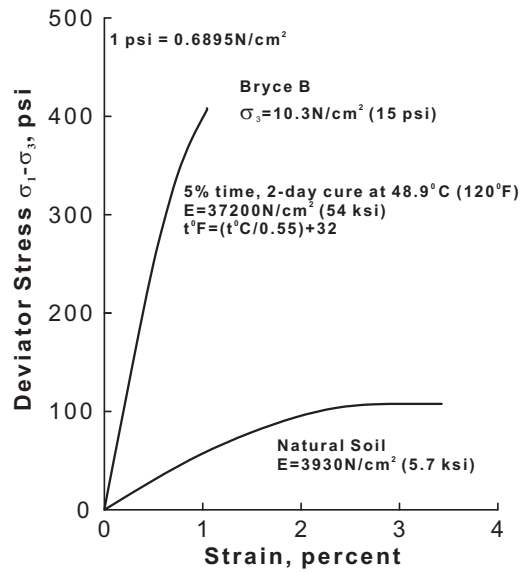


**Figure 3.7:** Typical Stress-Strain Curves for Natural and Lime Treated Soils [Transportation Research Board, 1987] (Reproduced from the Original Figure).

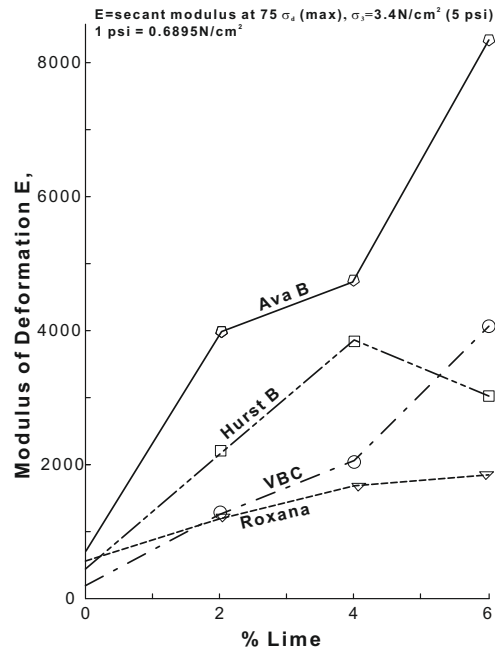


**Figure 3.8:** Immediate Effects of Lime Treatment without Curing on Modulus Deformation [Neubauer & Thompson, 1972] (Reproduced from the Original Figure).

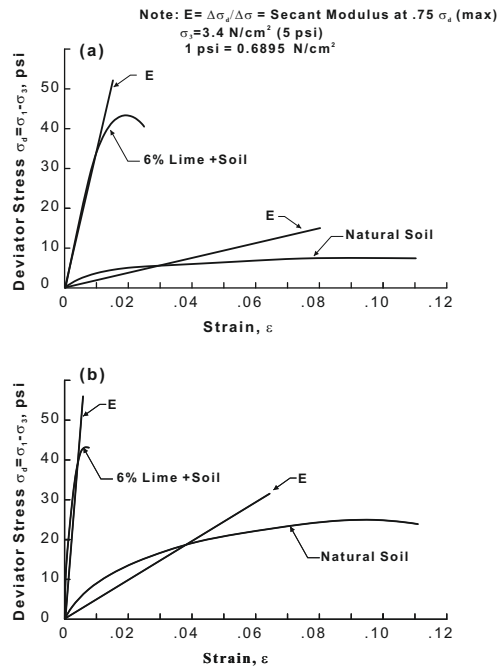


**Figure 3.9:** Typical Stress-Strain Curves for Immediate Effects of Lime Treatment (a) Vicksburg Buckshot Clay (b) Ava B. [McDonald, 1969] (Reproduced from the Original Figure).

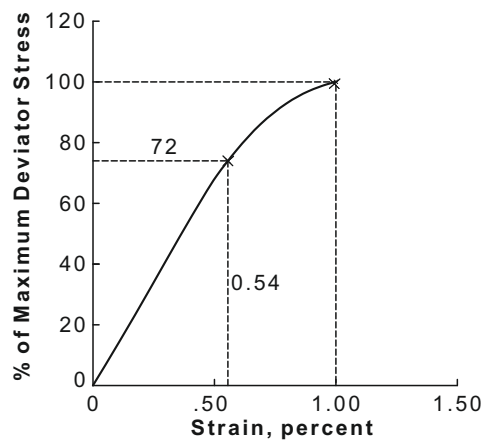


**Figure 3.10:** Generalized Stress-Strain Relationship for Cured Soil-Lime Mixtures [Thompson, 1966] (Reproduced from the Original Figure).

**Table 3.3:** Ranges of FDP-LSSs Studied in the ILLI-PAVE Preliminary Analyses

Case	$t_{AC}$ (in.)	$t_{LSS}$ (in.)	$E_{AC}$ (psi)	$E_{LSS}$ (psi)	$E_{Ri}$ (psi)	Sensitivity Variable
1	9	4	$1 \times 10^6$	$1.5 \times 10^4$	$1.0 \times 10^3$	$E_{Ri}$
2	9	22	$1 \times 10^6$	$1.0 \times 10^5$	$1.4 \times 10^4$	
3	9	22	$1 \times 10^6$	$1.5 \times 10^4$	$1.0 \times 10^3$	
4	9	4	$1 \times 10^6$	$1.0 \times 10^5$	$1.4 \times 10^4$	
5	9	4	$1 \times 10^5$	$1.5 \times 10^4$	$7.5 \times 10^3$	$E_{AC}$
6	9	22	$2 \times 10^6$	$1.0 \times 10^5$	$7.5 \times 10^3$	
7	9	22	$1 \times 10^5$	$1.5 \times 10^4$	$7.5 \times 10^3$	
8	9	4	$2 \times 10^6$	$1.0 \times 10^5$	$7.5 \times 10^3$	
9	3	4	$1 \times 10^6$	$1.5 \times 10^4$	$7.5 \times 10^3$	$t_{AC}$
10	15	22	$1 \times 10^6$	$1.0 \times 10^5$	$7.5 \times 10^3$	
11	3	22	$1 \times 10^6$	$1.5 \times 10^4$	$7.5 \times 10^3$	
12	15	4	$1 \times 10^6$	$1.0 \times 10^5$	$7.5 \times 10^3$	

quantification of the improvement in pavement responses, i.e., deflections, strains, and stresses, due to LSS is necessary to facilitate comparisons between FDP vs. FDP-LSS and CFP vs. CFP-LSS solutions. This is achieved in this section through FE modeling of both pavement types and comparing the analysis results.

### 3.2.1.1 Full-depth Asphalt Pavements on Lime Stabilized Soils

The motivation in this section was to investigate the differences in the FWD deflection profiles and predicted pavement responses, if any, between the FDPs and FDPs-LSS. In an effort to quantify these discrepancies in critical pavement responses and deflection values, ILLI-PAVE preliminary analyses were carried out for the typical ranges of layered pavement geometries and material properties (see Table 3.3). The ranges of inputs, i.e., the thickness of AC layer ( $t_{AC}$ ), the thickness of LSS layer ( $t_{LSS}$ ),  $E_{AC}$ ,  $E_{LSS}$  and  $E_{Ri}$ , were carefully chosen to cover most values of all FDPs-LSS found in Illinois [Pekcan *et al.*, 2007]. The depth of the untreated subgrade beneath the LSS layer was computed each time based on the total constant height of the FE analysis mesh. The similar FDP sections having the same properties but with no LSS were also analyzed using the ILLI-PAVE FE program.

The results of preliminary ILLI-PAVE analyses are presented for both LSS and no lime pavements using the average absolute errors (AAEs) of deflection values and critical pavement responses in Figures 3.11(a) and 3.11(b), respectively. AAE, also called mean absolute percentage error, or MAPE, is defined in Equation 3.3 where the measured value is the one obtained for FDP while the calculated one is for FDP-LSS.

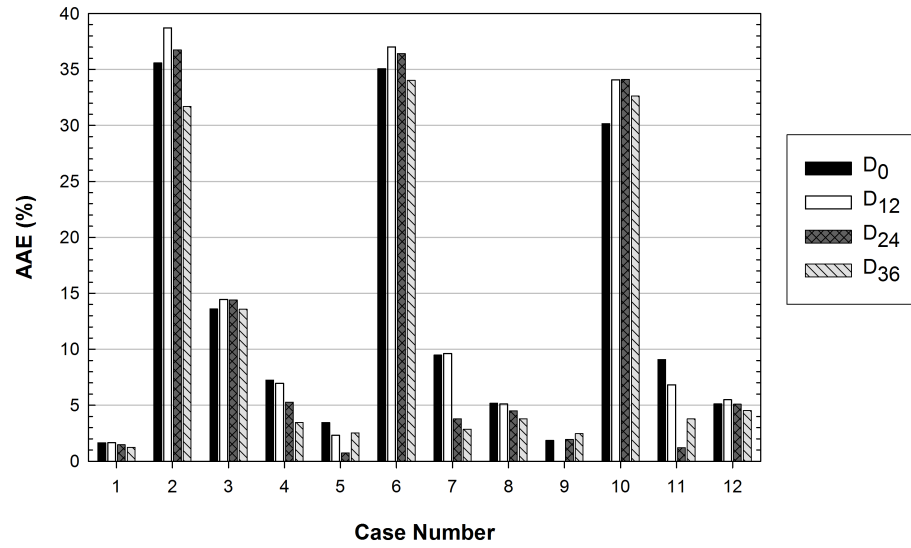
$$\text{Average Absolute Error (AAE)} = \left[ \frac{1}{n} \sum_{i=1}^n \left( \frac{\text{Measured}_i - \text{Actual}_i}{\text{Measured}_i} \right) \right] \times 100 \quad (3.3)$$

As shown in Figure 3.11(a), while the maximum AAE or difference in deflections can reach up to 39% for case 2, the total average difference for all deflection values is about 12%. Furthermore, in Figure 3.11(b), the total average differences for  $\epsilon_{AC}$ ,  $\epsilon_{SG}$ , and  $\sigma_{DEV}$  are approximately 18%, 18%, and 35%, respectively. This is in spite of the fact that the maximum differences can reach up to 38%, 60%, and 80% for  $\epsilon_{AC}$ ,  $\epsilon_{SG}$ , and  $\sigma_{DEV}$ , respectively. Therefore, the placement of a lime stabilized layer over the untreated subgrade considerably changed the overall responses of FDPs. Almost up to 40% of the differences in the deflection values certainly affect the accuracy of backcalculated layer moduli from the FWD deflection basins.

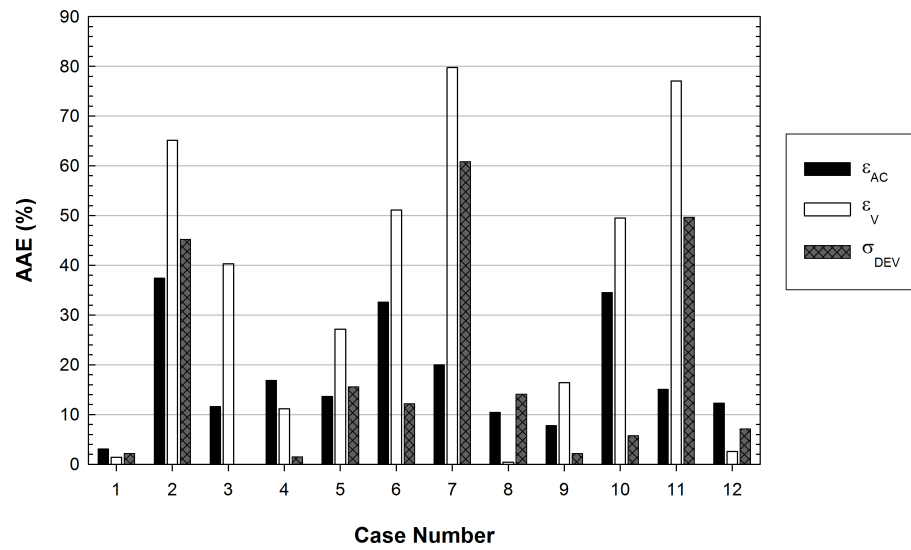
### 3.2.1.2 Conventional Flexible Pavements on Lime Stabilized Soils

To show the additional effect of lime stabilized soil layer on critical pavement responses and deflection profiles for CFPs, preliminary analyses were also needed. For this purpose, 20 different CFP-LSS sections were analyzed using the ILLI-PAVE FE program under the typical 9-kip FWD loading. The inputs were selected such that they included extensive ranges of material properties and thicknesses (see Table 3.4). The LSS layer was then replaced with natural subgrade and the analyses were repeated. This way, CFP and CFP-LSS critical pavement responses could be compared effectively. The deflection





(a) Deflection Basin Differences



(b) Critical Pavement Response Differences

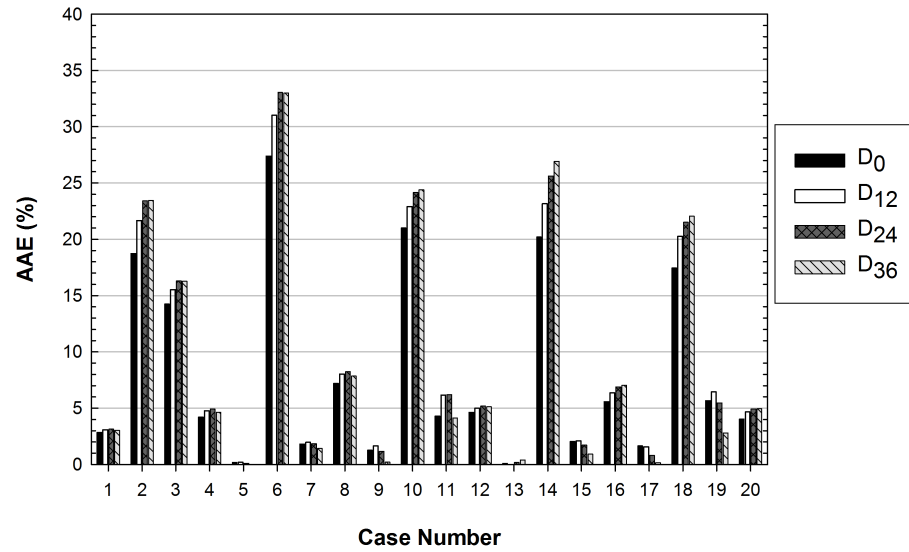
**Figure 3.11: ILLI-PAVE Comparisons between FDP-LSS and FDP with No Lime.**

**Table 3.4:** Ranges of CFP-LSSs Studied in the ILLI-PAVE Preliminary Analyses

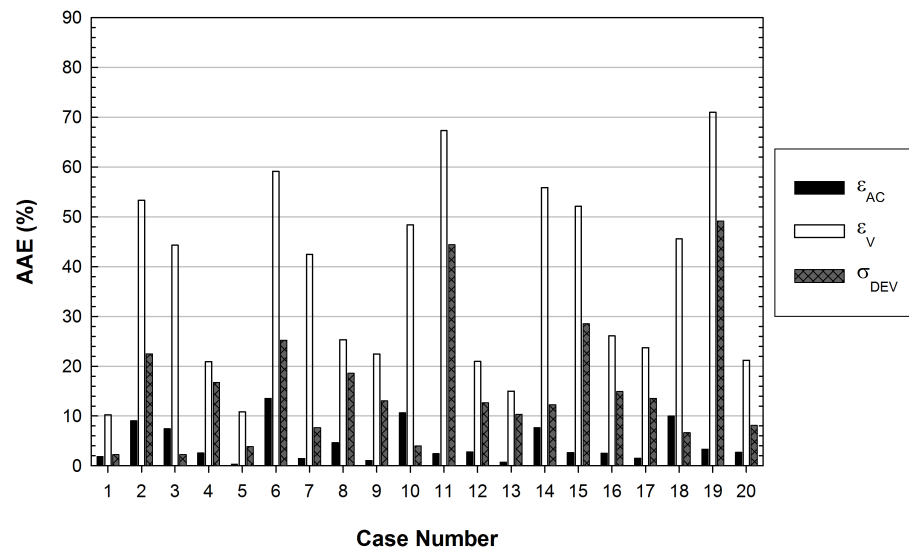
Case	$t_{AC}$ (in.)	$t_{GB}$ (in.)	$t_{LSS}$ (in.)	$E_{AC}$ (psi)	$K_{GB}$ (psi)	$E_{LSS}$ (psi)	$E_{Ri}$ (psi)	Sensitivity Variable
1	9	13	4	$1.0 \times 10^6$	$7.5 \times 10^3$	$1.5 \times 10^4$	$1.0 \times 10^3$	$E_{Ri}$
2	9	13	22	$1.0 \times 10^6$	$7.5 \times 10^3$	$1.0 \times 10^5$	$1.4 \times 10^4$	
3	9	13	22	$1.0 \times 10^6$	$7.5 \times 10^3$	$1.5 \times 10^4$	$1.0 \times 10^3$	
4	9	13	4	$1.0 \times 10^6$	$7.5 \times 10^3$	$1.0 \times 10^5$	$1.4 \times 10^4$	
5	9	13	4	$1.0 \times 10^6$	$3.0 \times 10^3$	$1.5 \times 10^4$	$7.5 \times 10^3$	$K_{GB}$
6	9	13	22	$1.0 \times 10^6$	$1.2 \times 10^4$	$1.0 \times 10^5$	$7.5 \times 10^3$	
7	9	13	22	$1.0 \times 10^6$	$3.0 \times 10^3$	$1.5 \times 10^4$	$7.5 \times 10^3$	
8	9	13	4	$1.0 \times 10^6$	$1.2 \times 10^4$	$1.0 \times 10^5$	$7.5 \times 10^3$	
9	9	13	4	$1.0 \times 10^5$	$7.5 \times 10^3$	$1.5 \times 10^4$	$7.5 \times 10^3$	$E_{AC}$
10	9	13	22	$2.0 \times 10^6$	$7.5 \times 10^3$	$1.0 \times 10^5$	$7.5 \times 10^3$	
11	9	13	22	$1.0 \times 10^5$	$7.5 \times 10^3$	$1.5 \times 10^4$	$7.5 \times 10^3$	
12	9	13	4	$2.0 \times 10^6$	$7.5 \times 10^3$	$1.0 \times 10^5$	$7.5 \times 10^3$	
13	9	4	4	$1.0 \times 10^6$	$7.5 \times 10^3$	$1.5 \times 10^4$	$7.5 \times 10^3$	$t_{GB}$
14	9	22	22	$1.0 \times 10^6$	$7.5 \times 10^3$	$1.0 \times 10^5$	$7.5 \times 10^3$	
15	9	4	22	$1.0 \times 10^6$	$7.5 \times 10^3$	$1.5 \times 10^4$	$7.5 \times 10^3$	
16	9	22	4	$1.0 \times 10^6$	$7.5 \times 10^3$	$1.0 \times 10^5$	$7.5 \times 10^3$	
17	3	13	4	$1.0 \times 10^6$	$7.5 \times 10^3$	$1.5 \times 10^4$	$7.5 \times 10^3$	$t_{AC}$
18	15	13	22	$1.0 \times 10^6$	$7.5 \times 10^3$	$1.0 \times 10^5$	$7.5 \times 10^3$	
19	3	13	22	$1.0 \times 10^6$	$7.5 \times 10^3$	$1.5 \times 10^4$	$7.5 \times 10^3$	
20	15	13	4	$1.0 \times 10^6$	$7.5 \times 10^3$	$1.0 \times 10^5$	$7.5 \times 10^3$	

profiles and critical pavement responses from the preliminary analyses are compared again using the computed AAEs, defined in Equation 3.3 where the measured value is the one obtained for CFP while the calculated one is for CFP-LSS.

The results are presented in Figures 3.12(a) and 3.12(b). The maximum AAE in deflection values (see Figure 3.12(a)) is observed to be 33% (Case 6) and the average of all deflection AAE values is calculated as 9%. The comparisons of critical pavement response, however, indicated higher variations. While the maximum AAE values for  $\epsilon_{AC}$ ,  $\epsilon_{SG}$ , and  $\sigma_{DEV}$  can reach up to 14% (Case 6), 71% (Case 19) and 49% (Case 19), respectively, the average AAE values are calculated as 4%, 37%, and 16%, for  $\epsilon_{AC}$ ,  $\epsilon_{SG}$ , and  $\sigma_{DEV}$ , respectively (see Figure 3.11(b)). Hence, accurate pavement responses could not be computed by neglecting the contribution of the LSS layer [Pekcan *et al.*, 2008b].



(a) Deflection Basin Differences



(b) Critical Pavement Response Differences

**Figure 3.12:** ILLI-PAVE Comparisons between CFP-LSS and CFP with No Lime.

### 3.3 ILLI-PAVE Database For Flexible Pavements

Randomly selected combinations of material and thickness inputs were provided to ILLI-PAVE to generate batch analyses. For this purpose, a MS Excel file was created for a given pavement to list  $t_{AC}$ ,  $t_{GB}$ ,  $E_{AC}$ ,  $K_{GB}$ ,  $E_{Ri}$  that are randomly chosen in the predefined ranges of properties for CFPs (see Figure 3.13). A batch program interface was written in Borland Delphi (see Figure 3.14) capable of producing ILLI-PAVE input files with the material and thickness properties obtained from the corresponding MS Excel file. This software mainly duplicates ILLI-PAVE preprocessor which was written using MS Visual Basic and is available to the researchers. By using this new program, named ILLI-PAVE auto analysis, numerous runs were made to cover the whole ranges of layer moduli and thicknesses as illustrated in Figure 3.15. Also developed using Borland Delphi, ILLI-PAVE auto analysis completely replaces the analysis engine embedded in ILLI-PAVE 2005 and is capable of extracting the deflections and critical pavement responses from the analyses to form a database consisting of inputs and outputs of the flexible pavement analyses (see Figure 3.16). This database, which inherently captured the nonlinear FE approximations, was then used to train and develop an ANN-based structural analysis toolbox containing several ANN models for forward and backcalculation analyses of flexible pavements.

The input files for ILLI-PAVE FE analyses were generated by randomly selecting values for each of the thickness and moduli combinations for different types of flexible pavements. A total of 24,000 ILLI-PAVE runs were made for FDP and 24,100 for CFP in order to fully cover the material property ranges given in Tables 3.5 and 3.6. The surface deflections corresponding to the locations of the FWD sensors and the critical pavement responses, i.e.,  $\epsilon_{AC}$ ,  $\epsilon_{SG}$ , and  $\sigma_{DEV}$ , directly at the centerline of the FWD loading were then extracted from the ILLI-PAVE output files.

The preliminary analyses proved that FDP-LSS pavements had to be analyzed separately to consider the contribution of lime stabilization and capture more accurate pavement

	A	B	C	D	E
1	tac	tbc	Eac	Kb	Eri
2	14.8	16.2	855140	8992	2200
3	6.2	6.9	1187354	3537	1568
4	5.7	6.1	1016992	10141	1093
5	13.7	5.1	906400	4708	5462
6	13.2	17	498775	3077	2846
7	9.2	17.3	1621869	4496	4048
8	14.3	6.3	752070	10954	1171
9	11.5	19.7	235824	4995	9374
10	3.9	12.7	1020721	9250	4848
11	5.3	14.9	1625715	7500	2102

**Figure 3.13:** Randomly Selected Inputs Shown in an MS Excel File for ILLI-PAVE Analyses.

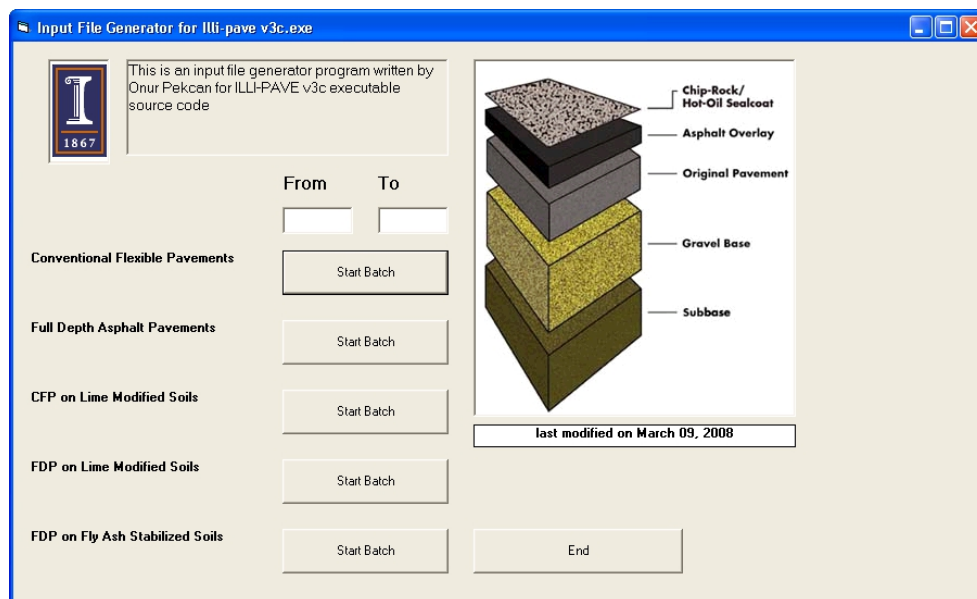


**Figure 3.14:** ILLI-PAVE Input Data Generator.

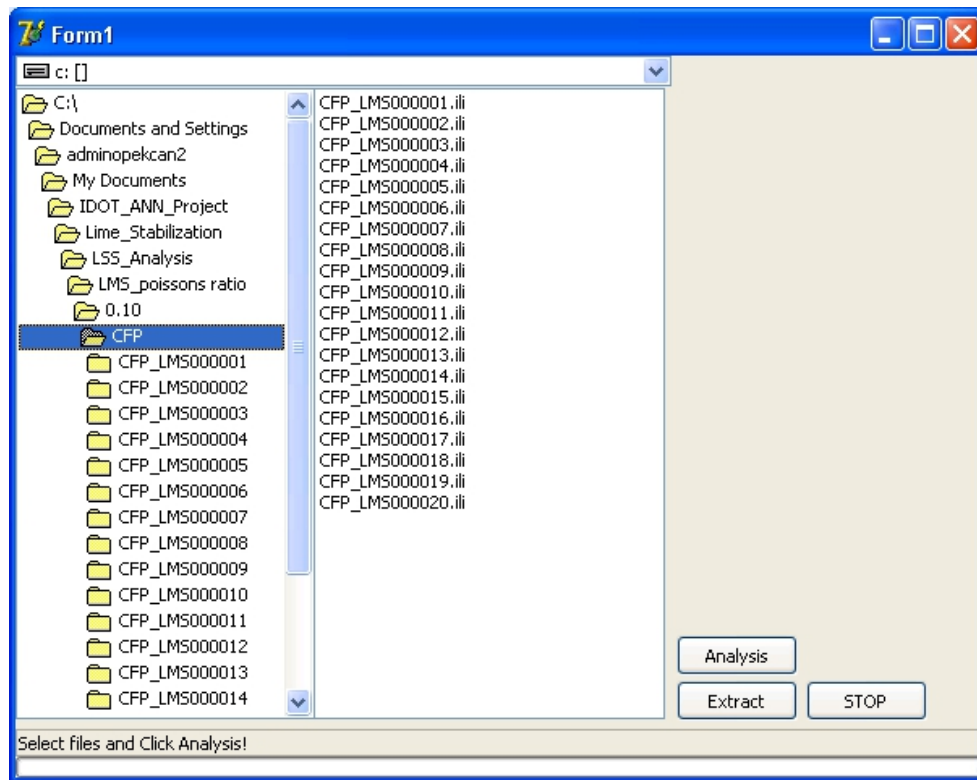


**Figure 3.15: ILLI-PAVE Auto Analysis Engine.**

	A	B	C	D	E	F	H	J	K	L	M
1	tac	tbc	Eac	Kb	Eri	do	d12	d24	d36	d48	d60
2	14.8	16.2	855140	8992	2200	6.82E+00	5.78E+00	4.94E+00	4.12E+00	3.35E+00	2.66E+00
3	6.2	6.9	1187354	3537	1568	1.71E+01	1.43E+01	1.08E+01	7.96E+00	5.65E+00	3.90E+00
4	5.7	6.1	1016992	10141	1093	1.99E+01	1.63E+01	1.21E+01	8.68E+00	6.05E+00	4.10E+00
5	13.7	5.1	906400	4708	5462	6.41E+00	5.37E+00	4.46E+00	3.60E+00	2.82E+00	2.14E+00
6	13.2	17	498775	3077	2846	1.06E+01	8.69E+00	7.06E+00	5.57E+00	4.26E+00	3.17E+00
7	9.2	17.3	1621869	4496	4048	8.20E+00	7.15E+00	5.85E+00	4.63E+00	3.55E+00	2.65E+00
8	14.3	6.3	752070	10954	1171	8.44E+00	7.22E+00	6.16E+00	5.11E+00	4.14E+00	3.26E+00
9	11.5	19.7	235824	4995	9374	1.27E+01	8.76E+00	6.05E+00	4.08E+00	2.67E+00	1.71E+00
10	3.9	12.7	1020721	9250	4848	1.93E+01	1.38E+01	8.74E+00	5.66E+00	3.57E+00	2.22E+00
11	5.3	14.9	1625715	7500	2102	1.56E+01	1.29E+01	9.67E+00	7.08E+00	5.02E+00	3.47E+00
12	4.9	10.1	1204649	8687	13302	1.13E+01	8.13E+00	5.05E+00	3.17E+00	1.93E+00	1.15E+00
13	10.9	21.1	170029	4413	9718	1.53E+01	9.96E+00	6.48E+00	4.15E+00	2.58E+00	1.58E+00
14	9.8	5.1	1371202	3921	11603	6.09E+00	5.06E+00	3.95E+00	2.97E+00	2.16E+00	1.52E+00
15	12.9	19.2	1691169	4073	13529	4.17E+00	3.55E+00	2.96E+00	2.39E+00	1.87E+00	1.42E+00
16	7.2	6.3	1894882	4722	10962	7.39E+00	6.12E+00	4.59E+00	3.33E+00	2.33E+00	1.58E+00
17	13.6	14.9	1029062	7747	9229	5.26E+00	4.35E+00	3.57E+00	2.85E+00	2.21E+00	1.66E+00
18	11.7	10.5	1538563	11591	4614	5.90E+00	5.14E+00	4.33E+00	3.53E+00	2.80E+00	2.16E+00
19	4.1	14.1	280172	8958	7949	2.24E+01	1.32E+01	6.93E+00	4.01E+00	2.37E+00	1.46E+00
20	9.2	19.4	412630	7533	4752	1.34E+01	1.03E+01	7.49E+00	5.31E+00	3.67E+00	2.48E+00
21	8.9	11.6	1841268	3864	9871	6.49E+00	5.55E+00	4.40E+00	3.37E+00	2.49E+00	1.78E+00

**Figure 3.16: Sample MS Excel Database Used to Train ANN Models.**

**Table 3.5:** Geometries and Material Properties of Full-Depth Flexible Pavements Analyzed

Material Type	Thickness (in.)	Material Model	Elasticity Modulus (ksi)	Poisson's Ratio
Asphalt Concrete (AC)	5-24	Linear Elastic	100 - 2000	0.35
Fine Grained Subgrade (SG)	$(300 - t_{AC})$	Nonlinear Analysis with Bilinear Model	1 - 14	0.45

**Table 3.6:** Geometries and Material Properties of Conventional Flexible Pavements Analyzed

Material Type	Thickness (in.)	Material Model	Elasticity Modulus (ksi)	Poisson's Ratio
Asphalt Concrete (AC)	3-15	Linear Elastic	100 - 2000	0.35
Granular Base (GB)	4-22	Nonlinear K- $\theta$ Model	3 - 12	0.35 for $K \geq 5$ ksi 0.40 for $K < 5$ ksi
Fine Grained Subgrade (SG)	$(300 - t_{AC} - t_{GB})$	Nonlinear Analysis with Bilinear Model	1 - 14	0.45

responses for forward and backcalculation purposes. Sufficiently wide ranges of material and geometry properties of flexible pavements on LSS were analyzed to form a database for training ANNs to model the complex and nonlinear relations between the pavement properties and the responses. Table 3.7 lists the typical ranges of FDP-LSS pavement geometries and material properties selected to represent field conditions for establishing the ANN database. A total of 26,000 ILLI-PAVE analyses were performed to fully capture the ranges defined in Table 3.7. To make sure that ANN models had the ability to perform correctly for representative field conditions, the ranges of layer thickness values and material property inputs were extended up to 20% beyond the actual field values. It was also guaranteed that training was done properly and poor performances of ANN models in the ranges of typical field conditions and thicknesses were prevented.

The reported differences from preliminary analyses also confirmed that accuracy of FWD based backcalculated results for CFP-LSS could be improved when properly taking into account the LSS layer in the analyses. Therefore, CFP-LSS sections were analyzed under FWD loading with extensive ranges of material and geometry properties to develop an ILLI-PAVE FE database. Critical pavement responses and deflection profiles were stored along with corresponding inputs. Typical ranges of CFP-LSS pavement geometries and material properties are given in Table 3.8. A total of 30,000 analyses were carried out with ILLI-PAVE to form the database. This database was also used for training of ANN models for the inverse pavement analysis or backcalculation.

### **3.4 ANN Structural Models**

The multi-layered, feed-forward backpropagation type neural networks are mainly implemented for complex valued network level problems. In this project, backpropagation type ANNs were trained for the backcalculation of pavement layer moduli using the previously developed database with the input and output variables. Trained ANN models



**Table 3.7:** Geometries and Material Properties of Full-Depth Flexible Pavements on Lime Stabilized Soils Analyzed

Material Type	Thickness (in.)	Material Model	Elasticity Modulus (ksi)	Poisson's Ratio
Asphalt Concrete (AC)	4-24	Linear Elastic	100 - 2500	0.35
Lime Stabilized Subgrade (LSS)	4-20	Linear Elastic	16 - 150	0.31
Fine-grained Subgrade (SG)	$(300 - t_{AC} - t_{LSS})$	Nonlinear Analysis with Bilinear Model	1 - 15	0.45

**Table 3.8:** Geometries and Material Properties of Conventional Flexible Pavements on Lime Stabilized Soils Analyzed

Material Type	Thickness (in.)	Material Model	Elasticity Modulus (ksi)	Poisson's Ratio
Asphalt Concrete (AC)	3-18	Linear Elastic	100 - 2500	0.35
Granular Base (GB)	4-22	Nonlinear K- $\theta$ model	3 - 16	0.35 for $K \geq 5$ ksi 0.40 for $K < 5$ ksi
Lime Stabilized Subgrade (LSS)	4-20	Linear Elastic	16 - 150	0.31
Fine-grained Subgrade (SG)	$(300 - t_{AC} - t_{GB} - t_{LSS})$	Nonlinear Analysis with Bilinear Model	1 - 15	0.45

were tested based on an independent data set within the ranges that they were trained. Approximately 1,000 runs of all the data sets were independently and randomly chosen considering the given ranges of material and geometry properties and used as the testing data sets for the verification of proper ANN learning. The remaining ILLI-PAVE runs in the data sets were used for the training and/or learning task. The ANN models trained to determine whether or not they were capable of producing the same database results (with the given inputs to obtain outputs or vice versa) were checked quickly in this manner. Although training of each ANN model required a long computation time, with the already set weighted connections, testing was much faster (on the order of micro-seconds). This advantage allows a field engineer to use trained ANN models as quick pavement analysis tools without the need for any complex inputs.

### **3.4.1 Forward Analysis Models**

There are a total of six ANN models designed to compute the responses of flexible pavements under a typical FWD loading. Two of them were developed for FDP and CFP pavements using the different geometries and layer properties. Although the input variables of these models are different, the outputs are the same for FDP-FW1 and CFP-FW1 and they are given in Table 3.9. Both models were developed to predict the surface deflection values  $D_0, D_{12}, D_{24}$ , and  $D_{36}$  as well as critical pavement responses, i.e.,  $\epsilon_{AC}$ ,  $\epsilon_{SG}$ , and  $\sigma_{DEV}$ . In addition, for both models, the ANN architectures were chosen to have two hidden layers with 60 neurons in each layer. This was according to the findings from similar ANN trainings performed by Ceylan et al. [2005]. Finally, the ANN models were trained for 10,000 epochs.

Similar to the forward models developed for FDP and CFP, two different ANN models were developed to calculate the responses of FDP-LSS and CFP-LSS pavements using the different geometries and layer properties. The input and output variables of the ANN models are also given in Table 3.9. FDP-LSS-FW1 and CFP-LSS-FW1 models were

**Table 3.9:** Forward Artificial Neural Network Models for Flexible Pavements

Name	Inputs	Outputs
FDP-FW1	$t_{AC}, E_{AC}, E_{Ri}$	$D_0, D_{12}, D_{24}, D_{36}, \epsilon_{AC}, \epsilon_{SG}, \sigma_{DEV}$
CFP-FW1	$t_{AC}, t_{GB}, E_{AC}, K_{GB}, E_{Ri}$	$D_0, D_{12}, D_{24}, D_{36}, \epsilon_{AC}, \epsilon_{SG}, \sigma_{DEV}$
FDP-LSS-FW1	$t_{AC}, t_{LSS}, E_{AC}, E_{LSS}, E_{Ri}$	$D_0, D_{12}, D_{24}, D_{36}$
FDP-LSS-FW2	$t_{AC}, t_{LSS}, E_{AC}, E_{LSS}, E_{Ri}$	$\epsilon_{AC}, \epsilon_{SG}, \sigma_{DEV}$
CFP-LSS-FW1	$t_{AC}, t_{GB}, t_{LSS}, E_{AC}, K_{GB}, E_{LSS}, E_{Ri}$	$D_0, D_{12}, D_{24}, D_{36}$
CFP-LSS-FW2	$t_{AC}, t_{GB}, t_{LSS}, E_{AC}, K_{GB}, E_{LSS}, E_{Ri}$	$\epsilon_{AC}, \epsilon_{SG}, \sigma_{DEV}$

developed to predict the surface deflection values  $D_0$ ,  $D_{12}$ ,  $D_{24}$ , and  $D_{36}$  using design thicknesses  $t_{AC}$ ,  $t_{LSS}$  and  $t_{GB}$  (see Table 3.9). Since it is often not desirable to have one ANN model to predict several different outputs at once - the prediction ability of the ANN model is negatively impacted when nonlinear mapping is done for too many output variables in one model - FDP-LSS-FW2 and CFP-LSS-FW2 models were also developed to predict this time the critical pavement responses using the same inputs. For all the models, the ANN architectures were chosen to have two hidden layers with 20 neurons in each layer. This was according to the findings from similar ANN trainings performed by Ceylan et al. [2005]. The ANN models were trained for 10,000 epochs.

One of the basic advantages of the developed ANN models is that they do not require complicated FE inputs that are either difficult or costly to obtain through laboratory and field characterizations for the analyses of flexible pavements. Yet, the solutions still need to consider the needed sophistication in analysis, such as the stress dependent subgrade behavior and the lime-stabilized subgrade layer, as an additional layer on top of the natural unmodified grade, and the realistic layered pavement structure of flexible pavements.

### 3.4.1.1 Performances of the Developed ANN Models

ANN forward calculation models developed for the analyses of flexible pavements were verified for satisfactory performance using the independent testing data extracted from the database of the ILLI-PAVE FE solutions. The performances of ANN models were indicated by comparing predictions with the ILLI-PAVE FE results using AAE values. Figure 3.17 shows the deflections predicted by ANN models at the FWD geophone locations  $D_0, D_{12}, D_{24}$ , and  $D_{36}$  to match very accurately with the ILLI-PAVE results with the given AAE values between 0.2 to 0.5%. The strains ( $\epsilon_{AC}$  and  $\epsilon_{SG}$ ) predicted using ANNs vary on the average by only 2.0% while the subgrade deviator stresses  $\sigma_{DEV}$  predicted change on the average by 1.4% from the ILLI-PAVE FE analysis results (see Figure 3.18). The results for CFPs are given in Figures 3.19 and 3.20 from the ANN model CFP-FW1. This model could predict the surface deflection values with an AAE value of at most 0.3%. Similarly, it was also successful in predicting the critical pavement responses  $\epsilon_{AC}$ ,  $\epsilon_{SG}$ , and  $\sigma_{DEV}$  with AAE values of 0.5%, 0.8%, and 1.8%, respectively. The results proved that very good agreement was achieved when trying to replace ILLI-PAVE solutions with ANN predictions.

Figure 3.21 shows the deflection values predicted using the ANN model FDP-LSS-FW1. Comparisons with ILLI-PAVE results produced AAE values between 0.2 to 0.4% with a maximum error of 1.4%. Figure 3.22 also indicates that the strains  $\epsilon_{AC}$  and  $\epsilon_{SG}$  predicted using ANNs vary on the average by only 0.9% and 1.0%, respectively. On the other hand, the deviator stresses  $\sigma_{DEV}$  predicted on the unmodified subgrade change on the average by 1.5% from the ILLI-PAVE FE analysis results. Even the largest error computed for the subgrade deviator stress corresponds to within 0.1 psi, which is a negligibly small value for all practical engineering design applications with the developed ANN models. This is especially important when considering up to 40% differences in predicted responses computed earlier between the FDP solutions with and without lime.

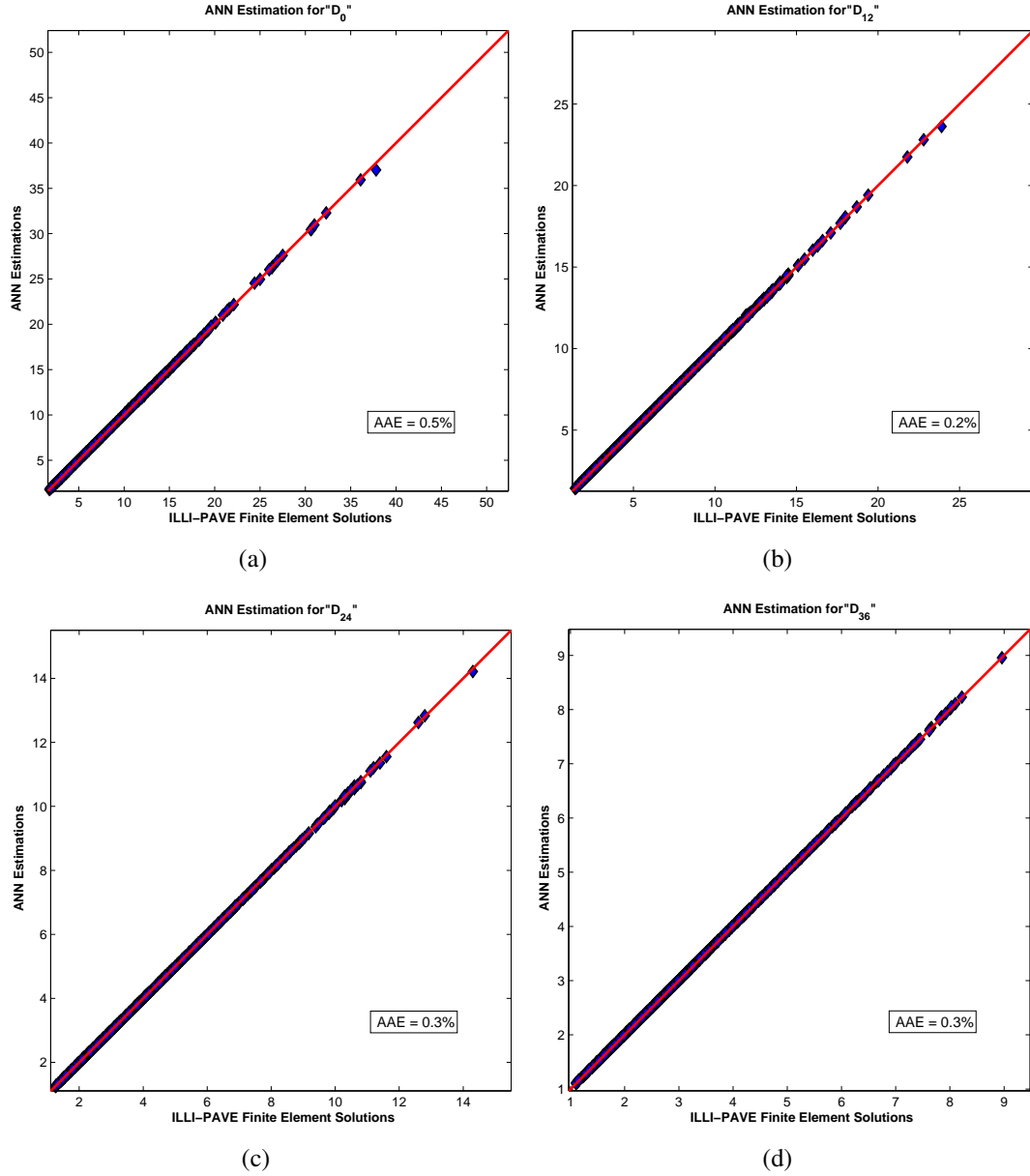


**Figure 3.17:** Comparisons of ANN Structural Model Predictions with ILLI-PAVE Results for Full-depth Asphalt Pavement Surface Deflections (in mils).

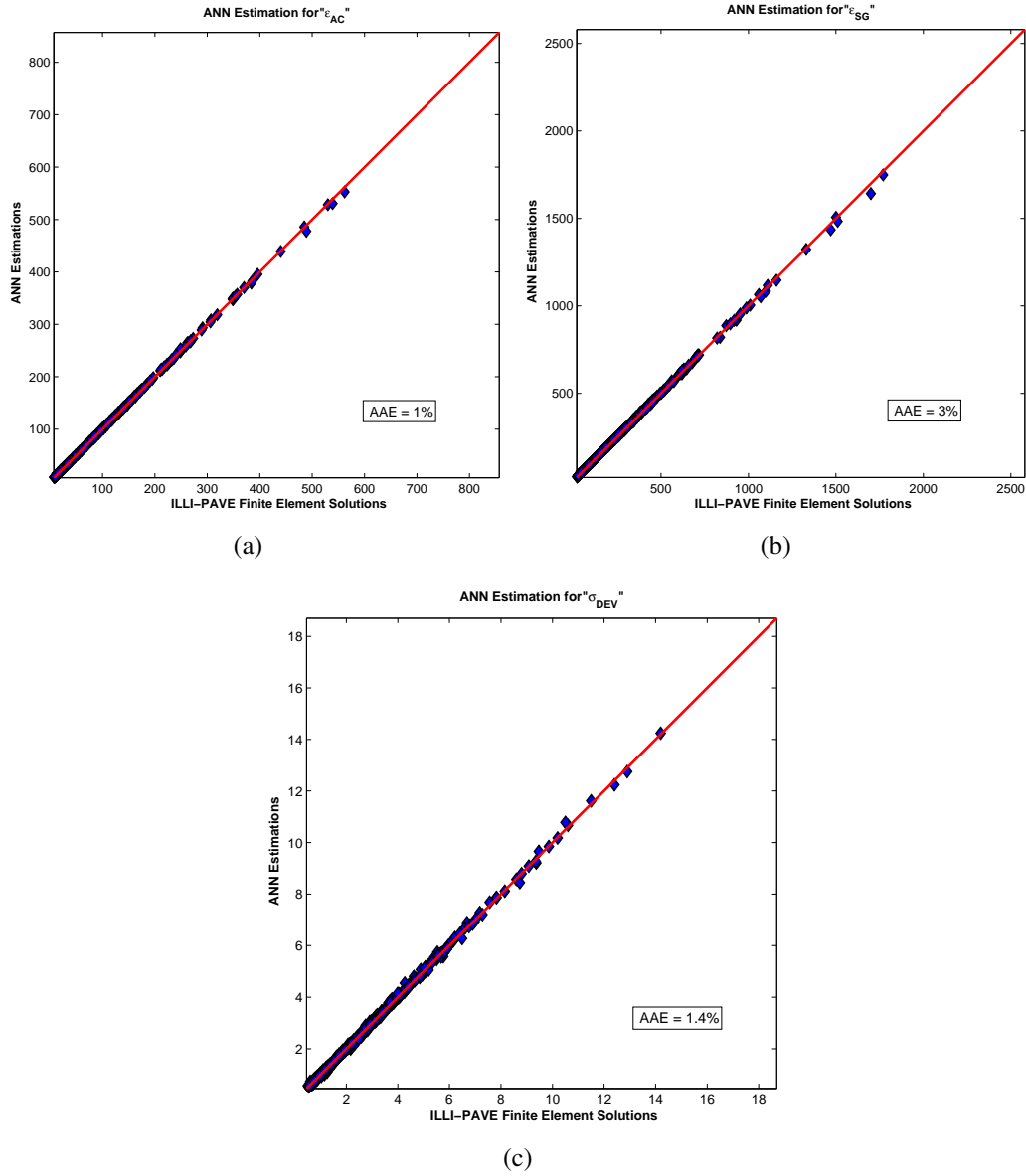


**Figure 3.18:** Comparisons of ANN Structural Model Predictions with ILLI-PAVE Results for Full-depth Asphalt Pavement Critical Pavement Responses (Strains in micro-strain and Stress in psi).

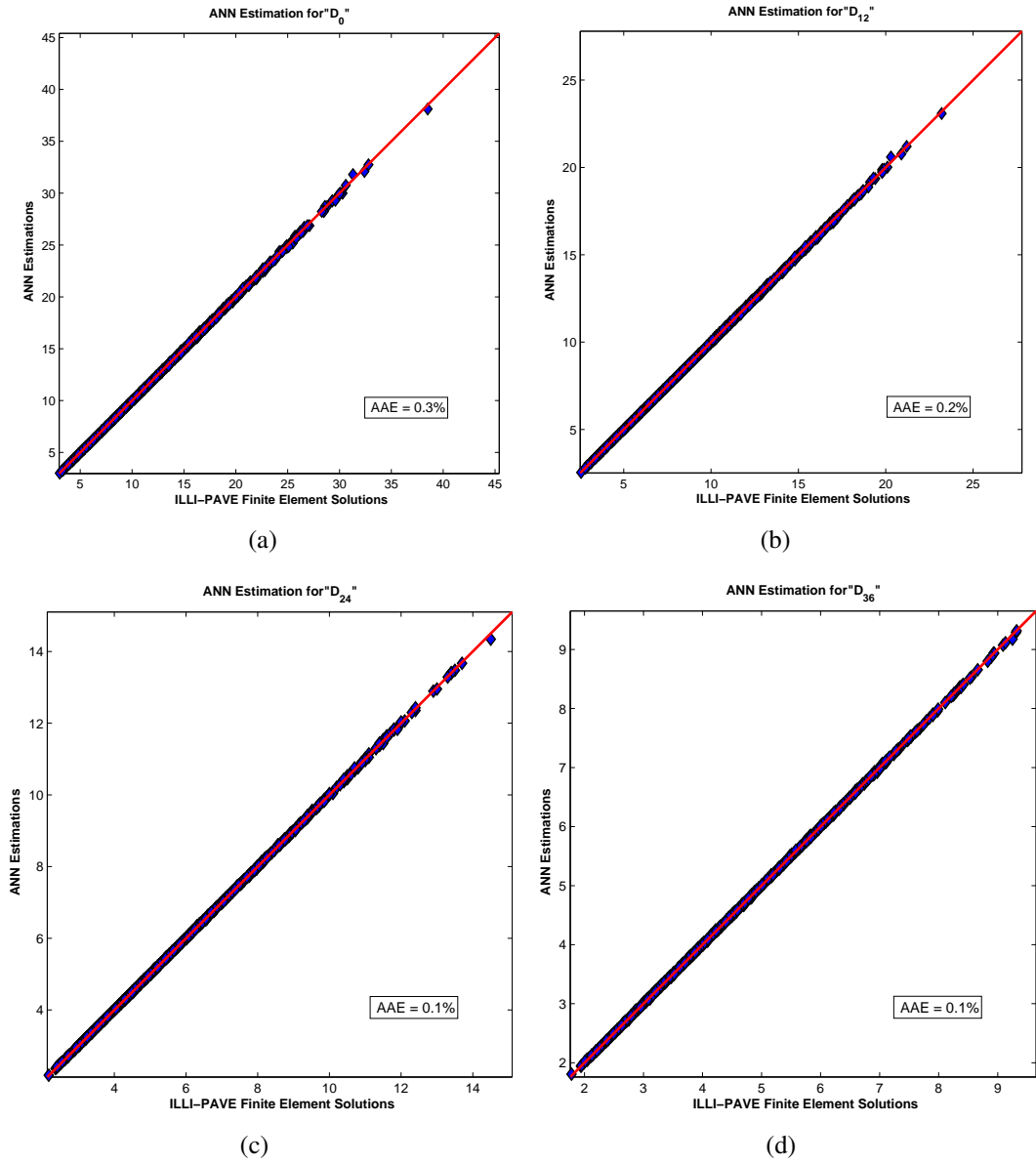
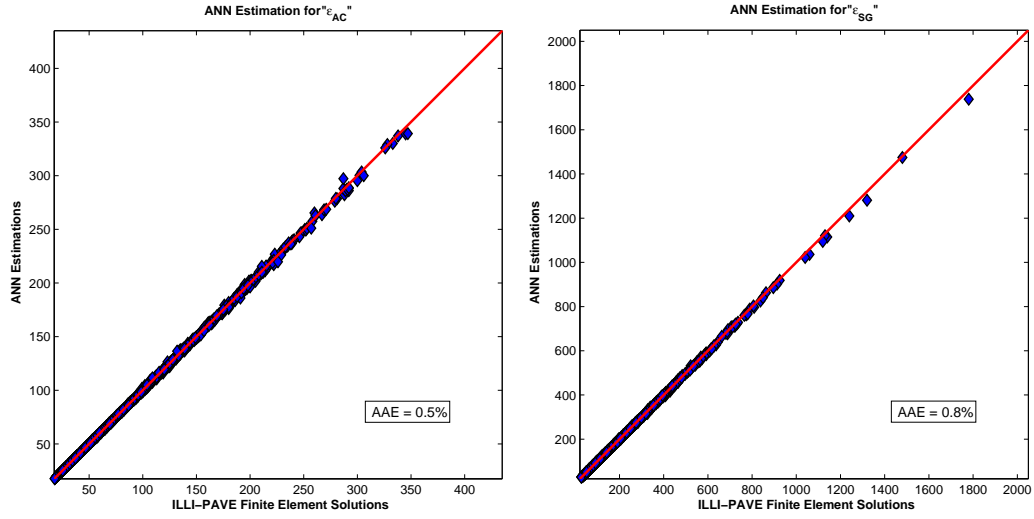
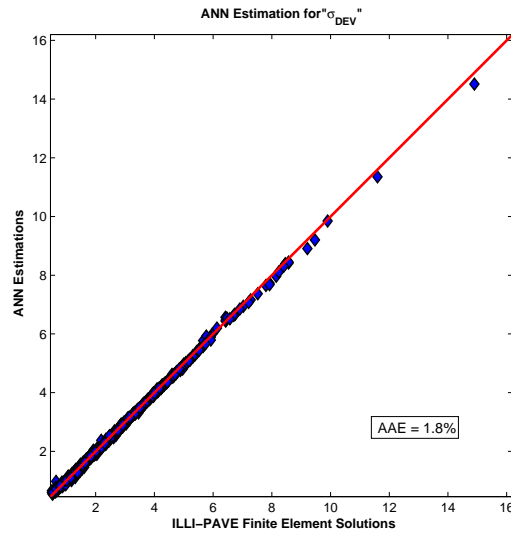


**Figure 3.19:** Comparisons of ANN Structural Model Predictions with ILLI-PAVE Results for Conventional Flexible Pavement Surface Deflections (in mils).



(a)

(b)



(c)

**Figure 3.20:** Comparisons of ANN Structural Model Predictions with ILLI-PAVE Results for Conventional Flexible Pavement Critical Pavement Responses (Strains in micro-strain and Stress in psi).



The ANN model predictions for CFP-LSS are given in Figures 3.23 and 3.24 for Models CFP-LSS-FW1 and CFP-LSS-FW2, respectively. Model FW-1 could predict the surface deflection values with an AAE value of at most 0.4%. For example, this error accounts for 0.05 mils in  $D_0$ . Similarly, model FW-2 was successful in predicting the critical pavement responses  $\epsilon_{AC}$ ,  $\epsilon_{SG}$ , and  $\sigma_{DEV}$  with AAE values of 0.9%, 1.5%, and 1.0%, respectively. Therefore, these results once again have proven that very good agreement could be achieved when trying to replace ILLI-PAVE FE solutions with ANN model predictions. In addition, the developed ANN models eliminated the need for complex FE inputs that are usually not easy to determine in the laboratory or in the field. Consequently, these ANN models can be used successfully for practical structural analyses of pavements. All of the developed ANN forward calculation models were embedded in the Artificial Neural Network for Professionals software (ANN-Pro).

### **3.4.2 Backcalculation Models**

ANNs are very powerful and versatile computational tools for organizing and correlating information for certain types of problems in which the complexity and/or intensiveness of data resources are predominant. As such, ANNs have been used as a new class of computationally intelligent modeling systems for solving many geotechnical and transportation engineering problems including the pavement layer backcalculation application [Meier, 1995]. Yet, pavement structural analysis tools used to train ANN models were mainly linear elastic and did not account for the realistic stress sensitivity of geomaterials. FE programs with the nonlinear, stress dependent geomaterial characterization need to be used to generate solution databases for developing ANN-based structural models. Such uses of ANN models were intended in this section to rapidly and more accurately backcalculate field or in-service pavement layer properties as well as to predict critical stress, strain and deformation responses of these pavements in real time from the measured FWD deflection data.

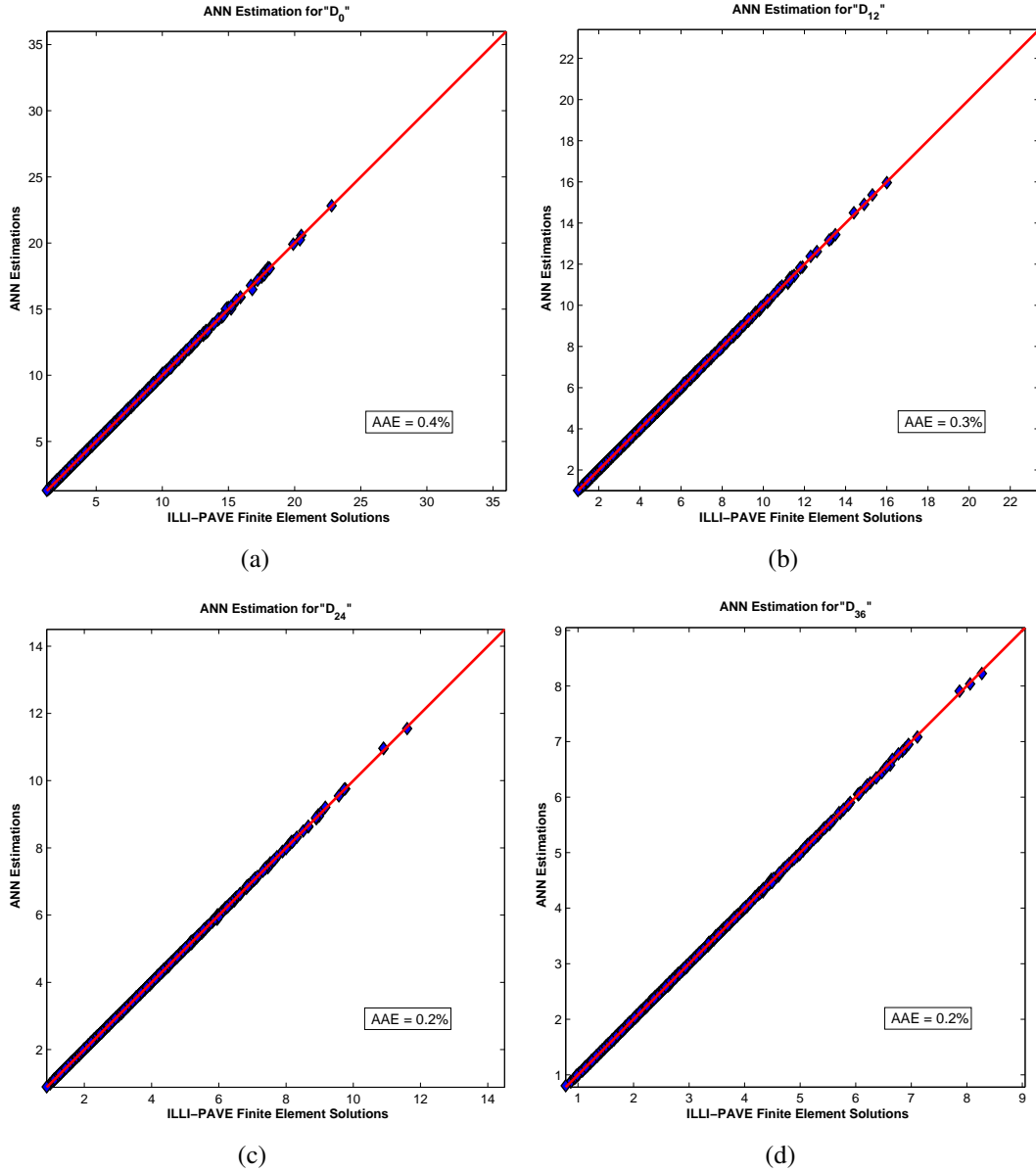
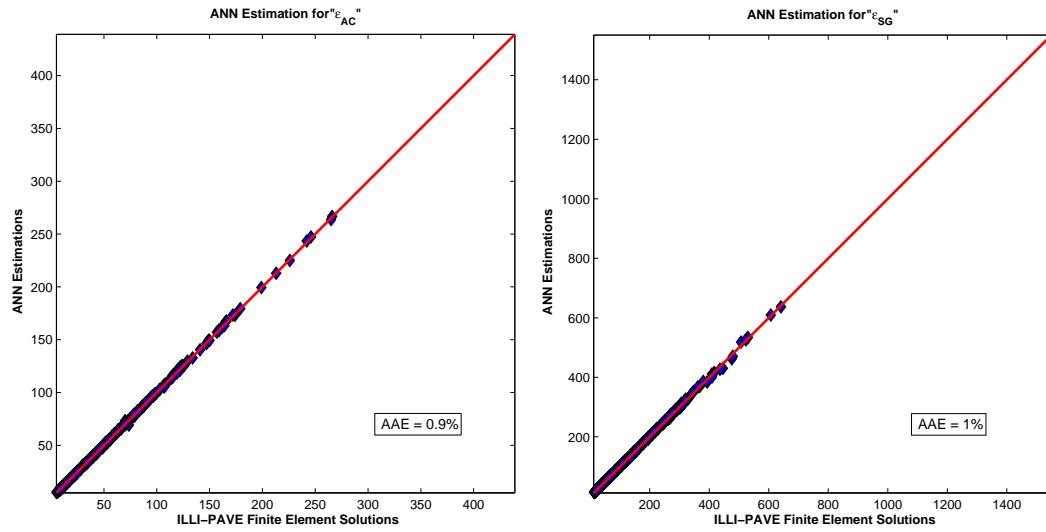
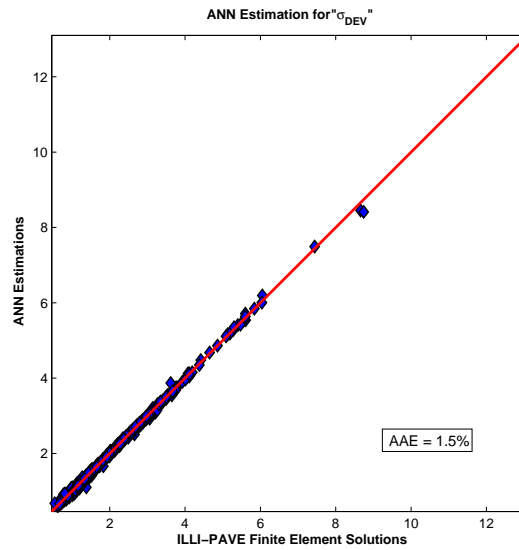


**Figure 3.21:** Comparisons of ANN Structural Model Predictions with ILLI-PAVE Results for Surface Deflections (in mils) of Full-depth Asphalt Pavements Built on Lime Stabilized Soils.



(a)

(b)



(c)

**Figure 3.22:** Comparisons of ANN Structural Model Predictions with ILLI-PAVE Critical Pavement Responses of Full-depth Asphalt Pavements Built on Lime Stabilized Soils (Strains in micro-strain and Stress in psi).

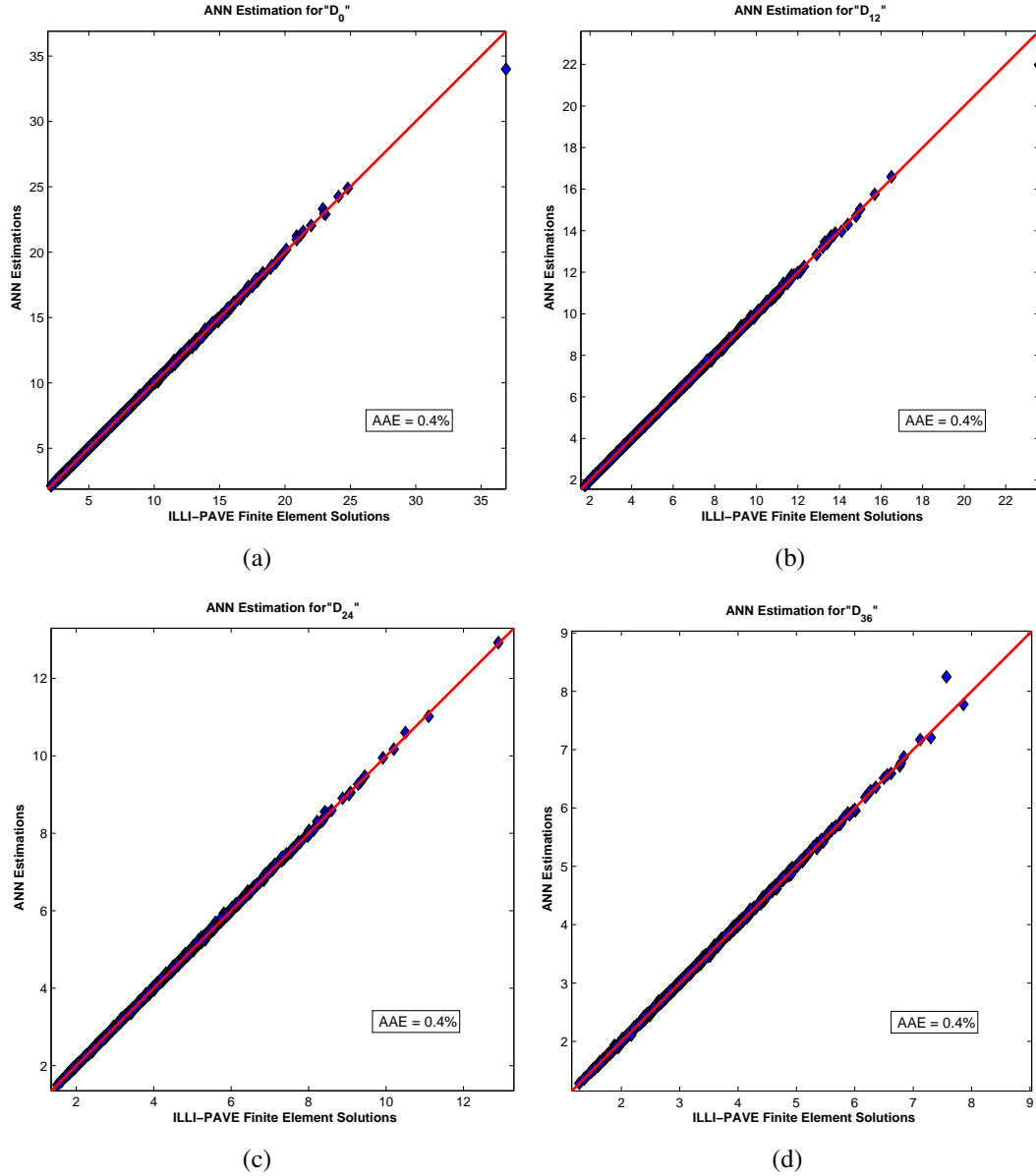
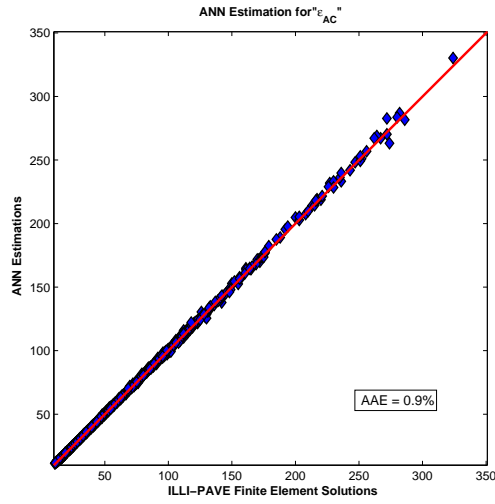
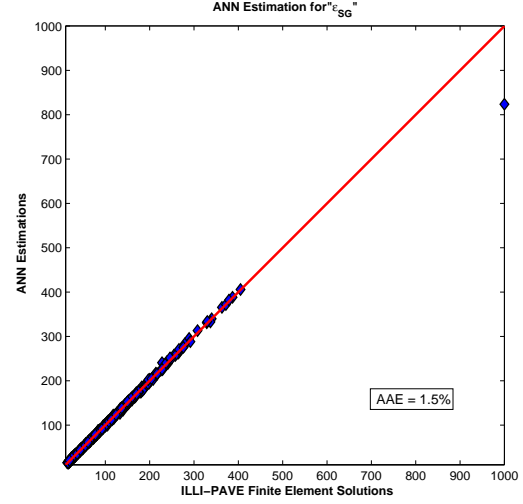


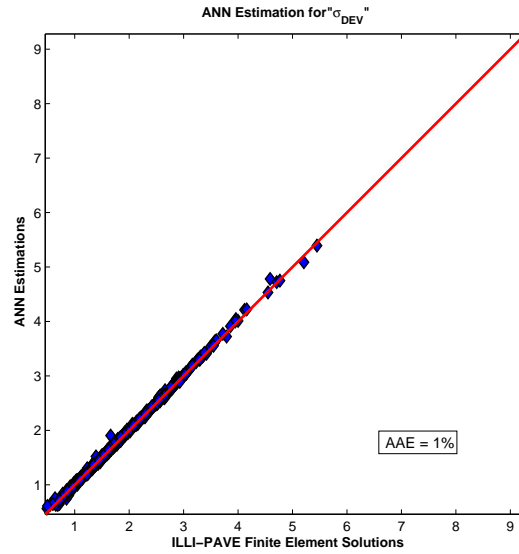
**Figure 3.23:** Comparisons of ANN Structural Model Predictions with ILLI-PAVE Results for Surface Deflections (in mils) of Conventional Flexible Pavements Built on Lime Stabilized Soils.



(a)



(b)



(c)

**Figure 3.24:** Comparisons of ANN Structural Model Predictions with ILLI-PAVE Critical Pavement Responses of Conventional Flexible Pavements Built on Lime Stabilized Soils (Strains in micro-strain and Stress in psi).

The ILLI-PAVE database that was explained in the previous section was used here for training of ANN models in an inverse way. Various backcalculation models were developed for the rapid estimation of pavement layer properties. Two hidden layers were used in all ANN models to have adequate nonlinear functional mapping for computing the pavement responses and moduli of all flexible pavement layers [Ceylan *et al.*, 2005]. The specific ANN models trained and their input and output variables are listed in Tables 3.10 through 3.13. All ANN models had 60 neurons in two hidden layers and they were trained for 10,000 epochs. The ANN models were then tested for their prediction abilities using 1,100 independent testing data sets for CFP and 1,000 testing data sets for FDP, FDP-LSS, and CFP-LSS pavements. The learning rates and the coefficients of momentum were adjusted and optimized to improve the ANN learning process when needed [Haykin, 1999].

FDP-BW1 and CFP-BW1 models predict the layer moduli values from FWD deflections, as indicated in Tables 3.10 and 3.11, for both FDP and CFP pavements. The CFP-BW2 model was trained to predict  $K_{GB}$  for CFPs with the CFP-BW1 results also used as inputs in addition to the FWD deflections. FDP-BW2 and CFP-BW3 models were developed to predict critical pavement responses directly from FWD deflections and layer thicknesses. In doing so, they can also calculate pavement responses without the need for a structural analysis model, such as the ILLI-PAVE FE program.

Similarly, the FDP-LSS-BW1 model uses the deflection values  $D_0$ ,  $D_{12}$ ,  $D_{24}$ , and  $D_{36}$  obtained from an FWD test and the pavement thicknesses  $t_{AC}$  and  $t_{LSS}$  of the FDP-LSS to predict  $E_{AC}$  and  $E_{Ri}$  at the same time. The FDP-LSS-BW2 model takes all inputs and outputs of BW1 and treats them as additional inputs to predict  $E_{LSS}$ . In other words, the use of BW2 requires successful implementation of BW1. After  $E_{AC}$  and  $E_{Ri}$  are estimated, they are then utilized as inputs for the BW2 model. Using the FDP-LSS-BW3 model, critical pavement responses can be calculated (Table 3.12).

Finally, four ANN models are developed for the backcalculation of CFP-LSS pavement layer properties. In all four ANN models developed, the deflection values  $D_0$ ,  $D_{12}$ ,  $D_{24}$ ,

**Table 3.10:** Backcalculation ANN Models for Full-Depth Asphalt Pavements

Name	Inputs	Outputs
FDP-BW1	$D_0, D_{12}, D_{24}, D_{36}, t_{AC}$	$E_{AC}, E_{Ri}$
FDP-BW2	$D_0, D_{12}, D_{24}, D_{36}, t_{AC}$	$\epsilon_{AC}, \epsilon_{SG}, \sigma_{DEV}$

**Table 3.11:** Backcalculation ANN Models for Conventional Flexible Pavements

Name	Inputs	Outputs
CFP-BW1	$D_0, D_{12}, D_{24}, D_{36}, t_{AC}, t_{GB}$	$E_{AC}, E_{Ri}$
CFP-BW2	$D_0, D_{12}, D_{24}, D_{36}, t_{AC}, t_{GB}, E_{AC}, E_{Ri}$	$K_{GB}$
CFP-BW3	$D_0, D_{12}, D_{24}, D_{36}, t_{AC}, t_{GB}$	$\epsilon_{AC}, \epsilon_{SG}, \sigma_{DEV}$

**Table 3.12:** Backcalculation ANN Models for Full-Depth Asphalt Pavements on Lime Stabilized Soils

Name	Inputs	Outputs
FDP-LSS-BW1	$D_0, D_{12}, D_{24}, D_{36}, t_{AC}, t_{LSS}$	$E_{AC}, E_{Ri}$
FDP-LSS-BW2	$D_0, D_{12}, D_{24}, D_{36}, t_{AC}, t_{LSS}, E_{AC}, E_{Ri}$	$E_{LSS}$
FDP-LSS-BW3	$D_0, D_{12}, D_{24}, D_{36}, t_{AC}, t_{LSS}$	$\epsilon_{AC}, \epsilon_{SG}, \sigma_{DEV}$

**Table 3.13:** Backcalculation ANN Models for Conventional Flexible Pavements on Lime Stabilized Soils

Name	Inputs	Outputs
CFP-LSS-BW1	$D_0, D_{12}, D_{24}, D_{36}, t_{AC}, t_{GB}, t_{LSS}$	$E_{AC}, E_{Ri}$
CFP-LSS-BW2	$D_0, D_{12}, D_{24}, D_{36}, t_{AC}, t_{GB}, t_{LSS}$	$\epsilon_{AC}, \epsilon_{SG}, \sigma_{DEV}$
CFP-LSS-BW3	$D_0, D_{12}, D_{24}, D_{36}, D_{48}, D_{60}, D_{72}, t_{AC}, t_{GB}, t_{LSS}, \epsilon_{AC}, \epsilon_{SG}, \sigma_{DEV}$	$K_{GB}$
CFP-LSS-BW4	$D_0, D_{12}, D_{24}, D_{36}, D_{48}, D_{60}, D_{72}, t_{AC}, t_{GB}, t_{LSS}, E_{AC}, E_{Ri}, K_{GB}$	$E_{LSS}$

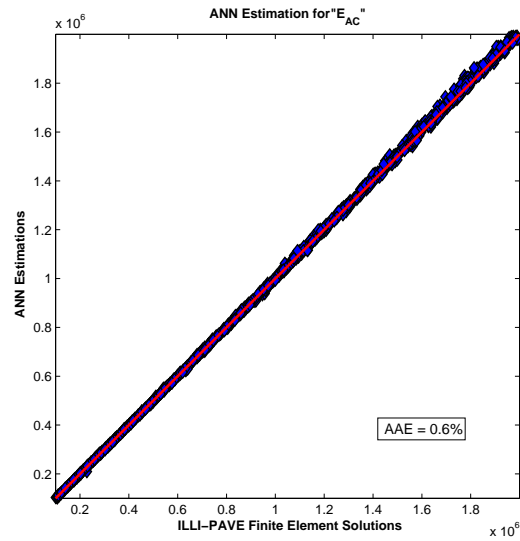
$D_{36}$ ,  $D_{48}$ ,  $D_{60}$ , and  $D_{72}$  obtained from FWD testing and the pavement thicknesses  $t_{AC}$ ,  $t_{GB}$ , and  $t_{LSS}$  were used as inputs. The CFP-LSS-BW1 model is used to backcalculate just the layer moduli  $E_{AC}$  and  $E_{Ri}$ , while the CFP-LSS-BW2 model predicts the critical pavement responses  $\epsilon_{AC}$ ,  $\epsilon_{SG}$ , and  $\sigma_{DEV}$ . These are the first two ANN models to run for a given problem set. A sequential approach thereby employed computes next the remaining GB and LSS layer properties such that the CFP-LSS-BW3 model uses the critical pavement responses obtained from the CFP-LSS-BW2 model to determine  $K_{GB}$ . Similarly, the CFP-LSS-BW4 model requires the CFP-LSS-BW3 output  $K_{GB}$  to determine  $E_{LSS}$  accurately (Table 3.12). In practice, models 3 and 4 may produce less accurate results since the errors can be cumulative.

#### **3.4.2.1 Performances of the Developed ANN Models**

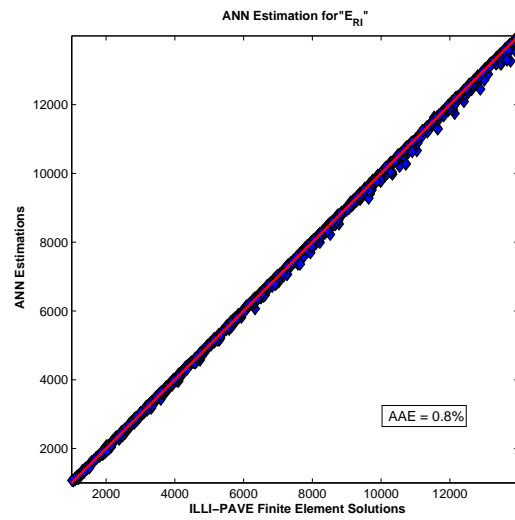
The performances of the developed ANN models are illustrated in Figures 3.25 to 3.26 along with the computed AAE values. Figures 3.25 and 3.27 indicate that the asphalt concrete moduli of both FDP and CFP pavements were predicted with the lowest AAEs when compared to those of the base and subgrade nonlinear modulus model parameters. Usually,  $K_{GB}$  was found to be the most difficult to predict, although in this case, the combined use of the CFP-BW1 and CFP-BW2 models worked quite effectively for improving predictions. All critical pavement responses were also predicted quite successfully with AAE values less than 6.1% corresponding to very low and almost negligible values of actual strain and stress magnitudes (see Figures 3.26 and 3.28).

ANN model performances for backcalculated FDP-LSS pavement layer moduli are given in Figures 3.29(a) to 3.29(c). The AAEs given indicate that the FDP-LSS-BW1 model could predict ILLI-PAVE solutions within very low 1.3% and 2.1% AAEs for  $E_{AC}$  and  $E_{Ri}$ , respectively, while the accuracy of the FDP-LSS-BW2 model for the prediction of  $E_{LSS}$  remains within a very low AAE of 2.3%. All critical pavement responses were also predicted quite successfully (see Figure 3.30). The maximum AAE value of 3.2% was



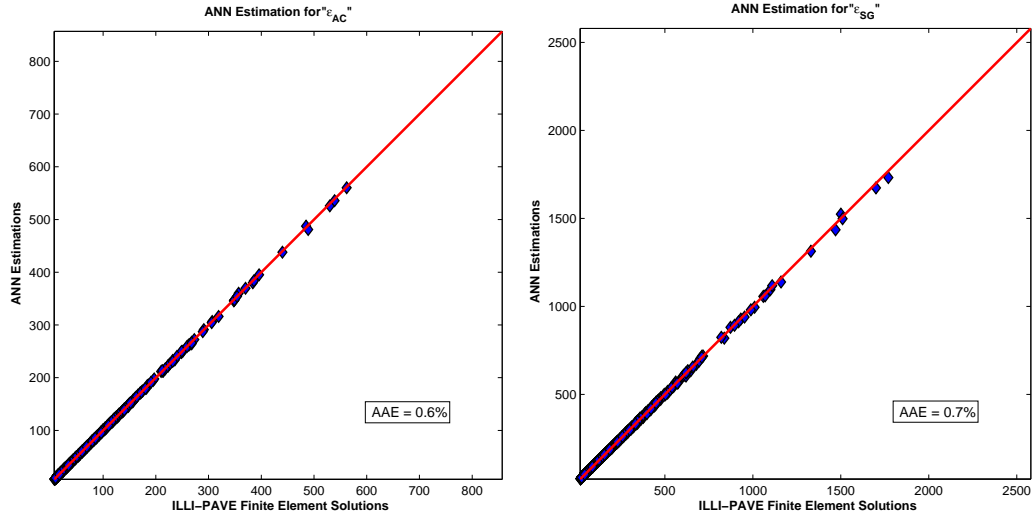


(a)



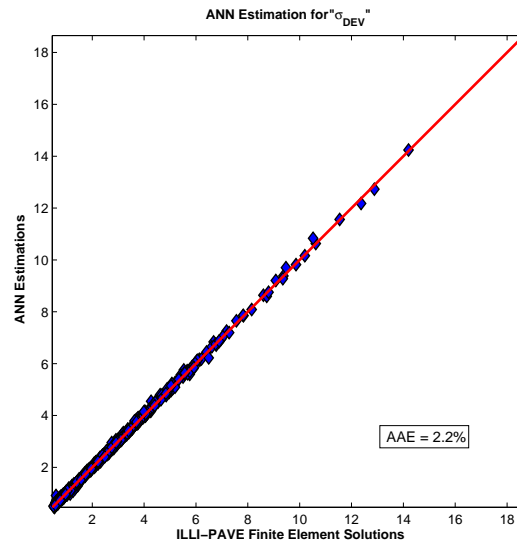
(b)

**Figure 3.25:** Performances of ANN Backcalculation Models for Predicting Layer Moduli (in psi) of Full-depth Asphalt Pavements.



(a)

(b)



(c)

**Figure 3.26:** Performances of ANN Backcalculation Models for Predicting Critical Pavement Responses of Full-depth Asphalt Pavements (Strains in micro-strain and Stress in psi).

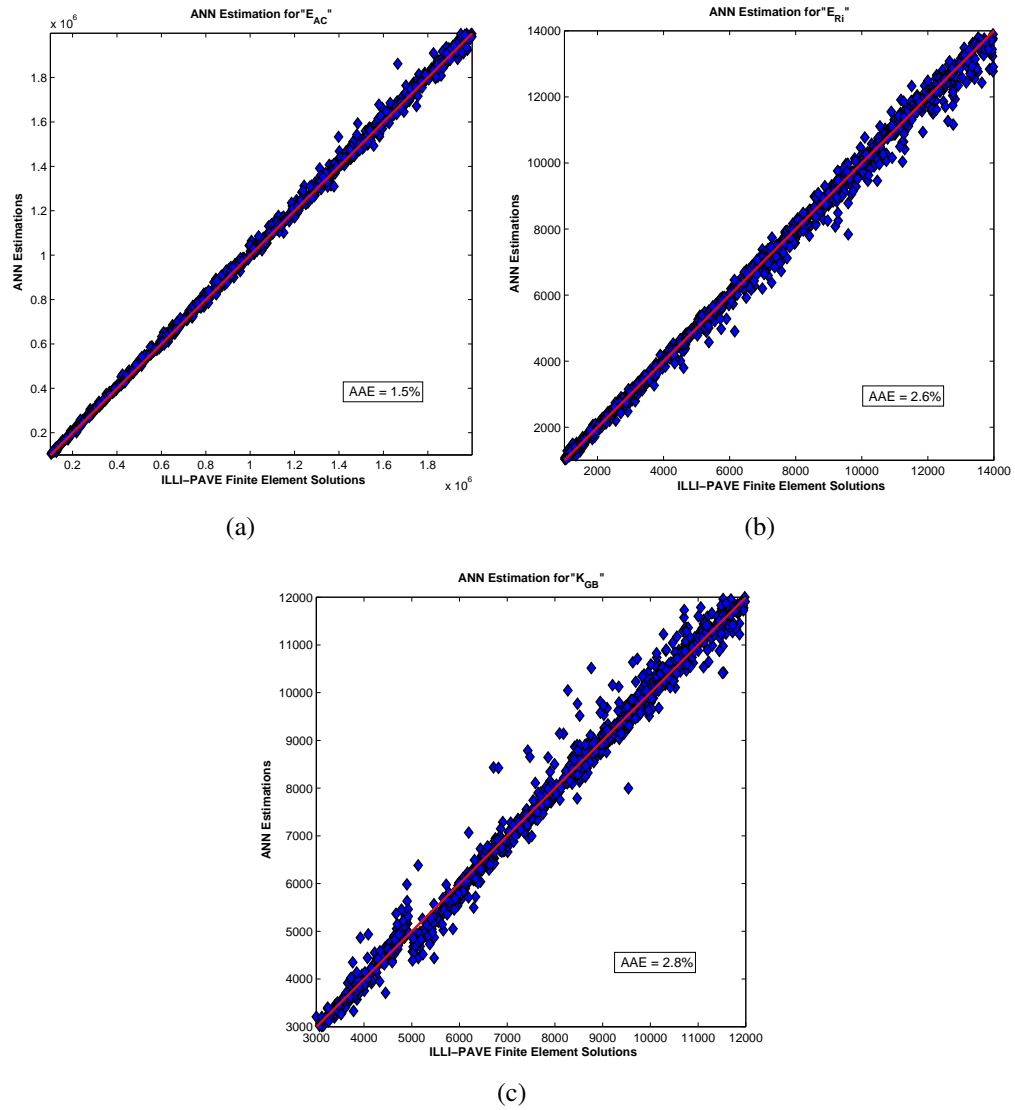
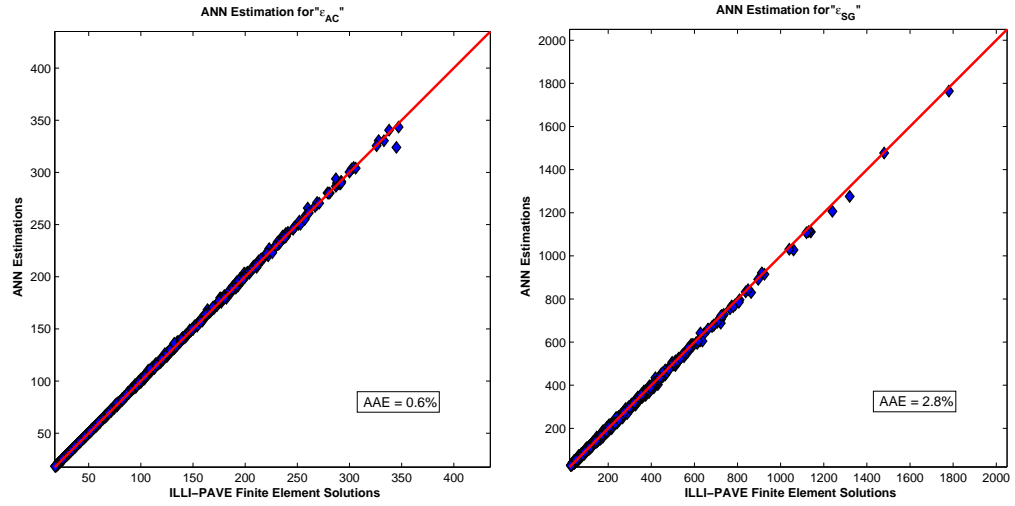
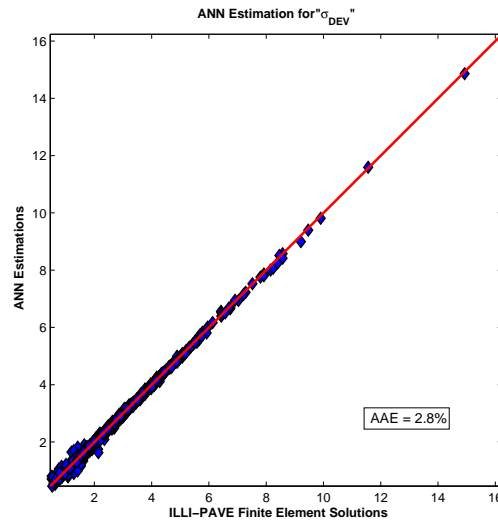


**Figure 3.27:** Performances of ANN Backcalculation Models for Predicting Layer Moduli (in psi) of Conventional Flexible Pavements.



(a)

(b)



(c)

**Figure 3.28:** Performances of ANN Backcalculation Models for Predicting Critical Pavement Responses of Conventional Flexible Pavements (Strains in micro-strain and Stress in psi).

obtained for the subgrade deviator stress and the strain predictions had much lower AAE values.

Comparisons of CFP-LSS pavement layer moduli predictions with ILLI-PAVE results are given in Figures 3.31(a) through 3.31(d) with the corresponding AAE values [Pekcan *et al.*, 2008a]. The CFP-LSS-BW1 model could predict  $E_{AC}$  and  $E_{Ri}$  values in the ILLI-PAVE database within AAE values of 2.1% and 4.7%, respectively. In addition, AAE values from the CFP-LSS-BW2 model are 0.9%, 6.1%, and 4.6% for  $\epsilon_{AC}$ ,  $\epsilon_{SG}$ , and  $\sigma_{DEV}$ , respectively (see Figure 3.32). The predictions of  $K_{GB}$  and  $E_{LSS}$  layer properties, however, produced slightly higher AAE values of 2.7% and 6.6%, respectively. It was observed that the layer properties that could not be predicted with high accuracy by CFP-LSS-BW3 and CFP-LSS-BW4 usually belonged to the pavement sections with extremely thick LSS and GB layers. In practice, however, these pavement geometries are very rare in Illinois and often not constructed with proper quality control and quality assurance practices.

### 3.5 Field Validation

The performances of the developed ANN models were deemed to be adequately verified using the testing data sets by the good comparisons of ANN model predictions with the ILLI-PAVE results. However, it is always necessary to validate ANN model performances using actual field data especially when the training database has been created synthetically such as in this case using the ILLI-PAVE FE analyses. For this purpose, field data were collected from three highway condition assessment and rehabilitation projects provided by the IDOT Bureau of Materials and Physical Research and used for the performance validations of the developed ANN models. The field data included both the FWD results as well as the information and test results obtained from cored pavement sections collected from the FWD locations. Note that most of the FDP sections in Illinois are built on

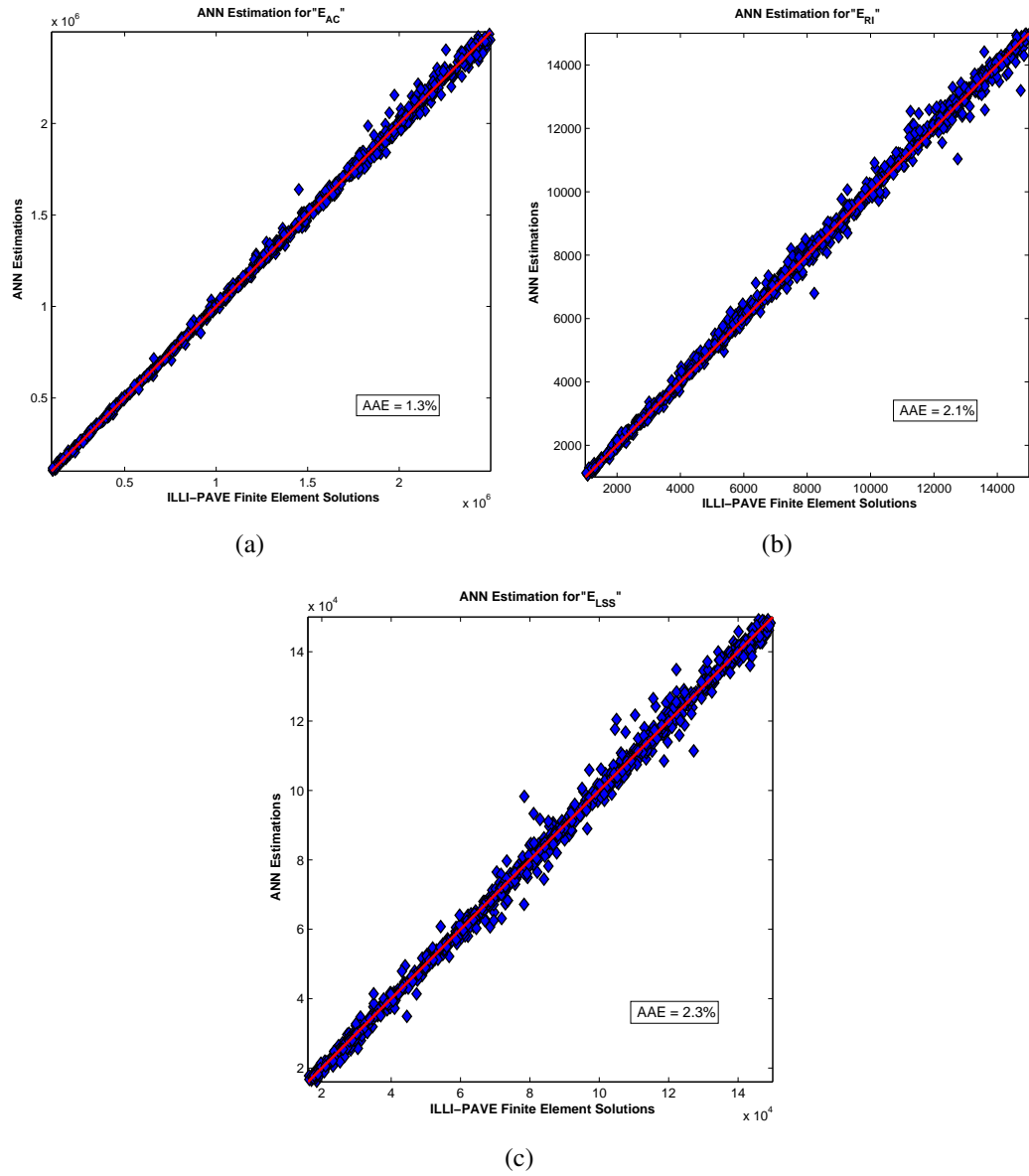
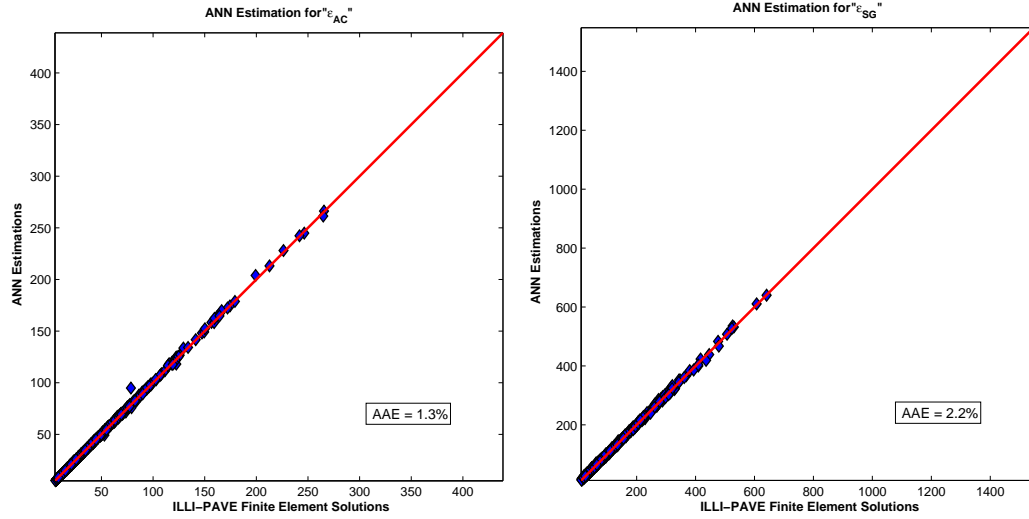
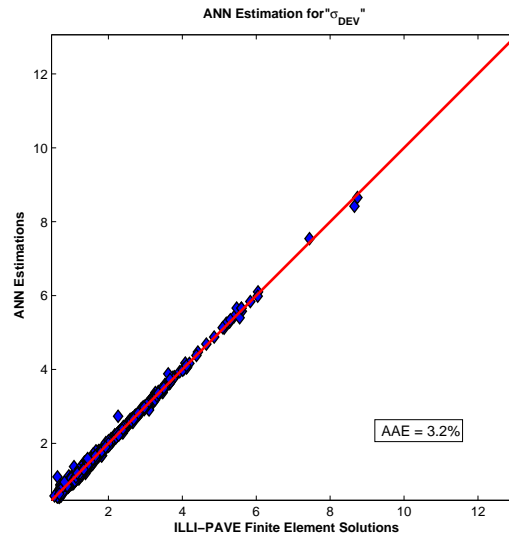


**Figure 3.29:** Performances of ANN Backcalculation Models for Predicting Layer Moduli (in psi) of Full-depth Asphalt Pavements Built on Lime Stabilized Soils.



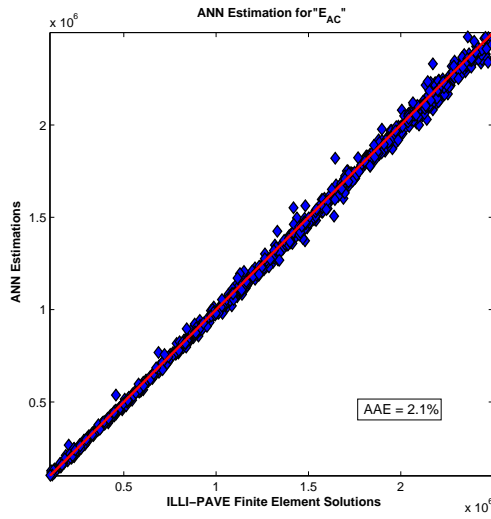
(a)

(b)

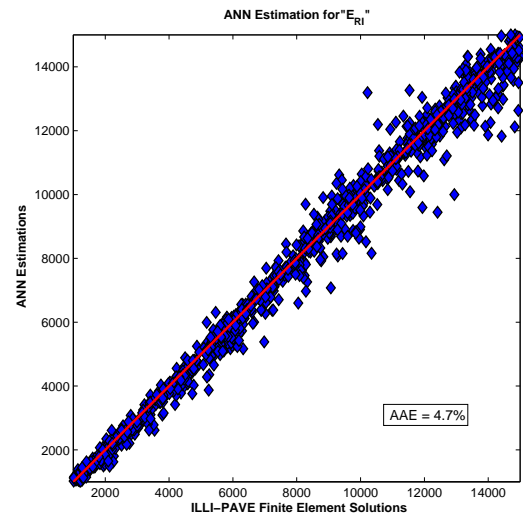


(c)

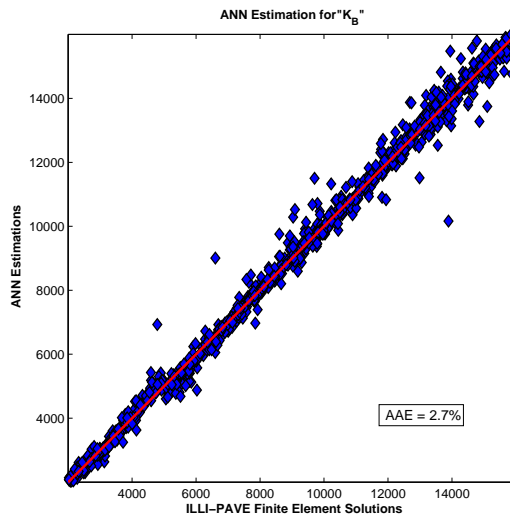
**Figure 3.30:** Performances of ANN Backcalculation Models for Predicting Critical Pavement Responses of Full-depth Asphalt Pavements Built on Lime Stabilized Soils (Strains in micro-strain and Stress in psi).



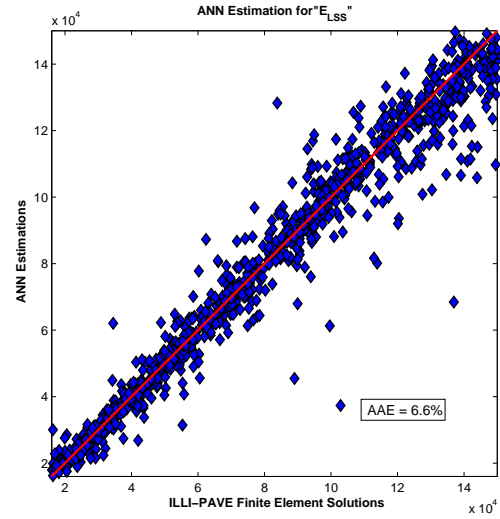
(a)



(b)



(c)



(d)

**Figure 3.31:** Performances of ANN Backcalculation Models For Predicting Layer Moduli (in psi) of Conventional Flexible Pavements Built on Lime Stabilized Soils.



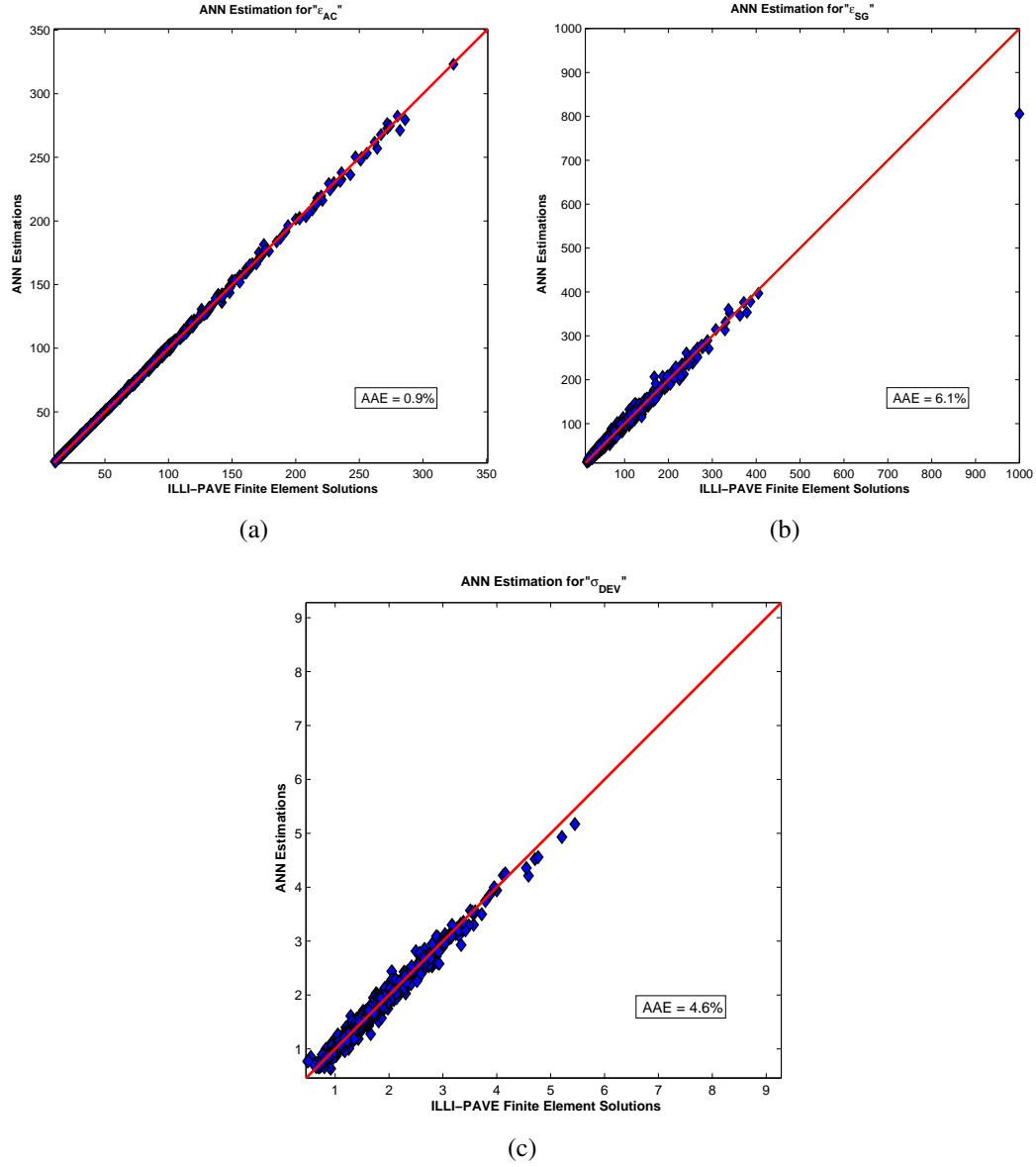


**Figure 3.32:** Performances of ANN Backcalculation Models for Predicting Critical Pavement Responses of Conventional Flexible Pavements Built on Lime Stabilized Soils (Strains in micro-strain and Stress in psi).

lime stabilized soils although a very few sections also exist that are built on unmodified subgrade.

In addition, two sets of backcalculation algorithms, given below in Equations 3.6 to 3.9, for  $E_{AC}$  and  $E_{Ri}$  were chosen from the previous studies and/or current practice and used to further verify ANN model predictions for comparisons. Equations 3.4 to 3.7, referred to hereafter as Hill's algorithms [Hill & Thompson, 1988], were separately developed with and without the consideration of existing LSS layers in FDPs, whereas, Equations 3.8 and 3.9, referred to hereafter as Thompson's algorithms, were developed only for FDPs without taking into account LSS layers [Thompson, 1989]. Note that Thompson's algorithms provide the set of equations currently in use by IDOT for FDP layer modulus backcalculation. All of these equations were developed based on ILLI-PAVE solutions and the statistical regression analyses of the field collected data, FWD test results with standard 9,000 lb. loading, with a minimum correlation coefficient  $R^2$  of 0.98 reported in the literature. In these equations, no temperature correction was included in backcalculation to account for different field pavement temperatures based on seasonal and daily temperature fluctuations.

*Hill's Equations for No-Lime Sections:*

$$\begin{aligned} \log(E_{AC}) = & 3.516 - 5.045 \log(D_0 - D_{24}) - 0.479 \frac{(D_0 - D_{36})}{(D_{12} - D_{24})} \\ & + 4.082 \log(D_{12} - D_{36}) + 1.237 \frac{(D_0 - D_{24})}{(D_{12} - D_{36})} \end{aligned} \quad (3.4)$$

$$\begin{aligned} E_{Ri} = & -136.1 + 106.4 \frac{\log(D_{24})}{\log(D_{36})} - 3.33 \left( \frac{D_{12}}{D_{36}} \right) + 87.78 \frac{\log(D_{12})}{\log(D_{24})} \\ & - 58.75 \frac{\log(D_{12})}{\log(D_{36})} - 4.27 \log(D_{12} - D_{24}) \end{aligned} \quad (3.5)$$

*Hill's Equations for Lime Stabilized Sections:*

$$\begin{aligned}\log(E_{AC}) = & 2.824 - 4.083 \log(D_0 - D_{12}) + 3.478 \log(D_0 - D_{24}) \\ & - 0.375 \log(D_{12} - D_{36}) - 0.382 \frac{(D_{12} - D_{36})}{(D_{12} - D_{24})}\end{aligned}\quad (3.6)$$

$$\begin{aligned}E_{Ri} = & 46.71 + 23.74 \frac{\log(D_{24})}{\log(D_{36})} - 89.72 \left(\frac{D_{24}}{D_{36}}\right) + 335.69 \log\left(\frac{D_{24}}{D_{36}}\right) \\ & - 13.17 \log(D_{24} - D_{36}) + 5.20 \frac{(D_{12} - D_{36})}{(D_{12} - D_{24})}\end{aligned}\quad (3.7)$$

*Thompson's Equations:*

$$\begin{aligned}\log(E_{AC}) = & 1.846 - 4.902 \log(D_0 - D_{12}) + 5.189 \log(D_0 - D_{24}) \\ & - 1.282 \log(D_{12} - D_{36})\end{aligned}\quad (3.8)$$

$$E_{Ri} = 24.7 - 5.41 D_{36} + 0.31 (D_{36})^2 \quad (3.9)$$

where  $E_{AC}$  and  $E_{Ri}$  are in ksi and  $D_0$ ,  $D_{12}$ ,  $D_{24}$ , and  $D_{36}$  are in mils.

### **3.5.1 US 50 (FAP 327, old FA 409)**

US 50 is located in both St. Clair County and Clinton County in Illinois. The design pavement section is 9.5 in. of HMA built on unmodified subgrade. The FWD data belonging to test section K in St. Clair County and section M2 in Clinton County were analyzed. The pavement temperature was reported to be 95°F for both sections on the day of FWD tests. Figures 3.33(a) to 3.33(d) show the performances of the ANN models developed for FDP pavements in comparison to the predictions from Hill's and Thompson's backcalculation algorithms (Equations 3.4, 3.5, 3.8 and 3.9) for  $E_{AC}$  and  $E_{Ri}$ .

### **3.5.2 US 20 (FAP 301, old FA 401)**

US 20 is located in Stephenson County in Illinois. The design pavement section is 13 in. of HMA built on unmodified subgrade. The FWD tests were performed on both sections A and B, which are approximately 200 ft. in length. The pavement temperature was reported to be 99°F for both sections on the day of FWD tests. Figures 3.34(a) to 3.34(d) show the performances of the ANN models developed for FDP pavements in comparison to the predictions from Hill's and Thompson's backcalculation algorithms (Equations 3.4, 3.5, 3.8 and 3.9) for  $E_{AC}$  and  $E_{Ri}$ .

### **3.5.3 Roseville Bypass**

Roseville Bypass is a connector road to accommodate US-67 traffic. The design pavement cross section consists of 14 in. of HMA and a 12 in. thick LSS layer. The FWD tests were performed on part C of the Roseville Bypass, which is a connector road approximately 300 ft. in length. The pavement temperature was reported as 97°F along the road during the FWD tests. Figures 3.35(a) to 3.35(d) show the performances of the ANN models developed for FDP-LSS pavements in comparison to the predictions from Hill's and Thompson's backcalculation algorithms (Equations 3.6, 3.7, 3.8 and 3.9) for  $E_{AC}$  and  $E_{Ri}$ .

### **3.5.4 Staley Road**

Staley Road runs in north-south direction and is located on the west end of the City of Champaign in Champaign County, Illinois. The design pavement cross section consists of 12 in. of HMA constructed on LSS with a thickness of 12 in. The FWD tests were performed along a 2-mile stretch of highway. The pavement temperature was reported as 75°F along the road on the day of FWD tests. Figures 3.36(a) to 3.36(d) show the performances of the ANN models developed for FDP-LSS pavements for Staley road in

comparison to the predictions from Hill's and Thompson's backcalculation algorithms (Equations 3.6, 3.7, 3.8 and 3.9) for  $E_{AC}$  and  $E_{Ri}$ .

### **3.5.5 High Cross Road (FA 808)**

High Cross Road is located in the southeast corner of the City of Urbana in Champaign County, Illinois. The pavement cross section from original design consists of 11 in. of hot mix asphalt (HMA) surface on top of 11 in. of LSS. The FWD tests were performed along highway sections 201 and 201B. The total length of highway mileage for the FWD data collection was approximately 2.28 miles. The pavement temperature was approximately 54°F when the FWD tests were performed. Figures 3.37(a) to 3.37(d) show the backcalculation performances of the ANN models developed for FDP-LSS pavements for High Cross Road in comparison to the predictions from Hill's and Thompson's backcalculation algorithms (Equations 3.6, 3.7, 3.8 and 3.9) for  $E_{AC}$  and  $E_{Ri}$ .

For all the field validation performances shown in Figures 3.35 to 3.37, ANN-LSS models captured the AC modulus of FDP-LSS pavements practically the same with both Hill's and Thompson's algorithms. This is possibly due to the fact the effect of LSS is mostly pronounced in the estimation of  $E_{Ri}$  and the AC layer moduli are not affected significantly by the presence of the LSS layer. However, Hill's equations, developed for the FDP-LSS pavements, produced overall better and more comparable estimates with the ANN models. This was clearly indicated as Hill's  $E_{Ri}$  predictions were better centered on the 45-degree equality line with the ANN predictions whereas  $E_{Ri}$  values predicted by Thompson's algorithms were in general much lower in magnitude than the ANN results. A possible explanation of this is linked to the nonlinear stress dependent modulus behavior of the fine-grained subgrade soils as shown in Figure 3.5. As the wheel load deviator stresses become lower under the LSS layer, typically higher moduli are predicted for the untreated subgrade layer by the ANN models in comparison to those estimated by Thompson's algorithm.

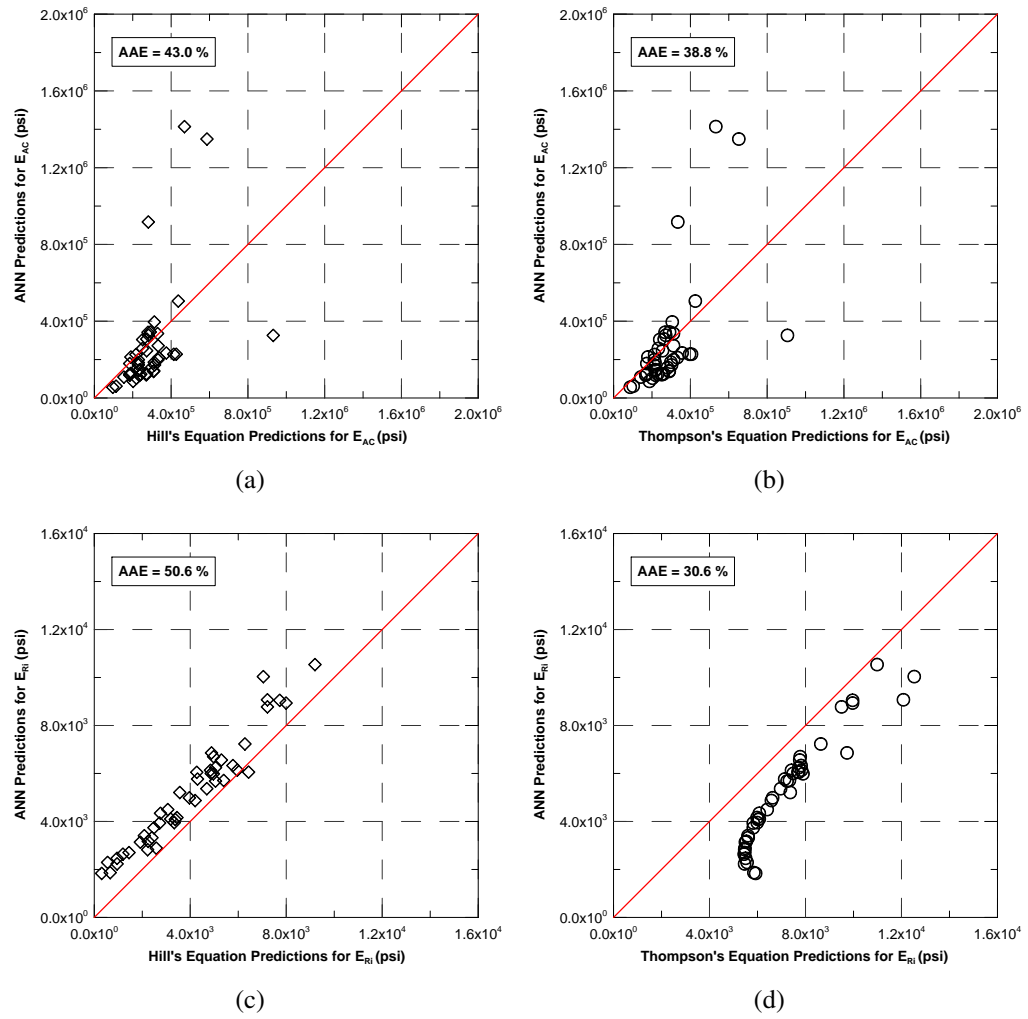


**Figure 3.33:** Performances of FDP ANN Models for US 50.

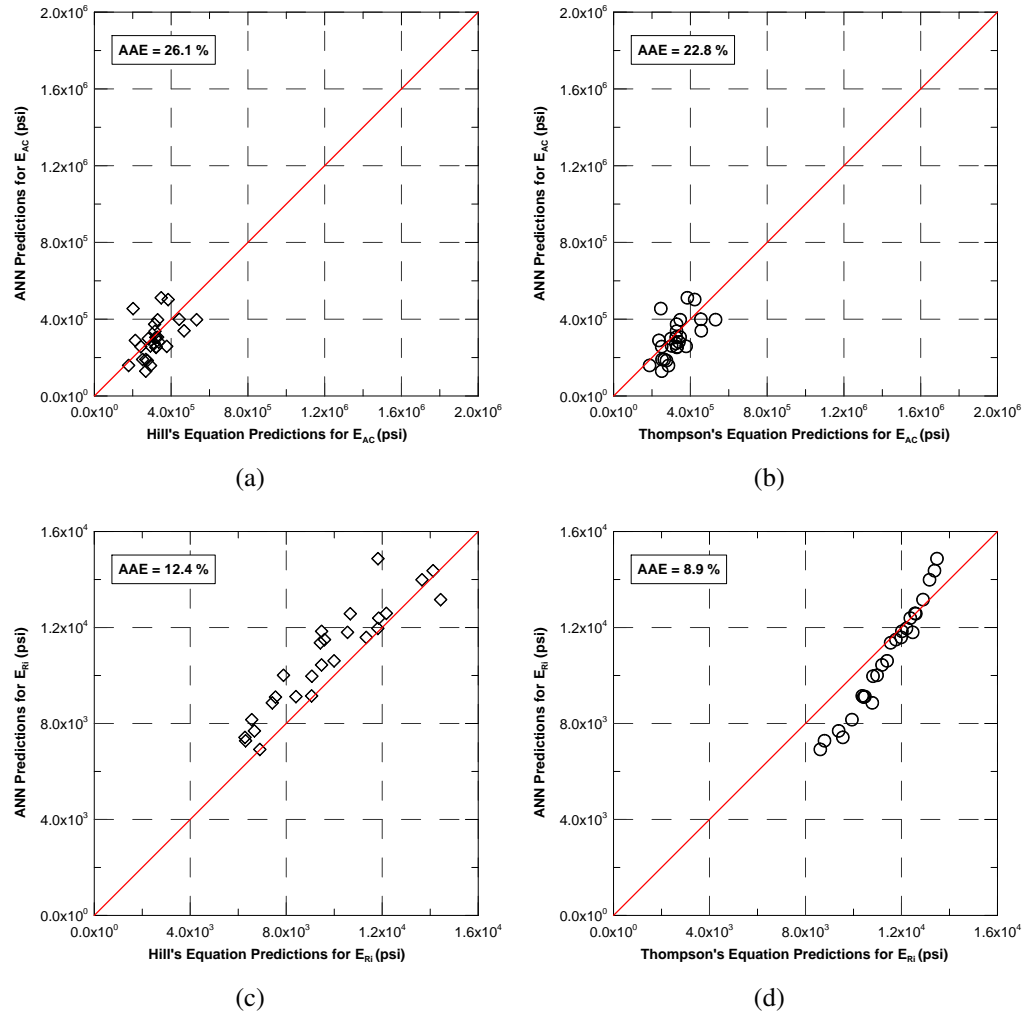


**Figure 3.34:** Performances of FDP ANN Models for US 20.

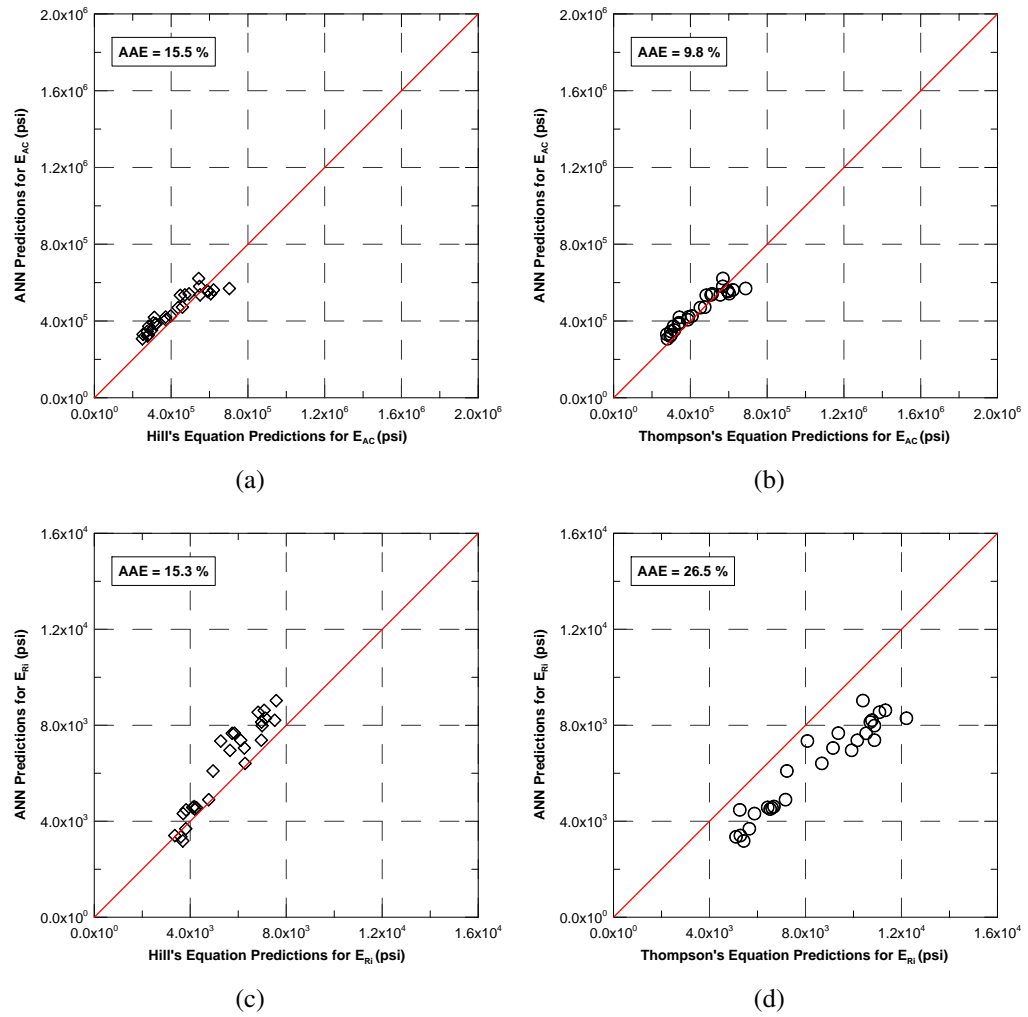


**Figure 3.35:** Performances of FDP-LSS ANN Models for Roseville Bypass.



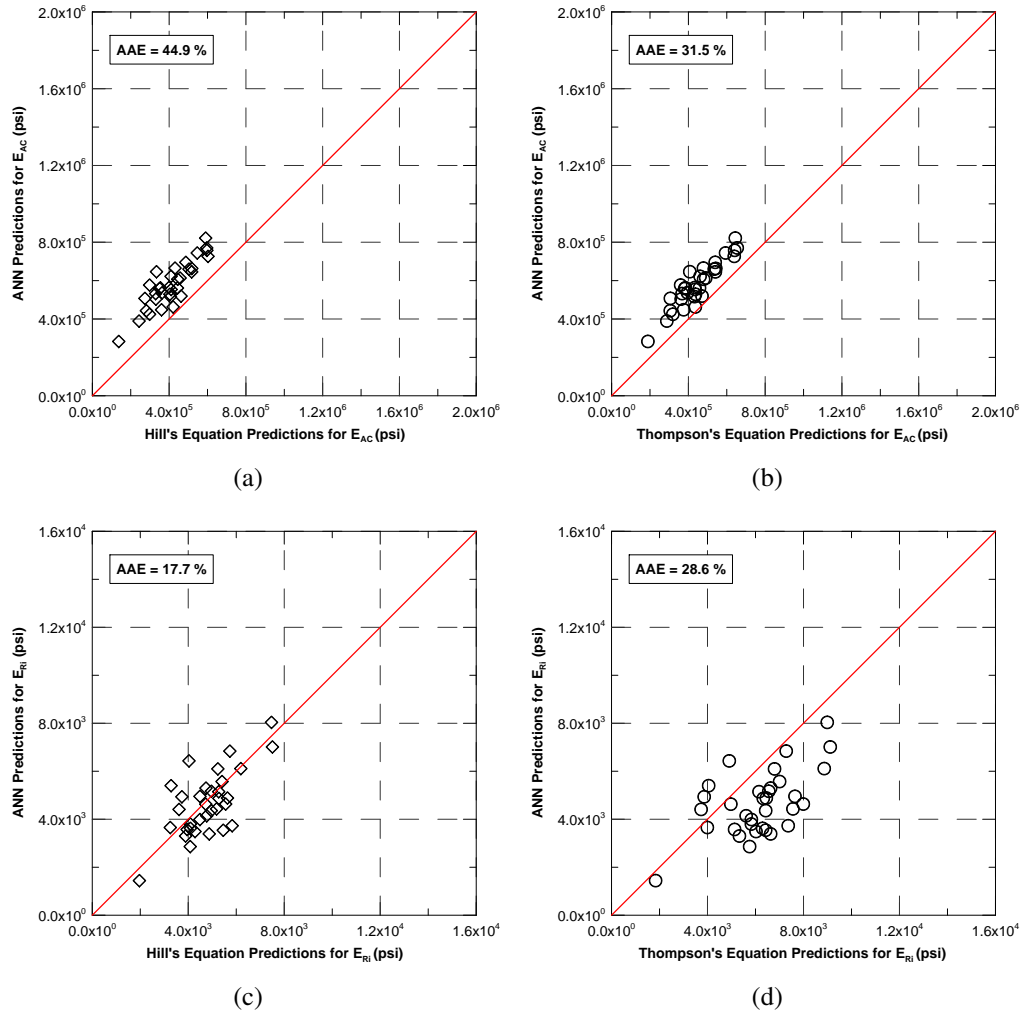


**Figure 3.36:** Performances of FDP-LSS ANN Models for Staley Road.

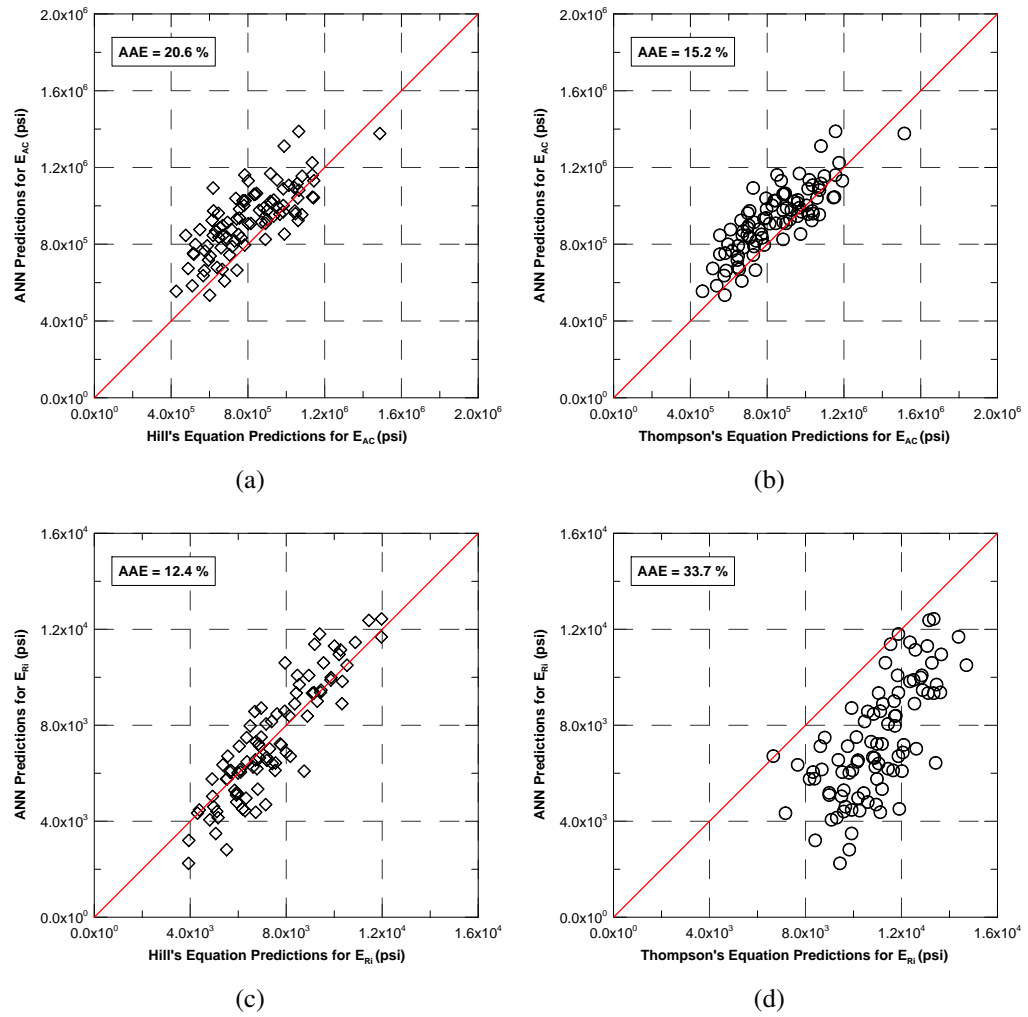


**Figure 3.37:** Performances of FDP-LSS ANN Models for High Cross Road.

The field validation performances for FDPs are shown in Figures 3.33 to 3.34. Similar to FDP-LSS, ANN models developed for FDPs captured the AC modulus practically the same with both Hill's and Thompson's algorithms. Hill's equations, developed for the estimation of  $E_{Ri}$  of FDPs, produced overall better and more comparable estimates with the ANN models. This was clearly indicated as Hill's  $E_{Ri}$  predictions were better centered on the 45-degree equality line with the ANN estimates whereas  $E_{Ri}$  values predicted by Thompson's algorithms were in general much lower in magnitude than the ANN results.

Some of the variability in the presented data can also be attributed to variations in the actual constructed thicknesses of both HMA and LSS layers. Not all the field pavement thicknesses were verified with collected pavement cores. To overcome this difficulty in the future, field thicknesses should be determined at the FWD locations. Alternatively, sensitivities of the backcalculation models to imprecise layer thicknesses should be better assessed and possibly made more robust.

### **3.5.6 Sand Pit Road (Henry County)**

Sand Pit Road was one of the very few CFP sections that were analyzed among all other FWD data. The design pavement section is 3.5 in. of HMA and 16 in. of GB built on unmodified subgrade. Pavement temperatures show large variations throughout the road, changing from 63°F to 88°F on the day of FWD tests. Figures 3.38(a) and 3.38(b) show the performances of the developed ANN models for backcalculating  $E_{AC}$  and  $E_{Ri}$  layer properties of CFPs in Henry County, Illinois in comparison to the Thompson's algorithm predictions given in Equations 3.10 and 3.11 [Thompson, 1989]. In addition,  $K_{GB}$  estimation along the road is given in Figure 3.38(c). Some of the results of backcalculation analyses for  $K_{GB}$  are not shown here since they are found to be not meaningful. However, these stations are included when  $E_{AC}$  and  $E_{Ri}$  are shown on the corresponding Figures.

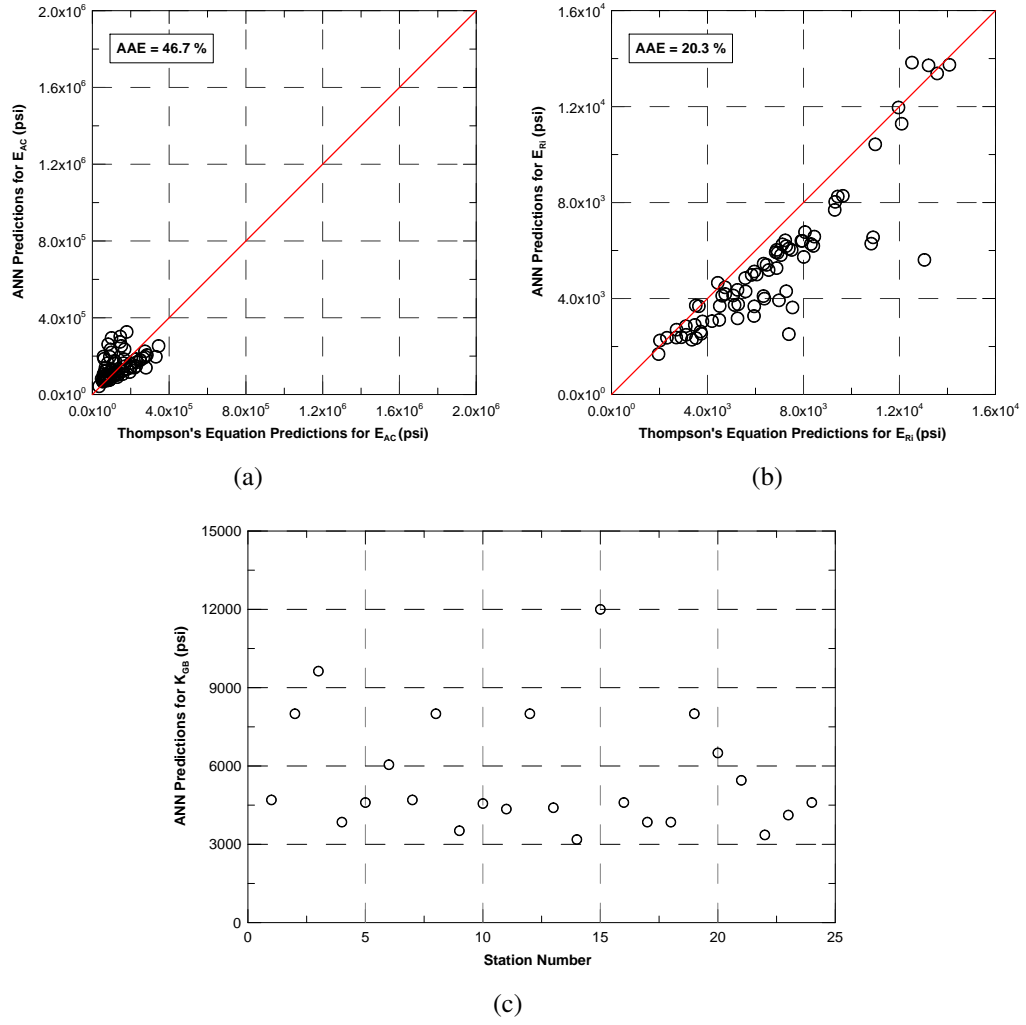


**Figure 3.38:** Performances of CFP ANN Models for Sand Pit Road.

$$\log(E_{AC}) = 1.31 + 8.01 \frac{D_{12}}{D_0} - 13.0 \frac{D_{24}}{D_{12}} + 6.58 \frac{D_{36}}{D_{24}} - 0.081D_0 + 0.096D_{12} \quad (3.10)$$

$$E_{Ri} = 24.1 - 5.08D_{36} + 0.28D_{36}^2 \quad (3.11)$$

### 3.6 Summary

In this chapter, first information was collected on the types, and typical geometries and layer properties of different flexible pavements existing in the State of Illinois. Then, the ILLI-PAVE FE program was used as an advanced structural model for solving deflection profiles and responses of the identified typical Illinois flexible pavements including Full-depth Asphalt Pavements, Full-depth Asphalt Pavements on Lime Stabilized Soils, Conventional Flexible Pavements, and Conventional Flexible Pavements built on Lime Stabilized Soils. Pavement deflection and response databases established from the ILLI-PAVE FE solutions in this manner covered all combinations of the different pavement geometries, layer thicknesses, and layer moduli.

Then, both forward and backcalculation types of ANN models were developed. Different ANN model network architectures were trained successfully to determine the optimum architectures that best captured the behavior of the Illinois pavement sections. In addition, several different network architectures were trained for directly predicting the critical pavement responses, such as the maximum horizontal tensile strain at the bottom of HMA layer or the vertical stress/strain on top of subgrade, from the FWD deflection basins.

In an effort to validate ANN backcalculation models, FWD test data already available at the IDOT Bureau of Materials and Physical Research from previous IHR studies were collected for establishing a comprehensive field FWD database from pavements in Illinois, with known layer thicknesses and material properties. Examples of such previous studies with available FWD test data are the US 50, US 20, Staley Road, High Cross Road, Roseville Bypass, and Sand Pit Road projects. The validation database established this way from the field FWD data was fully utilized in a comprehensive effort to validate the ANN models developed for robustness and accuracy in predicting the pavement layer moduli and critical pavement responses directly from FWD testing.

# **Chapter 4**

## **Soft Computing Based System Analyzer: SOFTSYS**

### **4.1 Introduction**

In the previous chapter of this thesis, it was shown that properly trained ANN models are capable of backcalculating flexible pavement layer moduli and predicting pavement critical responses with average errors much smaller than those obtained with the statistically formulated algorithms developed by Thompson [1989]. Since these models are based on inverse mapping of inputs and outputs, their performances may suffer from ill-posedness due to the nature of problem. As a reliable alternative to those, a quick and robust backcalculation method is presented in this chapter. The new method uses two major soft computing techniques: (i) GAs as powerful search and optimization tools and (ii) ANNs as a fast and reliable pavement analysis engine. Combining these techniques makes the method very powerful and extends its capabilities to a point where it can be used in the inverse analysis of various geomechanical systems. This novel method is therefore called Soft Computing Based System Analyzer, which is abbreviated as SOFTSYS.

### **4.2 Basics of SOFTSYS**

SOFTSYS is a pavement evaluation tool to facilitate real time pavement condition assessment and develop pavement rehabilitation strategies. It interprets FWD test results and performs pavement structural analysis based on the Finite Element Method (FEM). FEM provides modeling of pavement structure's behavior resulting from applied wheel

loading to compute pavement deflections. Unlike the linear elastic theory commonly used in pavement analysis, nonlinear unbound aggregate base and subgrade soil characterization models are used in the FEM. This accounts for the typical hardening behavior of unbound aggregate bases and the softening of fine-grained subgrade soils under increasing stress states. The results of nonlinear FEM have been proven to be consistent with the deflections obtained from nondestructive testing of pavements. Since FEM internally captures the nonlinear material properties to simulate the real pavement behavior, SOFTSYS has an inherent capability of incorporating these properties as the pavement foundation.

When the FEM is used as the structural analysis technique, the convergence of SOFTSYS is extremely slow. To solve this problem efficiently, ANNs are used as a quick and precise pavement structural analysis tool for predicting pavement deflection profiles, since they work much faster than mathematical models and can still perform similar higher-order-function approximations as FEM. Training of ANNs is accomplished based on the results of nonlinear FE analyses of pavements. In SOFTSYS, ILLI-PAVE FE software was selected to provide an advanced pavement structural model for solving deflection profiles and responses. ILLI-PAVE can analyze any flexible pavement geometry, i.e., full-depth and conventional flexible pavements, due to an applied static loading.

The development stages of ANN forward models are provided in Chapter 3. First, a broad range of model input parameters of the pavement layers (layer moduli and thicknesses) is created in a database. Then, randomly selected combinations of the model parameters are entered into ILLI-PAVE. Analyses are conducted for the simulation of FWD tests. Multi-layered, feed-forward backpropagation ANNs [Wythoff, 1993] are then trained to capture the nonlinear relationships between the input model parameters and output variables (deflections) of ILLI-PAVE. The developed ANN model is ultimately used for computing pavement surface deflections based on the known pavement layer moduli and thicknesses.

The next stage in the development of SOFTSYS is the use of GAs to search the solution space formed by FE analyses. The major contribution of GAs is that they are highly robust and noise tolerant [Ghaboussi, 2001, 2010]. Using GAs increases the speed by performing fitness based intelligent search. In SOFTSYS, GAs work as a stochastic search with the operators inspired by natural evolution. The major components of GAs are the genotype / phenotype representation of model parameters of the problem domain (i.e., pavement layer moduli), fitness function (mathematical expression as a measure of the difference between the surface deflections obtained by the FWD test and the ones calculated from the ANN model), selection scheme, crossover method, and mutation. A collection of model input parameters within a reasonable range is created randomly to create the database of all possible combinations of pavement layer material properties including material moduli and the given design thickness of the pavement. These parameters are then fed as testing data set into the ANN model to compute the corresponding deflection profiles. The testing of all data sets created by GAs is done within one second, which is quite fast. In theory the testing time is also insensitive to number of testing examples. GAs then sort input data set based on the imposed fitness function calculated using the outputs of ANN results and the deflection profile obtained by FWD testing. Nature-inspired evolution operators (selection, crossover, and mutation) are then applied to the so called parents and to their offspring to establish the most satisfactory data set for the surface profile obtained from FWD.

#### **4.2.1 SOFTSYS Algorithm and Implementation**

The individual components of SOFTSYS were explained briefly in the previous section. In this section, the SOFTSYS algorithm is explained step by step for implementation purposes. The details are given to further clarify the coding. These are expected to form guidelines for obtaining robust solutions in SOFTSYS.



---

**Algorithm 1** SOFTSYS Algorithm

---

**Require:** Pavement type, backcalculation model, Falling Weight Deflectometer (FWD) data

```
1: for each FWD data do
2:   Initialize random population of phenotypes (i.e., pavement moduli)
3:   Run Artificial Neural Network model with the phenotypes as inputs
4:   Evaluate fitness of population using the fitness function
5:   while Termination Criteria Not Satisfied do
6:     Encode phenotypes into genotypes for bit string representation
7:     Select parents for reproduction
8:     Recombine parents and form child genotypes
9:     Mutate child genotypes
10:    Decode genotypes into phenotypes
11:    Go to step 3
12:  end while
13:  print backcalculated pavement layer moduli
14: end for
```

---

#### 4.2.1.1 Defining Pavement Type and Backcalculation Model

When SOFTSYS is started, the pavement type needs to be input. In addition, the properties of the pavement that need to be backcalculated are also entered. They can also be embedded using predefined backcalculation models, the development of which will be explained in the next section.

- SOFTSYS can backcalculate layer properties of FDPs, FDP-LSSs and CFPs.
- Based on the pavement category selected, the corresponding ANN structural model has to be introduced into the system. The ANN model parameters (so called phenotypes for genetic algorithms) are extracted from the selected model.

#### 4.2.1.2 Entering FWD Data

When FWD tests with typical 9-kip loading are conducted on any road section, the deflections obtained from the FWD testing are entered as an input file into the system.

- For real time applications, the deflection values ( $D_0$ ,  $D_8$ ,  $D_{12}$ ,  $D_{18}$ ,  $D_{24}$ ,  $D_{36}$ ,  $D_{48}$ ,  $D_{60}$  and  $D_{72}$ ) can be entered online.

- For offline analyses (after the FWD test is carried out on each station of the road), an input file is generated consisting of the deflection values for each station.
- In addition to FWD deflections, the conditions of the road (i.e., any comment of the technician, description of any observed crack, joint, etc.) and weather information (i.e., temperature) need to be entered into the system.

#### **4.2.1.3 Population Initialization**

Random populations of phenotypes, i.e., AC modulus ( $E_{AC}$ ), lime stabilized layer modulus ( $E_{LSS}$ ), and subgrade soil modulus ( $E_{Ri}$ ), etc., are created at this stage. The user is queried for the ranges, i.e., maximum and minimum values, of phenotypes. The number of bits necessary to represent the phenotype is found using the minimum and maximum values of the phenotypes. A uniform random number generator is then used to create the population of phenotypes.

- The maximum number of generations for analysis is entered;
- The population size (recommended value is a minimum of 100) is asked if not specified already;
- The probabilities of crossover and mutation are input;
- The maximum number of bits to represent the phenotype is determined based on the range of pavement properties;
- The chromosome length is then kept constant throughout GA evaluations.

#### **4.2.1.4 Running ANN Forward Analysis**

The trained ANN model is run with the randomly created phenotypes as inputs.

- The phenotypes are normalized to the range specified by the developed model (for example, the inputs and outputs are normalized to [-1, 1] and [0.1, 0.9], respectively);

- Run the ANN program with the number of training data sets is 0 and that of testing data is the population size. The results of ANN model runs are then obtained, and the deflection values are scaled back to ranges of the developed model and reported.

#### 4.2.1.5 Fitness Evaluation of Population

The fitness of each member is calculated using the fitness function.

- Depending on the number of FWD outputs, abbreviated as “d” and typically 4 ( $D_0$ ,  $D_{12}$ ,  $D_{24}$ , and  $D_{36}$ ), the fitness of each member is calculated using the formula given in Equation 4.1;
- The fitness vector is then formed for the whole population;

$$Fitness = \frac{1}{1 + \sqrt{\sum_{i=1}^d \left[ \left[ 1 + \left( \frac{FWD_i - ANN_i}{FWD_i} \right) \right]^\varpi \right] - 1}} \quad (4.1)$$

where  $\varpi$  is selected to be 2 to emphasize the difference between the calculated and measured deflections.

#### 4.2.1.6 Checking Termination Criterion

This stage is where the termination of the SOFTSYS algorithm is checked against several different criteria. If generation is less than the maximum number of generations or the fitness is less than 1 (for practical purposes it is specified less than 0.9999), then the algorithm needs to be run for at least one more generation.

- If the generation number is greater than the maximum number of generations or the value of any of the members of the population in the fitness vector is equal to 1 (or specified by the user such as 0.95), then stop running SOFTSYS and report the member with the highest fitness, its fitness value, and the generation number on the screen and print them to a file. Otherwise go to the next step.

#### **4.2.1.7 Encoding Variables**

The variables are converted, i.e., encoded, from phenotypes into genotypes (bit string representation) using bit, i.e., base 2, conversion. The chromosome is then formed using a string of bits, 0 or 1. Encoding can be performed using different techniques such as permutation encoding or tree encoding, the suitability of which needs to be studied depending on the problem to be solved using GAs.

#### **4.2.1.8 Selection of Child Genotypes**

In this stage, parents are combined to form child genotypes.

- According to the specified selection algorithm, such as the roulette wheel or tournament selection, select the new parents to create the offspring;
- The parents are then paired in order, i.e., 1-2, 3-4, etc.

#### **4.2.1.9 Crossover and Mutation of Variables**

Given the probability of crossover and mutation, these operations are performed in order to produce the offspring. First, crossover operators (single point, two point, uniform, etc.) are applied to the parent chromosomes. Each pair produces two offspring after the application of this operator. Then some genes (i.e., bits) of the offspring chromosomes are replaced by their logical complement (i.e., mutation).

#### **4.2.1.10 Decoding of Genotypes**

After the crossover and mutation have been performed, the offspring genotypes are converted into phenotypes based on the number of bits each variable presents through base 10 conversions. One generation cycle is completed at the end of these operations. The program is run based on the specified number of generations, or until the desired fitness is achieved. For proper termination of SOFTSYS some other criteria can be used, such

as the loss of diversity in the population, etc. When the termination criterion is satisfied, SOFTSYS produces the backcalculated properties of the pavement.

#### **4.2.2 Development of SOFTSYS Models**

In this section, the development stages of SOFTSYS models are explained. The parameter settings used in the design of the GA search are given. Since the parameters used for training of ANNs were already provided in the Chapter 3, they are not repeated here. Then the importance of choosing appropriate parameters is discussed in the light of findings of the SOFTSYS models.

SOFTSYS backcalculation models were developed using the ILLI-PAVE synthetic database. These models were then used to backcalculate pavement layer properties using the field FWD data. It was assumed that the performances of these models would be similar when tested using real FWD data. The validity of this assumption is limited by the ability of the FE program to capture field responses successfully under a given FWD loading. Usually the dynamic characteristics of FWD tests and the differences between the actual traffic loading and time history of FWD loading create unforeseen differences. Especially in the case of thick pavements, the effect of the AC layer's viscoelasticity may be dominating the measured responses. However, this thesis did not focus on highlighting the differences between elastic and viscoelastic layer properties. It is rather limited to ILLI-PAVE FE models.

The performances of ANN models used as the forward analysis engine in SOFTSYS were given in Figures 3.17, 3.21, 3.19 and 3.23 for FDPs, FDP-LSSs, CFPs and CFP-LSSs, respectively. The excellent performances of the ANN models proved that they would not affect the accuracy of the SOFTSYS backcalculation models. In other words, ANN's ability to work as surrogate FE models in SOFTSYS necessitated carefully choosing the GA parameters since the accuracy would be mainly affected. The effective exploration of FEM based search space is then fully dependent on GA parameter selection.

In general, the performance of GAs depends on the following parameters [da Graça Lobo, 2000; De Jong, 1975]:

- Population Size,
- Probability of Mutation,
- Probability of Crossover,
- Number of Generations,
- Chromosome Size.

The selection of the above parameters for the pavement layer backcalculation problem plays an important role [Reddy *et al.*, 2004, 2002] in obtaining accurate responses. Therefore, sensitivity analyses were carried out to determine a proper set of these parameters. For this purpose, the ILLI-PAVE synthetic database created using FDP analyses was used. SOFTSYS analyses were performed to backcalculate  $E_{AC}$  and  $E_{Ri}$  for a randomly chosen synthetic station. The selection strategy was chosen to be the tournament selection without replacement. The effect of population size was investigated by analyzing the same station with population sizes of 100 - 500 - 1,000 and 5,000. Each size was used three times to eliminate the effect of randomness. Usually, the very best results are reported if GAs are used for analysis. The evolution of fitness with the number of generations is presented in Figure 4.1 for different populations. In general, as population size is increased there is greater opportunity to obtain better “best fitness” values. However, the population size of 1,000 provided the same performance as that of 5,000 for at least two trials. Therefore, a population of 1,000 members was used throughout the backcalculation analyses.

Similar to population size, the number of generations also plays a crucial role on the performance of SOFTSYS for all practical purposes. Although ANN analyses that are guided by GAs happen very quickly, as the number of generations increases, the computational time required to report the backcalculated pavement properties increases.

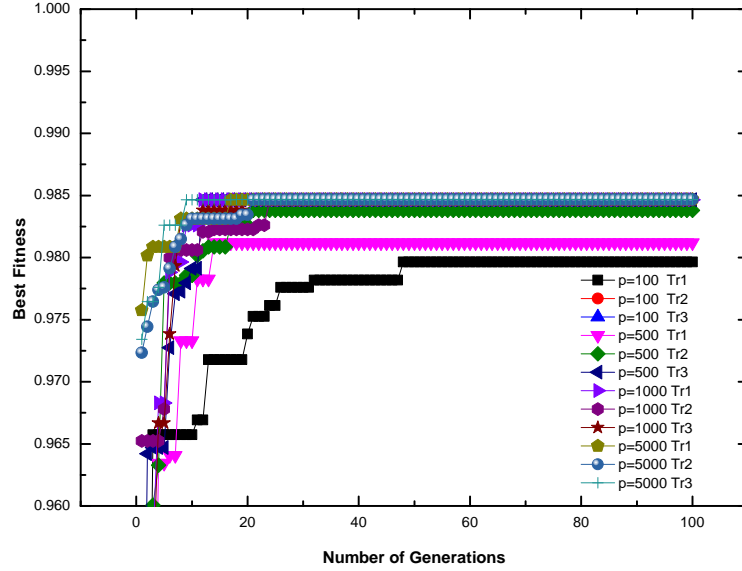


**Figure 4.1:** Effect of Population Size on the Performance of SOFTSYS for a Random IP-SYNTH Station.

The numbers of generations for SOFTSYS analyses were selected to be 20, 40, 60, 80, and 100. The evolution of fitness for different number of generations is shown in Figure 4.2. Some trials with lower numbers of generations did not produce good “best fitness” results. However, 100 generations were found to be satisfactory to obtain reliable and repeatable backcalculated moduli properties. Finally, an algorithm was implemented to cut off the additional generations if the best fitness value does not change for 40 generations. This cut-off algorithm only starts after the 50th generation to eliminate premature solutions.

The effects of crossover and mutation probabilities were investigated to obtain better solutions with GA searches. For this purpose, crossover probabilities,  $p_c$ , were selected to be 0.80, 0.85, 0.90, 0.95, and 1.00. Similarly, mutation probability,  $p_m$ , was changed from 0.01 to 0.00001. The results of different trials are given in Figures 4.3 and 4.4. According to Figure 4.3, all  $p_c$  values produced good “best fitness” results. As shown in Figure 4.4, the models with value of  $p_m$  greater than or equal to 0.001 showed better performances.

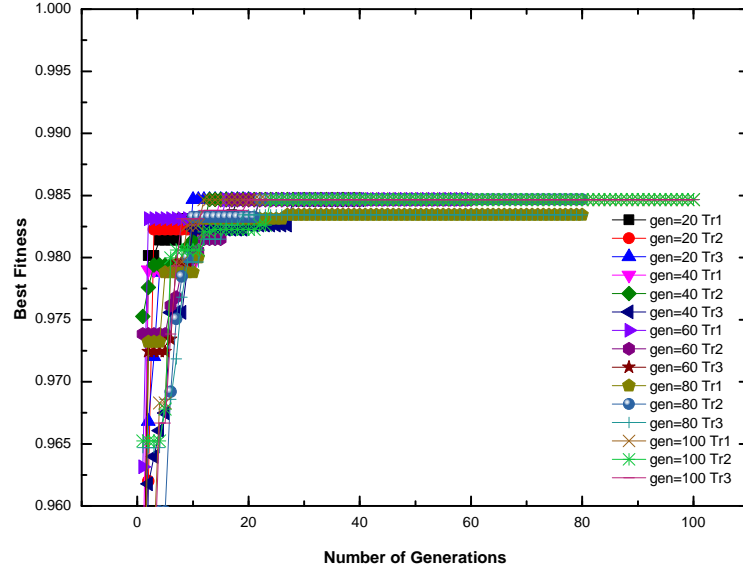


**Figure 4.2:** Effect of Number of Generations on the Performance of SOFTSYS for a Random IP-SYNTH Station.

Then, considering the effect of population size (previously specified to be 1,000) on both variables,  $p_c$  and  $p_m$  were chosen to be 0.85 and 0.001, respectively.

Finally, the effect of chromosome length was also studied for scalability purposes. However, SOFTSYS chromosome size was selected to be the longest whenever possible. In other words, the change of 1 bit in a chromosome was considered to be an important change in for engineering purposes. For example, if maximum value of  $E_{Ri}$  is 16,384 ksi ( $= 2^{14}$ ), then 14 bits were used to represent such values. The change of 1 bit will correspond to 1 psi. In some cases, 10 bits were used, which results in a 1-bit change producing a change of 16 psi.

### 4.3 SOFTSYS Validation with Synthetic Data Sets

There are a total of six backcalculation models developed for FDPs, FDP-LSSs, and CFPs. The descriptions of these models are given in Table 4.1 for the input and output



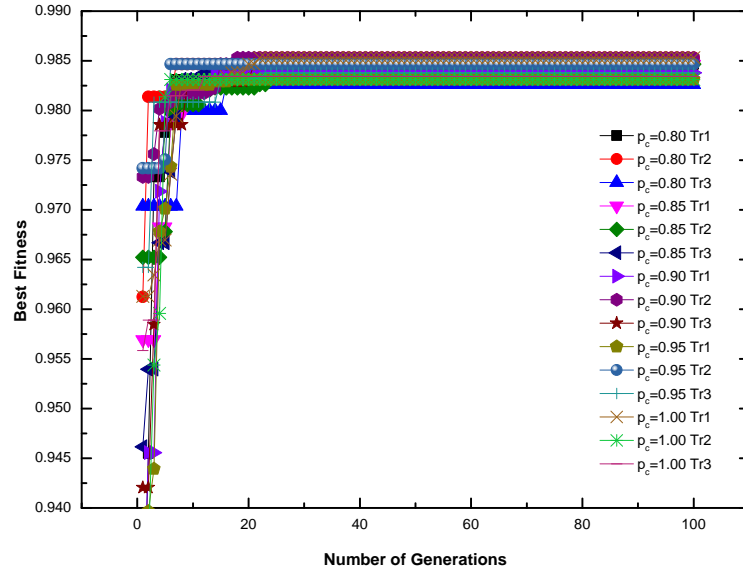


**Figure 4.3:** Effect of Crossover Rate,  $p_c$ , on the Performance of SOFTSYS for a Random IP-SYNTH Station.

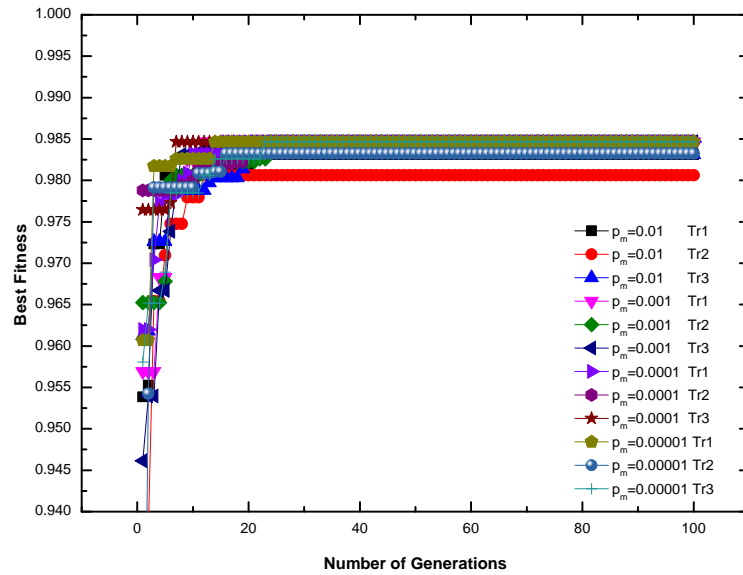


**Figure 4.4:** Effect of Mutation Rate,  $p_m$ , on the Performance of SOFTSYS for a Random IP-SYNTH Station.

**Table 4.1:** Descriptions of SOFTSYS Models Developed to Estimate Layer Moduli of Different Types of Pavements

Name	Inputs	Outputs
FDP-PM1-FWD4	$D_0, D_{12}, D_{24}, D_{36}, t_{AC}$	$E_{AC}, E_{Ri}$
FDP-PM1-FWD7	$D_0, D_{12}, D_{24}, D_{36}, D_{48}, D_{60}, D_{72}, t_{AC}$	$E_{AC}, E_{Ri}$
FDP-LSS-PM1-FWD4	$D_0, D_{12}, D_{24}, D_{36}, t_{AC}, t_{LSS}$	$E_{AC}, E_{LSS}, E_{Ri}$
FDP-LSS-PM1-FWD7	$D_0, D_{12}, D_{24}, D_{36}, D_{48}, D_{60}, D_{72}, t_{AC}, t_{LSS}$	$E_{AC}, E_{LSS}, E_{Ri}$
CFP-PM1-FWD4	$D_0, D_{12}, D_{24}, D_{36}, t_{AC}, t_{GB}$	$E_{AC}, K_{GB}, E_{Ri}$
CFP-PM1-FWD7	$D_0, D_{12}, D_{24}, D_{36}, D_{48}, D_{60}, D_{72}, t_{AC}, t_{GB}$	$E_{AC}, K_{GB}, E_{Ri}$

requirements. Two models for each flexible pavement, each of which uses different sensor information, are used. For example, for FDPs, the first model FDP-PM1-FWD4, predicts  $E_{AC}$  and  $E_{Ri}$  with the use of four sources of sensor information,  $D_0$ ,  $D_{12}$ ,  $D_{24}$ , and  $D_{36}$ , obtained from FWD tests in addition to the design AC thickness of FDP. Similarly, the second model FDP-PM1-FWD7 uses more sensors,  $D_0$ ,  $D_{12}$ ,  $D_{24}$ ,  $D_{36}$ ,  $D_{48}$ ,  $D_{60}$ , and  $D_{72}$ , to predict the same properties of FDP. Both models use the same ANN forward structural model, which replaces ILLI-PAVE successfully. The performance of the corresponding ANN model (FWD-FW1) with only four deflections was provided in the previous chapter; the AAE values obtained using the ANN forward model to predict 7 deflections are similar to those of FWD-FW1. The models developed for FDP-LSS and CFP were developed with the same approach, i.e., they use different sensor information, 4 and 7, to predict corresponding moduli values. The predicted values for FDP-LSS are  $E_{AC}$ ,  $E_{LSS}$ , and  $E_{Ri}$  and those for CFP are  $E_{AC}$ ,  $K_{GB}$ , and  $E_{Ri}$ . Finally, these SOFTSYS models also take design thicknesses as inputs [Pekcan *et al.*, 2009].

The performances of SOFTSYS models were measured using the synthetic FWD data. Unlike ANN backcalculation models, the number of stations used to test the performance of SOFTSYS was kept limited since SOFTSYS understandably requires more computation time than does ANN. For this purpose, 20 stations for FDPs were randomly selected from the ILLI-PAVE database generated for training ANNs. The database was named as IP-SYNTH. In the case of FDP-LSSs and CFPs, the number of stations used in testing is increased to 30 to sample the database more uniformly, since there are more properties to predict for these pavements.

### **4.3.1 Full-depth Asphalt Pavements**

Figures 4.5(a) and 4.5(b) provide the performance summaries of the SOFTSYS FDP-PM1-FWD4 model for predicting pavement layer moduli. The values of AAE are very close to 2%, which indicates that pavement layer moduli were predicted quite successfully using FDP-PM1-FWD4. In addition, the progress curves of GAs implemented in this SOFTSYS model are given in Figures 4.6(a) to 4.6(b) for stations randomly selected from the IP-SYNTH FWD database. These curves simply represent the growth of member fitness of the population through generations. Best fitness values are also reported on the progress graphs to show that deflections obtained using that specific member of the population are in conformity with the ones in the FWD database. Finally, the growths of the average fitness of all population members are shown together with fittest member of each generation. Best fitness is different than maximum fitness in that it represents the highest maximum fitness through generations. In conclusion, it is shown that SOFTSYS reaches the satisfactory fitness values at very early stages, i.e., the first 10 or 20 generations when its performance is tested using synthetic data. Still, in order to effectively apply the genetic pressure on the members of the population and to obtain better results, the algorithm continues to run until 400 generations. This has adverse effects on the total

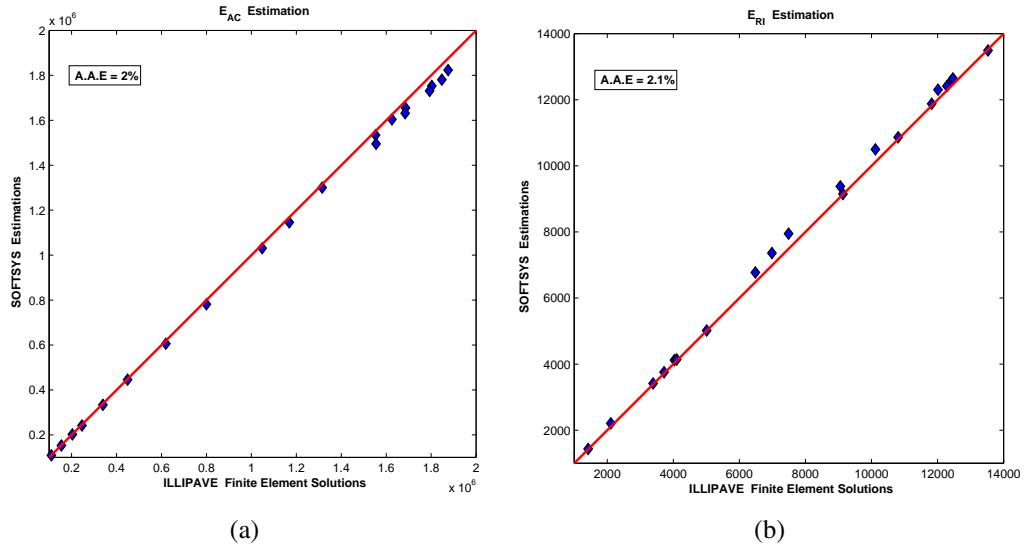


**Figure 4.5:** Performances of SOFTSYS Backcalculation Models for Predicting Layer Moduli (in psi) of Full-depth Asphalt Pavements Using  $D_0$ ,  $D_{12}$ ,  $D_{24}$  and  $D_{36}$  as Inputs.

computational time of SOFTSYS and can be optimized. Nonetheless running for more generations improves the chances of obtaining reliable results.

The second model, FDP-PM1-FWD7, was developed to be able to use more sensor information  $D_{48}$ ,  $D_{60}$ , and  $D_{72}$  when available. Figures 4.7(a) and 4.7(b) provide the performances of this model when tested with IP-SYNTH data. The AAE values obtained for both  $E_{AC}$  and  $E_{Ri}$  are 0.7%, which indicates that SOFTSYS predictions improved when compared to the structural prediction model using only four deflections. Therefore, when analyzing field data, it would be better to run the model using seven deflections, which provides more accurate solutions. It is concluded that both models developed to predict  $E_{AC}$  and  $E_{Ri}$  can be reliably used for field analyses.

### 4.3.2 Full-depth Asphalt Pavements on Lime Stabilized Soils

There are also two backcalculation models, FDP-LSS-PM1-FWD4 and FDP-LSS-PM1-FWD7, for predicting  $E_{AC}$ ,  $E_{LSS}$ , and  $E_{Ri}$  by using information from four and seven FWD deflection sensors, respectively. The SOFTSYS model

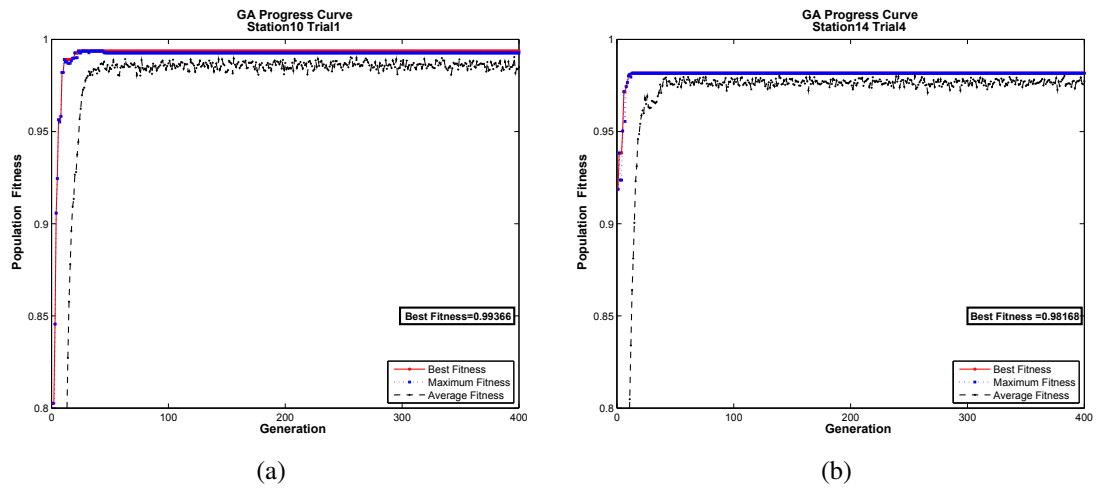


**Figure 4.6:** Progress Curves of SOFTSYS Model FDP-PM1-FWD4 for Random IP-SYNTH Stations.

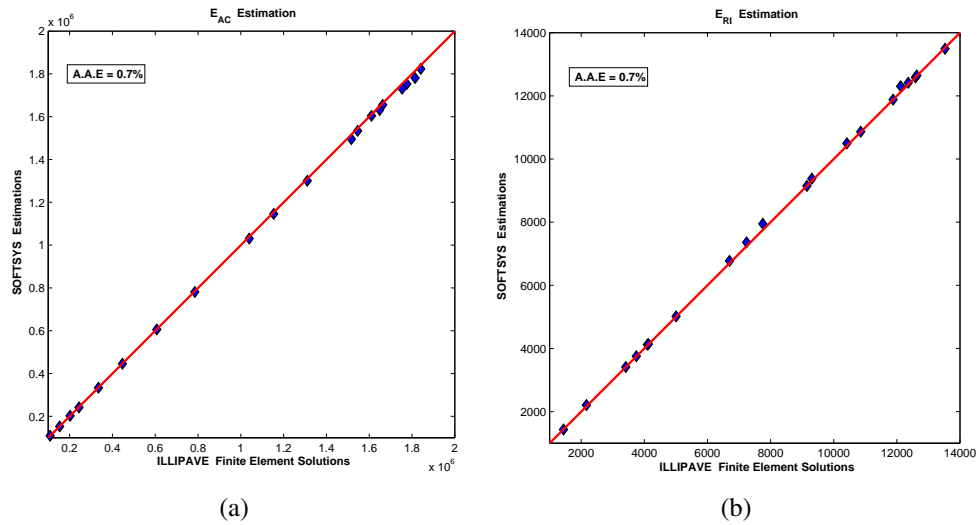


**Figure 4.7:** Performances of SOFTSYS Backcalculation Models for Predicting Layer Moduli (in psi) of Full-depth Asphalt Pavements Using Seven Deflections.

FDP-LSS-PM1-FWD4 performances for backcalculated FDP-LSS pavement layer moduli are given in Figures 4.8(a) to 4.8(c). The AAEs given indicate that the FDP-LSS-PM1-FWD4 model could predict ILLI-PAVE solutions within very low 2.7%, 9.5% and 1.7%, respectively for  $E_{AC}$ ,  $E_{LSS}$  and  $E_{Ri}$ . Similarly, FDP-LSS-PM1-FWD7 performances for backcalculated FDP-LSS pavement layer moduli are given in Figures 4.9(a) to 4.9(c). The accuracy of the FDP-LSS-PM1-FWD7 model for the prediction of  $E_{Ri}$  improved by 1.1%. Meanwhile the accuracy for the prediction  $E_{AC}$  remains within a very low AAE of 3.3%. However, it can be seen that the accuracy of  $E_{LSS}$  got worse by 3.5% when seven deflections are used in SOFTSYS for predictions of FDP-LSSs. This is the opposite of what was expected from a structural backcalculation model that uses more deflections. When the results were investigated, it was observed that the FWD stations for which  $E_{LSS}$  could not be predicted well had either very thick AC layers or a high modulus for the AC layer, which resulted in high flexural rigidity for the AC layer. The deflection basin parameters are affected mostly by the asphalt layer's rigidity. Therefore, the contribution of the LSS layer is not pronounced, which results in poor estimates of LSS layer properties. Finally, both of these models were able to reach the same fitness values at about the same number of generations.

### 4.3.3 Conventional Flexible Pavements

The SOFTSYS model predictions for CFP are given in Figures 4.10 and 4.11 for Models CFP-PM1-FWD4 and CFP-PM1-FWD7, respectively. Figures 4.10(a) to 4.10(c) show that the first model could predict the layer moduli  $E_{AC}$  and  $E_{Ri}$  with AAE values of less than 1.9%. However, the prediction of  $K_{GB}$  produced 16.9% AAE when using four deflection sensors. It was observed that the layer properties that could not be predicted with high accuracy by CFP-PM1-FWD4 usually belonged to the pavement sections with extremely thick AC layers (more than 10 in.) and/or high AC layer moduli. In practice, however, these pavement geometries are very rare in Illinois. Nonetheless, the outliers were kept in

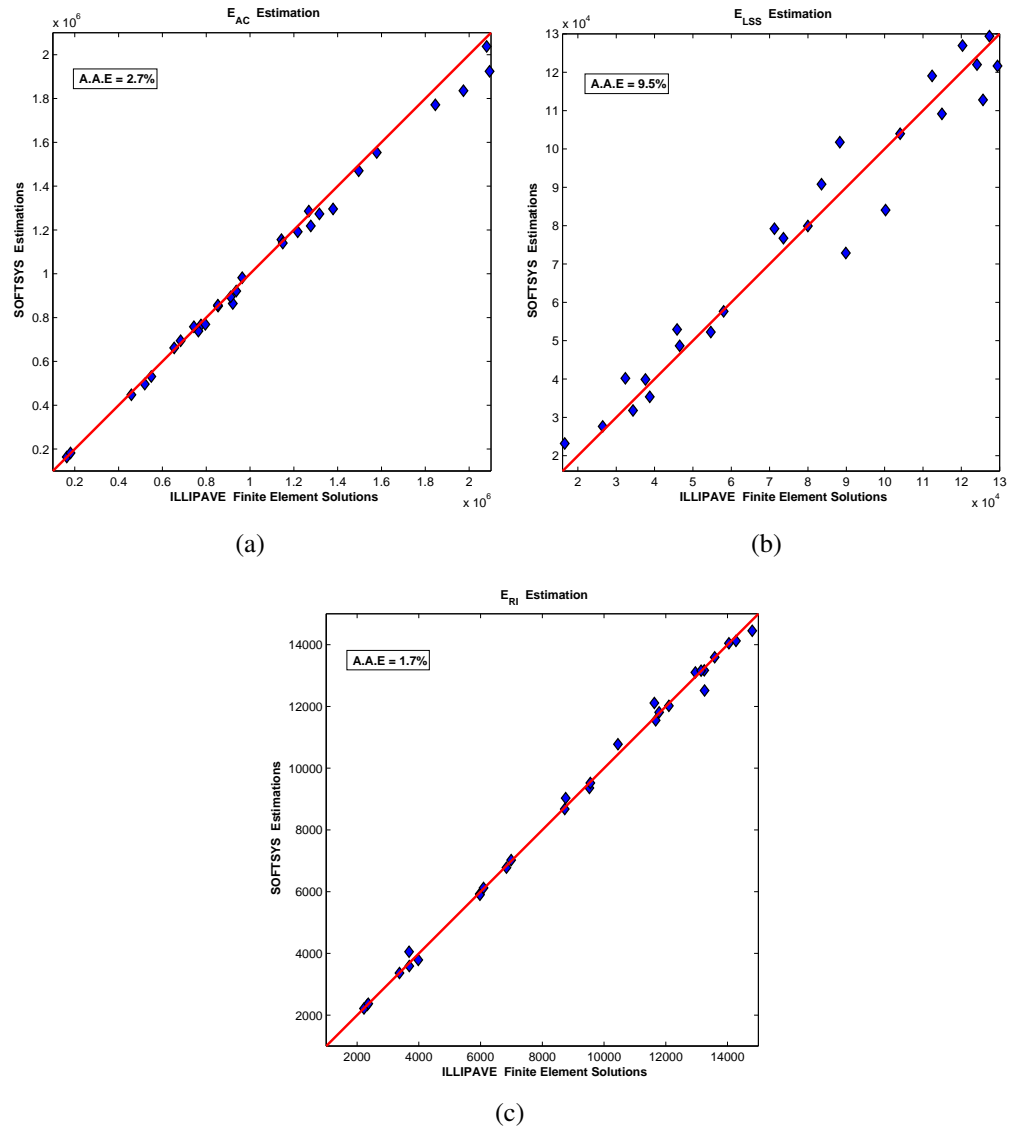


**Figure 4.8:** Performances of SOFTSYS Backcalculation Models for Predicting Layer Moduli (in psi) of Full-depth Asphalt Pavements Built on Lime Stabilized Soils Using Four Deflections.

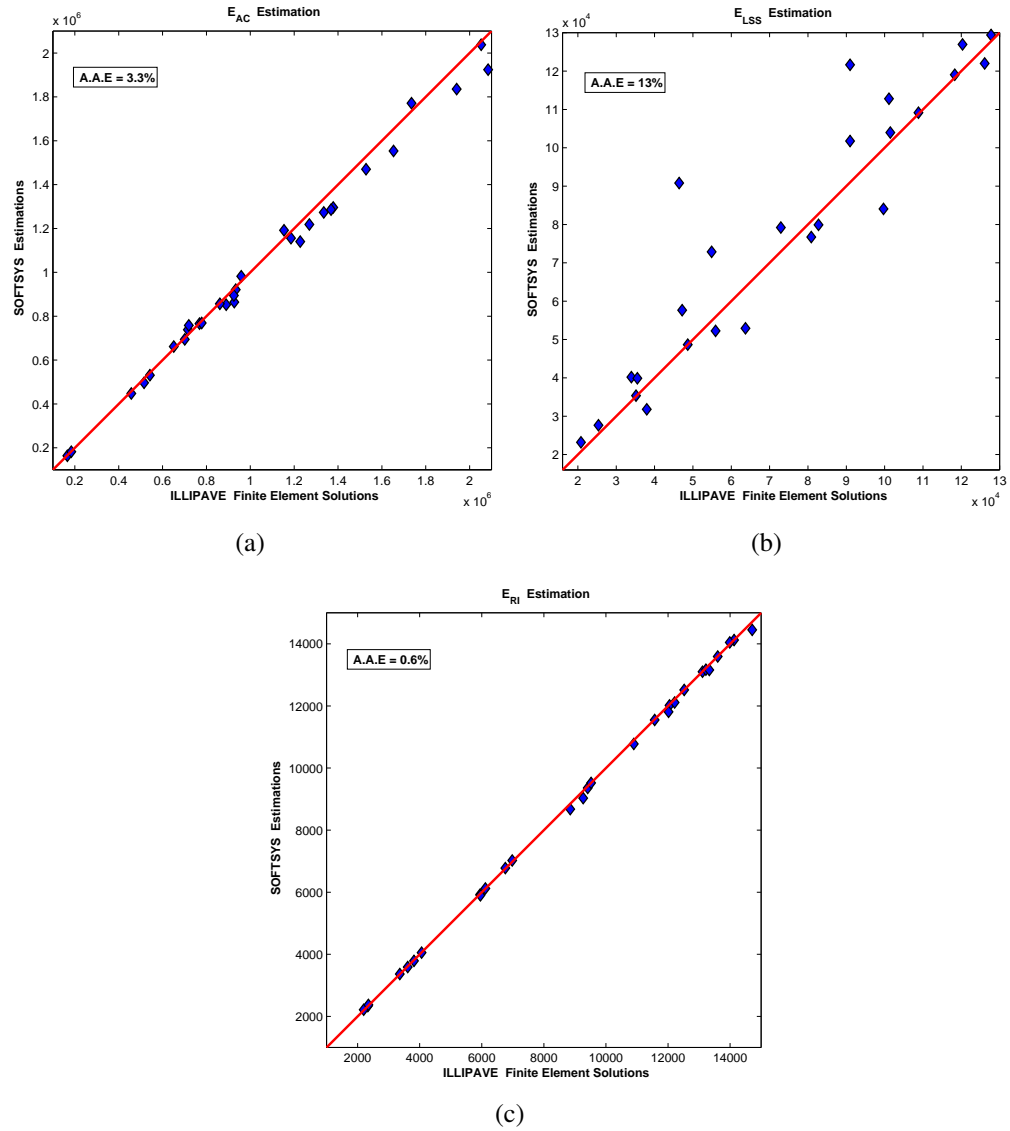


**Figure 4.9:** Performances of SOFTSYS Backcalculation Models for Predicting Layer Moduli (in psi) of Full-depth Asphalt Pavements Built on Lime Stabilized Soils Using Seven Deflections.



the predictions to provide warnings for the end-users and to guide them when searching the reason for the poor performances of SOFTSYS. Finally, increasing the number of deflections to predict the layer moduli properties was not helpful; the AAEs increased by an average of 1.3% as shown in Figures 4.11(a) to 4.11(c). When the analyses were investigated, it was seen that the same deflection profiles were obtained with different combinations of  $E_{AC}$ ,  $E_{Ri}$  and  $K_{GB}$ . However, it was observed that either the modulus of the AC layer was found to be very high ( 2,000 ksi) or the AC layer is thick (> 7 in.) or both happen at the same time.

## **4.4 Field Validations**

In this section, the performances of SOFTSYS models developed to predict layer moduli properties are verified using the field data. The details of the field conditions, FWD testing and the design properties of the flexible pavements used in this study are already given in Chapter 3.5. Therefore only the performances of SOFTSYS models are provided in this section. When using the field data, two sets of backcalculation algorithms, referred to as Hill's algorithms and Thompson's algorithms, given in Chapter 3.5 are used. This also facilitates the comparison of SOFTSYS model predictions with those estimated using ANN backcalculation models. Finally, a discussion is provided to compare SOFTSYS and ANN model predictions when they are used for backcalculation of pavement layer moduli.

### **4.4.1 US 50 (FAP 327, old FA 409)**

The FDP SOFTSYS model predictions for US 50 are shown in Figures 4.12(a) to 4.12(d). SOFTSYS model FDP-PM1-FWD4 was used to analyze the FWD data. This model captured the AC modulus with results almost identical to those produced by both Hill's and Thompson's algorithms; the AAE values obtained were about 15% for both algorithms. Hill's equation, developed for the estimation of  $E_{Ri}$  of FDPs, produced 52.9% AAE value.

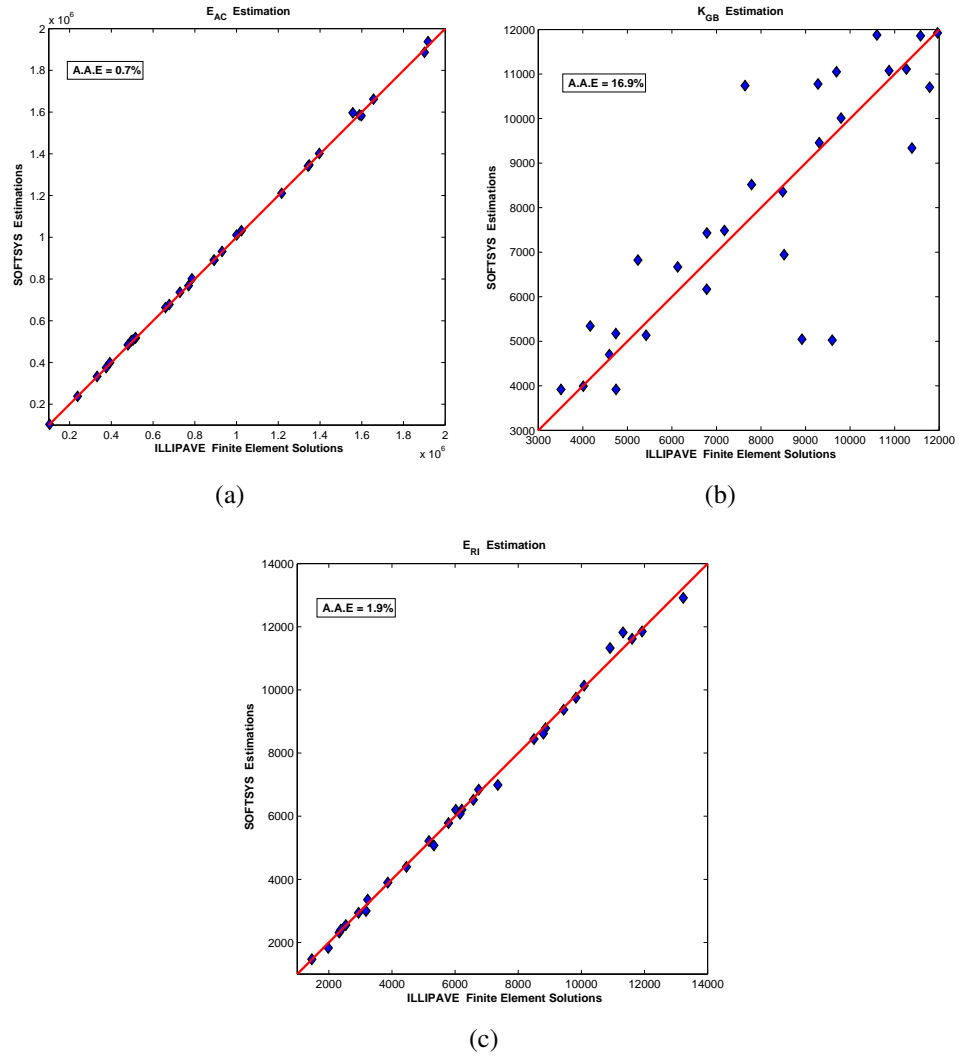


**Figure 4.10:** Performances of SOFTSYS Backcalculation Models for Predicting Layer Moduli (in psi) of Conventional Flexible Pavements Using Four Deflections.

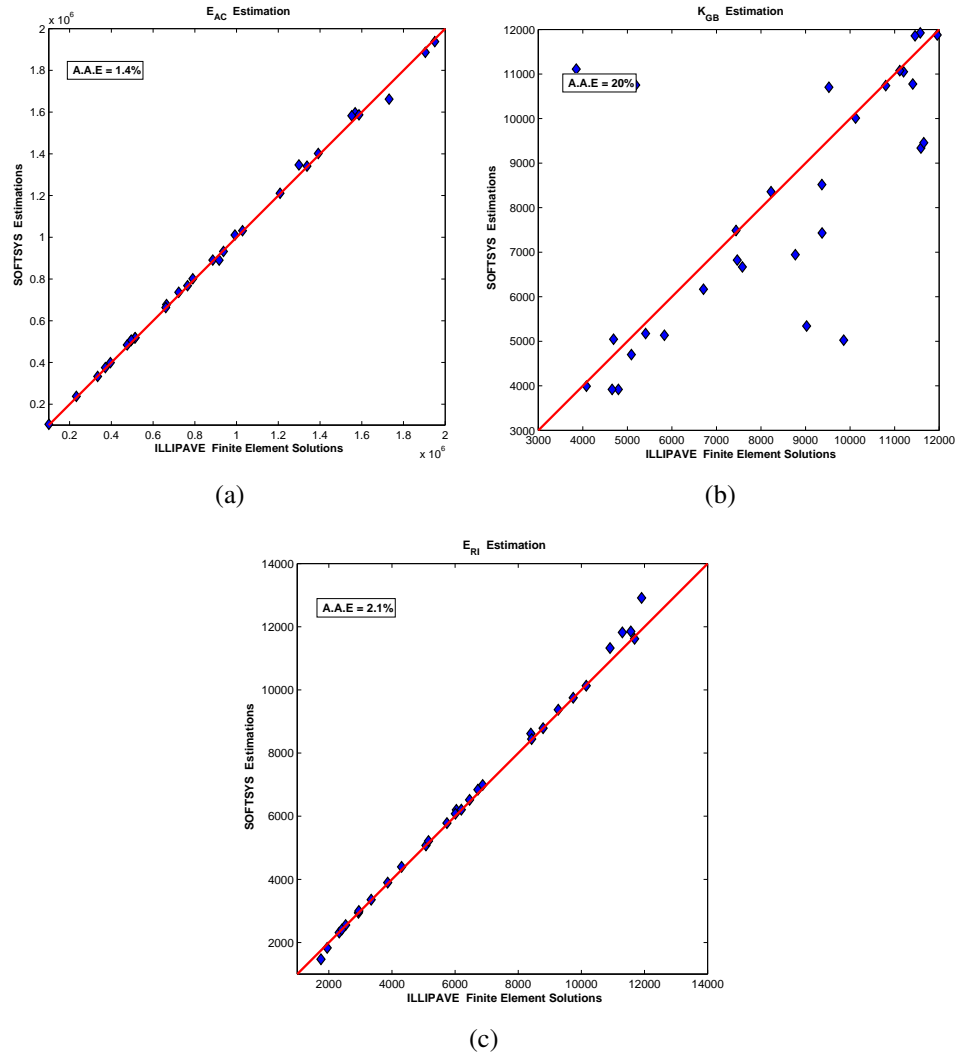


**Figure 4.11:** Performances of SOFTSYS Backcalculation Models for Predicting Layer Moduli (in psi) of Conventional Flexible Pavements Using Seven Deflections.

However, Thompson's algorithm produced overall better and more comparable estimates with the SOFTSYS models. This was clearly indicated as Thompson's  $E_{Ri}$  predictions were better centered on the 45-degree equality line with the SOFTSYS estimates, whereas  $E_{Ri}$  values predicted by Hill's algorithms were in general much higher in magnitude than the SOFTSYS results. The best fitness value obtained from the SOFTSYS solutions was 0.996251 among all the stations. The average number of generations to reach the best fitness was 22. Finally, when the estimations for  $E_{AC}$  are investigated carefully, it was seen that for three stations SOFTSYS produced unreasonably high moduli values for the AC layer. To eliminate such values, appropriate initial ranges of  $E_{AC}$  before GA search could be initiated based on the pavement temperature that was measured during the FWD loading. This would improve the prediction performance of other variables as well.

The comparison of SOFTSYS models with ANN backcalculation models can also be made based on Hill's and Thompson's algorithms. From Figures 3.33 and 4.12, it can easily be seen that SOFTSYS models performed much better compared to ANN models, although ANN backcalculation models produced better estimates when tested with the synthetic ILLI-PAVE database. The predictions of SOFTSYS for  $E_{AC}$  are at least 23.6% better compared to those of ANN models. The improvement in the prediction of  $E_{Ri}$  was found to be 16.2% when SOFTSYS is used instead of ANN-based backcalculation models when Thompson's algorithm was used. The performance of SOFTSYS when Hill's algorithm was comparable to those of ANNs. This also verifies that SOFTSYS models can predict  $E_{AC}$  and  $E_{Ri}$  more reliably when used for field analyses.

#### **4.4.2 US 20 (FAP 301, old FA 401)**

Figures 4.13(a) to 4.13(d) show the SOFTSYS model predictions for US 20. Since only four deflection data are obtained from the FWD testing, SOFTSYS model FDP-PM1-FWD4 was used in the analyses. The results obtained showed that the AC modulus was predicted with almost the same accuracy as for both Hill's and Thompson's

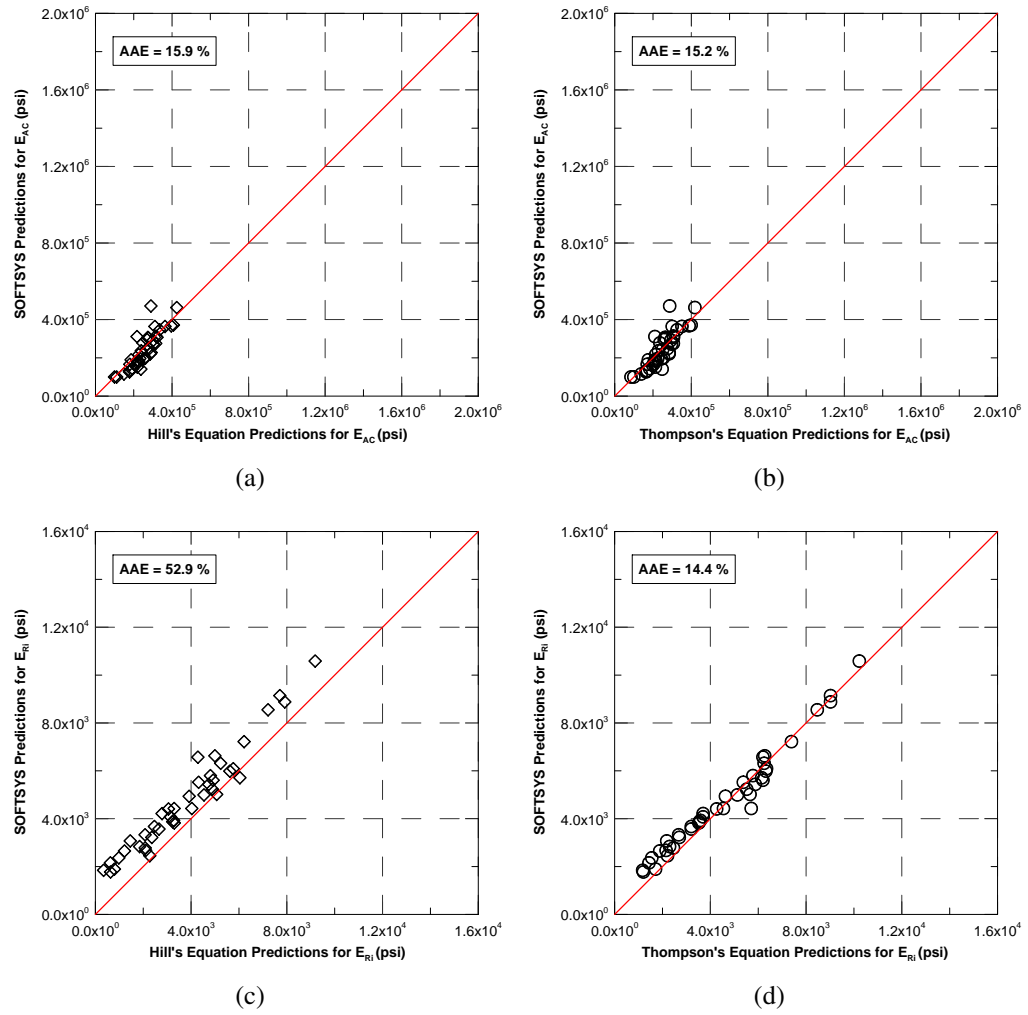


**Figure 4.12:** Performances of FDP-PM1-FWD4 SOFTSYS Model for US 50.

algorithms. The AAE values obtained were about 16.5% and 12.4% for Hill's algorithms and Thompson's algorithms, respectively. Similarly, AAE values produced for the estimation of  $E_{Ri}$  were 10.1% and 6.0% for both algorithms. Thompson's algorithm produced estimates overall better and more comparable with the SOFTSYS models. The best fitness value obtained from the SOFTSYS solutions was 0.982988 among all the stations. The average number of generations to reach the best fitness was 24. When the analyses results were investigated, some outliers were found especially in the prediction of  $E_{AC}$ . SOFTSYS produced much lower moduli values for the AC layer, although this was not expected when the temperature data was taken into account. SOFTSYS tried to match the higher deflection values obtained from the field by lowering the AC layer moduli. This type of data can either be eliminated, as it is an outlier for FWD deflection database or precautions may be taken when the GA search is initialized to improve the prediction performance. Then the minimum value of AC modulus can be adjusted accordingly.

The comparison of SOFTSYS models with ANN backcalculation models can also be made using Figures 3.34 and 4.13. Accordingly, SOFTSYS models performed better compared to ANN models when FA401 FWD data were used in the analyses. The predictions of SOFTSYS for  $E_{AC}$  are at least 9.6% better compared to those of ANN models. The improvement in the prediction of  $E_{Ri}$  was also found to be at least 2.3%. Both analyses showed that SOFTSYS can be used reliably and with a higher accuracy in analyzing FWD data compared to using ANN based models.

#### **4.4.3 Roseville Bypass**

Figures 4.14(a) to 4.14(d) show SOFTSYS model predictions for the Roseville Bypass. There were only four deflection data obtained from the FWD testing and therefore SOFTSYS model FDP-LSS-PM1-FWD4 was used in the analyses. The results obtained showed that the AC modulus was predicted with almost the same accuracy as for both Hill's and Thompson's algorithms. The AAE values obtained for predicting AC modulus

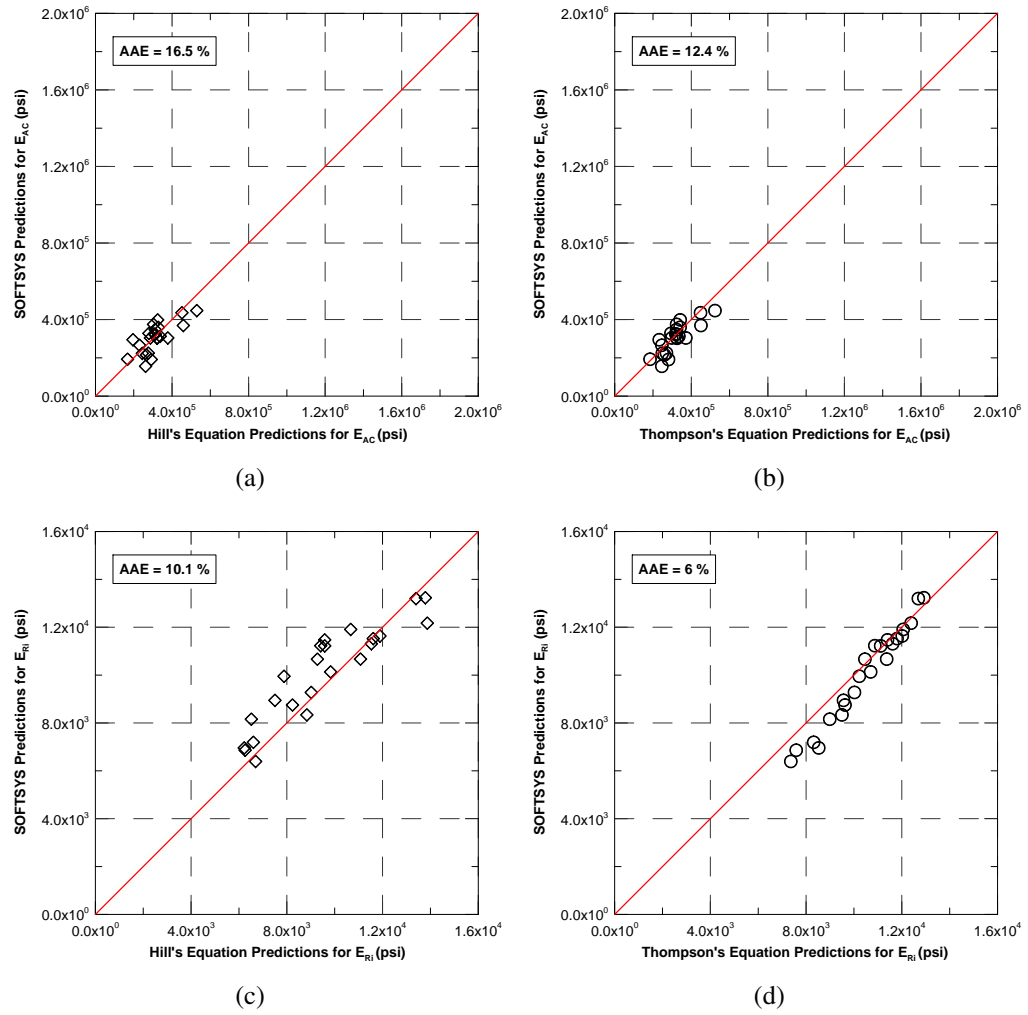


**Figure 4.13:** Performances of FDP-PM1-FWD4 SOFTSYS Model for US 20.

were 15.6% and 11.0% for Hill's algorithm and Thompson's algorithm, respectively. Similarly, the AAE value produced for the estimation of  $E_{Ri}$  was 9.0% using Hill's algorithm. Thompson's algorithm, however, produced much higher AAE values when SOFTSYS models are used for comparison. The inspection of the data actually showed that SOFTSYS can capture  $D_{36}$  perfectly, which is actually used in backcalculating the  $E_{Ri}$  value in Thompson's algorithm. However, the predicting together the combination of all layer moduli,  $E_{AC}$ ,  $E_{LSS}$  and  $E_{Ri}$  resulted in much higher AAEs using SOFTSYS. This is an indication of a uniqueness issue in the definition of the backcalculation problem since this means that the same  $D_{36}$  value may correspond to the response obtained for different combinations of pavement layer moduli values in the case of FDPs. To overcome this problem, the initial ranges of GAs for  $E_{Ri}$  can be chosen based on the  $D_{36}$  value; or an algorithm that takes all the deflections into account can be used to backcalculate the pavement layer moduli for comparison purposes. The best fitness value obtained from the SOFTSYS solutions was 0.996187 among all the stations. The average number of generations to reach the best fitness was 31. The average layer modulus for the LSS layer was reported to be 32 ksi, which was found to be consistent considering the short-term curing of the lime stabilized layer. The coefficient of variation in the LSS layer moduli throughout the FWD stations was reported to be 0.72.

Figures 3.35 and 4.14 compare SOFTSYS models with ANN backcalculation models for layer moduli prediction. Since the predictions with the ANN models were quite successful for the Roseville Bypass, SOFTSYS models could not perform any better compared to the ANN models. Still, the predictions of SOFTSYS were improved by about 6.3% for  $E_{Ri}$  when Hill's algorithms were used. Both analyses show that SOFTSYS can be used reliably and with a higher accuracy in analyzing FWD data compared to using ANN based models.



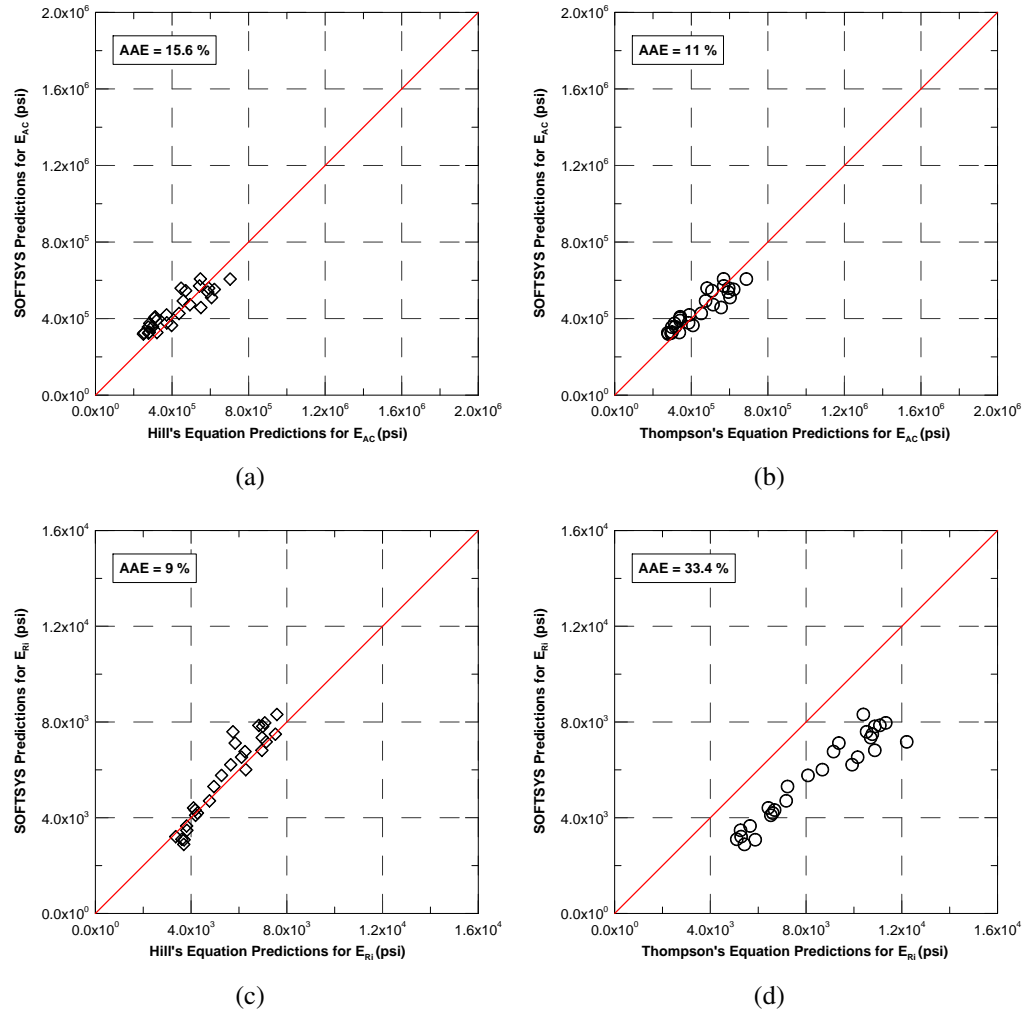


**Figure 4.14:** Performances of FDP-LSS-PM1-FWD4 SOFTSYS Model for Roseville Bypass.

#### 4.4.4 Staley Road

Figures 4.15(a) to 4.15(d) show SOFTSYS model predictions for Staley Road. SOFTSYS model FDP-LSS-PM1-FWD4 was used for backcalculating layer properties of FDP-LSS. The results obtained showed that the AC modulus was predicted with almost the same accuracy for both Hill's and Thompson's algorithms. The AAE values obtained for predicting AC modulus were 15.7% and 14.5% for Hill's and Thompson's algorithms, respectively. Similarly, AAE values produced for the estimation of  $E_{Ri}$  were 16.0% and 15.7% for Hill's and Thompson's algorithms, respectively. The inspection of the data actually showed a similar problem occurred when analyzing Roseville Bypass. That is, SOFTSYS can capture  $D_{36}$  perfectly, which is actually used in backcalculating the value of  $E_{Ri}$  in Thompson's algorithm. However, all layer moduli in combination  $E_{AC}$ ,  $E_{LSS}$  and  $E_{Ri}$  resulted in much higher predictions with SOFTSYS. The alternative approaches for the solution of this problem can be applied for Staley Road data too. The best fitness value obtained from the SOFTSYS solutions was 0.996187 among all the stations. The average number of generations to reach the best fitness was 32. Similar GA performances were also observed in the analyses of Roseville Bypass. Therefore, it can be concluded that the number of generations needed increases with the number of layers in order to improve predictions. The average layer modulus for the LSS layer was reported to be 22 ksi, which was found to be a little lower considering the short-term curing of the lime stabilized layer. In addition, the coefficient of variation in LSS layer moduli throughout the FWD stations was reported to be 0.43, which needs to be taken into account while reporting the results of backcalculation analysis.

The comparison of SOFTSYS models with ANN backcalculation models can also be made based on Hill's and Thompson's algorithms. Figures 3.36 and 4.15 showed that SOFTSYS models performed much better compared to ANN models although both approaches produced similar estimates when tested with the synthetic ILLI-PAVE database.

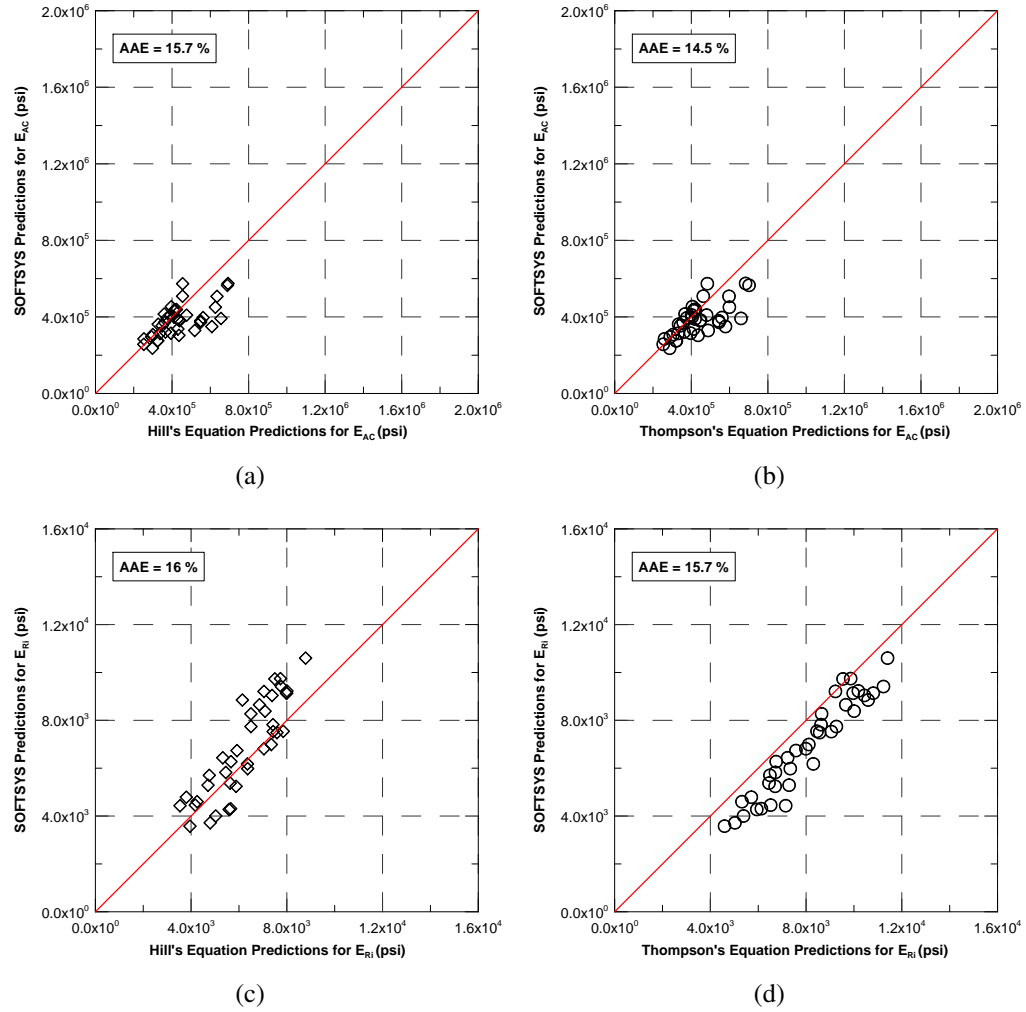


**Figure 4.15:** Performances of FDP-LSS-PM1-FWD4 SOFTSYS Model for Staley Road.

The predictions of SOFTSYS for  $E_{AC}$  are at least 17.0% better compared to those of ANN models. The improvement in the prediction of  $E_{Ri}$  was found to be at least 1.7% when SOFTSYS is used instead of ANN based backcalculation models.

#### 4.4.5 High Cross Road (FA 808)

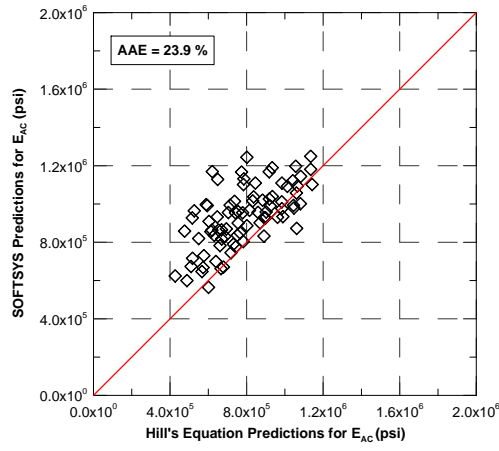
Figures 4.16(a) to 4.16(d) show SOFTSYS model predictions for High Cross Road. SOFTSYS model FDP-LSS-PM1-FWD4 was used for backcalculating layer properties of FDP-LSS. The results obtained showed that the AC modulus was predicted with almost the same accuracy for both Hill's and Thompson's algorithms. The AAE values obtained

for predicting AC modulus were 23.9% and 18.2% for Hill's and Thompson's algorithms, respectively. Similarly, AAE values for the estimation of  $E_{Ri}$  were 9.9% and 31.1% for Hill's and Thompson's algorithms, respectively. Unfortunately, the inspection of the FWD data and the results actually showed the similar problem occurred when analyzing both Roseville Bypass and Staley Road. SOFTSYS captured  $D_{36}$  perfectly, which is actually used in backcalculating the value of  $E_{Ri}$  in Thompson's algorithm. However, all layer moduli in combination,  $E_{AC}$ ,  $E_{LSS}$  and  $E_{Ri}$ , resulted in much higher predictions with SOFTSYS. Therefore alternative formulas that take into account all deflections can be used to improve the estimations for  $E_{Ri}$ . Exact matches of the deflection profiles were observed, which resulted in the best fitness values of the SOFTSYS solutions to be 1.00, which was an excellent performance of SOFTSYS models. The average number of generations to reach the best fitness was 27 for all the stations. The average layer modulus for LSS layer was reported to be 86 ksi, which suggests that long-term curing of the lime stabilized layer should be considered when backcalculating the modulus of LSS layer. In addition, the coefficient of variation in LSS layer moduli throughout the FWD stations was reported to be 0.47, which is similar to those obtained in the previous field analyses.

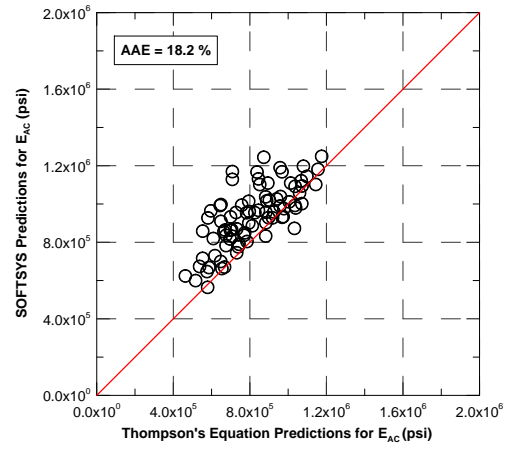
The comparison of SOFTSYS models with ANN backcalculation models can also be made based on Hill's and Thompson's algorithms. Figures 3.37 and 4.16 show that SOFTSYS models performed much better compared to ANN models when estimating  $E_{Ri}$ , although both models produced similar estimates when tested with the synthetic ILLI-PAVE database. The improvement in the prediction of  $E_{Ri}$  was found to be at least 2.5% when SOFTSYS is used instead of ANN based backcalculation models. However, the predictions of SOFTSYS for  $E_{AC}$  are 3.0% worse compared to those using ANN models.

#### **4.4.6 Sand Pit Road (Henry County)**

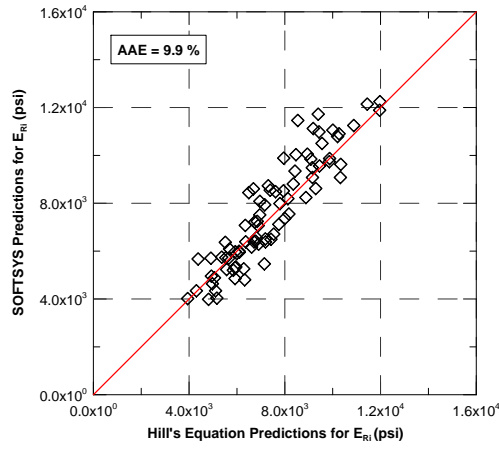
Figures 4.17(a) to 4.17(b) show SOFTSYS model predictions for Sandy Pit Road. SOFTSYS model CFP-PM1-FWD4 was used for backcalculating layer properties of CFP.



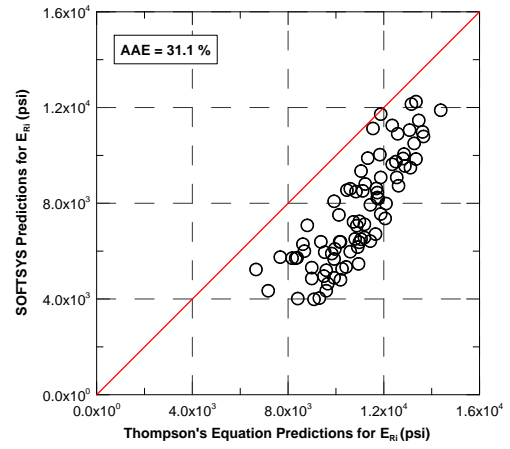
(a) Hill's Algorithm for  $E_{AC}$



(b) Thompson's Algorithm for  $E_{AC}$



(c) Hill's Algorithm for  $E_{Ri}$



(d) Thompson's Algorithm for  $E_{Ri}$

**Figure 4.16:** Performances of FDP-LSS-PM1-FWD4 SOFTSYS Model for High Cross Road.

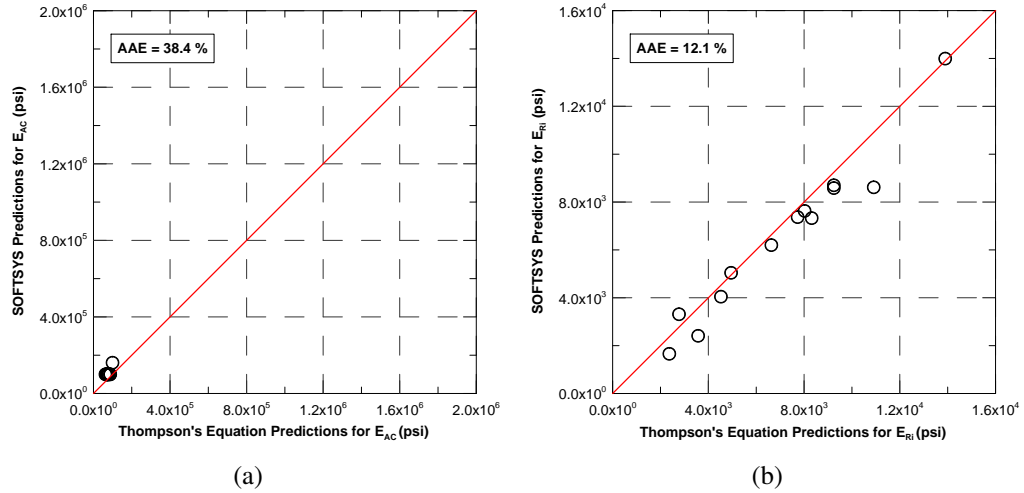


**Figure 4.17:** Performances of CFP-PM1-FWD4 SOFTSYS Model for Sand Pit Road.

Thompson's algorithms were used alone to predict the AC modulus and the value of  $E_{Ri}$ . The AAE values obtained for predicting  $E_{AC}$  and  $E_{Ri}$  were 38.4% and 12.1% when Thompson's algorithms were used. The deflection profiles obtained could not be used to produce high correlations. The maximum best fitness value of SOFTSYS solutions was 0.846255. The average number of generations to reach the best fitness was 29 for all the stations. The average layer modulus for the GB layer was 5 ksi. However, large variations were observed throughout the FWD stations when estimating  $K_{GB}$ . The coefficient of variation in GB layer moduli throughout the FWD stations was 0.69.

The comparison of SOFTSYS models with ANN backcalculation models can be made using only Thompson's algorithms. Figures 3.38 and 4.17 show that SOFTSYS models performed much better compared to using ANN models when predicting both  $E_{AC}$  and  $E_{Ri}$  values for CFPs. The predictions of SOFTSYS for  $E_{AC}$  are about 8.3% better compared to those of ANN models. The improvement in the prediction of  $E_{Ri}$  was also found to be noticeable and reported to be 8.2% when SOFTSYS was used instead of ANN based backcalculation models.

## 4.5 Comparison of SOFTSYS with ANN-PRO

The main objective of this thesis is to backcalculate the pavement layer properties reliably and quickly. For this purpose, two approaches were presented in this thesis. In addition, a comparison between these approaches was made using the field data obtained from Illinois pavements. These results showed in practice that SOFTSYS can be used more reliably than ANN backcalculation models. However, there are also some differences between the two approaches which may make one approach advantageous over the other when a backcalculation analysis is performed.

- SOFTSYS can search and identify all possible solutions that may be a candidate for the solution of backcalculation problems. ANN models, on the other hand, only provide a deterministic solution after they are trained properly. Considering the variability and noise in the FWD data, an end-user may be interested in all the solutions that may satisfy the deflection profile obtained from the field. Then, a decision can be made based on experience and/or other known information about the road (i.e. pavement surface temperature, design thickness, etc.). Therefore, the SOFTSYS approach provides more thorough backcalculation analysis results.
- SOFTSYS is often slower compared to ANN backcalculation methods; however, it provides more realistic results since it uses forward FE analysis, which does not suffer from the ill-posedness problems. This provides an advantage since the actual field data may contain high variability and noise. If this was the case, ANN models would have to be re-trained with noise capable databases.
- The adjustment or selection of many GA model parameters implemented in SOFTSYS does not play an important role in the predictions, whereas, model parameters selected in training ANN backcalculation models do affect the results considerably. SOFTSYS can converge to the same results in a longer period of time through more generations. The most important parameter in SOFTSYS is the

mutation rate because it simply creates diversity in the population space. However, the selection of ANN parameters, i.e., the number of hidden layers, number of nodes in these layers, etc., plays a crucial role as the parameters directly interfere with the accuracy of the ANN models. Therefore, SOFTSYS provides more flexibility to the end-user when a new set of models needs to be developed.

- ANN backcalculation methods may easily suffer from the problem of memorization when they are not properly trained. The cross validation must be made to eliminate this risk. However, SOFTSYS does not suffer from such a problem since it is based on forward FE analysis, which is less susceptible to overfitting.
- The identification of uniqueness problems can only be realized in the training of ANN backcalculation models using the predictions for testing data sets. Note that the training is generally performed using the synthetic deflection data in order to have much less variability and, therefore, include fewer non-unique cases to train. On the contrary, SOFTSYS can provide much more information about the uniqueness (or insensitiveness) problems occurring using either synthetic or field data, because SOFTSYS can provide multiple solutions since the analyses are repeated. This is a great advantage when analyzing multi-layered pavements where non-unique (or insensitive) solutions are obtained.

## **4.6 Summary**

In this chapter, a novel and robust methodology is presented to backcalculate the pavement layer moduli using a hybrid system of two soft computing methodologies, ANNs and GAs as an alternative solution strategy to the ANN based backcalculation method presented in Chapter 3.

First, the details of the algorithm and the implementation of SOFTSYS were described. Then SOFTSYS backcalculation models developed to backcalculate pavement layer



moduli were provided. Verification of the SOFTSYS model was made using the synthetic ILLI-PAVE database developed previously for flexible pavements including Full-depth Asphalt Pavements, Full-depth Asphalt Pavements on Lime Stabilized Soils and Conventional Flexible Pavements.

In an effort to fully validate SOFTSYS backcalculation models, FWD test data already available from previous IHR studies were used with known pavement layer design thicknesses and material properties. Examples of such previous studies with available FWD test data are the US 50, US 20, Staley Road, High Cross Road, Roseville Bypass, and Sand Pit Road projects. The validation database established in this way from the field FWD data was fully utilized in a comprehensive effort to validate the SOFTSYS models developed for robustness and accuracy in predicting the pavement layer moduli directly from FWD testing. Finally, a comparison was made between the predictions of ANN based backcalculation models and SOFTSYS models.

In summary, SOFTSYS was shown to feature high reliability and robustness for predicting accurate and repeatable results from FWD test data, which are essential for nondestructive evaluation of pavements.

# Chapter 5

## Backcalculation of Layer Thickness and Moduli for Flexible Pavements

### 5.1 Introduction

A typical pavement structure, as shown in Figure 5.1, can be described using four different properties [Selezneva *et al.*, 2002], which need to be determined in order to have an overall pavement rehabilitation strategy:

- Layer description (e.g., surface, overlay, base, and subgrade);
- Material type description of pavement layers;
- Layer thickness; and
- Layer thickness variability.

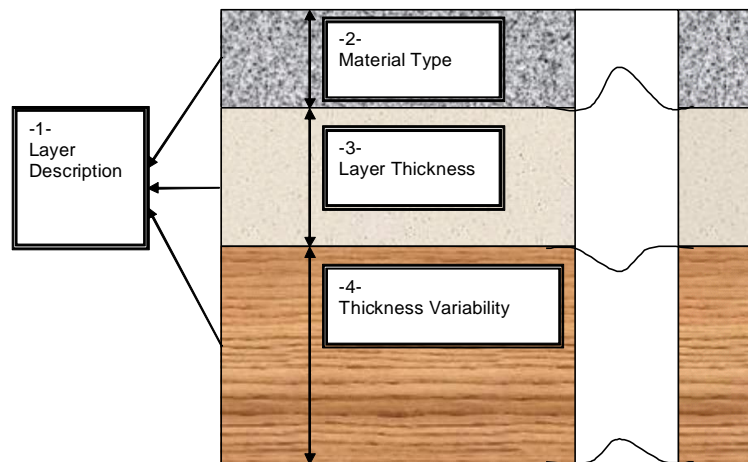


**Figure 5.1:** Typical Pavement System Geometry and Properties to be Determined.

In this chapter, SOFTSYS is implemented for interpreting the results of FWD tests using an innovative approach. SOFTSYS is a computational method to estimate the

properties of pavement layers. Among those, the layer thickness plays the crucial role in determining the pavement's remaining life since it is a major factor contributing to the structural adequacy of the pavement. The outstanding contribution of SOFTSYS is that it is able to reliably estimate an asphalt concrete layer's thickness in addition to its modulus. Using only FWD test results (i.e., deflections) as inputs, SOFTSYS calculates all the necessary properties for pavement evaluation. To do this, SOFTSYS uses a combination of nontraditional computing tools, such as ANNs and GAs. Using quick and robust algorithms in SOFTSYS, real-time field evaluation of pavements becomes feasible, as well as verification of as-constructed pavement design properties.

With the main focus being on infrastructure renewal, the proposed algorithm brings innovation in the areas of FWD testing and structural layer thickness and property evaluations of in-service pavements. The SOFTSYS algorithm applies to data collection and real-time analyses using the ILLI-PAVE based structural model without the need for pavement coring or additional GPR testing for thickness determinations. Being robust and accurate, SOFTSYS can be used to assess the construction quality to achieve a significant improvement in estimation of as-constructed pavement properties. This approach has the potential to minimize traffic disruptions and extended pavement lane closures, and as a result, improves both mobility and safety of our highways.

### **5.1.1 Significance**

One of the main objectives of this study is to develop integrated solutions to transportation problems by explicitly capturing the interactions between the vehicle, driver/traveler, and the infrastructure. Considering that in freight transportation heavy truck axle/wheel loads cause the most damage and deterioration of highway pavements, an integrated solution to nondestructive pavement condition evaluation would be best accomplished by collecting both typical and overloaded truck wheel loads from weigh-in-motion stations and applying to the pavement similar or equivalent load magnitudes during the FWD tests. Such

pavement-vehicle interaction that causes nonlinear pavement deformation trends under increasing load levels would be better captured using the SOFTSYS approach, which essentially takes into account the nonlinearity of pavement base and subgrade layers through ILLI-PAVE FE solutions. Thus, the advantage of the SOFTSYS approach would be in the robust and accurate interpretations of the FWD data collected at different load magnitudes. By determining thickness profiles and layer properties of in-service pavements from the results of FWD testing, the novel methodology SOFTSYS could improve new and rehabilitated pavement thickness designs for a major benefit to the asset management of a nation's transportation network.

### **5.1.2 Objective**

Knowing pavement layer thicknesses is critical to predicting pavement performance, establishing pavement load carrying capacity, and developing pavement maintenance and rehabilitation strategies. Accurate determination of pavement layer thicknesses usually requires destructive coring and sampling from the pavement section. This is usually not desirable since it damages functionality of a pavement and disrupts traffic. Moreover, thickness measurements obtained from only a few extracted cores may not always represent the thickness profile adequately. It is important to ensure that the thicknesses of materials being placed by the contractor are acceptably close to specifications [Sener *et al.*, 1998].

The layer thickness information, a key structural design input, is required for many types of analyses, including backcalculation of pavement moduli, mechanistic analysis of pavement structures, and performance modeling. Due to poor workmanship and/or limitations of construction equipment used to build roads, construction quality of pavements may not be at a desired level. This might cause the thickness constructed on-site to be considerably different than the designed thickness. Furthermore, in many cases, the lack of proper design documentation for existing roads makes it extremely difficult to rehabilitate certain pavements without the knowledge of pavement layer thicknesses.

Therefore, insufficient knowledge of layer thicknesses during pavement response testing is often a major limitation in pavement condition assessment. Current methods other than pavement coring used to determine the thicknesses require some advanced nondestructive testing equipment such as GPR, which is rather expensive. On the other hand, if FWD tests are conducted, for example, in 5 ft intervals of a road section for which abrupt change in the thickness is not expected, the thickness profile along the test section can be determined with reasonably good accuracy and in real time.

To address the current challenges, SOFTSYS is developed to perform the following tasks in real time as part of conducting FWD tests:

- Determine pavement thickness
- Estimate pavement moduli, and
- Identify pavement properties such as Poisson's ratio.

Models developed for SOFTSYS to predict thicknesses of flexible pavements are provided in this chapter. The developed backcalculation models were first validated with the ILLI-PAVE synthetic database. Then, they were used to capture the thicknesses of various types of flexible pavements previously used with SOFTSYS models developed only to predict moduli.

## **5.2 SOFTSYS Models for Thickness Determination**

SOFTSYS models to determine pavement layer thicknesses were developed based on the ones used for backcalculation of pavement layer moduli. In the previous chapter, these models used design thicknesses for reliably predicting pavement layer moduli. Therefore, their reliability is also based on the accuracy of thickness estimation. However, the thicknesses of pavement layers, especially those of the AC layer, may show large variations along the road due to several reasons. To illustrate this, the thickness information for

full-depth flexible pavements obtained from several projects constructed in the state of Illinois are provided in Table 5.1. It includes the planned (designed) AC thickness of FDP in addition to the minimum, maximum, and average constructed thicknesses obtained from cores taken along these projects. This table also provides the thickness variation determined by the cores taken for each project. The constructed thickness data suggest that the average value of variation in the AC layer's thickness was 14.9% of design thickness. For some projects, the constructed thickness was different than the design thickness by 28.2%. Using this data set, it was concluded that the constructed thicknesses can be considerably different than the design thickness, which may result in erroneous predictions for layer properties when a backcalculation model uses the design thickness information as input. Still, the data presented in this table provide very valuable information when the accuracy of a thickness prediction is questioned using any method. Finally, it should be noted that due to the nature of the problem, the variability of layer thickness increases as the number of layers in the pavement section increases.

In total, 10 thickness backcalculation models were developed for FDPs, FDP-LSSs, and CFPs. Table 5.2 provides the input and output properties needed for these models. Among them the first two models, FDP-PM2-FWD4 and FDP-PM2-FWD7, belong to FDPs developed to use different sensor information when available. For example, the first model FDP-PM2-FWD4, predicts  $t_{AC}$ ,  $E_{AC}$ , and  $E_{Ri}$  with the use of four sensor information obtained from FWD;  $D_0$ ,  $D_{12}$ ,  $D_{24}$ , and  $D_{36}$ . This model also predicts the thickness of the AC layer in addition to the pavement layer moduli [Pekcan *et al.*, 2010]. Similarly, the second model FDP-PM2-FWD7, uses seven sensors,  $D_0$ ,  $D_{12}$ ,  $D_{24}$ ,  $D_{36}$ ,  $D_{48}$ ,  $D_{60}$ , and  $D_{72}$ , to predict the same properties of FDP including the thickness of the AC layer. These SOFTSYS models use the same ANN forward structural model that was already used successfully to predict the pavement layer moduli (FDP-PM1-FWD4 and FDP-PM1-FWD7) in the previous chapter.

**Table 5.1:** Asphalt Thickness Variability for Various Flexible Pavements Constructed in the State of Illinois

<i>Project Number</i>	<i>Planned Thickness (in.)</i>	<i>Avg. Thickness (in.)</i>	<i>Min. Thickness (in.)</i>	<i>Max. Thickness (in.)</i>	<i>Standard Deviation (in.)</i>	<i>C.O.V. (%)</i>	<i>Number of Cores</i>
1	13.5	14.1	12.2	16	0.98	6.97	37
2	14.2	14.58	12.4	18.2	0.76	5.19	43
3	11.5	11.57	10.5	12.8	0.45	3.9	45
4	16.5	16.66	16.5	16.8	0.11	0.68	5
5	15.2	16.34	13	18.6	1	6.15	54
6	12.5	13.4	11.6	15.7	0.92	6.87	22
7	13	13.48	11.4	16.3	0.87	6.46	48
8	12.75	13.16	12.7	14	0.46	3.51	9
9	12.5	14.2	13.8	14.6	0.57	3.98	2
10	12.75	13.46	12.7	14.2	0.45	3.31	12
11	12	12.41	11.4	13.8	0.78	6.32	11
12	12.5	12.66	11.7	13.4	0.52	4.13	7
13	14	14.17	11.9	15.7	1.37	9.65	10
14	15.75	16.35	15.8	17.4	0.39	2.4	43
15	15	15.54	14.1	16.9	0.54	3.48	73
16	15	15.77	15	17	0.46	2.92	63
17	14	14.5	13.5	16.5	0.63	4.36	52
18	13.2	14.37	13.8	15.1	0.67	4.63	3
19	9.5	10.15	9	11.5	0.64	6.35	19
20	17	18.3	17.3	19	0.59	3.24	14
21	11.7	13	12.2	13.8	1.13	8.7	2
22	10	10.42	8.8	11	0.7	6.71	10
23	10	10.75	10.1	11.4	0.92	8.55	2
24	14.75	15.13	13.8	16.4	0.46	3.05	83
25	12.7	13.35	12.9	14	0.45	3.34	6
26	14	14.84	14.3	16.4	0.61	4.08	10
27	13.5	14.6	13.8	16	0.56	3.86	33
28	16.2	16.63	16.3	17.3	0.46	2.75	4
29	11.5	11.95	11.6	13	0.27	2.24	38

The models developed for estimation of layer thicknesses of FDP-LSSs (FDP-LSS-PM2-FWD4 and FDP-LSS-PM2-FWD7) use different number of sensors' information as in those used in FDPs. In addition to these, two more thickness prediction models (FDP-LSS-PM3-FWD4 and FDP-LSS-PM3-FWD7) are developed to predict the thickness of the AC layer by assuming that the design thickness of lime stabilized soil layer is known. The objective of developing these methods is to decrease the number of unknowns in the backcalculation problem and therefore reduce the ill-posedness. These models also eliminate the need for estimating thicknesses of layers underneath the AC layer since they generally show greater thickness variations.

The approach used in FDP-LSSs was also used to determine the thicknesses of CFP layers. Four different models, CFP-PM2-FWD4, CFP-PM2-FWD7, CFP-PM3-FWD4, and CFP-PM3-FWD7, were developed, which use 4- and 7- sensor inputs to predict AC layer thickness with or without the knowledge of design thickness of the GB layer. The predicted parameters for FDP-LSS and CFP also include pavement layer moduli  $E_{AC}$ ,  $E_{LSS}$ , and  $E_{Ri}$  for FDP-LSS and  $E_{AC}$ ,  $K_{GB}$ , and  $E_{Ri}$  for CFPs in addition to the thicknesses. Finally, the performances of all these SOFTSYS models were evaluated using the synthetic FWD data used to test the SOFTSYS models that only predict pavement layer moduli.

### 5.2.1 Full-depth Asphalt Pavements

Figures 5.2(a) to 5.2(c) provide the SOFTSYS FDP-PM2-FWD4 model's predictions of the AC layer thickness and moduli. The values of AAEs obtained for the estimation of  $t_{AC}$ ,  $E_{AC}$ , and  $E_{Ri}$  are 3.9%, 8.3%, and 1.6%, respectively. The values of AAEs being very close to 2.0% for  $E_{Ri}$  indicate that the SOFTSYS model worked very effectively to predict breakpoint resilient modulus of the subgrade layer. SOFTSYS was also able to capture the AC thickness successfully. The prediction of  $E_{AC}$  by SOFTSYS produced slightly higher AAE values compared to those reported for the other pavement properties. The best fitness values obtained from FDP-PM1-FWD4 predictions for randomly selected stations from the



**Table 5.2:** SOFTSYS Models Developed to Estimate Thicknesses and Moduli of Different Pavement Types

<b>Name</b>	<b>Inputs</b>	<b>Outputs</b>
FDP-PM2-FWD4	$D_0, D_{12}, D_{24}, D_{36}$	$t_{AC}, E_{AC}, E_{Ri}$
FDP-PM2-FWD7	$D_0, D_{12}, D_{24}, D_{36}, D_{48}, D_{60}, D_{72}$	$t_{AC}, E_{AC}, E_{Ri}$
FDP-LSS-PM2-FWD4	$D_0, D_{12}, D_{24}, D_{36}$	$t_{AC}, t_{LSS}, E_{AC}, E_{LSS}, E_{Ri}$
FDP-LSS-PM2-FWD7	$D_0, D_{12}, D_{24}, D_{36}, D_{48}, D_{60}, D_{72}$	$t_{AC}, t_{LSS}, E_{AC}, E_{LSS}, E_{Ri}$
FDP-LSS-PM3-FWD4	$D_0, D_{12}, D_{24}, D_{36}, t_{LSS}$	$t_{AC}, E_{AC}, E_{LSS}, E_{Ri}$
FDP-LSS-PM3-FWD7	$D_0, D_{12}, D_{24}, D_{36}, D_{48}, D_{60}, D_{72}, t_{LSS}$	$t_{AC}, E_{AC}, E_{LSS}, E_{Ri}$
CFP-PM2-FWD4	$D_0, D_{12}, D_{24}, D_{36}$	$t_{AC}, t_{GB}, E_{AC}, K_{GB}, E_{Ri}$
CFP-PM2-FWD7	$D_0, D_{12}, D_{24}, D_{36}, D_{48}, D_{60}, D_{72}$	$t_{AC}, t_{GB}, E_{AC}, K_{GB}, E_{Ri}$
CFP-PM3-FWD4	$D_0, D_{12}, D_{24}, D_{36}, t_{GB}$	$t_{AC}, E_{AC}, K_{GB}, E_{Ri}$
CFP-PM3-FWD7	$D_0, D_{12}, D_{24}, D_{36}, D_{48}, D_{60}, D_{72}, t_{GB}$	$t_{AC}, E_{AC}, K_{GB}, E_{Ri}$

IP-SYNTH FWD database are higher than those of FDP-PM2-FWD4. This is because it is generally much more difficult to predict thicknesses along with the pavement layer moduli.

The predictions obtained from the FDP-PM2-FWD7 model were improved with the use of seven sensors information as shown in Figures 5.3(a) to 5.3(c). The improvements are on the order of 2.0%, 3.6% and 0.9% for  $t_{AC}$ ,  $E_{AC}$ , and  $E_{Ri}$ , respectively. This shows that for the analysis of FDPs, use of more sensors should be preferred whenever the data are available. However, depending on the required accuracy, the first model always gives good predictions.

### 5.2.2 Full-depth Asphalt Pavements on Lime Stabilized Soils

There are two backcalculation models, FDP-LSS-PM2-FWD4 and FDP-LSS-PM2-FWD7, for predicting  $t_{AC}$ ,  $t_{LSS}$ ,  $E_{AC}$ ,  $E_{LSS}$ , and  $E_{Ri}$  simultaneously by using four and seven FWD deflections, respectively. The FDP-LSS-PM2-FWD4 model performance results for backcalculated pavement layer moduli and thicknesses are given in Figures 5.4(a) to 5.4(e). The AAEs given indicate that the FDP-LSS-PM2-FWD4 model could predict ILLI-PAVE solutions within the range of 12.6%, 35%, 8.8%, 79.4%, and 5.7% for  $t_{AC}$ ,  $t_{LSS}$ ,  $E_{AC}$ ,  $E_{LSS}$ , and  $E_{Ri}$ , respectively. Note that the predictions for the properties of AC layer and subgrade were at an acceptable level. Unfortunately, SOFTSYS predictions for  $t_{LSS}$  and  $E_{LSS}$  were not satisfactory. Figures 5.5(a) to 5.5(e) indicate that increasing the number of deflections helped to improve the accuracies of backcalculated properties of FDP-LSSs. Although there are substantial improvements in AAEs, it can be concluded that estimating the properties of lime stabilized layers of the FDP-LSSs is very difficult.

In order to estimate the thickness of the AC layer in FDP-LSSs, another model, FDP-LSS-PM3-FWD4, was developed for SOFTSYS, which assumed that the design thickness of the LSS layer is known prior to backcalculation analysis. The performance of this model for the backcalculated FDP-LSS pavement layer moduli and AC thickness is given in Figures 5.6(a) to 5.6(d). The corresponding AAE values obtained are 9.2%, 7.6%,

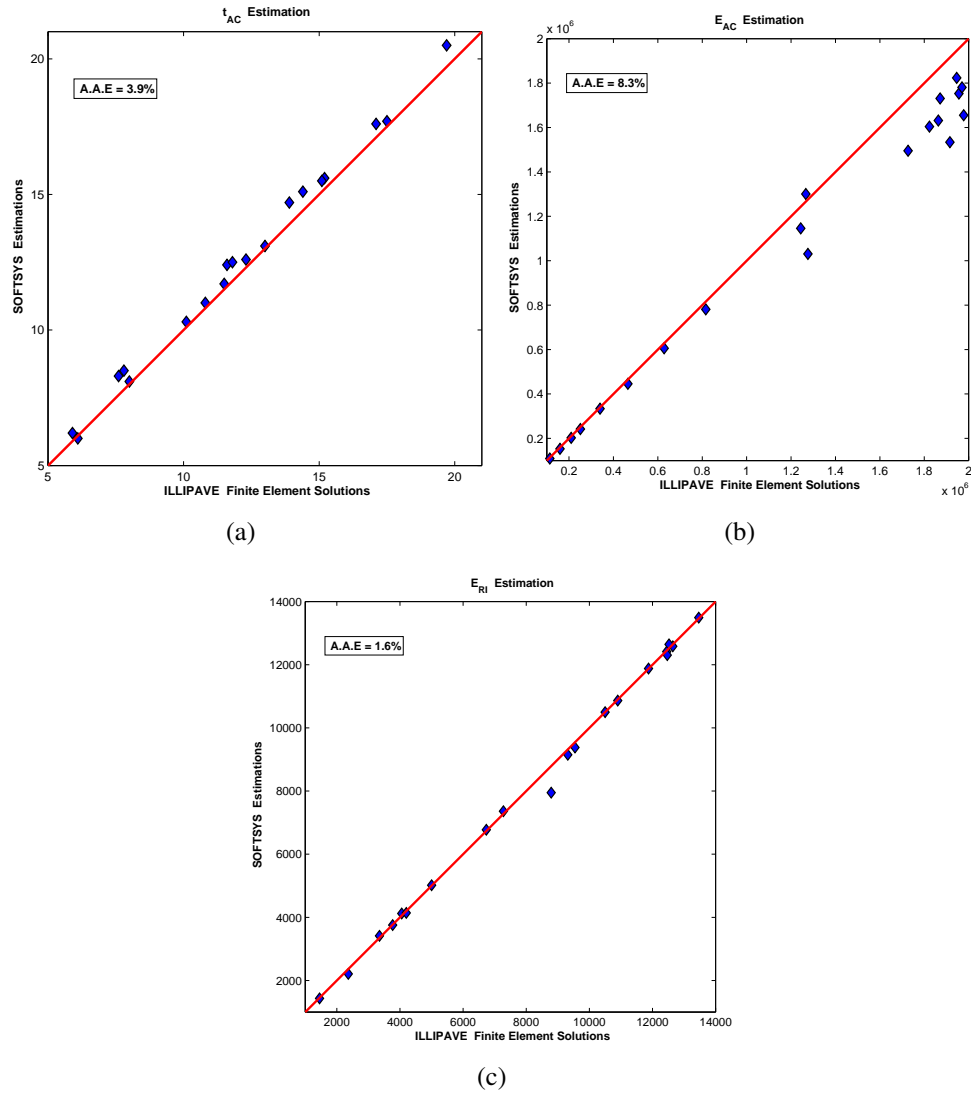


**Figure 5.2:** Performance Results of SOFTSYS Backcalculation Model FDP-PM2-FWD4 for Predicting AC Layer Thickness (in inches) and Layer Moduli (in psi) of Full-depth Asphalt Pavements Using Four Deflections.

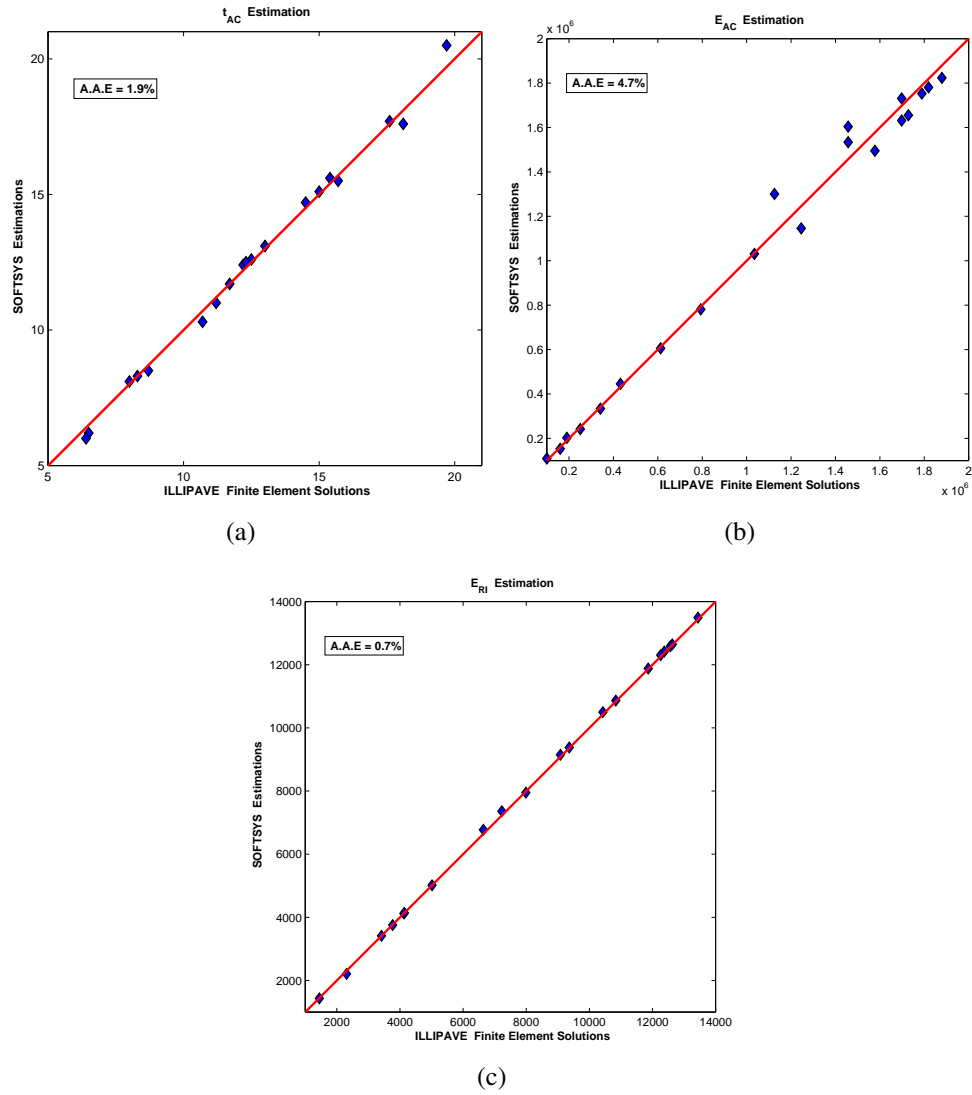


**Figure 5.3:** Performance Results of SOFTSYS Backcalculation Model FDP-PM2-FWD7 for Predicting AC Layer Thickness (in inches) and Layer Moduli (in psi) of Full-depth Asphalt Pavements Using Seven Deflections.

47.4%, and 3.2% for the prediction of  $t_{AC}$ ,  $E_{AC}$ ,  $E_{LSS}$ , and  $E_{Ri}$ , respectively. Increasing the number of FWD sensors (see Figures 5.7(a) to 5.7(d)) helped improve the prediction results; however, as with previous model, estimation of  $E_{LSS}$  was not very successful.

### 5.2.3 Conventional Flexible Pavements

The models developed for the estimation of CFP layer properties, including thicknesses of the AC layer and the GB layer, were similar to those developed for FDP-LSSs as explained in the previous section. Two backcalculation models, CFP-PM2-FWD4 and CFP-PM2-FWD7, were used for predicting  $t_{AC}$ ,  $t_{GB}$ ,  $E_{AC}$ ,  $K_{GB}$ , and  $E_{Ri}$  simultaneously. The difference between the two models is the number of FWD sensor inputs used in the backcalculation. The CFP-PM2-FWD4 model performance results for the backcalculated layer moduli and thicknesses are given in Figures 5.8(a) to 5.8(e). The AAEs obtained using this model are 4.4%, 49%, 8.9%, 43.4%, and 7.6% for  $t_{AC}$ ,  $t_{LGB}$ ,  $E_{AC}$ ,  $K_{GB}$ , and  $E_{Ri}$ , respectively. The SOFTSYS model could predict the properties of the AC layer and  $E_{Ri}$  successfully. Still, the prediction results for  $t_{LSS}$  and  $E_{LSS}$  were not at a desired level. Finally, Figures 5.9(a) to 5.9(e) indicate that increasing the number of deflections helped improve the accuracy of the backcalculated properties. As with FDP-LSSs, it can be concluded that estimating base layer properties of CFPs is also very hard.

Similarly, in order to estimate the layer moduli and thickness of the AC layer only, another set of SOFTSYS models was developed to assume the design thickness of GB layer as known. The performance results of the first model that uses only four deflections are given in Figures 5.10(a) to 5.10(d). The corresponding AAE values obtained are 5.0%, 10.6%, 47.7%, and 5.4% for the prediction of  $t_{AC}$ ,  $E_{AC}$ ,  $K_{GB}$  and  $E_{Ri}$ , respectively. The model that uses seven deflections (see Figures 5.11(a) to 5.11(d)) helped improve the prediction results by an average of 1.0% for AC layer properties and subgrade modulus. The AAE value obtained from the estimation of  $K_{GB}$  was still low, although it was improved by 25.1%.

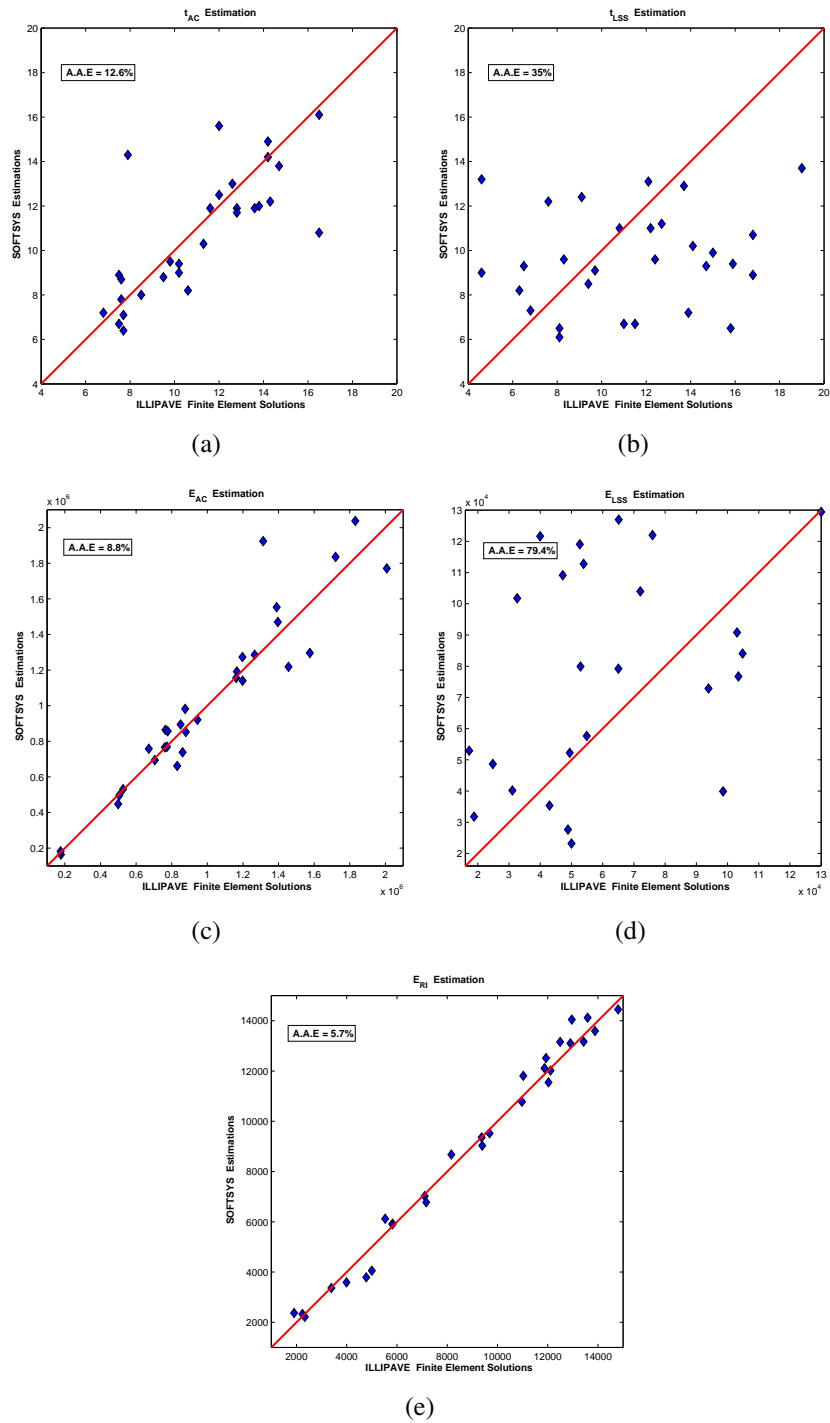


**Figure 5.4:** Performance Results of SOFTSYS Backcalculation Model FDP-LSS-PM2-FWD4 for Predicting Layer Thicknesses (in inches) and Layer Moduli (in psi) of Full-depth Asphalt Pavements Built on Lime Stabilized Soils Using Four Deflections.

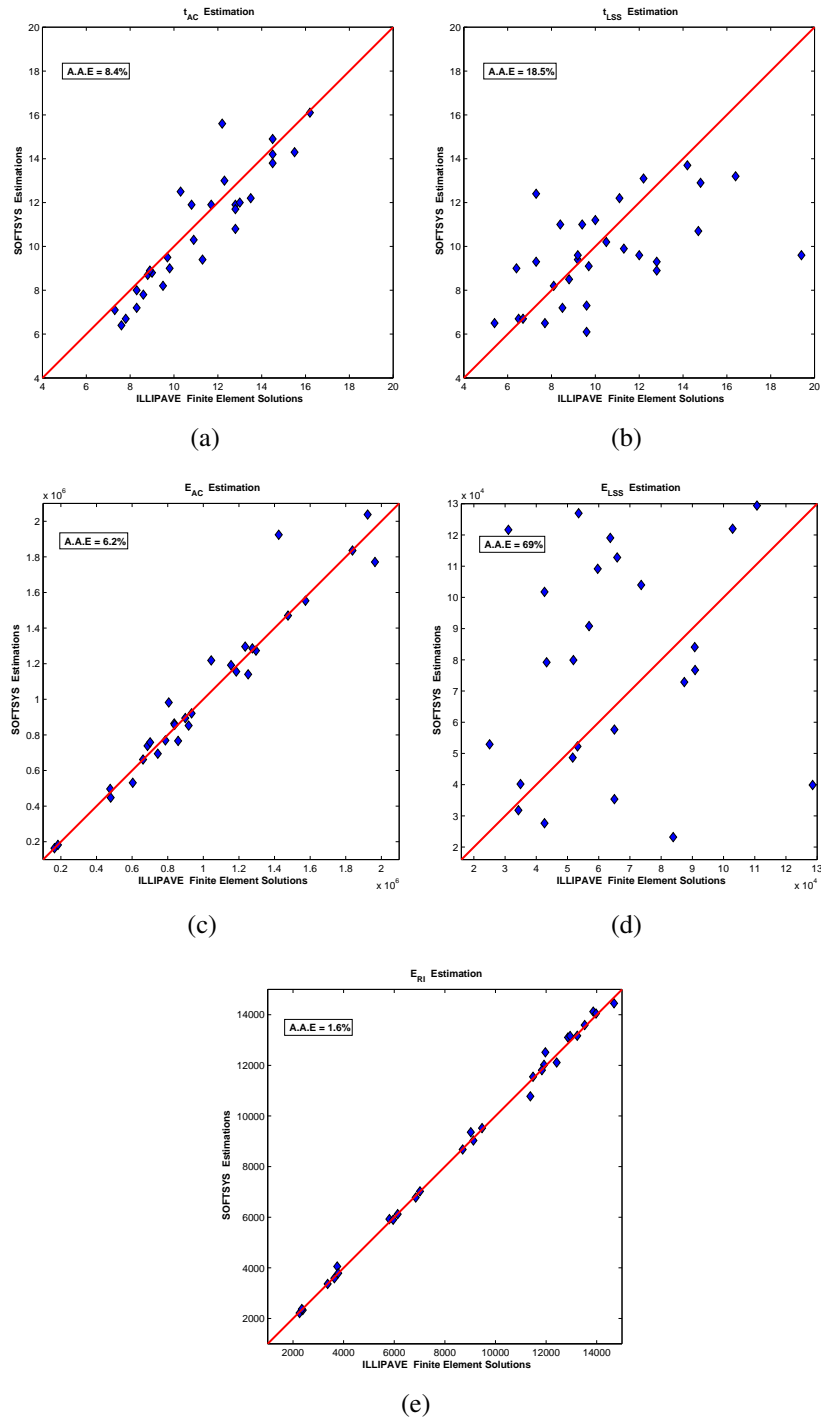


**Figure 5.5:** Performance Results of SOFTSYS Backcalculation Model FDP-LSS-PM2-FWD7 for Predicting Layer Thicknesses (in inches) and Layer Moduli (in psi) of Full-depth Asphalt Pavements Built on Lime Stabilized Soils Using Seven Deflections.

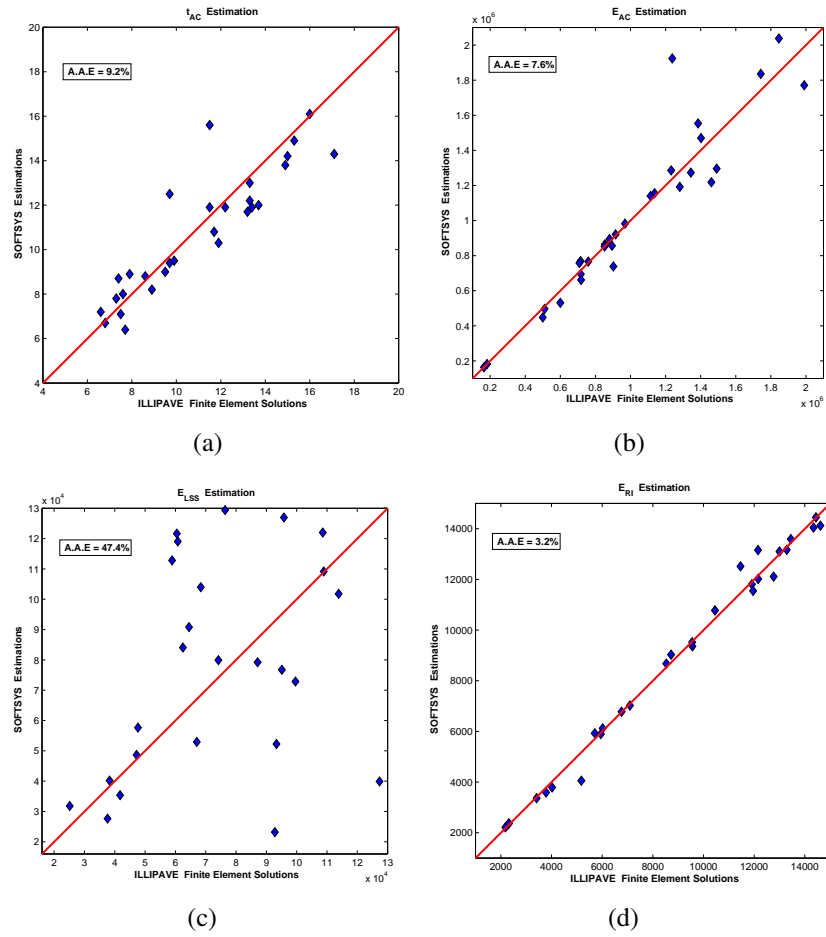


**Figure 5.6:** Performance Results of SOFTSYS Backcalculation Model FDP-LSS-PM3-FWD4 for Predicting AC Layer Thickness (in inches) and Layer Moduli (in psi) of Full-depth Asphalt Pavements Built on Lime Stabilized Soils Using Four Deflections.



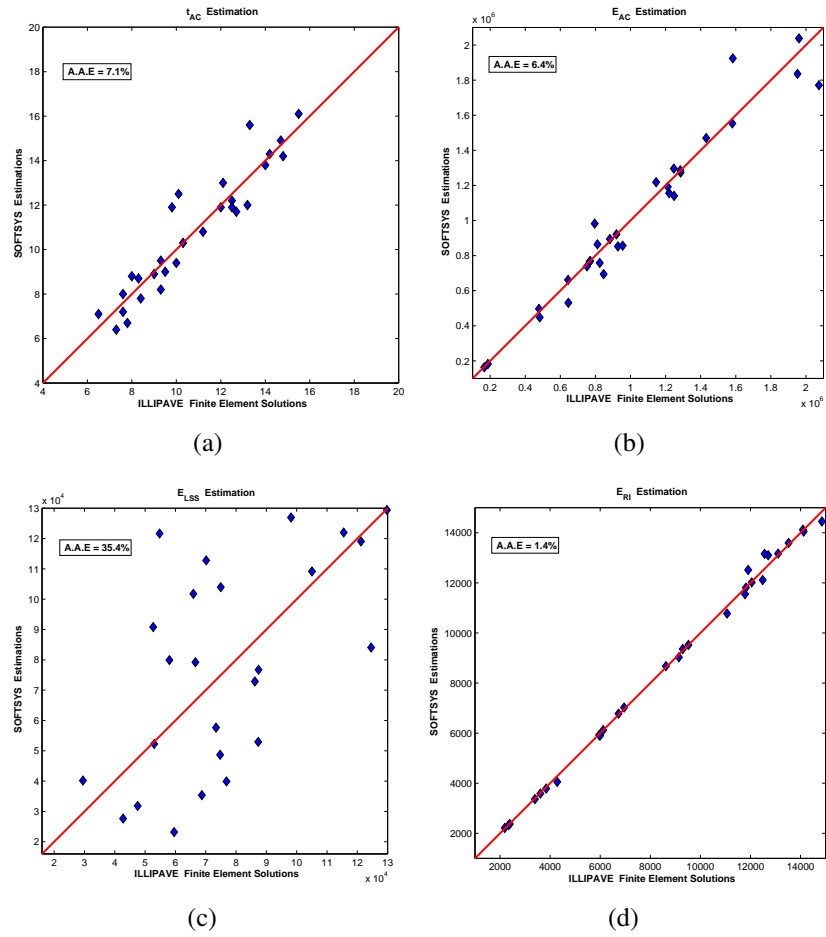


**Figure 5.7:** Performance Results of SOFTSYS Backcalculation Model FDP-LSS-PM3-FWD7 for Predicting AC Layer Thickness (in inches) and Layer Moduli (in psi) of Full-depth Asphalt Pavements Built on Lime Stabilized Soils Using Seven Deflections.

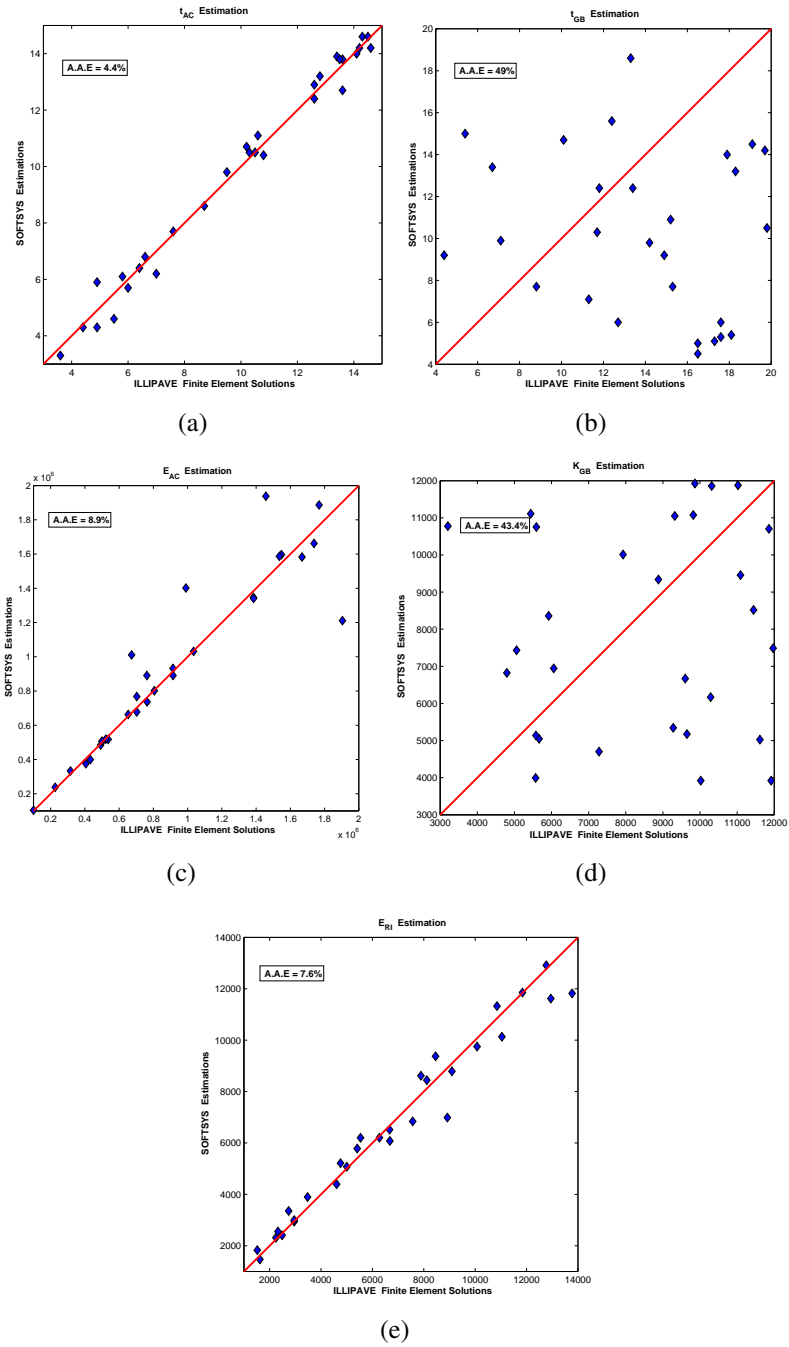


**Figure 5.8:** Performance Results of SOFTSYS Backcalculation Model CFP-PM2-FWD4 for Predicting Layer Thicknesses (in inches) and Layer Moduli (in psi) of Conventional Flexible Pavements Using Four Deflections.

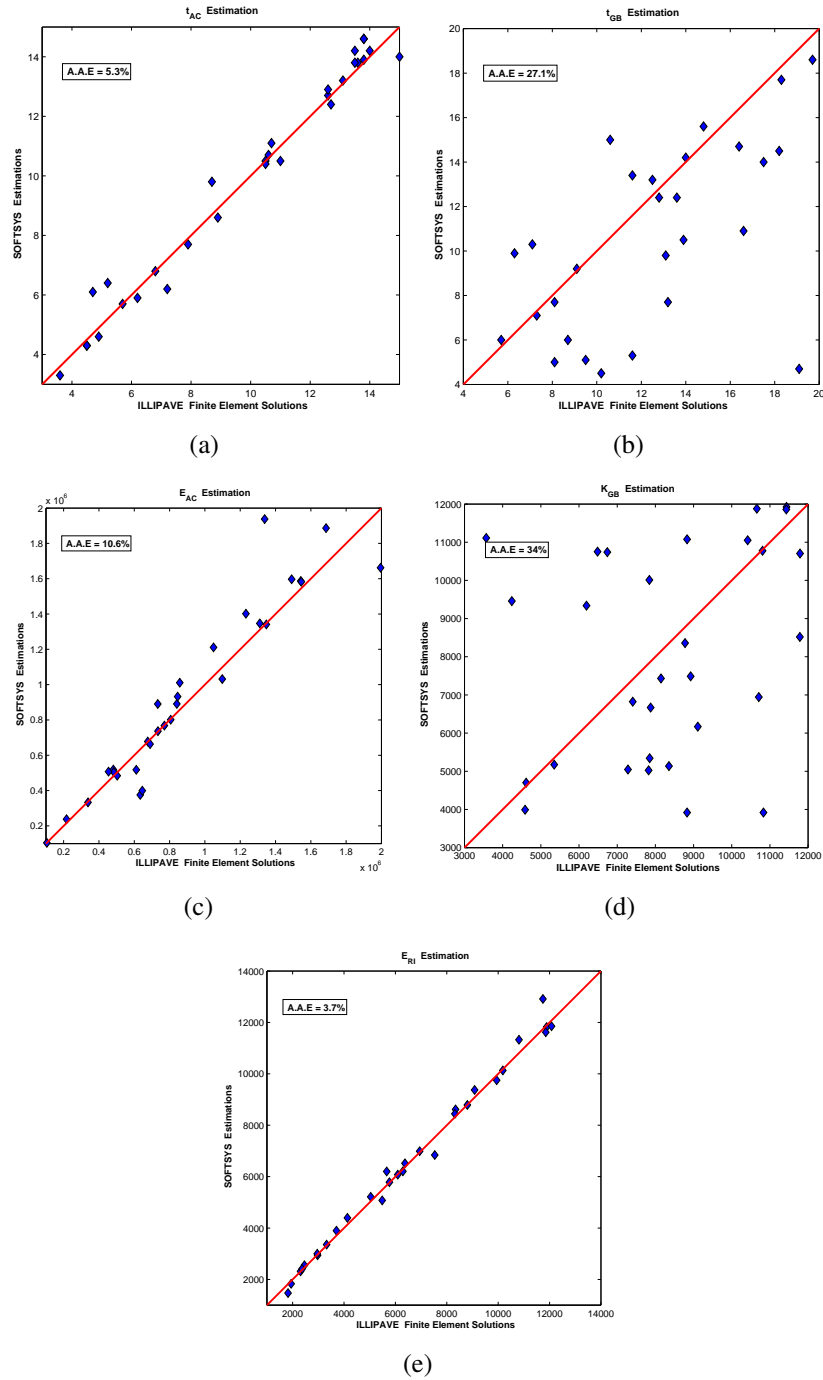


**Figure 5.9:** Performance Results of SOFTSYS Backcalculation Model CFP-PM2-FWD7 for Predicting Layer Thicknesses (in inches) and Layer Moduli (in psi) of Conventional Flexible Pavements Using Seven Deflections.

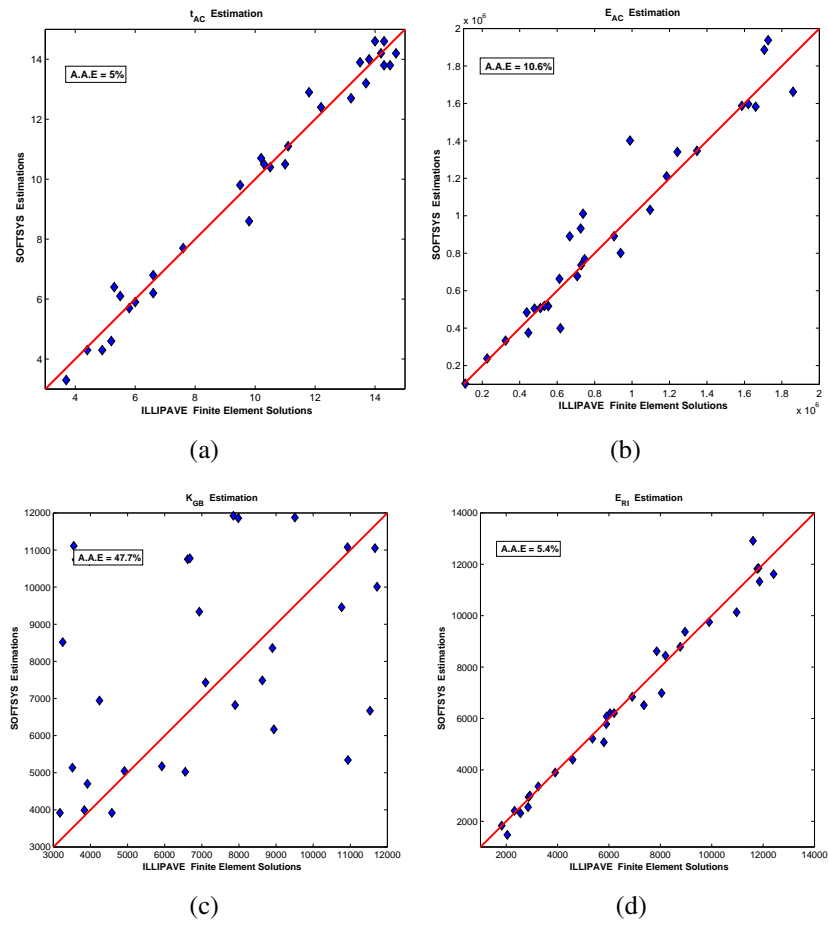


**Figure 5.10:** Performance Results of SOFTSYS Backcalculation Model CFP-PM3-FWD4 for Predicting AC Layer Thickness (in inches) and Layer Moduli (in psi) of Conventional Flexible Pavements Using Four Deflections.

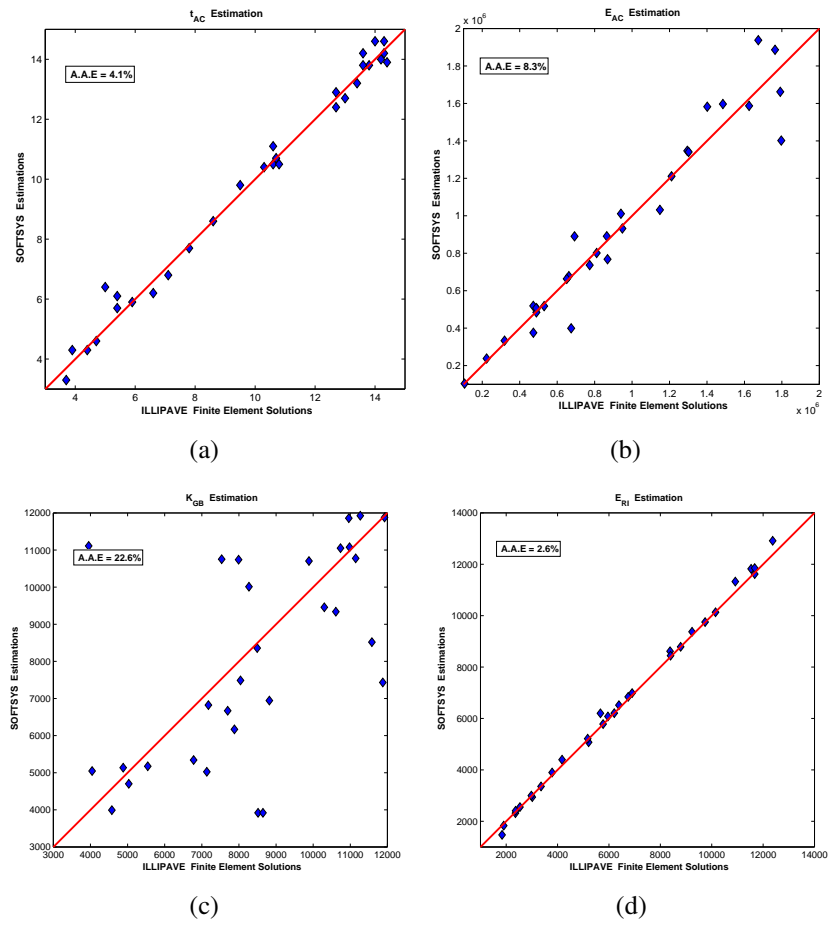


**Figure 5.11:** Performance Results of SOFTSYS Backcalculation Model CFP-PM3-FWD7 for Predicting AC Layer Thickness (in inches) and Layer Moduli (in psi) of Conventional Flexible Pavements Using Seven Deflections.

#### 5.2.4 Sensitivity and Uniqueness Issues for Three-Layered Systems

When the ILLI-PAVE synthetic database was used for verification, the performances of SOFTSYS models for backcalculating moduli and thickness of the mid-layer in FDP-LSSs and CFPs were not really good compared to the estimation of other layer properties. In this section, the reason behind this is explained by providing typical FE analysis results chosen from the ILLI-PAVE data set, which were used to train ANN forward models. In Table 5.3, a typical SOFTSYS result is provided for backcalculating of FDP-LSS properties for given synthetic FWD data. Different runs of SOFTSYS produced very close best fitness values. However, these best fitness values correspond to layer properties that show big differences.  $t_{LSS}$  values differ by almost 3 inches. In addition, the values of  $E_{LSS}$  are too different for the same best fitness value. These prove that for three-layered systems it is hard to predict the mid layer properties. Backcalculation processes for FDP-LSS are highly sensitive to small variations. Tables 5.4 and 5.5 are given in order to better explain the effect of a lime stabilized soil layer's thickness on pavement responses. Table 5.4 shows that even a big variation in the thickness of LSS layer does not affect the deflection responses on the surface of the pavement. This is because stress changes occur in the AC layer of the pavement. A similar behavior is also observed when the AC layer becomes softer (see Table 5.5). Finally, one can reach the same conclusion for the LSS layer modulus as it does not change the deflections measured on the pavement surface (shown in Table 5.6). These may result in inaccurate predictions for the modulus and thickness of the mid layer in FDP-LSS.

Unlike FDP-LSS, CFP backcalculation results may suffer from uniqueness issues, which is harder to handle compared to those created by sensitivity. In Table 5.7, a typical SOFTSYS result is provided for backcalculating CFP properties for given synthetic FWD data. The same best fitness values were obtained for different SOFTSYS analyses. However, these values correspond to layer properties with large variations.  $t_{GB}$  values

**Table 5.3:** Backcalculation Results of SOFTSYS for a Given FWD Data Chosen from ILLI-PAVE Database Developed for FDP-LSS

Best Fitness	$t_{AC}$ (in.)	$t_{LSS}$ (in.)	$E_{AC}$ (psi)	$E_{LSS}$ (psi)	$E_{Ri}$ (psi)	$D_0$ (mils)	$D_{12}$ (mils)	$D_{24}$ (mils)	$D_{36}$ (mils)
<b>ILLI-PAVE FWD DATA</b>	7.2	8.5	1218337	79216	2329	10.94	9.3	7.38	5.72
0.9946019	7.6	7.6	1147619	76490	2410	10.94	9.3	7.4	5.72
0.9946019	7.5	9	1242857	54447	2314	10.94	9.3	7.4	5.72
0.99785293	7.2	11	1348199	46631	2122	10.94	9.29	7.38	5.72
0.99785293	7	11.9	1433333	44098	2026	10.94	9.29	7.38	5.72
0.99635369	7.3	12	1306349	41238	2067	10.96	9.3	7.38	5.72

differ by almost 12 inches. In addition, the values of  $K_{GB}$  differ by almost 50% for the same best fitness value. These results prove that for CFP it is impossible to predict the mid layer properties unless another selection criterion is given. Tables 5.8 and 5.9 also explain the sensitivity issues for backcalculation of CFP properties. Changing the values of  $t_{GB}$  does not affect the surface deflections significantly when the AC layer modulus is too high (Table 5.8). Similar observations can be made when there is a very soft AC layer in the profile (Table 5.9). Finally, Table 5.10 shows that different values of  $K_{GB}$  do not greatly affect the surface deflections.

## 5.3 Field Validations

### 5.3.1 US 50 (FAP 327, old FA 409)

Figures 5.12(a) to 5.12(e) show SOFTSYS model predictions for US 50. There were only four deflections obtained from the FWD testing. Therefore SOFTSYS model FDP-PM2-FWD4 was used in the analyses. The results of backcalculation analyses showed that the AC modulus was predicted successfully; the AAE values obtained were about 19.8% and 24.8% for Hill's and Thompson's algorithms, respectively. Similarly, AAE

**Table 5.4:** Effect of Lime Stabilized Soil Layer's Thickness on Pavement Responses ( $t_{AC} = 8$  in.,  $E_{AC} = 900$  ksi,  $E_{LSS} = 100$  ksi,  $E_{Ri} = 9$  ksi)

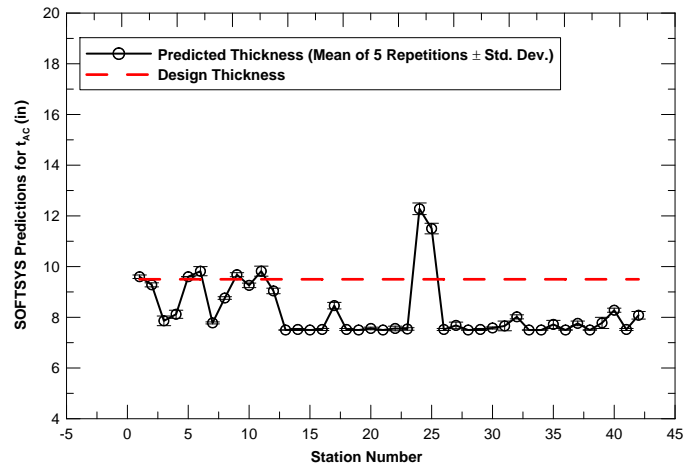
$t_{LSS}$ (in.)	$D_0$ (mils)	$D_{12}$ (mils)	$D_{24}$ (mils)	$D_{36}$ (mils)	$D_{48}$ (mils)	$D_{60}$ (mils)	$D_{72}$ (mils)	$\epsilon_{AC}$ ( $10^{-6}$ )	$\epsilon_{SG}$ ( $10^{-6}$ )	$\sigma_{DEV}$ (psi)	$\sigma_V$ (psi)
9	7.37	5.83	4.39	3.25	2.34	1.65	1.14	56.32	158.63	2.70	3.81
10	7.16	5.65	4.26	3.17	2.31	1.64	1.14	55.01	149.42	2.58	3.71
11	6.96	5.47	4.14	3.10	2.27	1.62	1.14	53.85	140.76	2.46	3.62
12	6.77	5.31	4.02	3.02	2.23	1.61	1.13	52.79	132.48	2.36	3.54
13	6.59	5.15	3.91	2.95	2.19	1.59	1.13	51.86	124.81	2.26	3.47
14	6.42	5.00	3.79	2.88	2.14	1.57	1.12	51.11	117.90	2.18	3.42
15	6.26	4.85	3.68	2.80	2.10	1.54	1.11	50.45	111.47	2.10	3.37

values produced for the estimation of  $E_{Ri}$  were 57.6% and 16.8% for the two algorithms. Thompson's algorithm produced overall better and more comparable estimates with the SOFTSYS model. The design thickness of the AC for US 50 was reported to be 9.5 in. for two different sections (K and M2) and SOFTSYS models produced generally lower estimates for thickness. The SOFTSYS analyses were repeated five times. The standard deviations of the thickness estimates are also shown in Figure 5.12(a). In general, the SOFTSYS model developed for backcalculating layer moduli only produced lower AAE values for predicting  $E_{AC}$ . Similarly, the estimations for  $E_{Ri}$  did not improve. The best fitness value obtained from all the SOFTSYS solutions was 0.998123 from all the stations where FWD data were collected. The average number of generations to reach the best fitness was 37 for all the stations.

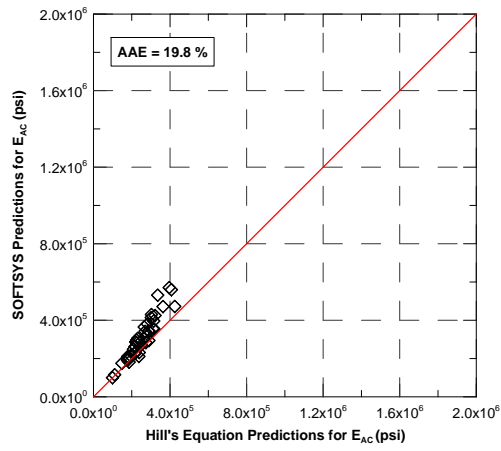
### 5.3.2 US 20 (FAP 301, old FA 401)

Figures 5.13(a) to 5.13(e) show SOFTSYS model predictions for US 20. Since only four deflections were obtained from the FWD testing, SOFTSYS model FDP-PM2-FWD4 was used in the analyses. The results showed that the AC modulus was predicted successfully;

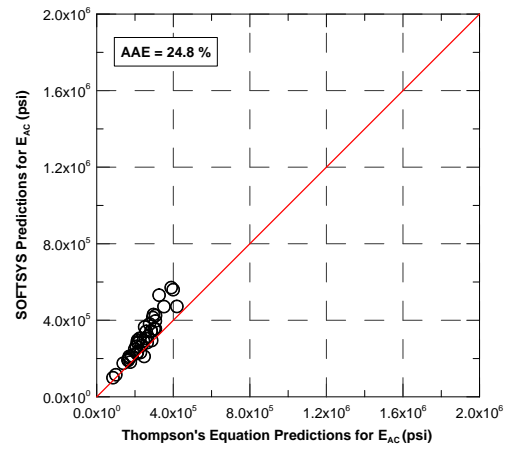




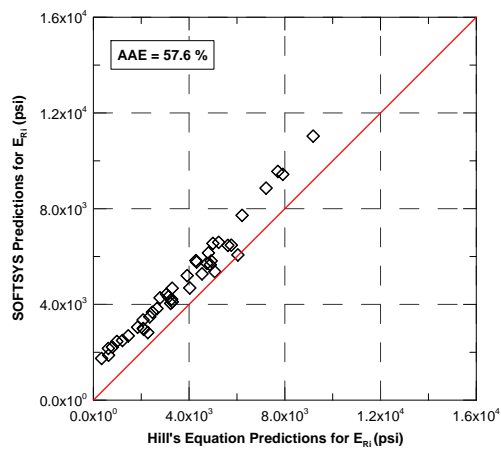
(a)



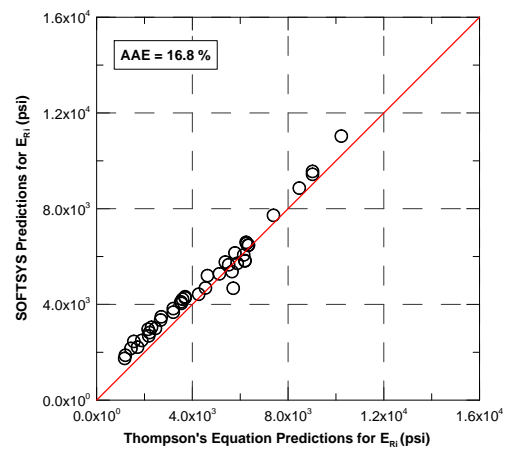
(b)



(c)



(d)



(e)

**Figure 5.12:** Performance Results of SOFTSYS Model FDP-PM2-FWD4 for US 50.

**Table 5.5:** Effect of Lime Stabilized Soil Layer's Thickness on Pavement Responses ( $t_{AC} = 8$  in.,  $E_{AC} = 500$  ksi,  $E_{LSS} = 100$  ksi,  $E_{Ri} = 9$  ksi)

$t_{LSS}$ (in.)	$D_0$ (mils)	$D_{12}$ (mils)	$D_{24}$ (mils)	$D_{36}$ (mils)	$D_{48}$ (mils)	$D_{60}$ (mils)	$D_{72}$ (mils)	$\epsilon_{AC}$ ( $10^{-6}$ )	$\epsilon_{SG}$ ( $10^{-6}$ )	$\sigma_{DEV}$ (psi)	$\sigma_V$ (psi)
9	8.77	6.48	4.70	3.39	2.39	1.64	1.11	73.81	197.10	3.29	4.42
10	8.50	6.25	4.56	3.31	2.36	1.64	1.12	71.98	183.66	3.10	4.25
11	8.25	6.04	4.42	3.24	2.32	1.63	1.12	70.45	171.31	2.93	4.10
12	8.01	5.84	4.29	3.16	2.29	1.62	1.13	69.03	159.76	2.77	3.97
13	7.79	5.65	4.16	3.08	2.25	1.61	1.13	67.82	149.25	2.64	3.85
14	7.59	5.47	4.03	3.00	2.21	1.59	1.13	66.95	139.96	2.51	3.76
15	7.40	5.30	3.91	2.93	2.17	1.58	1.12	66.19	131.42	2.40	3.69

**Table 5.6:** Effect of Lime Stabilized Soil Layer's Modulus on Pavement Responses ( $t_{AC} = 8$  in.,  $t_{LSS} = 12$  in.,  $E_{AC} = 900$  ksi,  $E_{Ri} = 9$  ksi)

$E_{LSS}$ (ksi)	$D_0$ (mils)	$D_{12}$ (mils)	$D_{24}$ (mils)	$D_{36}$ (mils)	$D_{48}$ (mils)	$D_{60}$ (mils)	$D_{72}$ (mils)	$\epsilon_{AC}$ ( $10^{-6}$ )	$\epsilon_{SG}$ ( $10^{-6}$ )	$\sigma_{DEV}$ (psi)	$\sigma_V$ (psi)
25	7.62	6.23	4.69	3.43	2.44	1.69	1.15	59.22	125.29	2.20	3.56
50	6.89	5.61	4.27	3.18	2.30	1.63	1.14	52.46	127.11	2.25	3.49
75	6.42	5.22	4.01	3.03	2.23	1.60	1.13	47.40	121.90	2.19	3.39
100	6.06	4.93	3.82	2.91	2.17	1.58	1.13	43.31	115.68	2.10	3.28

the AAE values obtained were about 22.7% and 15.3% for Hill's and Thompson's algorithms, respectively. Similarly, AAE values produced for the estimation of  $E_{Ri}$  were 14.8% and 5.7% for the two algorithms. Thompson's algorithm produced overall better and more comparable estimates with the SOFTSYS model. The design thickness of AC was reported to be 13 in. and SOFTSYS models produced generally lower estimates for thickness. The SOFTSYS analyses were repeated five times and the standard deviations of the thickness estimates are also shown in Figure 5.13(a). In general, the SOFTSYS model developed for only backcalculating layer moduli produced comparable AAE values. This proves that the idea of estimating thickness together with layer moduli actually works. The

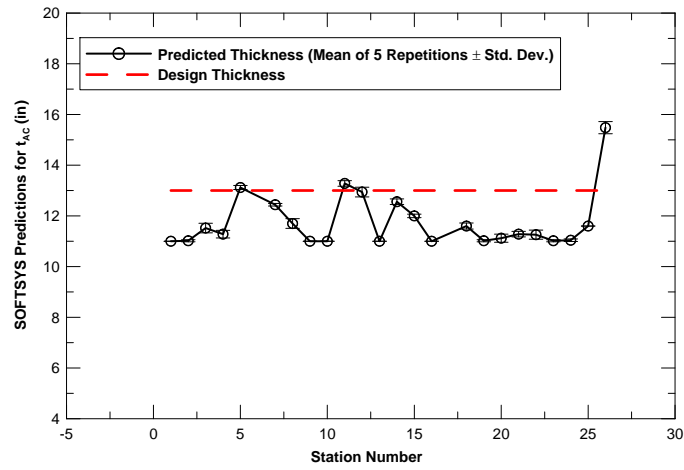
**Table 5.7:** Backcalculation Results of SOFTSYS for a Given FWD Data Chosen from ILLI-PAVE Database Developed for CFP

Best Fitness	$t_{AC}$ (in.)	$t_{GB}$ (in.)	$E_{AC}$ (psi)	$K_{GB}$ (psi)	$E_{Ri}$ (psi)	$D_0$ (mils)	$D_{12}$ (mils)	$D_{24}$ (mils)	$D_{36}$ (mils)
<b>ILLI-PAVE FWD DATA</b>	7.7	7.1	890593	11051	8790	9.8	7.73	5.54	3.86
1	7.8	10.8	883567	7038	9413	9.8	7.73	5.54	3.86
1	7.5	16.2	936455	8340	9400	9.8	7.73	5.54	3.86
1	7.9	4.4	853968	9405	8764	9.8	7.73	5.54	3.86
1	7.7	10	901892	7689	9260	9.8	7.73	5.54	3.86
0.99741769	7.9	14.4	853968	7100	9616	9.8	7.72	5.54	3.86

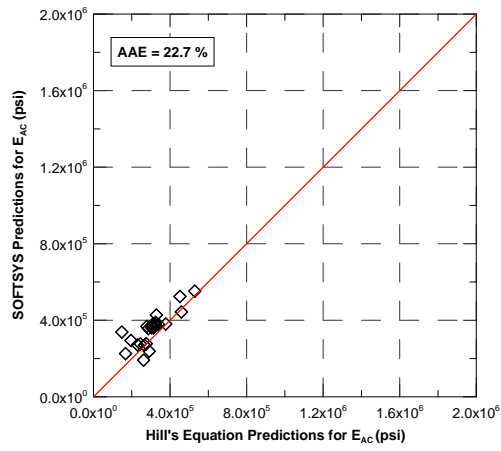
best fitness value obtained from all the SOFTSYS solutions was 0.982988 from all the stations where FWD data were collected. The average number of generations to reach the best fitness was 37 for all the stations.

### 5.3.3 Roseville Bypass

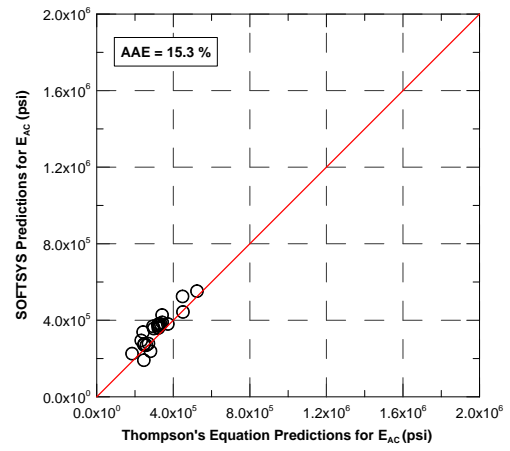
Figures 5.14(a) to 5.14(e) show SOFTSYS model predictions for Roseville Bypass. Since only four deflections were obtained from the FWD testing, SOFTSYS model FDP-LSS-PM3-FWD4 was used in the analyses. The FDP-LSS-PM2-FWD4 model was not used as its previous predictions for lime stabilized layer values were not good. The backcalculated results, however, showed very good agreement with the the results of the model used to predict layer moduli only. The advantage of this model is that it can also predict AC layer thickness without losing too much accuracy. The design thickness of the AC was reported to be 14 in. and the SOFTSYS model produced generally lower estimates for the thickness. The analyses were repeated five times and standard deviations are also shown in Figure 5.14(a). In general, the SOFTSYS model developed for only backcalculating layer moduli produced comparable AAE values. Again, this proves that the idea of estimating thickness together with layer moduli actually works. The best fitness



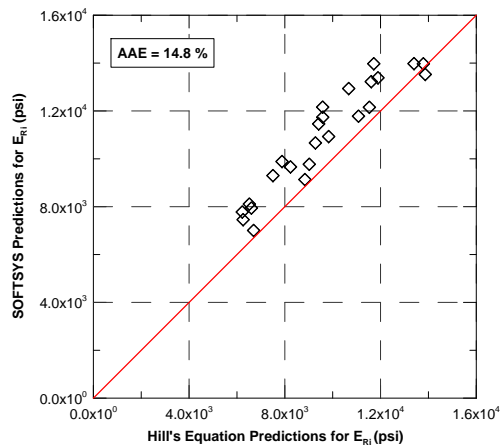
(a)



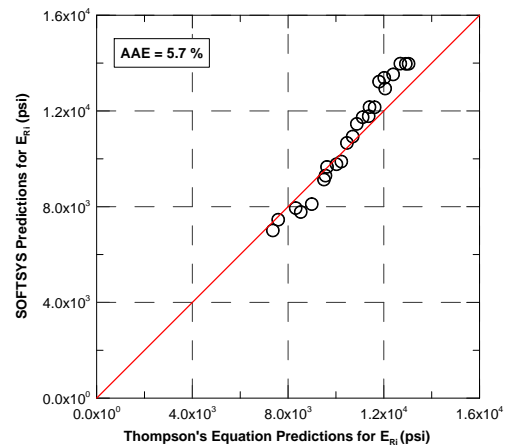
(b)



(c)



(d)



(e)

**Figure 5.13:** Performance Results of SOFTSYS Model FDP-PM2-FWD4 for US 20.

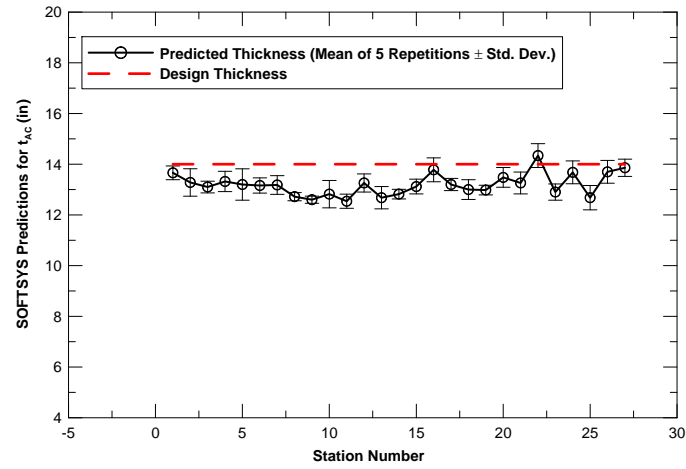
**Table 5.8:** Effect of Granular Base Layer's Thickness on Pavement Responses ( $t_{AC} = 9$  in.,  $E_{AC} = 1300$  ksi,  $K_{GB} = 5$  ksi,  $E_{Ri} = 9$  ksi)

$t_{GB}$ (in.)	$D_0$ (mils)	$D_{12}$ (mils)	$D_{24}$ (mils)	$D_{36}$ (mils)	$D_{48}$ (mils)	$D_{60}$ (mils)	$D_{72}$ (mils)	$\epsilon_{AC}$ ( $10^{-6}$ )	$\epsilon_{SG}$ ( $10^{-6}$ )	$\sigma_{DEV}$ (psi)	$\sigma_V$ (psi)
4	7.32	6.08	4.69	3.50	2.52	1.76	1.20	55.28	130.78	2.11	3.68
5	7.35	6.12	4.72	3.52	2.53	1.77	1.21	55.35	125.72	2.05	3.63
6	7.39	6.15	4.75	3.54	2.55	1.79	1.22	55.43	120.07	1.98	3.56
7	7.43	6.19	4.78	3.57	2.57	1.80	1.23	55.68	115.22	1.93	3.53
8	7.46	6.22	4.81	3.59	2.59	1.81	1.24	55.75	111.00	1.90	3.50
9	7.49	6.25	4.84	3.61	2.61	1.82	1.25	55.81	107.36	1.87	3.48
10	7.52	6.28	4.86	3.63	2.62	1.84	1.26	55.87	103.69	1.84	3.46
11	7.55	6.30	4.88	3.65	2.64	1.85	1.26	55.94	100.29	1.81	3.45
12	7.57	6.33	4.91	3.67	2.65	1.86	1.27	55.99	97.24	1.80	3.45
13	7.60	6.35	4.93	3.69	2.66	1.87	1.28	56.03	94.29	1.78	3.45
14	7.62	6.37	4.95	3.70	2.68	1.88	1.29	56.08	91.45	1.76	3.45
15	7.64	6.39	4.96	3.72	2.69	1.89	1.29	56.13	88.73	1.74	3.46
16	7.66	6.41	4.98	3.73	2.70	1.90	1.30	56.16	86.22	1.73	3.47
17	7.68	6.43	5.00	3.75	2.71	1.91	1.31	56.19	83.85	1.72	3.49
18	7.70	6.45	5.01	3.76	2.72	1.91	1.31	56.23	81.53	1.71	3.51

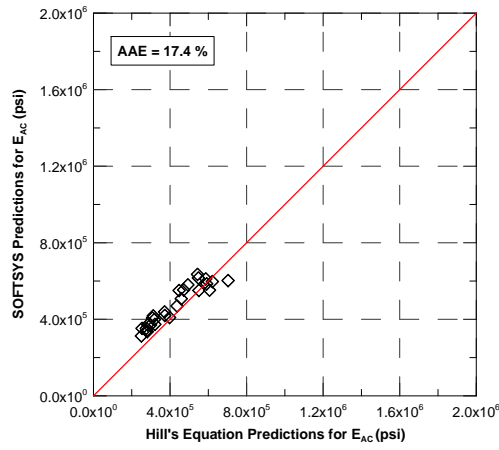
value obtained from the SOFTSYS solutions was 0.997363 from all the stations. The average number of generations to reach the best fitness was 25 for all the stations.

### 5.3.4 Staley Road

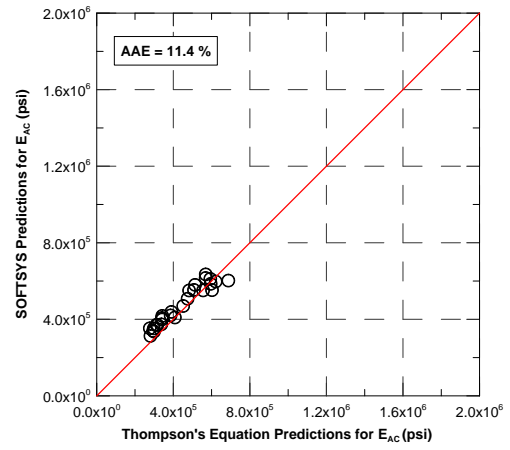
In this section, a comprehensive effort is described to further validate the prediction abilities of SOFTSYS models. For this purpose, field FWD data were first collected from Staley Road, in Champaign, Illinois, and used for performance validations of the developed SOFTSYS models. The Staley Road data included only FWD results along



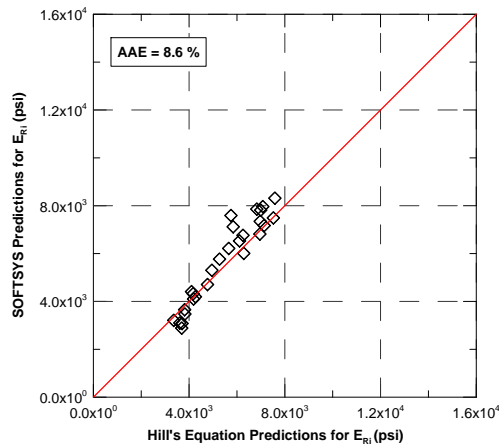
(a)



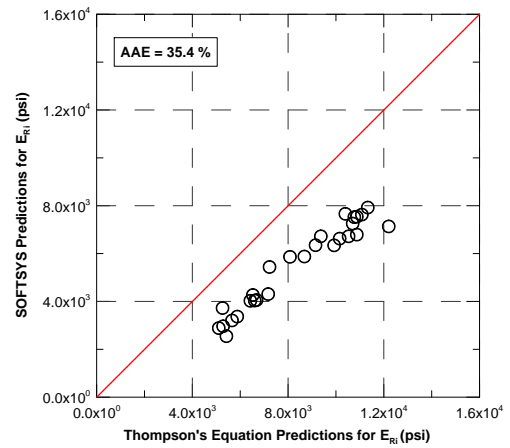
(b)



(c)



(d)



(e)

**Figure 5.14:** Performance Results of SOFTSYS FDP-LSS-PM3-FWD4 Models for Roseville Bypass.

**Table 5.9:** Effect of Granular Base Layer's Thickness on Pavement Responses ( $t_{AC} = 9$  in.,  $E_{AC} = 100$  ksi,  $K_{GB} = 5$  ksi,  $E_{Ri} = 9$  ksi)

$t_{GB}$ (in.)	$D_0$ (mils)	$D_{12}$ (mils)	$D_{24}$ (mils)	$D_{36}$ (mils)	$D_{48}$ (mils)	$D_{60}$ (mils)	$D_{72}$ (mils)	$\epsilon_{AC}$ ( $10^{-6}$ )	$\epsilon_{SG}$ ( $10^{-6}$ )	$\sigma_{DEV}$ (psi)	$\sigma_V$ (psi)
4	21.23	11.77	6.44	3.68	2.17	1.33	0.85	307.74	686.51	7.06	9.95
5	21.13	11.76	6.48	3.72	2.18	1.34	0.85	301.46	631.10	6.56	9.47
6	21.03	11.75	6.51	3.75	2.20	1.34	0.85	297.92	577.31	6.18	9.14
7	20.98	11.76	6.55	3.77	2.22	1.35	0.85	295.60	538.32	5.94	8.71
8	20.93	11.76	6.58	3.80	2.23	1.35	0.86	293.16	499.40	5.72	8.44
9	20.89	11.77	6.62	3.83	2.25	1.36	0.86	291.27	464.30	5.49	8.13
10	20.87	11.78	6.64	3.85	2.26	1.37	0.86	290.58	433.98	5.27	7.85
11	20.85	11.79	6.67	3.88	2.28	1.37	0.86	290.02	405.87	5.08	7.60
12	20.84	11.80	6.70	3.90	2.29	1.38	0.87	289.10	380.17	4.89	7.35
13	20.83	11.81	6.72	3.92	2.30	1.39	0.87	288.27	356.88	4.71	7.12
14	20.81	11.81	6.75	3.94	2.32	1.40	0.87	287.89	335.43	4.55	6.91
15	20.81	11.82	6.77	3.96	2.33	1.40	0.88	287.76	316.08	4.39	6.72
16	20.81	11.83	6.79	3.98	2.34	1.41	0.88	287.29	298.02	4.24	6.54
17	20.83	11.86	6.81	4.00	2.35	1.42	0.88	287.12	281.92	4.11	6.39
18	20.82	11.86	6.83	4.01	2.37	1.43	0.89	286.88	266.36	3.98	6.24

with the temperature information collected in August 2000, in warm weather conditions.

There were, however, no cores taken from the pavement sections at the FWD locations.

Staley Road runs in a north-south direction and is located on the west end of the city of Champaign in Champaign County, Illinois [see Figure 5.15(a) and 5.15(b)]. The design pavement cross section consists of 12 in. of HMA constructed on LSS with a thickness of 12 in. The FWD tests were performed on about 1,000 ft. of the highway stretch. The pavement temperature was approximately  $100^{\circ}F$  when the FWD tests were performed. Figure 5.16 shows the locations of FWD testing points along the pavement section. In

**Table 5.10:** Effect of Granular Base Layer's Stiffness on Pavement Responses ( $t_{AC} = 9$  in.,  $t_{GB} = 12$  in.,  $E_{AC} = 1300$  ksi,  $E_{Ri} = 9$  ksi)

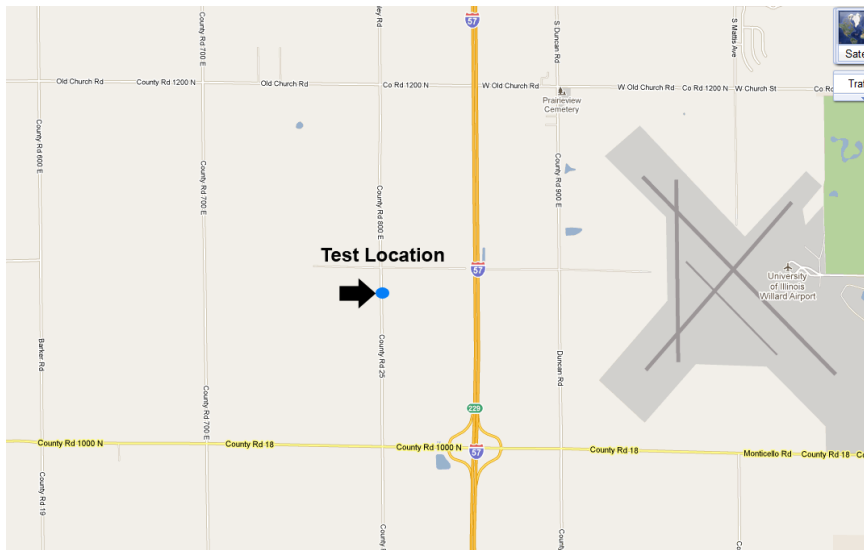
$K_{GB}$ (psi)	$D_0$ (mils)	$D_{12}$ (mils)	$D_{24}$ (mils)	$D_{36}$ (mils)	$D_{48}$ (mils)	$D_{60}$ (mils)	$D_{72}$ (mils)	$\epsilon_{AC}$ ( $10^{-6}$ )	$\epsilon_{SG}$ ( $10^{-6}$ )	$\sigma_{DEV}$ (psi)	$\sigma_V$ (psi)
1000	10.53	8.73	6.68	4.91	3.48	2.38	1.58	81.76	97.62	1.74	3.71
5000	8.88	7.19	5.39	3.90	2.72	1.84	1.22	74.67	122.15	2.14	3.87
10000	8.42	6.78	5.07	3.67	2.57	1.75	1.17	71.61	127.78	2.28	3.96
15000	8.11	6.50	4.87	3.54	2.49	1.71	1.15	68.94	130.95	2.34	3.94

this figure, the locations of existing metal plates on the road, and reference points that will continue to remain on the road are also shown for the sake of completeness.

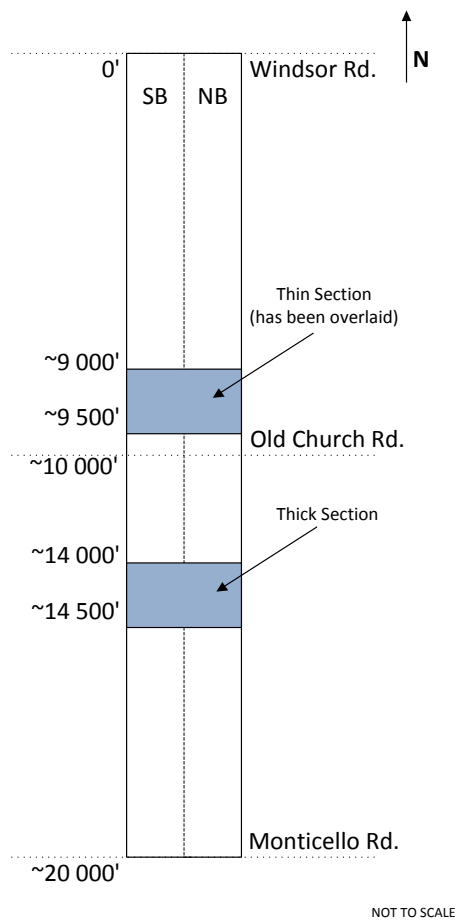
Two sets of GPR tests were performed along Staley Road in the same locations where FWD test data were obtained. The details of the GPR tests are provided in Table 5.11. The first set of GPR tests was performed to obtain the asphalt thickness data from the road, and the second one was aimed at verifying the first results and increasing reliability. In the first set of tests, North and South bound lanes of the test section were tested using both ground and air coupled antennae. In the second set of tests, only air coupled antenna were used to verify the previously determined asphalt thickness data. The GPR interpretations for both lanes (right wheel paths) are provided in Figures 5.17 and 5.18. The 1-GHz air antenna was able to capture the HMA and lime stabilized interfaces. However, the 2-GHz air antenna was able to verify only the HMA thickness, but not the lime stabilized interface. The interpretation of data collected with the ground coupled antenna did not produce meaningful results, which may be due to several reasons such as noise or moisture on the surface of the pavement.

The data obtained from GPR indicated that the constructed pavement thickness was generally thicker than the design thickness (by approximately 1 in.), although there were sections even thinner than the design thickness. The thickness data from the field were deemed to be essential to calibrate the GPR test results. For this purpose, the





(a) Map of Staley Road test location



(b) Layout of Staley Road test sections

**Figure 5.15:** Location of Staley Road and Test Sections.

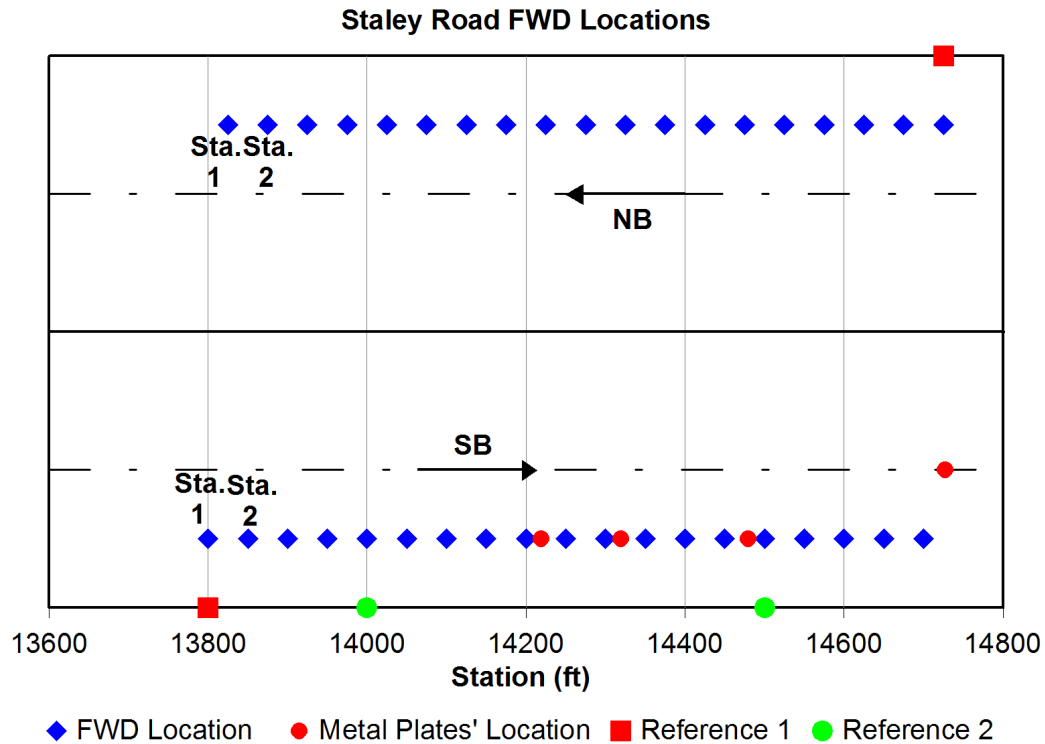
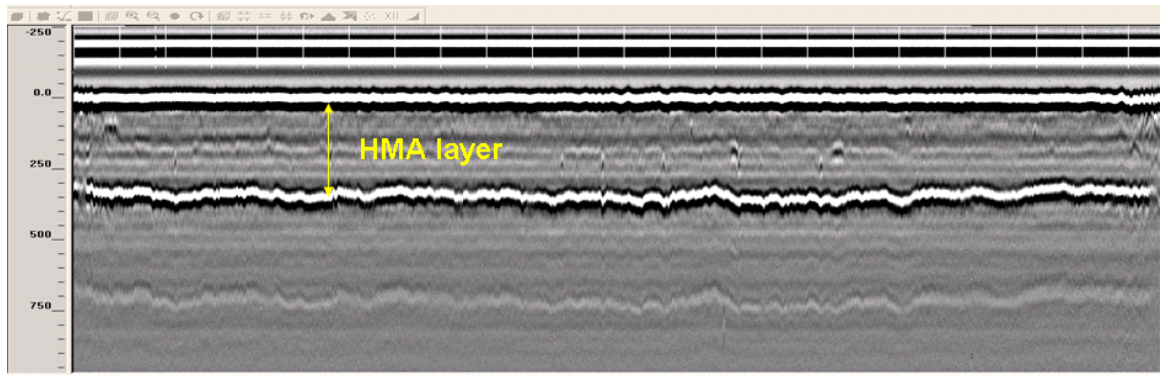


**Figure 5.16:** Locations of FWD Tests Along the Staley Road Sections.

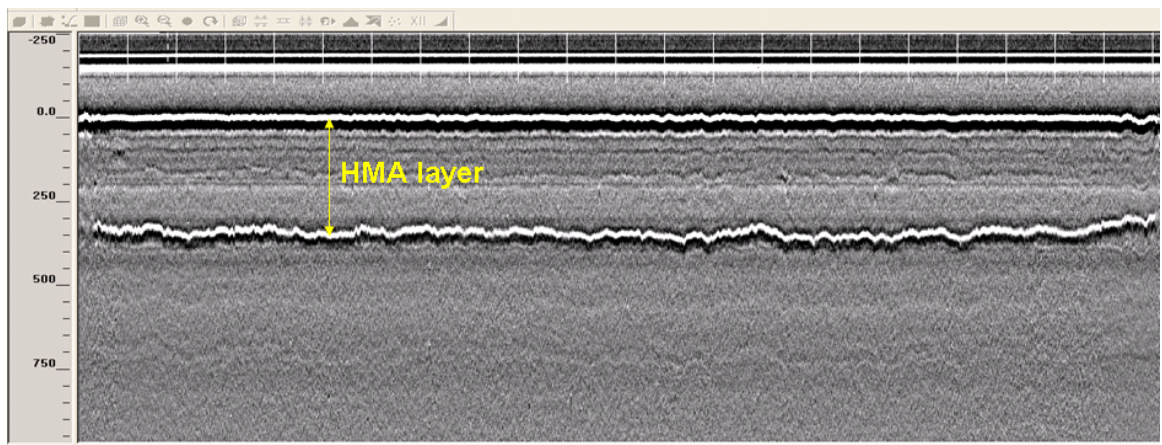
elevation data were obtained from the time when the road was constructed. There were three observation points identified within the pavement section where FWD tests were performed. These elevation points were then used to sufficiently compare GPR test results. Finally, the SOFTSYS predictions were also compared with the thickness data from both GPR testing and the construction thicknesses. No temperature correction was included in the backcalculation of pavement layer properties.

**Table 5.11:** GPR Test Conditions Along Staley Road Pavement Sections

	Test 1	Test 2
Section(ft)	13+800 => 14+750	13+800 => 14+750
Antenna Used	Ground + Air	Air
Air Condition	Clear (No rain 3 days before testing)	Clear (No rain 3 days before testing)

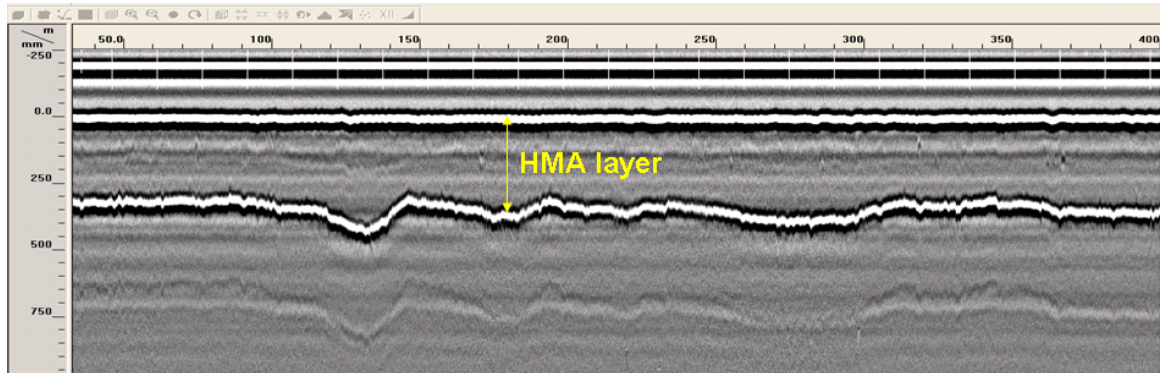


(a) 1-GHz Antenna

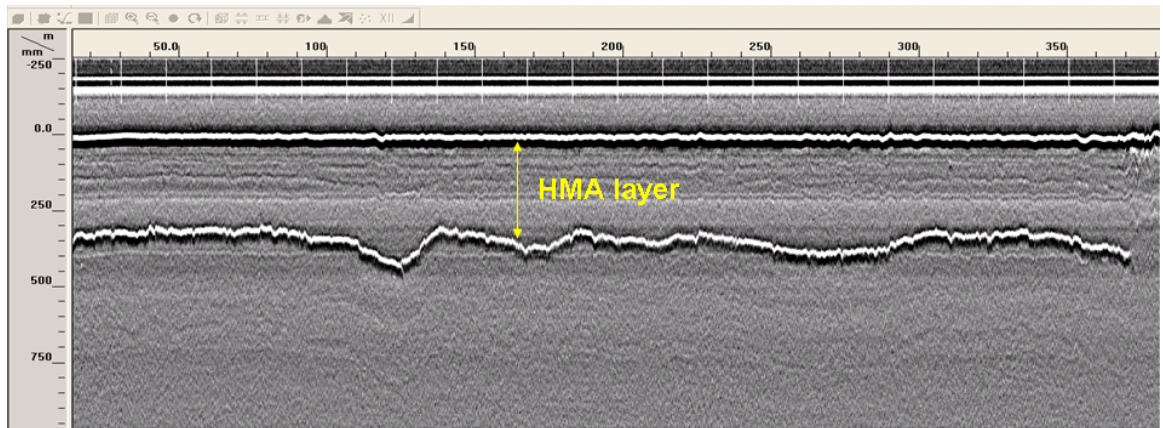


(b) 2-GHz Antenna

**Figure 5.17:** GPR Test Results: North Bound - Right Wheel Path.



(a) 1-GHz Antenna



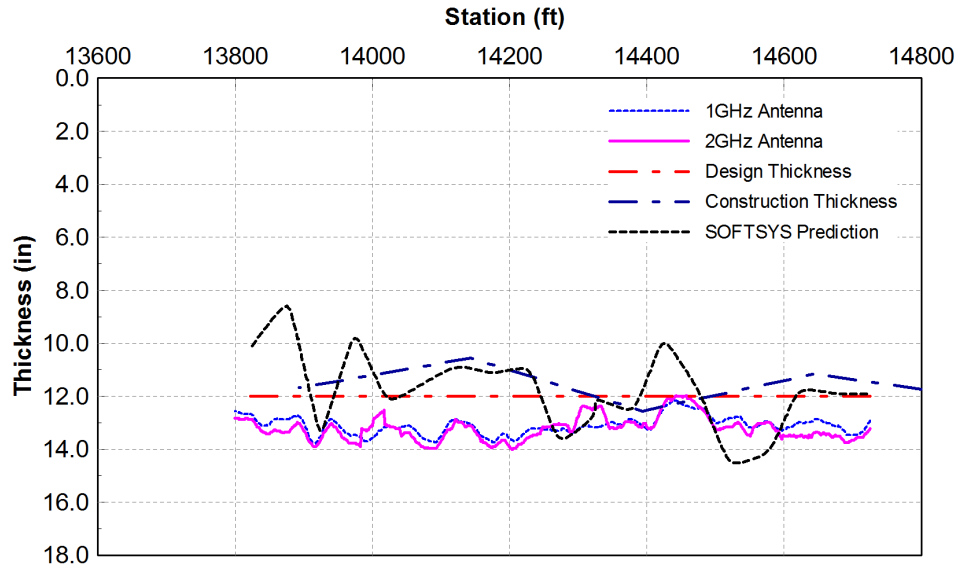
(b) 2-GHz Antenna

**Figure 5.18:** GPR Test Results: South Bound - Right Wheel Path.

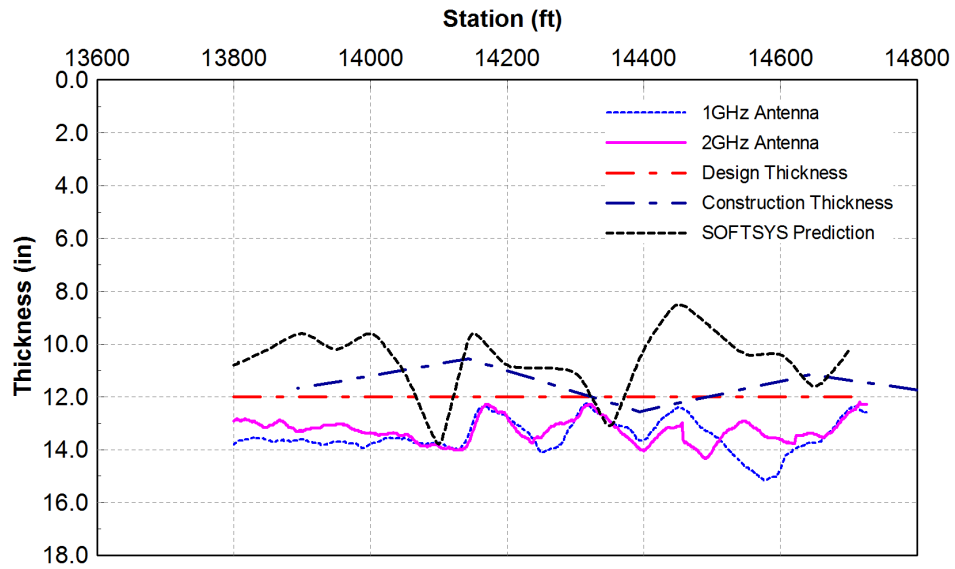
In an attempt to verify the SOFTSYS results, another model was developed to take into account the LSS layer (named FDP-LSS-PM3-FWD4) since Staley Road was built on lime modified soil. The design thickness of the LSS layer was used in the predictions. SOFTSYS predictions are given in Figures 5.19 to 5.21. The thicknesses obtained using the FDP-LSS-PM3-FWD4 model were in good agreement with the construction thicknesses on the North bound lane (see Figure 5.19(a)). On the other hand, SOFTSYS generally predicted lower thicknesses on the South bound lane (see Figure 5.19(b)). Finally, the SOFTSYS estimates for  $E_{AC}$ ,  $E_{LSS}$ , and  $E_{Ri}$  are also given in Figures 5.20 to 5.21. In general, the variations in AC layer thicknesses observed were attributed to the variability of the FWD test data.

### **5.3.5 High Cross Road (FA 808)**

Figures 5.22(a) to 5.22(e) show SOFTSYS model predictions for High Cross Road. There were only four deflections obtained from the FWD testing. Therefore SOFTSYS model FDP-LSS-PM3-FWD4 was used in the analyses. The results obtained from backcalculation analyses showed very good agreement with the the results of the corresponding model used only to predict layer moduli; the AAE values obtained for prediction of the AC modulus were about 19.2% and 14.2% for Hill's and Thompson's algorithms, respectively. Similarly, AAE values produced for the estimation of  $E_{Ri}$  were 9.6% and 34.0% for the two algorithms. Hill's algorithm produced overall much better and more comparable estimates with the SOFTSYS model. The design thickness of the AC was reported to be 11 in. and the SOFTSYS model produced very good estimates for thicknesses of the AC layer. The analyses were repeated five times and standard deviations are also shown in Figure 5.22(a). The best fitness value obtained from the SOFTSYS solutions was 1.00 from all the stations. The average number of generations to reach the best fitness was 75 for all the stations, which was much higher compared to the ones obtained from the analyses of the previously mentioned roads.



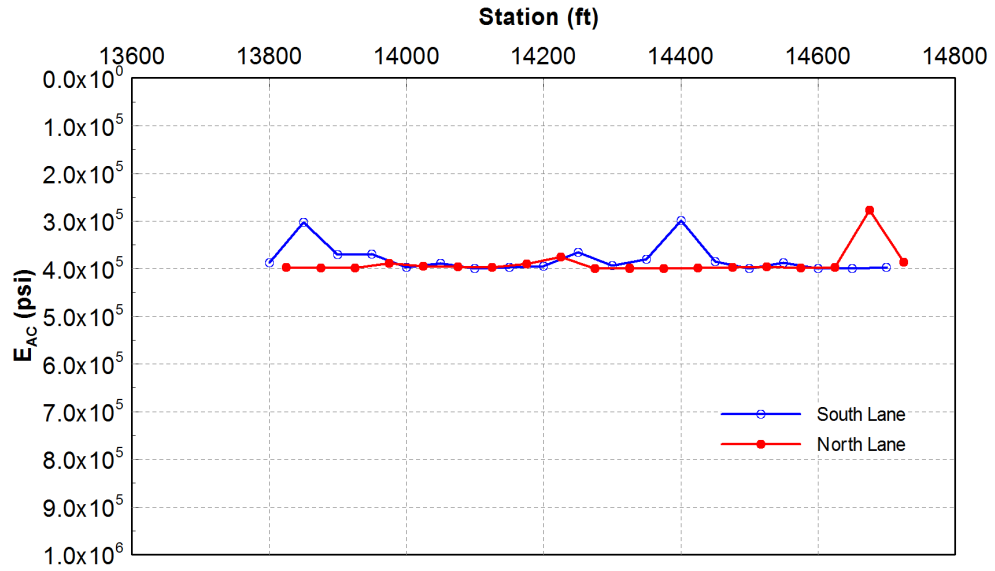
(a)  $t_{AC}$  North Bound - Right Wheel Path



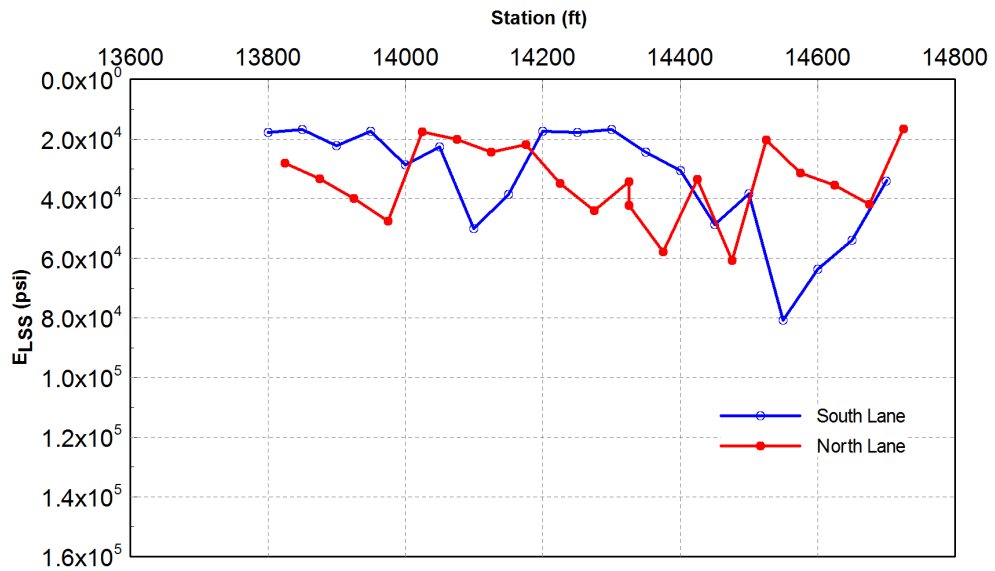
(b)  $t_{AC}$  South Bound - Right Wheel Path

**Figure 5.19:** Estimation of AC layer thicknesses using SOFTSYS FDP-LSS-PM3-FWD4 model on Staley Road in Illinois.





(a)



(b)

**Figure 5.20:** Estimation of Pavement Layer Properties Using SOFTSYS FDP-LSS-PM3-FWD4 Model on Staley Road in Illinois (cont.).

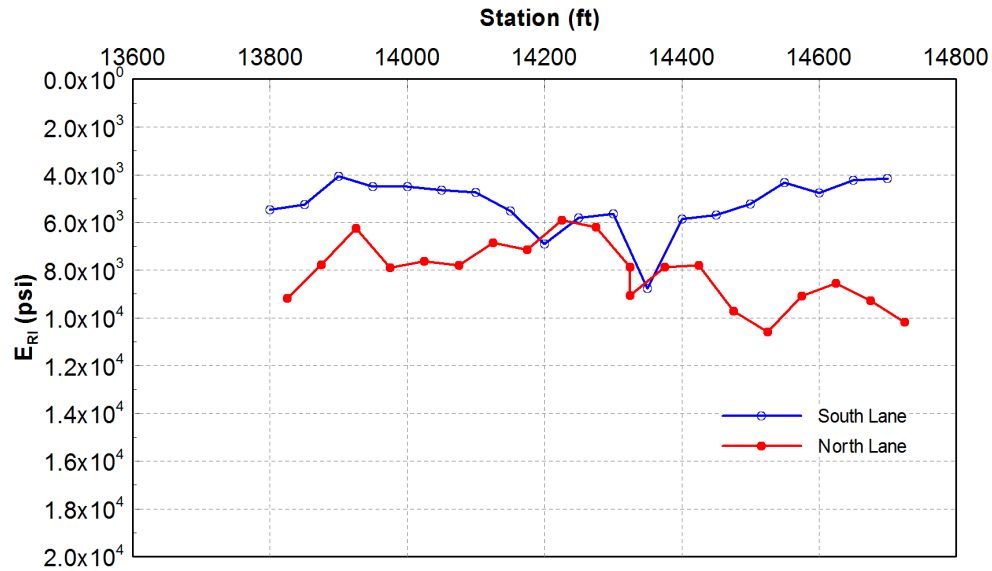
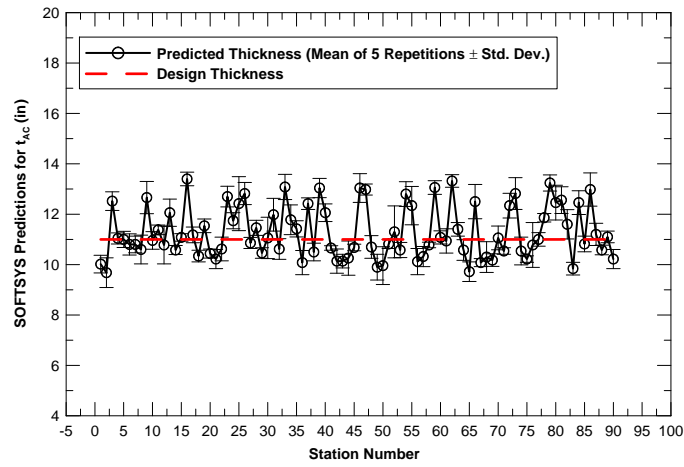


**Figure 5.21:** Estimation of Pavement Layer Properties Using SOFTSYS FDP-LSS-PM3-FWD4 Model on Staley Road in Illinois (cont.).

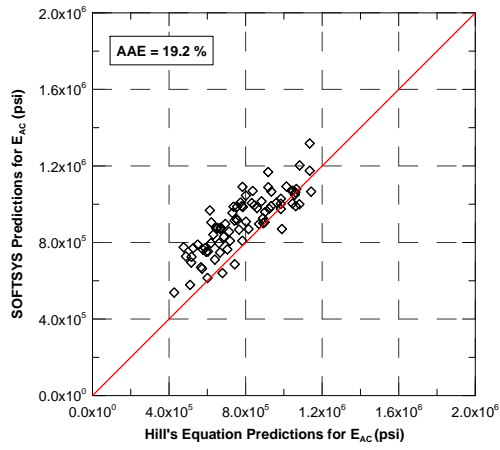
### 5.3.6 Sand Pit Road (Henry County)

SOFTSYS model CFP-PM2-FWD4 was used in the analysis of FWD data obtained from Sand Pit Road as it produced slightly better results than obtained using the CFP-PM3-FWD4 model. The CFP-PM2-FWD4 model takes the four deflections as inputs and predicts thicknesses of both AC and GB layers. In addition to the thicknesses, this model predicts layer moduli. The backcalculation analysis of Sand Pit Road was a challenging task since the FWD data had a lot of noise and/or variability; even the measurements taken on the same location had large variability. For example, the center deflections ( $D_0$ ) measured from three consecutive applications of FWD loading were different by about 40%. Therefore, FWD data were preprocessed to eliminate the ambiguities and the amount of data was greatly reduced. The design thickness of the AC was reported to be 3.5 in. and that of GB layer was 16.0 in. Figures 5.23(a) and 5.23(b) show the SOFTSYS model predictions for thickness of the AC and GB layers, respectively. Although SOFTSYS seems to produce meaningful results, they need to be interpreted cautiously since the best fitness values obtained from the SOFTSYS solutions

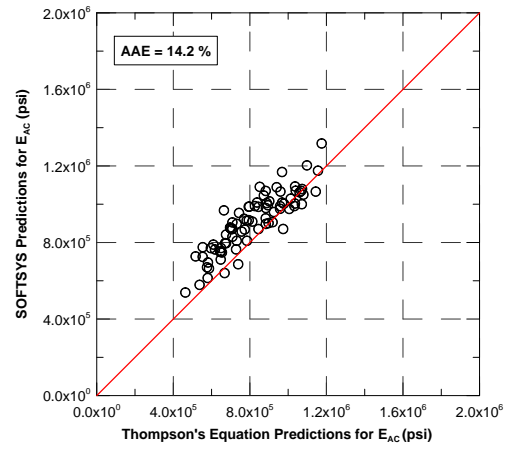




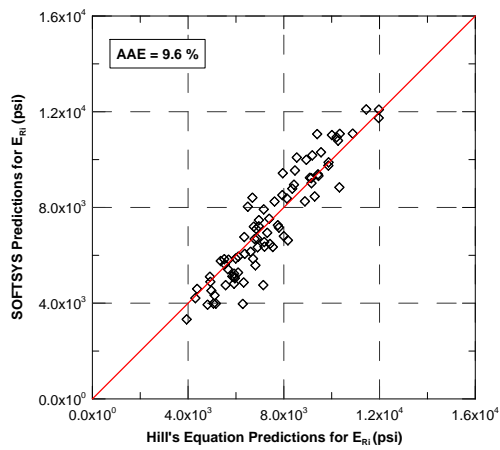
(a)



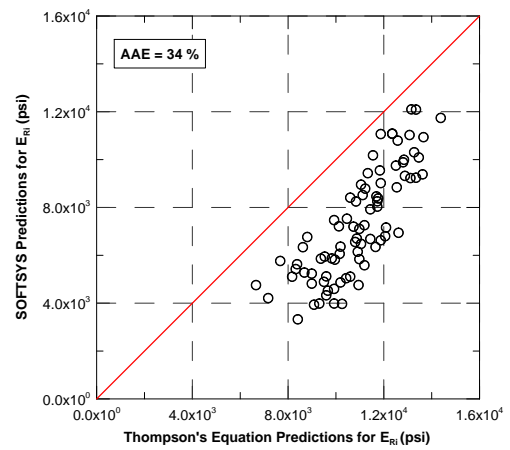
(b)



(c)



(d)



(e)

**Figure 5.22:** Performance Results of SOFTSYS FDP-LSS-PM3-FWD4 Models for High Cross Road.

were around 0.92 from all the stations. This means that the deflection profiles could not be matched fully. Finally, Figures 5.23(c) to 5.23(d) compare the SOFTSYS estimations for  $E_{AC}$  and  $E_{Ri}$  with Thompson's algorithm and Figure 5.23(e) shows the estimations of SOFTSYS for  $K_{GB}$  along the road. The CFP-PM2-FWD4 results may seem to be good; however, it should not be forgotten that the variability of FWD data was greatly reduced by eliminating the ones that create problems in backcalculation analysis. Therefore, this model's performance results need to be further validated through many other FWD data.

## 5.4 Summary

The development of the framework for SOFTSYS was refined as a new pavement analyzer to perform both forward and backcalculation analyses by the hybrid use of GA and ANN models, thus enabling Full-depth Asphalt Pavement analyses without knowledge of the pavement layer thicknesses. The newly developed SOFTSYS model performance results then needed to be validated with field FWD data.

The validation studies were first performed using the synthetic ILLI-PAVE database developed previously for flexible pavements including Full-depth Asphalt Pavements, Full-depth Asphalt Pavements on Lime Stabilized Soils, and Conventional Flexible Pavements. The promising results obtained from the validation of thickness and moduli models were then used to obtain AC layer thicknesses of pavements for the US 50, US 20, Staley Road, High Cross Road, Roseville Bypass, and Sand Pit Road projects. Layer moduli parameters were also estimated using SOFTSYS. In many cases, the performance results were compared to design thicknesses.

GPR was selected as the most reliable way of determining layer thicknesses of medium-to-long stretches of field pavement sections. In addition, construction thickness data were also obtained to determine the thicknesses of in-service pavements. The variability in the thickness as well as other pavement properties was a critical issue.

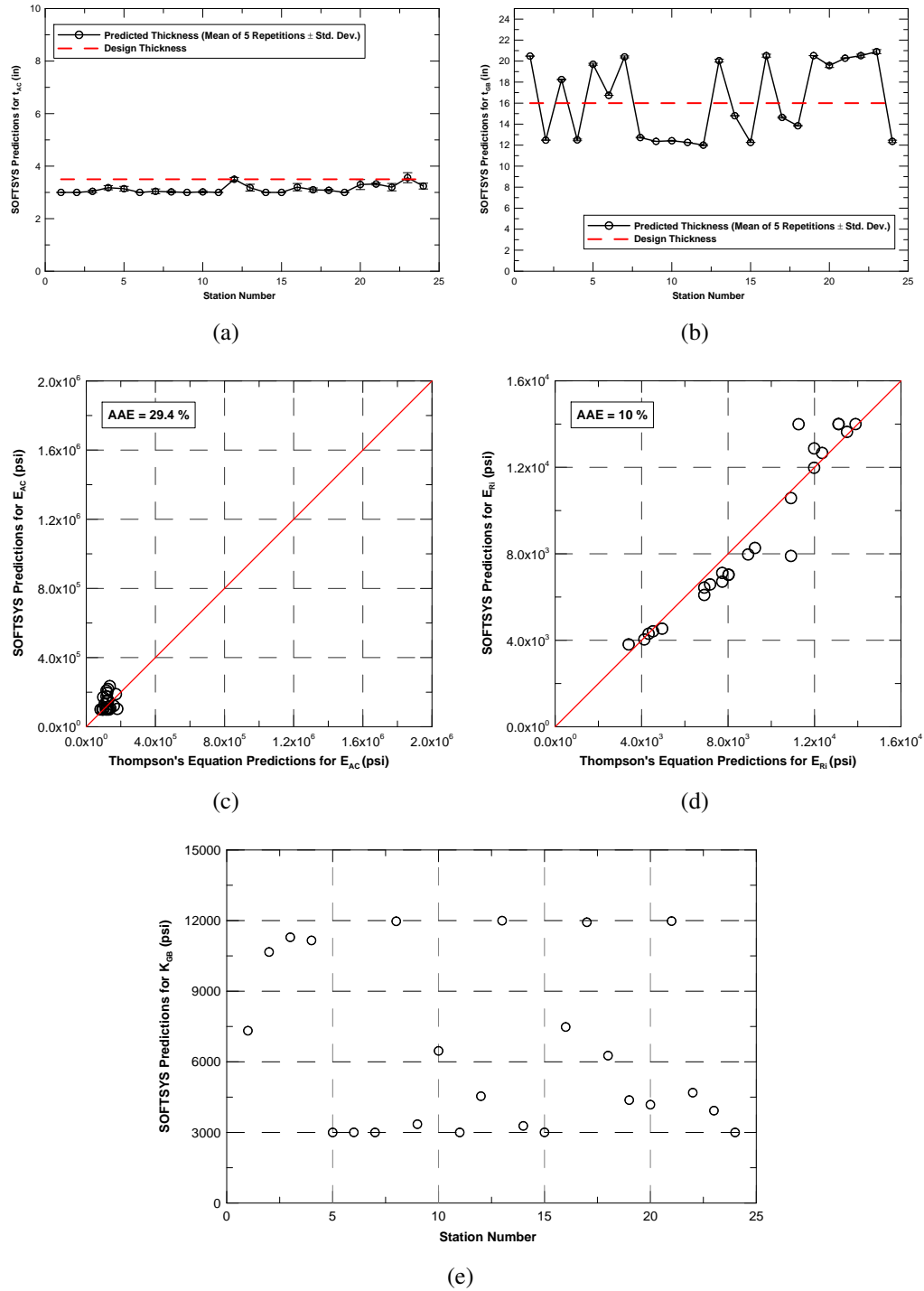


**Figure 5.23:** Performance Results of SOFTSYS CFP-PM2-FWD4 Model for Sand Pit Road.

Therefore, along with FWD testing, GPR testing was also conducted to obtain pavement thickness data. The SOFTSYS thickness predictions were then successfully validated through comparisons with the GPR test results and the thickness data from pavement section construction.

# **Chapter 6**

## **Summary, Conclusions, and Future Work**

### **6.1 Summary**

Assessment of pavement conditions in the field using the Falling Weight Deflectometer (FWD) requires backcalculation of layer moduli, which is generally performed using linear elastic pavement layer analysis tools. However, both the subgrade soils and unbound aggregate base/subbase layers exhibit nonlinear, stress-dependent geomaterial behavior. Sophisticated pavement structural models are needed to perform nonlinear analyses for more accurate solutions with fast computation schemes. This thesis first focused on the use of Artificial Neural Network (ANN) pavement structural models developed with the results of the ILLI-PAVE finite element (FE) program for FWD backcalculation and prediction of pavement critical responses. Then, with the successful application of ANN models, the emphasis was shifted towards the hybrid use of Genetic Algorithms (GAs) and ANNs to estimate the pavement layer properties, including pavement thicknesses, using only the FWD test data obtained from different types of flexible pavements.

First, information was collected on the types and typical geometries and layer properties of various flexible pavements in the State of Illinois. This information was crucial for conducting many ILLI-PAVE FE analyses and creating the synthetic pavement deflection basin database which represents the response/behavior of Illinois flexible pavements. Then, the ILLI-PAVE FE program, extensively tested and validated for over three decades, was used as an advanced structural model for solving deflection profiles and responses of the identified Illinois flexible pavements, including full-depth asphalt pavements,

full-depth asphalt pavements on lime stabilized soils, conventional flexible pavements, and conventional flexible pavements built on lime stabilized soils. Pavement deflection basins were created by the ILLI-PAVE FE runs under the standard 9,000 lb. FWD loading. Pavement deflection and response databases established in this manner from the ILLI-PAVE FE solutions covered all combinations of pavement geometries, layer thicknesses, and layer moduli.

Using these databases, both forward and backcalculation types of ANN models were developed. Different ANN model network architectures were searched and trained to determine the optimum architectures that best captured the behavior of the Illinois pavement sections. In each case, a portion of the ANN model training data was separated as an independent testing set to check the performance of the trained ANN architecture. Several network architectures were trained using different numbers of input parameters. Some of the network architectures were designed for directly predicting from the FWD deflection basins the critical pavement responses, such as the maximum horizontal tensile strain at the bottom of HMA layer or the vertical stress/strain on top of subgrade. These ANN models were intended for implementing the mechanistic-based pavement design concepts in Illinois.

In an effort to validate ANN backcalculation models, FWD test data already available from previous Illinois Highway Research (IHR) studies were collected for establishing a comprehensive field FWD database from pavements in Illinois with known layer thicknesses and material properties. Examples of such previous studies are the High Cross Road, Roseville Bypass, Staley Road, US 50, US 20, and Sand Pit Road projects. The validation database established in this way from the field FWD data was fully utilized in a comprehensive effort to validate the ANN models developed for robustness and accuracy in predicting the pavement layer moduli and critical pavement responses directly from FWD testing.

During the development of the ANN models, a professional ANN toolbox (ANN-Pro) was prepared as user-friendly software program with a graphical user interface to enable easy inputting of the FWD deflection data with pavement layer thicknesses and outputting of the ANN model predictions for forward and backcalculation structural analyses. The toolbox software program was updated in a way to directly read the FWD deflection data from the FWD testing equipment and print the pavement layer moduli and critical pavement response predictions in real time as the program output.

The second part of this thesis was the development of the framework SOFTSYS. It was proposed as a new pavement system analyzer to perform backcalculation analyses by the hybrid use of GA and ANN models thus enabling flexible pavement analyses with or without data about pavement layer thicknesses. Through the use of ANN models, SOFTSYS can also perform forward pavement analysis when needed. Similar to the ANN models, SOFTSYS model performances needed to be validated with the actual field data. Ground Penetrating Radar (GPR) was selected as an alternative nondestructive method of determining layer thicknesses of medium-to-long field pavement sections. In addition, construction thickness data were also required to determine the thicknesses of in-service pavements. The variability in the thickness as well as other pavement properties was a critical issue. Therefore, along with the FWD testing, GPR testing was also conducted to obtain pavement thickness data. The SOFTSYS thickness predictions were then successfully validated through comparisons with the GPR test results and pavement section construction thickness data. Finally, the sections analyzed using the ANN-based backcalculation models were also successfully analyzed using SOFTSYS to determine the thicknesses of pavement layers.

## 6.2 Conclusions

This thesis focused on the efficient use of soft computing methods to effectively solve the pavement layer backcalculation problem. The full potential of soft computing was also investigated using various techniques, whose capabilities were shown using the FWD data obtained from the field or the results of the ILLI-PAVE FE program. The following are the specific conclusions reached through this research study:

1. A suite of ANN models (available in the ANN-Pro software program) developed in this study for the analyses of full-depth asphalt and conventional flexible pavements, built on both natural and lime stabilized subgrades, proved that ANN model predictions for the backcalculated layer moduli and the critical pavement responses (i.e., the maximum horizontal tensile strain at the bottom of the HMA layer responsible for fatigue, and the vertical stress/strain on top of subgrade responsible for subgrade rutting conditions) were within very low average absolute errors of those obtained directly from the ILLI-PAVE FE solutions. Further, the excellent performance of the surrogate ANN structural models (forward models) proved that they could be used in lieu of FE analyses for the quick and accurate prediction of the surface deflections and the critical responses of full-depth and conventional flexible pavements found or constructed in Illinois.
2. The results of pavement structural modeling with the ILLI-PAVE FE program showed that improvements due to the constructed lime stabilized subgrade soil layer had to be captured separately in the analyses because there are significant differences between the critical pavement responses of full-depth pavements constructed on unmodified subgrade and lime stabilized subgrade. Therefore, to correctly model the pavement response and behavior with the lime stabilized subgrade soil layer, separate forward and backcalculation analysis approaches were developed to accurately



predict pavement deflection profiles and pavement critical responses under FWD loading.

3. The performances of ANN models developed for lime stabilized sections were validated with the field FWD data collected from three highway projects in Illinois. In addition, FWD data collected from other pavement test sections in Illinois and Henry County test sites were also used for field validation purposes. The low average absolute errors, compared to those from currently utilized ILLI-PAVE FE based algorithms, proved that ANN models could be reliably used to backcalculate layer moduli of flexible pavements built on both lime stabilized and natural subgrades. When compared with these regression-based backcalculation algorithms that do not consider lime-stabilized subgrade layers, the ANN models justifiably predicted higher subgrade moduli corresponding to the much lower wheel load deviator stresses found under the lime stabilized layer.
4. These comparisons showed that ANN forward and backward models did not require knowledge of advanced material property inputs and, therefore, through the implementation of ANN-Pro software, can be effectively used as quick and reliable backcalculation tools for the nondestructive evaluation of flexible pavements in Illinois.
5. This study primarily proved the effectiveness of the hybrid use of soft computing tools as robust and fast analyzers for both pavement and geomechanical systems. The focus of this work was to reliably obtain the thickness and moduli of flexible pavement layers using the results of the FWD test. However, the potential of the proposed methodology goes far beyond the use proposed in this work. The next generation of backcalculation software will use the same nondestructive techniques, but with different types of information, to extract more comprehensive conclusions about the pavements and geomaterial systems. For example, the backcalculation of Poisson's ratio was not addressed in this thesis; however, it can easily be incorporated

into SOFTSYS by considering it as an additional parameter instead of taking it as a constant.

6. Because it uses the ILLI-PAVE finite element program as the analysis engine, SOFTSYS, when compared to other backcalculation approaches, provides more advanced solutions for the proposed backcalculation problem. In addition, SOFTSYS also produces results much faster than conventional backcalculation programs because it uses ANNs to replace finite element solutions. Finally, SOFTSYS completely changes the way the ANN inversion method works. It offers a unique way of effectively searching the solution space induced by the parameters of a given mechanical system through GAs. This way of searching greatly reduces the ill-posedness of the ANN based inversion technique, which is highly prone to producing incorrect results in the case of nonlinear system properties.
7. Thickness variability was a real issue in the field, and coring was not always an option to determine layer thickness. The SOFTSYS framework was developed as an alternative way to backcalculate layer moduli. Its major contribution, however, is to predict HMA thicknesses of full-depth asphalt pavements constructed on both lime stabilized and no-lime subgrade and conventional flexible pavements.
8. When tested using the ILLI-PAVE synthetic database, SOFTSYS backcalculation models developed for pavement layer moduli produced larger absolute average errors compared to those of the ANN-based structural models. However, SOFTSYS models provide more accurate predictions when tested with field data. SOFTSYS models are therefore more robust considering field variability and have a better potential for use in field interpretations.
9. SOFTSYS models were shown to work effectively with the synthetic data obtained from ILLI-PAVE FE solutions. Some of the very promising SOFTSYS predictions indicated average absolute errors on the order of 2%, 7%, and 4% for the HMA thickness estimation of full-depth asphalt pavements, full-depth pavements on lime

stabilized soils, and conventional flexible pavements, respectively. The mid-layer properties of three layered flexible pavements, such as full-depth pavements on lime stabilized soils and conventional flexible pavements, could not be determined reliably because the FWD stress states created in these layers did not vary appreciably under thick and/or stiff asphalt concrete surfacings. This insensitivity produced non-uniqueness problem in backcalculation analyses.

10. The field validations of SOFTSYS with Staley Road FWD data produced meaningful results. Higher deflection values did correlate well with lower backcalculated HMA thickness values. In addition, the thickness data obtained from GPR testing matched reasonably well with predictions from SOFTSYS models, although in some locations the maximum difference between the two results could be up to 3 in. The variations in the observed HMA and lime stabilized soil layer thicknesses were attributed to the deflection data variability of FWD tests. The data obtained from GPR indicated that the constructed HMA thicknesses were generally thicker than the 12 in. design thickness (by approximately 1 in.), although there were sections that were even thinner than 12 in. The thickness data from the field were deemed essential to calibrate the GPR test results.
11. In general, conventional flexible pavements have much more variability in the FWD data collected when compared to those from full-depth asphalt pavements. Often the subgrade soils in CFPs are not stabilized, and the load distribution is realized through the stress-dependent granular base layer, which is greatly influenced by the quality of the aggregate materials. The layer interface between AC and base is not fully bonded either. Taken all together, these factors introduce challenges to the backcalculation analysis.
12. In the case of Henry County Road, the SOFTSYS models could not as accurately match the deflection profiles obtained from the FWD testing of CFPs as the profiles obtained from FDPs. The primary reason for poor matching was the generally higher

deflections obtained from the field when compared to the highest deflection values generated by ILLI-PAVE runs. Even when the lowest  $E_{AC}$  and  $E_{Ri}$  values were considered in the ILLI-PAVE database, some of the actual field deflections obtained from Henry County Road were still higher. Insufficiency of ILLI-PAVE database to produce exact deflection matching made SOFTSYS models unable to predict the layer properties and pavement thicknesses, which was an unsuccessful validation case for conventional flexible pavements.

13. Providing more deflection sensors as inputs increased the performance of SOFTSYS models in the case of FDPs. The same trend was also observed in the case of FDP-LSSs and CFPs while predicting  $E_{AC}$  and  $E_{Ri}$ . However, using more sensor information can decrease the best fitness and hence the accuracy of the models when including the mid-layer parameters,  $E_{LSS}$  for FDP-LSS, and  $K_{GB}$  for CFP. Therefore, for these types of pavements, it is recommended that the models with four deflections should be used when a greater precision is required.
14. In conclusion, the SOFTSYS framework is a preferred methodology over ANN models because it is more robust and capable of tolerating noise. The biggest advantage of the SOFTSYS framework is its ability to determine accurately the thickness of the AC layer in flexible pavements together with pavement layer moduli.
15. The analysis engine for SOFTSYS has been the ILLI-PAVE FE program. Therefore, the solutions from both SOFTSYS and ANN-Pro programs have the assumptions and limitations of ILLI-PAVE. One major assumption is that the various paving layers are intact; that is, no cracked or deteriorated pavements are allowed to produce FWD data from the field in performance comparisons. Therefore, the end-user should check for these assumptions before starting the backcalculation analyses.
16. The use of SOFTSYS models is recommended for newly paved roads because FWD deflection measurements are more uniform and there are no visible cracks on the

pavement surface. In addition, the application of SOFTSYS models can indicate construction quality by checking the as-constructed thicknesses in the field.

17. In pavement layer backcalculation, many parameters affect the accuracy of the predictions, such as noise in the FWD data, temperature variation throughout pavement layer depth and the spatial variation of subgrade support throughout the stations. Therefore, it is extremely hard to develop a single method that can effectively handle all the difficulties to be encountered. Although there are many uncontrolled parameters, only FWD deflections are used to predict the parameters of pavements, which may result in obtaining inaccurate solutions.

## **6.3 Future Work**

The objective of this thesis was to develop a robust methodology to obtain pavement layer properties quickly from backcalculation analyses of different types of pavements. Considering its scope, the objectives were achieved successfully. The following will improve both the performance and reliability of the proposed methods in this thesis:

1. SOFTSYS should be evaluated as an effective way to interpret information obtained from the excitation of pavement structures through the FWD test. The information needed was obtained by modeling of the FWD test using static loading schemes. However, the actual FWD loading is dynamic in nature, and therefore, the modeling should use a dynamic approach. This may or may not change the maximum deflections obtained from the FWD testing; however, it will provide the deflection-time histories of FWD sensors, which are very valuable sources of information that can be used to distinguish among different pavement layers.
2. The proposed SOFTSYS approach was only tested using a maximum of three pavement layers. However, SOFTSYS models need to be extended to different pavement types to show the potential of Genetic Algorithms when the number of

layers in pavement sections is increased. If this is the case, higher FWD loads should be used in pavement testing because different FWD load levels can provide more information about the nonlinear behavior of base/subbase and subgrade layers. In addition, since the pavements studied in this thesis were chosen from those constructed in Illinois, the validation of SOFTSYS needs to be extended for other pavement types. In that case, the forward analysis tools may be changed to adapt to different pavement conditions.

3. A preprocessing method is required to screen and eliminate the noise and inconsistencies from the collected FWD data. Such a method would ensure that the variability of data obtained from FWD can be minimized when the testing is performed repeatedly at the same spot along the road. Such a scheme in data selection can be easily embedded into SOFTSYS to use it before backcalculation analyses. An alternative way is to interpret the noise as a way of exciting the pavement structure to improve the performance of SOFTSYS. This was not done in this thesis.
4. The use of temperature information to constrain the search for SOFTSYS should be further investigated. Some utilized road data proved that SOFTSYS could converge to erroneous and unexpected results when predicting the  $E_{AC}$  of the flexible pavement. These estimation errors can be eliminated when pavement temperatures measured in the field are included in the analyses. However, investigation of this phenomenon is not straightforward because the temperature and stiffness correlations are also dependent on the type of asphalt mix and aging trends of asphalt.
5. Theoretically, the computational time for the SOFTSYS search algorithm should be very short in order to be compatible in run times with trained ANN models that replace the FE program. However, SOFTSYS runs take longer, although FWD backcalculation analyses need to be done in real time. The reason for this longer run-time is that SOFTSYS models were developed in this study using

MATLAB, which generally needs longer run times compared to the programs written in compiled languages. In addition, many functions used in SOFTSYS code are retrieved from the library files in MATLAB, which is a time-costly process when loading them into the computer's memory. Therefore, development of SOFTSYS should be continued using a compiled language, such as C, C++ or Fortran. In that case, the final product would run much faster for performing real-time FWD data analysis.

# References

- AASHTO. 1999. Determining the Resilient Modulus of Soils and Aggregate Materials (T307-99). *In: Standard Specifications for Transportation Materials and Methods of Sampling and Testing*. American Association of State Highway and Transportation Officials.
- Abdallah, I., & Nazarian, S. 2009. Rapid Interpretation of Nondestructive Testing Results Using Neural Networks. *Pages 1–19 of: Gopalakrishnan, Kasthurirangan, Ceylan, Halil, & Attoh-Okine, Nii (eds), Intelligent and Soft Computing in Infrastructure Systems Engineering*, vol. 259. Springer Berlin / Heidelberg.
- Abdallah, I., Ferregut, C., Nazarian, S., & Lucero, O. M. 2000. Prediction of Remaining Life of Flexible Pavements with Artificial Neural Networks Models. *Pages 484–498 of: D., S., Tayabji, & E., O., Lukanen (eds), Nondestructive Testing of Pavements and Backcalculation of Moduli: Third Volume ASTM STP 1375*. American Society for Testing and Materials.
- Alkasawneh, W. 2007. *Backcalculation of Pavement Moduli Using Genetic Algorithms*. Ph.D. thesis, University of Akron.
- Anderson, M. 1988. *Backcalculation of Composite Pavement Layer Moduli*. Ph.D. thesis, University of Kentucky.
- Anderson, M. 1989. A Data Base Method for Backcalculation of Composite Pavement Layer Moduli. *Pages 201–216 of: J., A., Bush III, & G., Y., Baladi (eds), Nondestructive Testing of Pavements and Backcalculation of Moduli, ASTM - STP 1026*. American Society for Testing and Materials.
- ARA Incorporated, ERES Consultants Division, & Program, National Cooperative Highway Research. 2004. *Guide for the Mechanistic-Empirical Design of New and Rehabilitated Pavement Structures*. Tech. rept. National Cooperative Highway Research Program.
- Bäck, T. 1996. *Evolutionary Algorithms in Theory and Practice*. Oxford University Press.
- Bäck, T., Fogel, D. B., & Michalewicz, Z. 1997. *Handbook of Evolutionary Computation*. Institute of Physics Publishing.



- Bäck, T., Fogel, D.B., & Michalewicz, Z. 2000. *Evolutionary Computation I: Basic Algorithms and Operators*. Institute of Physics Publishing.
- Baker, J. E. 1985. Adaptive Selection Methods for Genetic Algorithms. *Pages 101–111 of: Proceedings of the 1st International Conference on Genetic Algorithms*. L. Erlbaum Associates Inc. Hillsdale, NJ, USA.
- Basheer, I. A., & Najjar, Y. M. 1996. A Neural Network-Based Distress Model for Kansas JPCP Longitudinal Joints. *Pages 983–988 of: Intelligent Engineering Systems Through Artificial Neural Networks*, vol. 6. ASME.
- Beasley, D. 2000. Possible Applications of Evolutionary Computation. *Pages 4–18 of: Evolutionary Computation I: Basic Algorithms and Operators*. Berlin, Heidelberg, and New York: Institute of Physics Publishing.
- Beasley, D., Bull, D. R., & Martin, R. R. 1993. An Overview of Genetic Algorithms. 2. Research Topics. *University Computing*, **15**(4), 170–181.
- Booker, L.B., Fogel, D.B., Whitley, D., Angeline, P.J., & Eiben, A.E. 1997. Recombination. *In: Bäck, T., Fogel, D. B., & Michalewicz, Z. (eds), Handbook of Evolutionary Computation*, vol. 97. IOP Publishing and Oxford University Press, Philadelphia, PA.
- Burke, E., & Kendall, G. 2005. *Search Methodologies : Introductory Tutorials in Optimization and Decision Support Techniques*. Springer.
- Ceylan, H., Tutumluer, E., Gomez-Ramirez, F., Thompson, M.R., & Guclu, A. 2004. Neural Network-Based Structural Models for Rapid Analysis of Flexible Pavements with Unbound Aggregate Layers. *Pages 139–147 of: Proceedings of the 6th International Symposium on Pavements Unbound (UNBAR 6)*.
- Ceylan, H., Guclu, A., Tutumluer, E., & Thompson, M.R. 2005. Backcalculation of Full-depth Asphalt Pavement Layer Moduli Considering Nonlinear Stress-dependent Subgrade Behavior. *International Journal of Pavement Engineering*, **6**(3), 171–182.
- Ceylan, H., Guclu, A., Bayrak, M.B., & Gopalakrishnan, K. 2007. *Nondestructive Evaluation of Iowa Pavements: Phase I*. Tech. rept. Center for Transportation Research and Education, Iowa State University.
- Cox, E. 2005. *Fuzzy Modeling and Genetic Algorithms for Data Mining and Exploration*. Morgan Kaufmann.
- da Graça Lobo, F.M.P. 2000. *The Parameter-Less Genetic Algorithm: Rational and Automated Parameter Selection for Simplified Genetic Algorithm Operation*. Ph.D. thesis, Nova University of Lisboa.
- Darwin, C. 1859. *On the Origin of Species by Means of Natural Selection*.

- De Jong, K. A. 1975. *An Analysis of the Behavior of a Class of Genetic Adaptive Systems*. Ph.D. thesis, University of Michigan.
- De Jong, K. A. 2006. *Evolutionary Computation : A Unified Approach*. Cambridge, Massachusetts: MIT Press.
- Elliott, R.P., & Thompson, M.R. 1985. *Mechanistic Design Concepts for Conventional Flexible Pavements*. Tech. rept. University of Illinois at Urbana-Champaign.
- Freitas, A. A. 2002. *A Survey of Evolutionary Algorithms for Data Mining and Knowledge Discovery*. Springer-Verlag. Pages 819–845.
- Fwa, T.F., Tan, C.Y., & Chan, W.T. 1997. Backcalculation Analysis of Pavement-Layer Moduli Using Genetic Algorithms. *Transportation Research Record: Journal of the Transportation Research Board*, **1570**, 134–142.
- Ghaboussi, J. 2001. Biologically Inspired Soft Computing Methods in Structural Mechanics and Engineering. *Structural Engineering and Mechanics*, **11**(5), 485–502.
- Ghaboussi, J. 2010. Advances in Neural Networks in Computational Mechanics and Engineering. *Pages 191–236 of: Advances of Soft Computing in Engineering*, vol. 512. Springer Vienna.
- Ghaboussi, J., & Wu, X. 1998. Soft Computing with Neural Networks for Engineering Applications: Fundamental Issues and Adaptive Approaches. *Structural Engineering and Mechanics*, **6**(8), 955–969.
- Girosi, Federico, & Poggio, Tomaso. 1989. Representation Properties of Networks: Kolmogorov's Theorem is Irrelevant. *Neural Computation*, **1**(4), 465–469.
- Goktepe, A. B., Agar, E., & Lav, A. H. 2006. Advances in Backcalculating the Mechanical Properties of Flexible Pavements. *Advances in Engineering Software*, **37**(7), 421–431.
- Goldberg, D.E. 1989. *Genetic Algorithms in Search, Optimization, and Machine Learning*. Reading, Mass.: Addison-Wesley Pub. Co.
- Goldberg, D.E., & Kalyanmoy, D. 1991. *A Comparative Analysis of Selection Schemes Used in Genetic Algorithms*. Morgan Kaufmann. Pages 69–93.
- Gomez-Ramirez, F., & Thompson, M.R. 2001. *Characterizing Aircraft Multiple Wheel Load Interaction for Airport Flexible Pavement Design*. Tech. rept. University of Illinois at Urbana-Champaign.
- Gomez-Ramirez, F., Thompson, M. R., & Bejarano, M. 2002. ILLI-PAVE Based Flexible Pavement Design Concepts for Multiple Wheel Heavy Gear Load Aircraft. *In: Proceedings of the 9th International Conference on Asphalt Pavements, Copenhagen, Denmark*.

- Gucunski, N., & Krstic, V. 1996. Backcalculation of Pavement Profiles from Spectral-Analysis-of-Surface-Waves Test by Neural Networks Using Individual Receiver Spacing Approach. *Transportation Research Record: Journal of the Transportation Research Board*, **1526**, 6–13.
- Gucunski, N., Krstic, V., & Maher, M. H. 1998. Backcalculation of Pavement Profiles from the SASW Test by Neural Networks. *Pages 191–222 of: I., Flood, & N., Kartam (eds), Artificial Neural Networks for Civil Engineers: Advanced Features and Applications*.
- Harrington, P.B. 1993. Sigmoid Transfer Functions in Backpropagation Neural Networks. *Analytical Chemistry*, **65**(15), 2167–2168.
- Hausmann, M.R. 1990. *Engineering Principles of Ground Modification*. New York: McGraw-Hill.
- Haykin, S. S. 1999. *Neural Networks: A Comprehensive Foundation*. 2nd edn. Upper Saddle River, N.J.: Prentice Hall.
- Hertz, J., Palmer, R. G., & Krogh, A. S. 1991. *Introduction to the Theory of Neural Computation*. Addison-Wesley Pub. Co., Redwood City, Calif.
- Hicks, R. G., & Monismith, C. L. 1971. Factors Influencing the Resilient Response of Granular Materials. *Highway Research Record*, **345**, 15–31.
- Hill, H. J., & Thompson, M. R. 1988. *Early Life Study of the FA409 Full-Depth Asphalt Concrete Pavement Sections*. Tech. rept. University of Illinois Urbana - Champaign.
- Hoffman, M.S., & Thompson, M. R. 1981. *Nondestructive Testing of Flexible Pavements: Field Testing Program Summary*. Tech. rept. Illinois Department of Transportation.
- Holland, J. H. 1975. *Adaptation in Natural and Artificial systems: An Introductory Analysis with Applications to Biology, Control, and Artificial Intelligence*. Ann Arbor: University of Michigan Press.
- Ioannides, A. M., Alexander, D. R., Hammons, M. I., & Davis, C. M. 1996. Application of Artificial Neural Networks to Concrete Pavement Joint Evaluation. *Transportation Research Record: Journal of the Transportation Research Board*, **1540**, 56–64.
- Kameyama, S., Himeno, K., Kasahara, A., & Maruyama, T. 1997. Backcalculation of Pavement Layer Moduli Using Genetic Algorithms. *Pages 1375–1385 of: Eighth International Conference on Asphalt Pavements*, vol. 2.
- Khazanovich, L., & Roesler, J. 1997. DIPLOBACK: Neural-Network-Based Backcalculation Program for Composite Pavements. *Transportation Research Record: Journal of the Transportation Research Board*, **1570**, 143–150.

- Kim, Y., & Kim, Y. R. 1998. Prediction of Layer Moduli from Falling Weight Deflectometer and Surface Wave Measurements Using Artificial Neural Network. *Transportation Research Record: Journal of the Transportation Research Board*, **1639**, 53–61.
- Kolmogorov, A.N. 1957. On the Representation of Continuous Functions of Several Variables by Superposition of Continuous Functions of One Variable and Addition. *Dokl. Akad. Nauk SSSR*, **114**, 953–956.
- Kůrková, Věra. 1991. Kolmogorov's Theorem Is Relevant. *Neural Computation*, **3**(4), 617–622.
- Lacroix, A., Kim Y.R. Ranjithan S.R. 2008. Backcalculation of Dynamic Modulus from Resilient Modulus of Asphalt Concrete with an Artificial Neural Network. *Transportation Research Record: Journal of the Transportation Research Board*, **2057**, 107–113.
- Lee, Y. C., Kim, Y. R., & Ranjithan, S. R. 1998. Dynamic Analysis-Based Approach to Determine Flexible Pavement Layer Moduli Using Deflection Basin Parameters. *Transportation Research Record: Journal of the Transportation Research Board*, **1639**, 36–42.
- Lima, C.F., Sastry, K., Goldberg, D.E., & Lobo, F.G. 2005. Combining Competent Crossover and Mutation Operators: a Probabilistic Model Building Approach. *Proceedings of the 2005 Conference on Genetic and Evolutionary Computation*, 735–742.
- Little, D.N. 1999. *Evaluation of Structural Properties of Lime Stabilized Soils and Aggregates Vol. 1: Summary of Findings*. Tech. rept. National Lime Association.
- Liu, G. R., & Han, X. 2003. *Computational Inverse Techniques in Nondestructive Evaluation*. Boca Raton: CRC Press.
- Mayr, E. 1987. *Toward a New Philosophy of Biology: Observations of an Evolutionist*. Harvard University Press.
- McDonald, E.B. 1969. *Lime Research Study - South Dakota Interstate Routes. Four Year Report*. Tech. rept. South Dakota Department of Highways, Pierre.
- Mehrotra, K., Mohan, C.K., Ranka, S., & NetLibrary, Inc. 1997. *Elements of Artificial Neural Networks*. MIT Press Cambridge, MA.
- Meier, R., Alexander, D., & Freeman, R. 1997. Using Artificial Neural Networks as a Forward Approach to Backcalculation. *Transportation Research Record: Journal of the Transportation Research Board*, **1570**, 126–133.
- Meier, R. W., & Rix, G. J. 1993. An Initial Study of Surface Wave Inversion Using Artificial Neural Networks. *ASTM Geotechnical Testing Journal*, **16**(4), 425–431.

- Meier, R.W. 1995. *Backcalculation of Flexible Pavement Moduli from Falling Weight Deflectometer Data Using Artificial Neural Networks*. Ph.D. thesis, Georgia Institute of Technology.
- Meier, R.W., & Rix, G.J. 1994. Backcalculation of Flexible Pavement Moduli Using Artificial Neural Networks. *Transportation Research Record: Journal of the Transportation Research Board*, **1448**, 75–82.
- Meier, R.W., & Rix, G.J. 1995. Backcalculation of Flexible Pavement Moduli from Dynamic Deflection Basins Using Artificial Neural Networks. *Transportation Research Record: Journal of the Transportation Research Board*, **1473**, 72–81.
- Michalewicz, Z. 1996. *Genetic Algorithms + Data Structures = Evolution Programs*. 3rd edn. Berlin;New York: Springer-Verlag.
- Moseley, M. P., & Kirsch, Klaus. 2004. *Ground Improvement*. 2nd edn. London ; New York: Spon Press.
- Muhlenbein, H., & Schlierkamp-Voosen, D. 1993. Predictive Models for the Breeder Genetic Algorithm I. Continuous Parameter Optimization. *Evolutionary Computation*, **1**(1), 25–49.
- Neubauer, C.H., & Thompson, M. R. 1972. Stability Properties of Uncured Lime-Treated Fine Grained Soils. *Highway Research Record*, **381**, 20–26.
- Park, Seong-Wan, Park, Hee, & Hwang, Jung-Joon. 2010. Application of Genetic Algorithm and Finite Element Method for Backcalculating Layer Moduli of Flexible Pavements. *KSCE Journal of Civil Engineering*, **14**, 183–190.
- Pekcan, O., Tutumluer, E., & Thompson, M. R. 2006. Nondestructive Flexible Pavement Evaluation Using ILLI-PAVE Based Artificial Neural Network Models. *Pages 227–232 of: GeoCongress 2006: Geotechnical Engineering in the Information Technology Age*.
- Pekcan, O., Tutumluer, E., & Thompson, M.R. 2007. Analyzing Flexible Pavements on Lime-Stabilized Soils with Artificial Neural Networks. *Pages 587–596 of: Advanced Characterisation of Pavement and Soil Engineering Materials: Proceedings of the International Conference on Advanced Characterisation of Pavement and Soil Engineering, Athens, Greece*, vol. 1.
- Pekcan, O., Tutumluer, E., & Thompson, M.R. 2008a. Artificial Neural Network Based Backcalculation of Conventional Flexible Pavements on Lime Stabilized Soils. *Pages 1647–1654 of: Proceedings of the 12th International Conference of International Association for Computer Methods and Advances in Geomechanics (IACMAG)*.
- Pekcan, O., Tutumluer, E., & Thompson, M.R. 2008b. Quantifying Effects of Lime Stabilized Subgrade on Conventional Flexible Pavement Responses. *Pages 529–534 of: Advances in Transportation Geotechnics: 1st International Conference on Transportation Geotechnics*, vol. 1.

- Pekcan, O., Tutumluer, E., & Thompson, M.R. 2009. SOFTSYS for Backcalculation of Full-Depth Asphalt Pavement Layer Moduli. *Pages 679–687 of: BCR2A, Eighth International Conference on the Bearing Capacity of Roads, Railways, and Airfields.*, vol. 1.
- Pekcan, O., Tutumluer, E., & Ghaboussi, J. 2010. Soft Computing Methodology to Determine Pavement Thickness from Falling Weight Deflectometer Testing. *Pages 2621–2630 of: GeoFlorida 2010: Advances in Analysis, Modeling & Design (GSP 199).*
- Rada, G., & Witczak, M. W. 1981. Comprehensive Evaluation of Laboratory Resilient Moduli Results for Granular Material. *Transportation Research Record: Journal of the Transportation Research Board*, **810**, 23–33.
- Rasheed, K., & Hirsh, H. 1997. Using Case-Based Learning to Improve Genetic-Algorithm-Based Design Optimization. *Pages 513–520 of: Proceedings of the Seventh International Conference on Genetic Algorithms.*
- Reddy, M. A., Reddy, K. S., & Pandey, B. B. 2004. Selection of Genetic Algorithm Parameters for Backcalculation of Pavement Moduli. *International Journal of Pavement Engineering*, **5**(2), 81–90.
- Reddy, M.A., Murthy, M.S., Reddy, S.K., & Pandey, B.B. 2002. Backcalculation of Pavement Layer Moduli Using Genetic Algorithms. *Journal of Highway Research Board*, **66**, 1–10.
- Reed, R. D., & Marks, R. J. 1999. *Neural Smithing : Supervised Learning in Feedforward Artificial Neural Networks*. Cambridge, Mass.: The MIT Press.
- Roesset, J. M., & Shao, K. Y. 1985. Dynamic Interpretation of Dynaflect and FWD Tests. *Transportation Research Record: Journal of the Transportation Research Board*, **1022**, 7–16.
- Rosenblatt, F. 1958. The Perceptron: A Probabilistic Model for Information Storage and Organization in the Brain. *Psychological Review*, **65**(6), 386–408.
- Rumelhart, D.E., Hintont, G.E., & Williams, R.J. 1986. Learning Representations by Back-propagating Errors. *Nature*, **323**(6088), 533–536.
- Saltan, M., & Terzi, S. 2004. Backcalculation of Pavement Layer Parameters Using Artificial Neural Networks. *Indian Journal of Engineering and Materials Sciences*, **11**(1), 38–42.
- Saltan, M., & Terzi, S. 2008. Modeling Deflection Basin Using Artificial Neural Networks with Cross-validation Technique in Backcalculating Flexible Pavement Layer Moduli. *Advances in Engineering Software*, **39**(7), 588–592.
- Sastry, K., & Goldberg, D.E. 2004. Let's Get Ready to Rumble: Crossover Versus Mutation Head to Head. *Genetic and Evolutionary Computation–GECCO 2004: Genetic and Evolutionary Computation Conference, Seattle, WA, USA.*

- Sastry, K., Goldberg, DE, & Kendall, G. 2005. *Introductory Tutorials in Optimization, Search, and Decision Support Methodologies*. Chap. Genetic Algorithms: A Tutorial, pages 97–125.
- Selezneva, O.I., Jiang, Y. J., & Mladenovic, G. 2002. *Evaluation and Analysis of LTPP Pavement Layer Thickness Data*. Final Report FHWA-RD-03-041.
- Sener, J. C., Smith, R. M., Garz, M. D., Murgel, G. A., Hamilton, R. W., & Haws, D. R. 1998. Pavement Thickness Evaluation by GPR Survey in Idaho. *Pages 236–249 of: Structural Materials Technology III*, vol. 3400.
- Shahin, M.Y. 2005. *Pavement Management for Airports, Roads, and Parking Lots*. 2nd edn. New York: Springer Science.
- Sharma, S., & Das, A. 2008. Backcalculation of Pavement Layer Moduli from Falling Weight Deflectometer Data Using an Artificial Neural Network. *Canadian Journal of Civil Engineering*, **35**(1), 57–66.
- Spears, W. M., & De Jong, K. D. 1991. On the Virtues of Parameterized Uniform Crossover. *Pages 230–236 of: In Proceedings of the Fourth International Conference on Genetic Algorithms*.
- Syswerda, G. 1989. Uniform Crossover in Genetic Algorithms. *Pages 2–9 of: Proceedings of the 3rd International Conference on Genetic Algorithms*. Morgan Kaufmann Publishers Inc.
- Thompson, M. R. 1966. Shear Strength and Elastic Properties of Lime-Soil Mixtures. *Highway Research Record*, **139**, 1–14.
- Thompson, M.R. 1987. ILLI-PAVE Based Full Depth Asphalt Concrete Pavement Design Procedure. *In: Proceedings of 6th International Conference on Structural Design of Asphalt Pavements*.
- Thompson, M.R. 1989. ILLI-PAVE Based NDT Analysis Procedures. *Pages 487–501 of: J., A., Bush III, & G., Y., Baladi (eds), Nondestructive Testing of Pavements and Backcalculation of Moduli, ASTM - STP 1026*. Philadelphia: American Society for Testing and Materials.
- Thompson, M.R. 1992. ILLI-PAVE Based Conventional Flexible Pavement Design Procedure. *Pages 222–230 of: Proceedings of 7th International Conference on Asphalt Pavements*, vol. 1.
- Thompson, M.R. 1994. ILLI-PAVE Based Thickness Design Concepts and Practices for Surface Treatment Pavements. *Pages 507–526 of: Proceedings of 4th International Conference on the Bearing Capacity of Roads and Airfields*, vol. 1.
- Thompson, M.R., & Elliott, R.P. 1985. ILLI-PAVE Based Response Algorithms For Design of Conventional Flexible Pavements. *Transportation Research Record: Journal of the Transportation Research Board*, **1043**, 50–57.

- Thompson, M.R., & Robnett, Q.L. 1979. Resilient Properties of Subgrade Soils. *Journal of Transportation Engineering ASCE*, **105**, 71–89.
- Transportation Research Board. 1987. *Lime Stabilization: Reactions, Properties, Design, and Construction, State of the Art Report: 5*. Tech. rept.
- Transportation Research Board. 1999. *Use of Artificial Neural Networks in Geomechanical and Pavement Systems*. Transportation Research Circular - (E-C012).
- Tutumluer, E. 1995. *Predicting Behavior of Flexible Pavements with Granular Bases*. Ph.D. thesis, Georgia Institute of Technology.
- Tutumluer, E., & Meijer, R.W. 1996. Attempt at Resilient Modulus Modeling Using Artificial Neural Networks. *Transportation Research Record: Journal of the Transportation Research Board*, **1540**, 1–6.
- Ullidtz, P. 1973. The Use of Dynamic Plate Loading Tests in Design of Overlays. In: *Proceedings of the Conference on Road Engineering in Asia and Australia, Kuala Lumpur*.
- Ullidtz, P., & Stubstad, R.N. 1985. Analytical-Empirical Evaluation Using the Falling Weight Deflectometer. *Transportation Research Record: Journal of the Transportation Research Board*, **1022**, 36–44.
- Uzan, J., Scullion, T., Michalek, CH, Parades, M., & Lytton, RL. 1988. *A Microcomputer Based Procedure for Backcalculating Layer Moduli from FWD Data*. Tech. rept. Texas Transportation Institute.
- Uzan, J., Lytton, R.L., & Germann, F.P. 1989. General Procedure for Backcalculating Layer Moduli. *Pages 201–216 of: J., A., Bush III, & G., Y., Baladi (eds), Nondestructive Testing of Pavements and Backcalculation of Moduli, ASTM - STP 1026*. Philadelphia: American Society for Testing and Materials.
- Vakili, J. 2008 (1-6 October 2008). A Simplified Method for Evaluation of Pavement Layers Moduli Using Surface Deflection Data. *Pages 4314–4319 of: Proceedings of the 12th International Conference of International Association for Computer Methods and Advances in Geomechanics (IACMAG)*.
- Van der Loo, J.M. 1982. Simplified Method for Evaluation of Asphalt Pavements. *Pages 475–481 of: Proceedings of the 5th International Conference on Structural Design of Asphalt Pavements, The Netherlands*, vol. 1.
- Williams, T. P., & Gucunski, N. 1995. Neural Networks for Backcalculation of Moduli from SASW Test. *Journal of Computing in Civil Engineering*, **9**(1), 1–8.
- Wythoff, B. J. 1993. Backpropagation Neural Networks. A Tutorial. *Chemometrics and Intelligent Laboratory Systems*, **18**(2), 115–155.
- Zadeh, Lotfi A. 1994. Fuzzy Logic, Neural Networks, and Soft Computing. *Communications of the ACM*, **37**(3), 77–84.



# Vita

Onur Pekcan was born in Ankara, Turkey, in 1978. He obtained his B.S. degree from the Civil Engineering Department of Middle East Technical University (METU) in Ankara. He then started working as a research assistant at METU and obtained his M.S. degree in Geotechnical Engineering in 2001. In 2004, he came to do his Ph.D. at the University of Illinois at Urbana-Champaign (UIUC). He also holds an M.S. degree from the Computer Science Department at UIUC.

During his Ph.D. years, he mainly worked on the characterization of pavements and geomaterials using nondestructive testing methods using soft computing techniques. He was actively involved in three research projects funded by Illinois Department of Transportation (IDOT), NEXTRANS Center, and Tensar International Corporation, Inc. He has authored and co-authored several technical papers and reports. He also developed three major software programs: ANN-Pro, a software for forward and backcalculation analysis of flexible pavements, SOFTSYS, a soft computing based system analyzer; and TENSAR, a finite element program for the analysis and design of pavements reinforced with geosynthetics.

Onur also worked as a teaching assistant. He was selected as one of the five Computer Science Outstanding Teaching Assistants for Spring 2010. He had previously been named to the list of Excellent Teachers for the Fall 2009 and Spring 2010 semesters, as ranked by their students. He also holds the 2010 Graduate Teacher Certificate from the Center for Teaching Excellence. Onur was also two times the winner of the Computing Habitat Programming Competition at the Siebel Center for Computer Science.